Expanding the arsenal against leishmaniasis: Clemastine/Tamoxifen chimera as potential antileishmanials

VICTOR DE-SOUSA-AGOSTINO

Expanding the arsenal against leishmaniasis: Clemastine/Tamoxifen chimera as potential antileishmanials

A thesis submitted in partial fulfilment of the requirements for the degree of Doctor of Philosophy from the University of Durham

Victor de Sousa Agostino

Supervisor: Prof. Patrick G. Steel

Co-Supervisor: Prof. Paul W. Denny

Department of Chemistry

January 2023

Abstract

Leishmaniasis is a complex group of vector-borne zoonosis caused by parasites of the *Leishmania* genus. The prediction of annual cases of visceral leishmaniasis and cutaneous leishmaniasis combined is of more than 1 000 000 cases, with up to 20 000 deaths per year. The treatment of leishmaniasis relies on a few drugs presenting multiple shortcomings, which makes the discovery of new treatments urgent. In recent years, clemastine **27** and tamoxifen **28** have been identified in repurposing strategies and shown to display potent anti-leishmanial activity against both *in vitro* and *in vivo* models of the disease. Both molecules were proposed to target the same enzyme, inositol phosphorylceramide synthase (IPCS), which is found in the parasite but not in the host. These molecules also share similar chemical features, such as an aminoalkoxy side chain and a diaryl system. In this project, it was hypothesised that these chemical features are responsible for their antileishmanial activity. Therefore, the goal was to design and synthesise hybrid molecules between clemastine and tamoxifen and improve their antileishmanial activity. Firstly, a library of 40 compounds was synthesised varying the nature of the diaryl carbinol core and the aminoalkoxy side chain. Using a classic resazurin-based assay, all compounds were screened for antiparasitic activity against *L. major* and *L. amazonensis* promastigotes, and HepG2 cells for the evaluation of their cytotoxicity against human cells. Seven compounds with an EC_{50} < 2 μM against both species, and a selectivity index > 10 were the selected for testing against other two species of *Leishmania* promastigotes epidemiologically relevant in South America (*L. braziliensis* and *L. infantum*) as well as against two species of intracellular amastigotes (*L. amazonensis* and *L. infantum*). All compounds were highly active against *L. braziliensis* promastigotes, displaying EC_{50} values below 1 μM, and 6/7 compounds had EC_{50} approximate to 2 μM against *L. infantum*. In addition, they displayed promising activity against *L. infantum* amastigotes (EC_{50} ≤ 2 μM), but were slightly less active against *L. amazonensis*. Analogues **110** and **111** had the highest activity across the four species of promastigotes tested, and the most active compound against the intracellular amastigotes was **130**. Collectively, these results contributed towards raising insights regarding the structure-activity relationship of this library, which led to the selection of clemastine/tamoxifen hybrids with high antileishmanial potency. Ongoing and future efforts are to explore the mechanism of action of this library. For this, two techniques were chosen to be explored; chemical proteomics, which makes use of chemical probes for the identification of binding proteins, and resistance selection followed by genomic sequencing, which allows for the identification of genes associated with the compound activity.

Acknowledgements

Firstly, I would like to thank Prof. Patrick Steel and Prof. Silvia Uliana. You believed in me and gave me the opportunity of working in this project, even though I had never done any synthetic chemistry before in my life. Thank you for all the guidance and advice, for listening to me and helping me whenever I was lost, and for being the best examples of leadership I could find in my career so far. I would also like to thank Prof. Paul Denny for all the help, guidance, and ideas throughout. A special thanks to Prof. Adriano Coelho for your friendship and wisdom. Finally, I would like to thank the Global Challenges Research Fund and the NTD Network for all the funding that allowed me to pursue the dream of becoming a doctor.

Life without friends is simply boring and lonely. I would like to thank the good souls I have met during this time and that have made my life lighter when I was so far away from home. Alberto, Trishla and Sam, thank you for being the first ones to embrace me and make me feel included. Angelo, thank you for all the support and wise words you gave me throughout this process, it would have been much more difficult without your friendship. Exe, Jaime and Jonathan, thank you for sharing with me this experience, for all your warmth and for making me feel home. Elizabeth, Sinthujah and Felipe, in the final year of my PhD you were the ones who helped me stay positive, so thank you for all the shared laughs. To all the neighbours in the JAGW group, thank you for your kindness and amusing energy. And, finally, to my girls Courtney, Michaela, Vanessa, Katherine and Telyn, thank you for being my family in Durham, for all the Girl's Nights and simple everyday moments that made life better. I would also like to thank to the wonderful people I have met in the past and that made my walk to the Present easier. To Cris and Carol, thank you for being the first ones to believe that I could become someone in science and to see in me what I could not. To

Migottão, thank you for bringing up different points of view and reflections about life that brought sense to my world. To Gabriel, Victor, Larissa, Alisson, Christian, Henrique and Vinicius, thank you for listening to my complaints, making me laugh and bringing me joy in the moments of need. To Nandy, thank you for being one of the best people I have ever met, the one I can always count on and feel the greatest with.

To my parents Claudio and Jane, my brother Gustavo and my grandma Bia, there are no words that can describe my gratitude to you. You are my best friends and the most important people of my life, the solid base in which I can safely grow. Thank you for teaching me to never give up on my dreams and to persist when times are difficult. You are the biggest examples of what it means to battle in life and win, and how love is transformative. None of this would be possible without you and all your love. I love you deeply. To my grandma Mela and aunt Leia, even though you both rest in God's arms now, I would like to express my gratitude for all the wisdom you shared throughout your life and that helped making me who I am today.

Declaration

The work presented in this thesis was carried out in the Department of Chemistry at Durham University between March 2019 and December 2022. All work is the author's own except for collaborative which is acknowledged where appropriate. No part of this work has been submitted for any other degree at this, or any other University.

Statement of copyright

List of abbreviations

°C	Degrees Celsius
Ar	Aromatic group
AUR1	Inositol phosphorylceramide synthase catalytic subunit
br	Broad, in IR spectroscopy
CerS	Ceramide Synthase
CL	Cutaneous Leishmaniasis
cm^{-1}	wavenumbers
d	doublet, in ^{1}H NMR spectroscopy
DAG	Diacylglycerol
DCL	Diffuse cutaneous leishmaniasis
DCM	Dichloromethane
DsCL	Disseminated cutaneous leishmaniasis
EC_{50}	Half maximal effective concentration
EDG	electron donating group
et al.	et alia, “and others”
EWG	electron withdrawing group
g	grams
GSK	GlaxoSmithKline, pharmaceutical company
h	Hour
HIV	Human immunodeficiency virus
HTS	High throughput screening
Hz	Hertz

IC_{50}	Half maximal inhibitory concentration
IPC	Inositol phosphorylceramide
IPCS	Inositol phosphorylceramide synthase
IR	Infrared
J	coupling constants
kDa	Kilo Dalton
LCB	Sphingoid long-chain base
LCL	Localized cutaneous leishmaniasis
LCMS	Liquid chromatography-mass spectrometry
Lmj	*Leishmania major*
LmjIPCS	*Leishmania major* inositol phosphorylceramide synthase
LPP	Lipid phosphate phosphatase
LST	Leishmanin skin test
M	mass
m	multiplet, in ^{1}H NMR spectroscopy
mM	millimolar
MoA	Mode of action
m/z	mass-to-charge ratio
MCL	Mucocutaneous Leishmaniasis
mg	milligrams
mL	milliliter
mmol	Milli mol
NADPH	Nicotinamide adenine dinucleotide phosphate
NMR	Nuclear Magnetic Resonance
NO	Nitric oxide

PC	Phosphatidylcholine
Ph	Phenyl
pH	Hydrogen ionization constant
PI	Phosphatidylinositol
ppm	parts per million
q	quartet, in ^{1}H NMR spectroscopy
R&D	Research and Development
ROS	Reactive oxygen species
RT	Room temperature
s	singlet, in ^{1}H NMR spectroscoopy
SAR	structure-activity relationship
SERM	Selective estrogen receptor modulator
SPT	Serine palmitoyltransferase
t	triplet, in ^{1}H NMR spectroscopy
Tf	Triflate
THF	Tetrahydrofuran
TLC	Thin layer chromatography
VL	Visceral Leishmaniasis
WHO	World Health Organization
WT	Wild Type
δ	Chemical Shift
μM	Micromolar
ν_{max}	wavenumber of absorbance maximum

Table of contents

1. Introduction

1.1. Overview

Leishmaniases are a complex group of vector-borne zoonosis caused by parasites of the *Leishmania* genus. The broad diversity of clinical manifestations is related to both the patient's immunological response and the parasite species, making the diagnosis and treatment more challenging. In addition, the treatment of leishmaniasis relies on a few drugs presenting multiple shortcomings, including severe side effects and decrease in responsiveness, which is mostly associated with the selection of resistant strains. This makes the discovery of new alternative treatments an urgent need. As a way of overcoming time and financial problems related to the drug development process, repurposing existing treatments represents an alternative strategy. As a result of this strategy, clemastine **27** and tamoxifen **28** were identified to display a potent anti-leishmanial activity. Both molecules have been proposed to target the same enzyme, inositol phosphorylceramide synthase (IPCS), which is found in the parasite but not in the host. The goal of this project was to design and synthesise tamoxifen/clemastine chimera molecules based on the common chemical features shared by them as a way of improving their antileishmanial activity and selectivity.

Chapter 1 will present the project background, introducing the leishmaniases and the main concepts on drug discovery strategies. Additionally, this chapter also provides discussions regarding the sphingolipid biosynthetic pathway as a source of drug targets and previous work of the group concerning clemastine **1** and tamoxifen **2** anti-leishmanial activity. Chapter 2 is composed of the project hypothesis as well as the overall and specific aims. Chapter 3 describes the synthesis of the clemastine/tamoxifen hybrids, followed by the primary anti-promastigote assay against

L. major. Chapter 4 will provide the results of further activity evaluation of this library, including the structure-activity relationship studies developed. The initial attempts on exploring the mechanism of action of most active compounds are described in Chapter 5. Finally, conclusions and future work are described in Chapter 6, whilst experimental details and procedures will be detailed on Chapter 7. A list of the references used are presented in Chapter 8.

1.2 *Leishmania spp* and the Leishmaniases

The etiological agents of human leishmaniases, a complex group of devastating diseases with a wide clinical spectrum, comprise over 20 species of protozoa of the *Leishmania* genus[1]. Being part of the Trypanossomatidae order and Kinetoplastea class, these protozoa are characterized by a single flagellum and an organelle called kinetoplast, located in the mitochondria adjacent to the flagellar basal body [2,3]. Clinical manifestations of the disease are dependent on the parasite species and host immunological response, resulting in either visceral (VL) [4] or tegumentary/cutaneous leishmaniasis (CL) [5–7]. The latter can manifest in different types: mucocutaneous (MCL), localized (LCL), diffuse (DCL) and disseminated (DsCL)[1].

Tegumentary leishmaniases are endemic in approximately 100 countries and territories worldwide, spread in all continents, as stated by the World Health Organization (WHO) (Figure 1.1). The countries with the highest occurrence of the disease are Brazil, Peru, Iran, Syria, Algeria, Saudi Arabia and Afghanistan. Several species can lead to CL, such as *L. major*, *L. amazonensis*, *L. tropica* and *L. mexicana* [1,6]. VL is highly prevalent in Bangladesh, India, Ethiopia and Nepal, being mostly caused by *Leishmania donovani,* as well as in Brazil, where *Leishmania infantum* is the prevalent species [8–10]. According to WHO, there were approximately 14 000 reported cases of VL in 2020, and more than 200 000 cases for CL. However, these

numbers are underestimated; the prediction of new annual cases of VL by WHO relies on 90 000, leading to about 20 000 deaths per year. For CL, the estimate is of approximately 1 million new cases yearly. In total, about 1 billion people are at risk of infection in endemic areas around the world [11].

Parasites are transmitted by several species of female hematophagous sandflies within the genus *Phlebotomus*, in the Old World (Africa, Europe and Asia) and *Lutzomyia*, in the New World (America) [12–14]. Approximately 30 species of sandflies are potential vectors for *Leishmania*. Natural hosts include a variety of wild animals, such as rodents, marsupials and xenarthrans, which characterize this disease as a zoonosis [14]. However, the infection has adapted to urban environments, which led to a transmission independent to the wild reservoirs .

Status of endemicity of cutaneous leishmaniasis worldwide, 2020

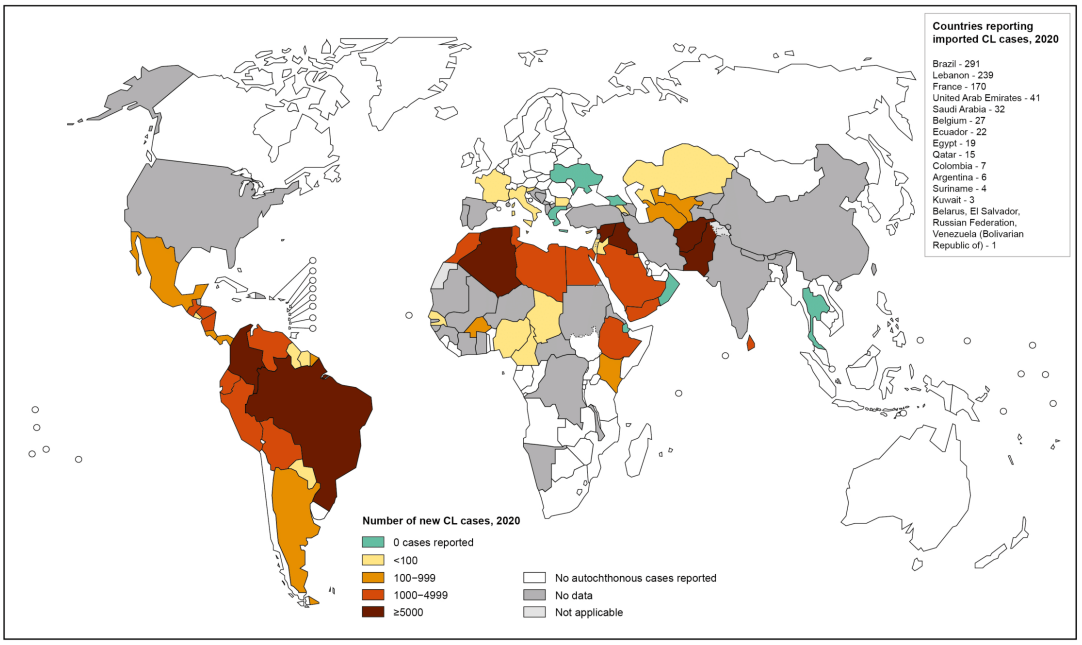

Data Source: World Health Organization
Map Production: Control of Neglected Tropical Diseases (NTD)
World Health Organization

World Health Organization

Status of endemicity of visceral leishmaniasis worldwide, 2020

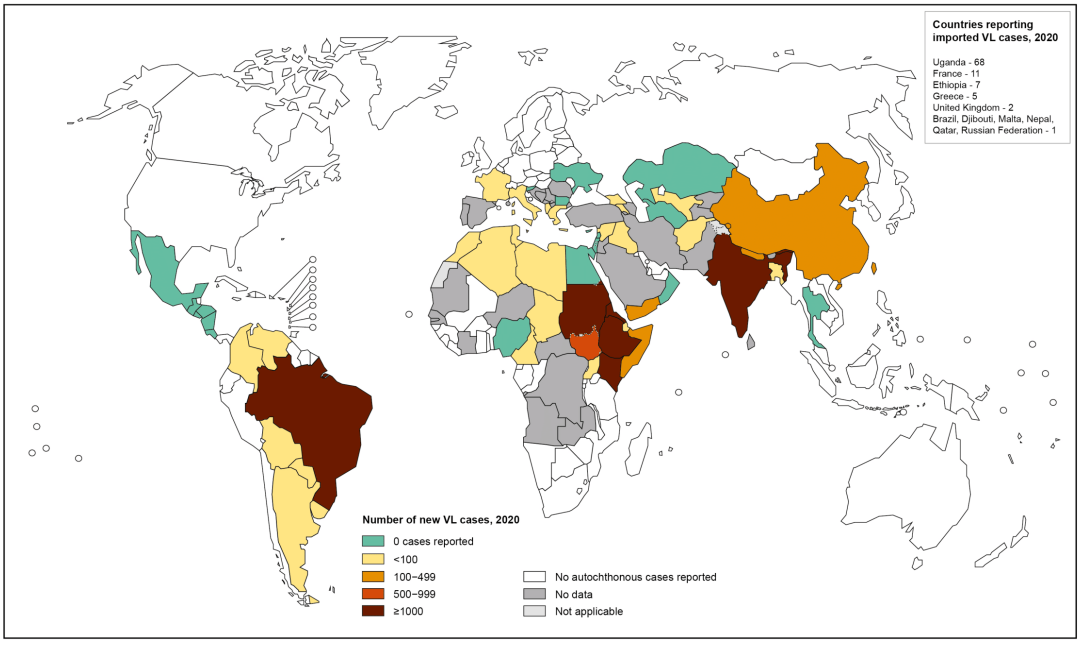

Data Source: World Health Organization
Map Production: Control of Neglected Tropical Diseases (NTD)
World Health Organization

World Health Organization

Figure 1.1. Endemicity of CL and VL worldwide in 2020 (WHO).

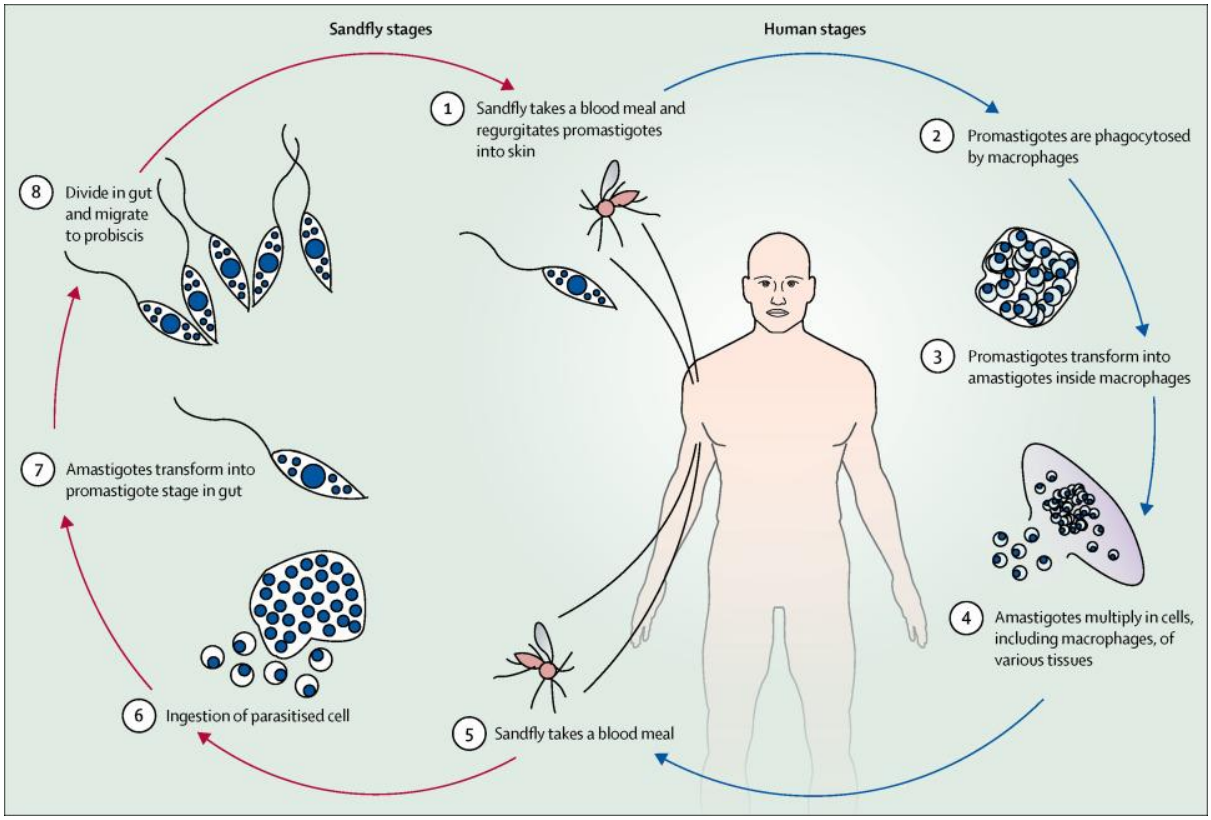

Figure 1.2. Parasitic life cycle of *Leishmania spp*. Reproduced from Burza et al (2018), *The Lancet*, with permission by Elsevier.

The parasite has a dimorphic life cycle that reflects the two host environments inhabited (Figure 1.2) [1]. The cycle starts in the gut of the sandfly, where the parasites are found in the promastigote form (elongated body and visible flagellum). There, the parasite is able to replicate and mature to its infective form, the metacyclic promastigote. During the blood meal, metacyclic promastigotes are regurgitated together with the insect's saliva into the mammal host's dermis. Parasites are then phagocytosed by both local (macrophages) and recruited (neutrophils) immune cells. The macrophage is classically considered the parasite's main host cell whilst neutrophil infection has been proven to be important in the spread and maintenance of the infection, functioning as "Trojan horses" to macrophages [15,16]. Once in the macrophage phagolysosome, a number of biochemical signals, in particular the low pH (between 4 and 5), induces the metamorphosis of the parasite to the amastigote

form (round body and internal flagellum). In this form, the parasite encounters optimal metabolic conditions for respiration, catabolism of substrates and construction of macromolecules [17]. Amastigotes replicate until the host cell is lysed, leading to parasite release. The released amastigotes are either phagocytosed by other macrophages, maintaining the infection in the host, or taken up by uninfected sandflies during blood meals. Amastigotes are able to disseminate both through the vascular and lymphatic systems, reaching lymph nodes and, consequently, liver, spleen, and bone marrow [1,4,7]. However, for reasons that are not yet understood, the ability to infect these organs is restricted to the causative agents of visceral leishmaniasis only [4].

1.2.1. Clinical manifestations

1.2.1.1 Tegumentary leishmaniasis

The tegumentary leishmaniasis can be split in four sub-categories; localised cutaneous (LCL), disseminated (DsCL), diffuse (DCL) and mucocutaneous (MCL) [1,6,7,18,19]. LCL is caused by a broad number of species, including *L. amazonensis*, *L. tropica*, *L. major*, *L. aethipica* and *L. mexicana*, being the most common clinical variant. LCL is characterized by nonspecific ulcerating lesions that are often mistaken for fungal and bacterial infections, or neoplasms. Interestingly, different parasite species worldwide lead to different ulcerating lesions, making the proper diagnosis even more difficult since there is no consistent pattern. The ulcers usually develop at the site of the sandfly bite; however, parasites can spread via the lymphatic system. The lesions may spontaneously heal depending on the parasite species.

DCL and DsCL [6,20] are rarer forms of cutaneous leishmaniasis and can be a late progression of LCL. DCL is characterized by multiple non-tender and non-ulcerating papules widespread in the body. It is classically caused by *L. amazonensis*, *L. aethiopica* and *L. mexicana* in patients who lack a cellular immune response which

explain the absence of ulcers. Affected patients show a negative leishmanin skin test (LST) and their dermis is strongly infiltrated with parasites, indicating an uncontrolled infection due to anergic immune response. In contrast, DsCL is characterized by about ten polymorphic lesions in the skin in at least two parts of the body, usually being associated with mucosal involvement. This variant is present in Latin America and it is mostly caused by *L. braziliensis*. In contrast to DCL, patients affected by the DsCL show few parasites in the lesions, positive LST and highly activated immune cells. Both forms are highly difficult to treat, with rate failure of at least 75% of the cases.

MCL [6], a late progression form of other cutaneous leishmaniases, is a severe form of the disease more common in the Americas, caused by infections with species from the *Viannia* subgenus, such as *L. braziliensis*. This clinical form is characterised by destructive and highly disfiguring mucosal lesions, mostly in the nasal septum, palate and lips, due to metastasis of the parasite to the host's mucosa. MCL is hard to treat and, if not diagnosed early, is potentially lethal. The reasons for this are multiple and include the fact that it is commonly associated with secondary infections, besides being proven to affect immunocompromised individuals

Despite the fact that the tegumentary leishmaniases are not fatal, they are strongly related with social stigma that are proven to trigger several mental health issues [21–23]. Amongst increased anxiety and depression, an estimated 70% of all patients experience reduced quality of life and social exclusion that are sustained by misconceptions regarding disease and its transmission. Because of the stigma, individuals avoid seeking treatment because they are ashamed of being exposed in public, which potentially leads to unfortunate disease outcomes [24]. In addition, scarred patients are prone to have less educational and employment opportunities [24,25].

Altogether, the leishmaniases contribute to continuous cycles of poverty that only exacerbate the severity of this disease on affected areas.

1.2.1.2. Visceral Leishmaniasis

VL is the most severe form of leishmaniasis, caused by *L. donovani* and *L. infantum* [1,10,26]. It is a silent immunosuppressing disease, characterized by pancytopenia, spleen-hepatomegaly and non-protective hypergammaglobulinemia, that is commonly asymptomatic until the patient becomes immunocompromised. Because of its immunosuppressing effects, the disease can be fatal within 2 years after infection, usually because of secondary infections and severe anaemia. When co-infected with HIV, it becomes an important challenge to treat both diseases, as their immunosuppressing effects are synergistic on the cellular immune response [9,27]. Consequently, as with MCL, a prevalence of HIV is associated with higher predisposition to VL in endemic areas, making patients more likely to develop life-threatening complications, including opportunistic infections.

1.2.2. Current treatments

The treatment of leishmaniases is limited to a few drugs and most of them have been in use for a long time without significant upgrading [28–30]. The therapeutic arsenal currently available includes pentavalent antimonials **1** and **2**, amphotericin B **3**, miltefosine **4**, paromomycin **5** and pentamidine **6** (Figure 1.3).

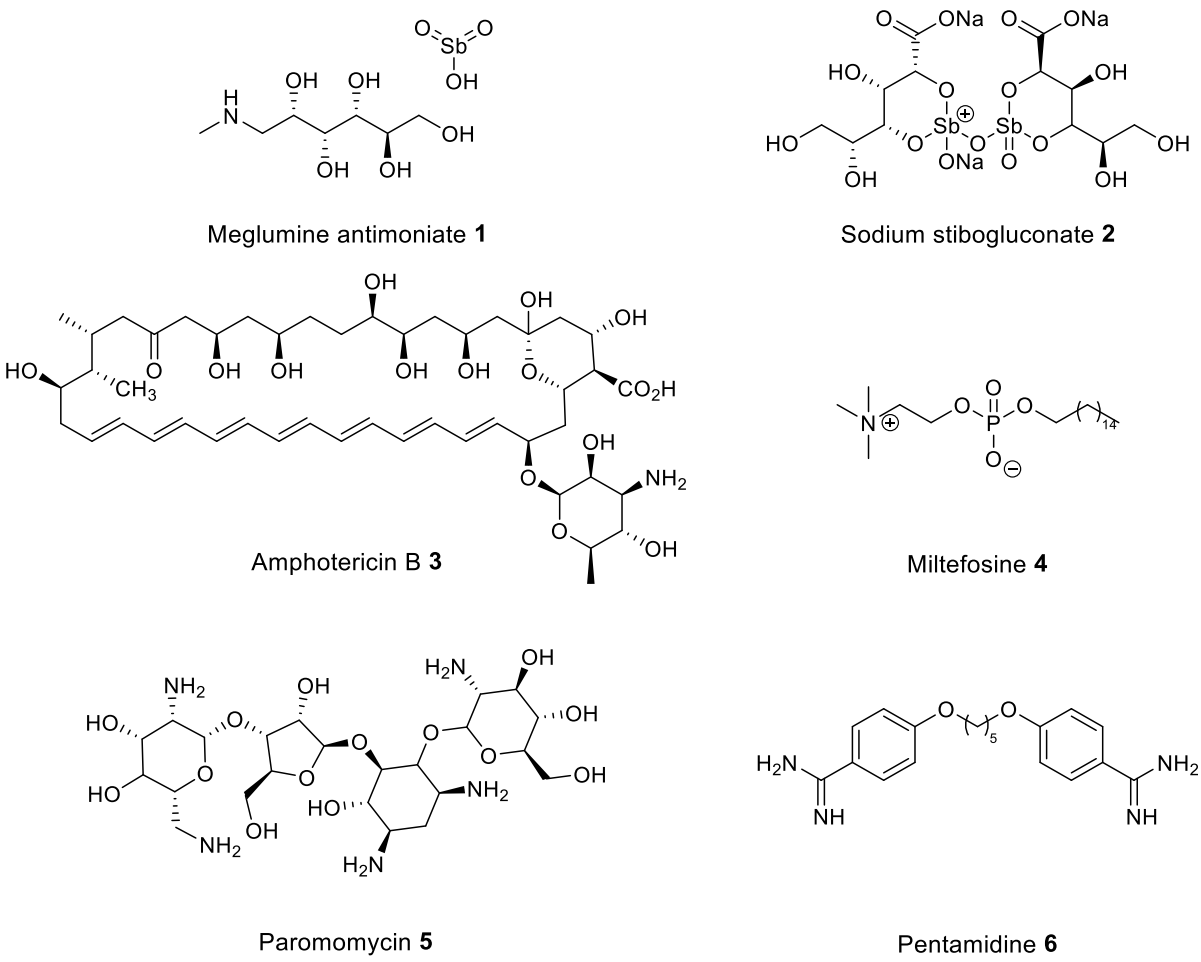

Figure 1.3. Current drugs used in the treatment of leishmaniasis.

Trivalent antimonials were proposed in 1914 by Gaspar Vianna to treat patients diagnosed with CL in Sao Paulo, Brazil. In the 1920s, the pentavalent antimonials were introduced by researchers in India as a less toxic alternative for this treatment [31]. Since then, meglumine antimoniate **1** and sodium stibogluconate **2** have been used as first line option both for CL and VL in most endemic countries. Given their high toxicity [32], antimonials are administered intralesionally in mild cases of CL, and intravenously in other cases. There is even a higher death risk in malnourished patients with advanced visceral leishmaniasis when treated with pentavalent antimonials, which represents a substantial impact on the poorest communities [26,33]. In the 1980s, it was reported in India a significant increase of the therapeutic failure in the treatment of VL, reaching a failure rate of 60-70% by 1995 [34,35]. For this reason,

antimonials are no longer used in India, as well as in certain areas in Nepal and Bangladesh. Similarly, in Brazil, a failure rate over 40% in patients with CL has been reported [36,37]. However, meglumine antimoniate **1** is still the first option for the treatment of tegumentary leishmaniasis. The mechanism of action of these drugs are not yet completely elucidated, although it is well known that the trivalent antimony is the active form of the compound. Activity is associated with interference at the beta-oxidation of fatty acids and glycolysis processes in the parasite, which leads to depletion of intracellular ATP-levels [38].

In 1960, amphotericin B **3**, a known antifungal drug, was reported as an alternative treatment to non-responsive patients with MCL [39]. A few years later, amphotericin B **3** was also shown to be effective in the treatment of VL [40,41]. It is proposed that the mechanism of action involves the disruption of the parasite membrane through the formation of membrane pores [42]. This membrane disruption is potentially a cause of host cell toxicity, which can lead to kidney failure [43,44]. To address this, liposomal formulations of the drug were developed in an attempt to reduce the high toxicity of amphotericin B deoxycholate [43,45]. Even though this formulation is currently recommended by WHO as the first-choice drug, mostly for VL treatment, its high cost and difficulties in storage obstruct its use in most endemic countries.

Miltefosine **4**, a phosphatidylcholine analogue, firstly developed as an anti-cancer drug, was approved in 2002 for VL treatment in India [46,47]. In contrast with all the other treatments, which need parenteral administration, miltefosine **4** is the first, and currently only, oral treatment for VL. The side-effects of this drug are generally considered manageable since they are mostly gastrointestinal. However, miltefosine **4** has a strong teratogenic potential, which is a problem for early treatment of pregnant

woman. In addition, it has a long half-life which has been associated with the selection of drug-resistant lines or the development of more virulent strains [46,48]. Consistent with this, relapse in treatment has been seen in at least 20% of patients infected with *L. donovani*, together with decrease in responsiveness in other cases. As with the other drugs miltefosine exhibits polypharmacology with multiple modes of actions. For example, evidence has been found for the induction of an apoptosis-like death in parasites [48]. Although there have been clinical trials that confirmed activity of miltefosine against CL, its use is currently restricted for the treatment of VL [37,49]. In Brazil, miltefosine was approved in 2017 for the treatment of canine VL [50,51]. This was very controversial considering miltefosine is the only orally available drug and its use has not been established in Brazil yet for the treatment of human leishmaniasis.

Paromomycin **5** is an aminoglycoside antibiotic first described in 1968 [52], and subsequently proposed as an antileishmanial topical treatment for CL in 1985 [29]. The drug was also explored as a treatment for VL [53,54]. However, activity varied when tested in other territories, where different parasite strains are more common [55]. Due to this geographical heterogeneity in efficacy and lower cure rates compared to other drugs, sole use of paromomycin **5** has been discontinued. Nonetheless, more recently, it has been shown that the combination of paromomycin **5** and antimonials enables the possibility for shorter treatment courses and this is now a recommended WHO regimen [56].

Pentamidine **6** is a diamidine synthesised on the 1930s and present severe toxic side-effects, such as cardiotoxicity and metabolic disturbances [57]. Even though pentamidine **6** presents unsatisfactory activity against VL and there was high rate of relapse in patients treated, the drug is still used in South America for the treatment of infections by *L. guyanensis* [58].

In most endemic countries association schemes are not applied on the treatment of leishmaniasis, and single drug treatments are used instead. Combination therapy is usually related with lower doses and reduction of side effects, making use of different mechanisms of action to enhance therapeutic efficiency [28,30,59,60]. Most importantly, it is an important strategy to avoid the selection of resistant strains, which has already been reported for pentavalent antimonials and miltefosine. An example of that is the guideline recently released by WHO for the treatment of VL patients co-infected with HIV. The scheme involves the use of liposomal amphotericin B together with miltefosine, which led to 88% efficacy rate against 55% obtained with current standard treatment [30,61].

In summary, leishmaniasis is a very complex group of diseases, where different clinical manifestations are related to both the patient's immunological response and the parasite species. Considering that methods for species-specific diagnosis are not available outside research facilities (hospitals in affected areas, for example), the assessment of species-specific treatment has not been properly investigated [62]. The current therapeutic arsenal induces serious side effects, leading to several disorders ranging from nephro-hepatotoxicity to teratogenicity [1,28]. The mode of administration is also a concern, considering all treatments available – but miltefosine – are parenterally administrated, requiring special infrastructure in endemic regions, leading to decreased treatment adhesion. In addition, the decrease in the responsiveness to treatment to several of the current treatments due to the selection of resistant strains [63], together with the other shortcomings listed, suggests that the discovery of new treatments for this disease is urgent.

1.3. Drug discovery

1.3.1 Introduction

The search for new targets and drugs that can lead to new treatments is a challenging process that involves high cost and a long time [64]. The estimated cumulative expenditure that leads to the registration of a new chemical entity (NCE) can be up to 3 billion dollars and takes approximately 15 years of research [65]. The pipeline can be generally split into two phases; the first, known as the exploratory phase, includes all *in vitro* and *in vivo* preclinical data that precedes clinical development in humans, which is the development phase (Figure 1.4) [66,67]. The exploratory phase starts with the mining of hit molecules by *in vitro* screening of a library of molecules. Hit molecules are defined as compounds that display the desired activity in a primary screening [67,68]. The most known strategies for the screening of compounds are divided between target-based and phenotypic screening [69], which will be further discussed in sections 1.3.2 and 1.3.3. Once identified, hit molecules go through a series of tests that confirm their activity as well as deconvolute their molecular target, and consequently, the mechanisms of action (MoA) [70]. The hit-to-lead optimization process involves the chemical optimisation of the hits identified, generating structure-activity relationship (SAR) data. This process results in a chemical lead, which is defined as a drug-like molecule that is synthetically feasible, metabolically stable, and non-toxic [68]. Promising lead compounds undergo further biological characterization *in vivo*, such as toxicology assays, pharmacokinetic and pharmacodynamic studies, and the use of *in vivo* models of the disease for preclinical evaluation. At the end of the exploratory phase, the most promising lead molecule is chosen as a development candidate, which is the NCE selected for clinical studies in humans [67]. The development phase starts with Phase I clinical trials to investigate

potential safety issues, followed by the evaluation in affected patients in Phase II and III clinical trials.

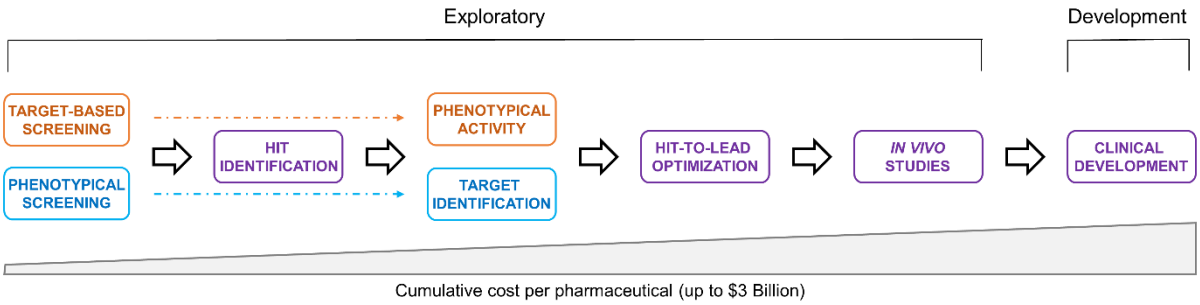

Figure 1.4. Drug discovery pipeline.

1.3.2. Target-based screening

The use of known and validated molecular targets to screen a library of compounds is called target-based screening [71]. With the great advances in molecular biology techniques, it has become more feasible to identify genes – and further macromolecules, such as proteins and lipids – that play important and/or essential roles in diseases [70,72,73]. A target-based approach is usually simpler and easier to implement when activity is simplified to a protein-substrate interaction [74]. Another advantage of knowing the molecular target is the broad range of techniques that can be applied to understand and chemically optimise lead compounds. For example, crystallography and computational modelling can be powerful tools to aid the rational design of molecules, leading to a smaller selection of compounds with a high probability of achieving the desired activity. This process can significantly decrease the time spent synthesizing molecules for further *in vitro* screening. Successfully developed molecules using this strategy are the several tyrosine kinase inhibitors used in the treatment of cancer, such as gefitinib **7** and sunitinib **8**, which target EGFR and VEGFR/PDGFR, respectively, as well as antivirals raltegravir **9** and zanamivir **10**, which target the HIV integrase and the influenza neuraminidase, respectively (Figure

1.5) [69]. Structural data, however, is only accessible for a few macromolecules, mostly soluble proteins, reflecting challenges in producing and crystallising certain classes of macromolecules, such as membrane-bound proteins [70]. In addition, a target-based approach must be followed by confirming phenotypical activity. It is not uncommon for molecules that have been developed in a target-based approach to fail to translate into clinical results, either not showing sufficient activity or acting differently than expected when applied in more complex environments [69].

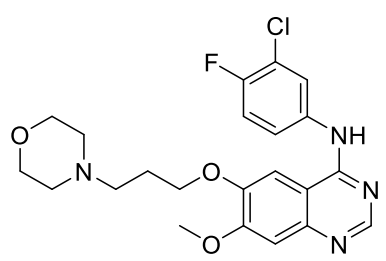

Gefitinib **7**

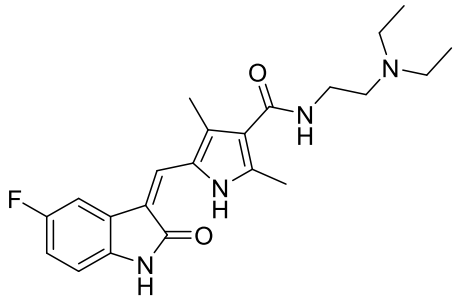

Sunitinib **8**

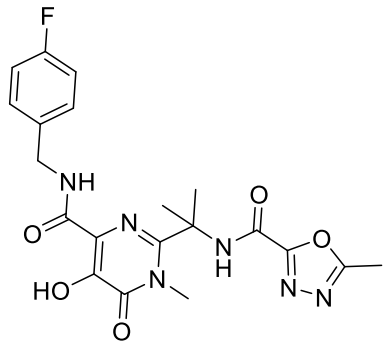

Raltegravir **9**

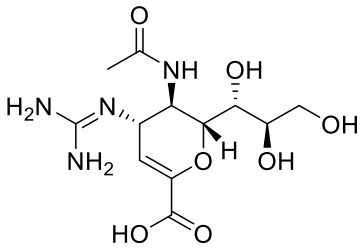

Zanamivir **10**

Figure 1.5. Compounds discovered using target-based screening strategies.

1.3.3 Phenotypic screening

In a phenotypic approach, the search is focused on a desired phenotype, such as elevating serotonin levels in synapses in the treatment of depression or eliminating microorganisms from infections [75]. The strongest advantage of phenotypic screening

is the unbiased nature of the process, which better captures the complexity of biological systems by using whole cell systems or even animal models, instead of isolated protein targets [69,75]. An example is the discovery of daclatasvir **11** for the treatment of Hepatitis C, which was assayed against a model of human cells expressing the virus replicon. This system was able to robustly predict the inhibition of HCV replication *in cellulo* [75]. Another example tackled the modulation of PCSK9 protein, which led to lower LDL cholesterol levels in humans when reduced [73]. A compound library was screened against mammalian cells and the assay readout was decrease in PCSK9 levels. This led to the identification of R-IMPP **12**, which specifically binds to human ribosomes and inhibits the translation of PCSK9 mRNAs [73]. Such novel mechanism could only be addressed in a phenotypic screening, considering that the complexity of the cellular translation machinery would not be reproduced in a target-based screening. Assays that fail in translating the biological context reliably in the screening may mislead the selection of relevant molecules for treating the disease. Furthermore, without knowing the molecular targets, it becomes challenging to work on the optimization of lead compounds as well as moving these compounds into the development phase.

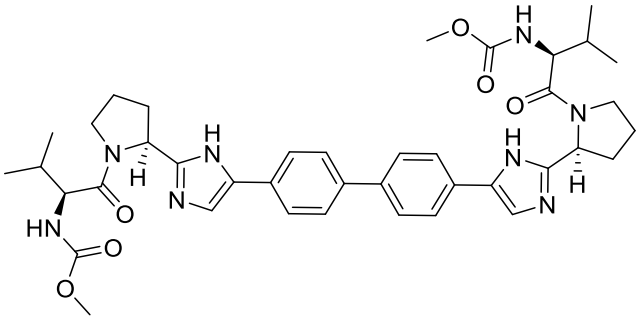

Daclatasvir **11**

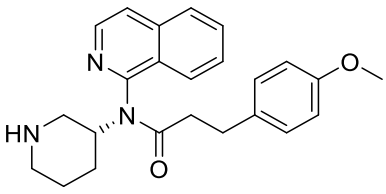

R-IMPP **12**

Figure 1.6. Compounds discovered using phenotypic screening strategies.

1.3.4. Drug repurposing, repositioning, and rescue

As mentioned above, the search for new drugs is expensive, laborious, time-consuming, and risky. As a subset of both target-based and phenotypical approaches, drug repositioning has become an attractive alternative to the traditional *de novo* drug discovery [76,77]. This strategy is characterized by repurposing a known and approved drug for new uses against another disease. Benefits behind drug repurposing include much faster development, considering an approved drug usually has a well described safety profile and considerable knowledge regarding its use. This strategy is also cheaper when compared to traditional techniques. It is estimated to cost approximately US$300 million to bring a repurposed drug to the market for a new indication [78]. The repositioning of drugs is well known in the treatment of leishmaniasis as, with the exception of pentavalent antimonials, all current treatments were originally developed to target other diseases [79]. In this project, the focus was to start from approved drugs that were previously suggested to be repurposed as antileishmanials. As a result of that, tamoxifen and clemastine were both found to be suitable drugs, which will be further discussed in Section 1.5.

1.4. Sphingolipids

1.4.1. Structure and general function

Sphingolipids are a subset of lipids with amphipathic properties and are of great structural importance in the constitution of eukaryotic membranes. In addition, they are also key components in a diverse range of intracellular signalling processes, such as cell recognition, differentiation and growth, membrane traffic and apoptosis [80,81]. These molecules are assembled from three main chemical components: (1) a sphingoid long-chain base (LCB), which is the backbone of all sphingolipids; (2) a fatty acid attached to C-2 via an amide bond; and (3) a hydrophilic head group bound to the hydroxyl group at C-1 (Figure 1.7) [82]. Sphingolipids exhibit structural diversity due to the broad range of variations in chain length, saturation and hydroxylation coming from the numerous combinations of different headgroups and fatty acyl chains.

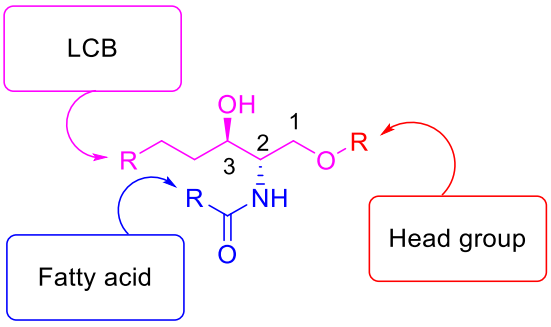

Figure 1.7. Sphingolipid general chemical structure.

1.4.2. Biological significance in Leishmania

Sphingolipids, together with sterols, compose the lipid rafts, which are membrane microdomains crucially important for membrane trafficking. In *Leishmania*, sphingolipids represent approximately 10% of their membranes [83,84]. *Denny et al* (2004) [85] produced a *Leishmania major* mutant strain that is sphingolipid-free by knocking down serine palmitoyltransferase (SPT), an early enzyme in the *de novo*

sphingolipid biosynthesis (further discussed in Section 1.4.3). They showed that a parasite lacking sphingolipids was defective in membrane trafficking and signalling transduction, but also overexpressed glycoconjugates, such as lipophosphoglycan (LPG) and proteophosphoglycan (PPG). The parasites were unable to undergo differentiation from procyclic to metacyclic promastigote. In contrast, *de novo* sphingolipid synthesis was shown to be unnecessary in intramacrophage amastigotes, suggesting that they scavenge mammalian sphingolipids, such as sphingomyelin, and metabolise them intracellularly.

1.4.3. De novo *synthesis of sphingolipids*

Sphingolipid biosynthesis starts in the endoplasmic reticulum with the condensation of palmitoyl CoA **13** with L-serine **14** by serine palmitoyl transferase [82,84] (Figure 1.6). This reaction provides 3-ketodihydrosphingosine that is enantioselectively reduced by 3-hydrosphingosine reductase, a NADPH-dependent enzyme, to give dihydrosphingosine **15**. These early steps of the biosynthetic pathway are conserved among all eukaryotes. From dihydrosphingosine **15**, there is a divergence between species. In mammals and trypanosomatids dihydrosphingosine is N-acylated and unsaturated to afford ceramide **16**, whilst in plants and fungi, the LCB is first hydroxylated and further N-acylated, forming phytoceramide **17** [82]. Ceramides can undergo other modifications, such as phosphorylation to form ceramide-1-phosphate, which is an important cell signalling molecule with antagonistic functions in comparison with ceramide. Sphingosine is a ceramide degradation product and can either be recycled to form new sphingolipids or be further phosphorylated to sphingosine-1-phosphate, which can be degraded to restore fatty acids.

The N-acylation step of ceramides is catalysed by different ceramide synthases (CerS) with different preferences for fatty acid chains, contributing to the diversity of sphingolipids. Ceramides/phytoceramides, known as simple sphingolipids, are transported to the Golgi complex by vesicular transport or via the ceramide transfer (CERT) protein. There, further sphingolipid complexity is achieved when ceramides are coupled with different headgroups, increasing the structural diversity of these molecules. In mammals and some protozoa, such as *Plasmodium spp*, sphingomyelin **18** is obtained in a reaction catalysed by sphingomyelin synthase with phosphatidylcholine **19** (PC) [86]. In contrast, in plants, fungi and trypanosomatids, ceramides are mostly combined with phosphatidylinositol **22** (PI) to afford inositol phosphorylceramide **20**/**21** (IPC), a reaction catalysed by the inositol phosphorylceramide synthase (IPCS) [82,84]. As a byproduct of both sphingomyelin **18** and IPC **20**/**21** formation, diacylglycerol **23** (DAG) is produced. Within the trypanosomatids, *Trypanosome spp* also produces sphingomyelin, however IPC **20** is the major sphingolipid synthesised [87].

Sphingolipids can also be produced by the recycling and degradation pathway, in which ceramides are recycled from sphingolipids and glycosphingolipids [82]. *Leishmania* parasites express inositol phosphosphingolipid phospholipase C-like (ISCL), an enzyme that carries a promiscuous degrading activity for sphingomyelin from the host, as well as endogenous IPC. This scavenging process predominantly occurs in the intramacrophage amastigote and is believed to be crucial for amastigote survival in the acidic environment, differentiation, and virulence [88,89].

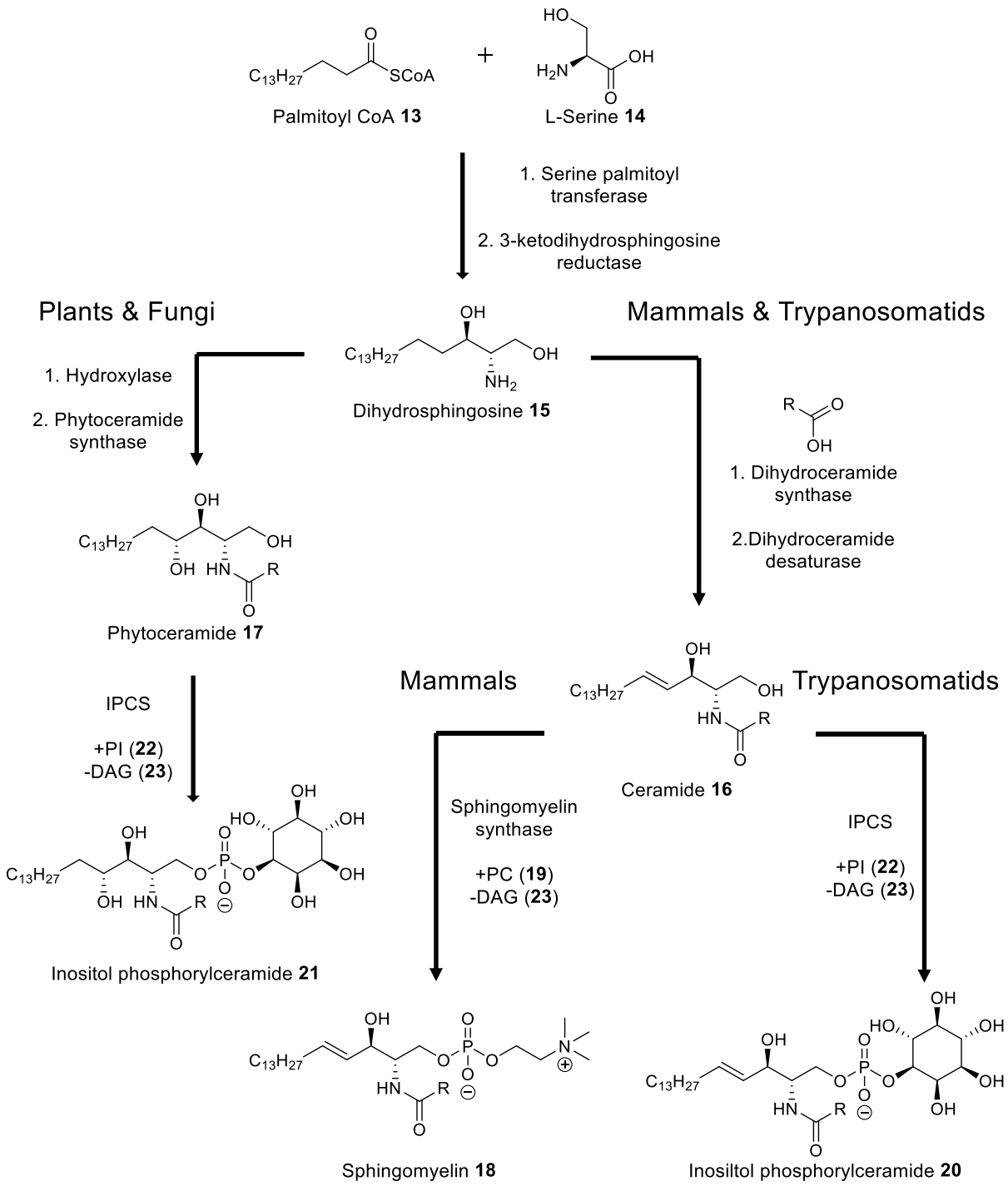

Figure 1.8. *De novo* biosynthetic pathway of sphingolipids

1.5. Previous work on inositol phosphorylceramide synthase

1.5.1. Drug target in fungi

Investigations on the mechanism of action of antifungal aureobasidin A **24** (Figure 1.7) in *Saccharomyces cerevisiae* revealed IPCS as the drug target. The gene

AUR1, named after the natural product, is responsible for the expression of the enzyme [90]. This knowledge allowed for the chemical validation of IPCS as a drug target in pathogenic fungi, such as *Candida albicans* and *Aspergillus spp* [90–92]. Study of lines in which *AUR1* expression was suppressed showed that the yeast could not survive due to ceramide accumulation and indicated that IPCS is essential [92]. Other natural product antifungals, rustmicin/galbanolide A **25** and khafrefungin **26** (Figure 1.7), have also been shown to inhibit fungal IPCS at nanomolar concentration [92].

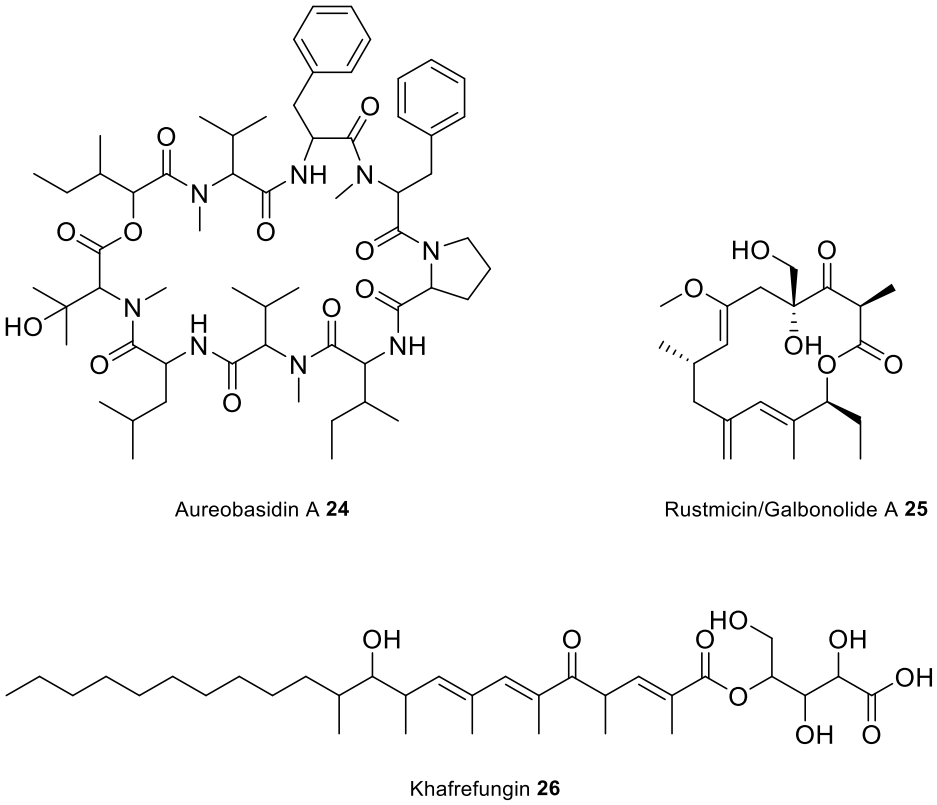

Figure 1.9. Antifungal compounds that target IPCS

1.5.2. Characterisation and function in Leishmania

The gene that encodes the enzyme responsible for the synthesis of IPC **20** in *Leishmania* was identified in 2006 by Denny [88]. The genome sequence of *L. major* was screened using a conserved motif shared by three enzymes: lipid phosphate phosphatase (LPP), fungal IPCS, and mammalian sphingomyelin synthase. A single-

copy gene with unknown function (*Lmj*IPCS) was identified to encode a putative membrane-bound protein of 38kDa and 338 amino acids. *Lmj*IPCS has been predicted to have six transmembrane domains.

As seen in both the fungal IPCS and animal sphingomyelin synthase, the kinetoplastid orthologues have a conserved catalytic triad composed of two histidine (His264 and His220) and one aspartate (Asp268) residues. These are postulated to be oriented towards the lumen of the Golgi apparatus [88]. The enzyme is conserved across *Leishmania* species as well as *Trypanosoma*, with a sequence identity of 48% for *T. cruzi* and 41% for *T. brucei* (Figure 1.10). The same catalytic triad is present in human sphingomyelin synthases, however the identity is only 25% with respect to the *Lmj*IPCS (Figure 1.10).

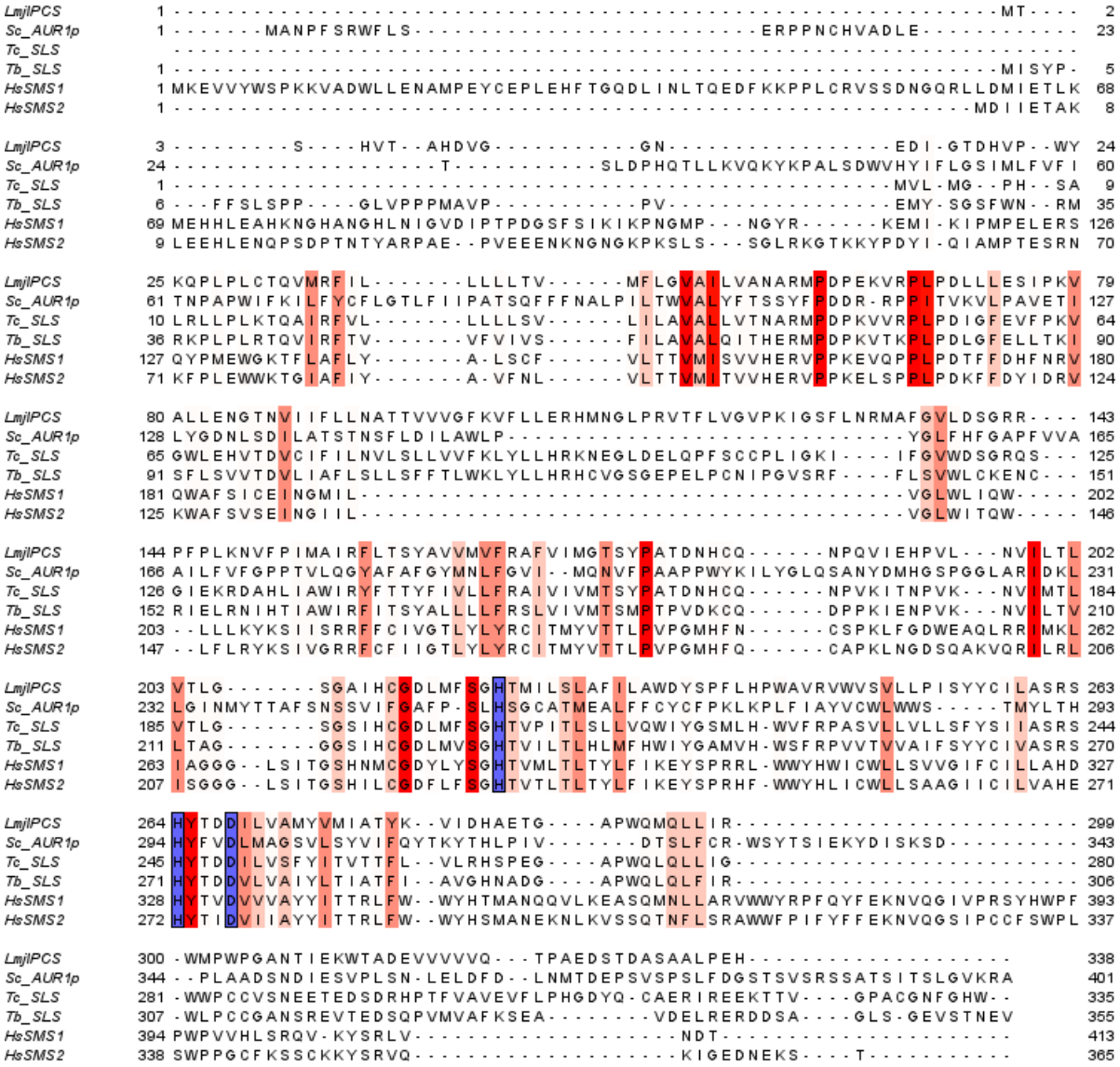

Figure 1.10. Alignment of sphingolipid synthases protein sequences of different species using Clustal Omega. *Lmj*IPCS: *L. major* IPCS (E9AFX2); *Tc*_SLS: Sc_AUR1p: *S. cerevisiae* IPCS; *T. cruzi* sphingolipid synthase (PBJ73426); *Tb*_SLS: *T. brucei* sphingolipid synthase (B3A0L9); *Hs*SMS1: human sphingomyelin synthase 1 (accession Q86VZ5); HsSMS2: human sphingomyelin synthase 2 (accession Q8NHU3). Residues that are similar across species are highlighted in shades of red, in which the strongest the colour, the more similar the sequences. In purple are highlighted the conserved residues that compose the catalytic triad.

After expression in *S. cerevisiae*, the *Lmj*IPCS was found to be responsible for the conversion of ceramide into IPC **20** [88,93]. Subsequently, Mina *et al* developed a yeast extract-based cell-free assay for further biochemical characterisation of the

enzyme [93,94]. The assay consisted in using a *S. cerevisiae* mutant strain expressing *Lmj*IPCS, from which microsomal membranes enriched with the enzyme were purified and confirmed to retain enzymatic activity. The enzyme mediates both the removal of phosphoinositol from PI **22**, producing DAG **23** in the process, and the subsequent conversion of ceramide into IPC **20**. Therefore, it was concluded that the biochemical mechanism occurs via a double displacement or ping-pong bi-bi mechanism (Figure 1.9).

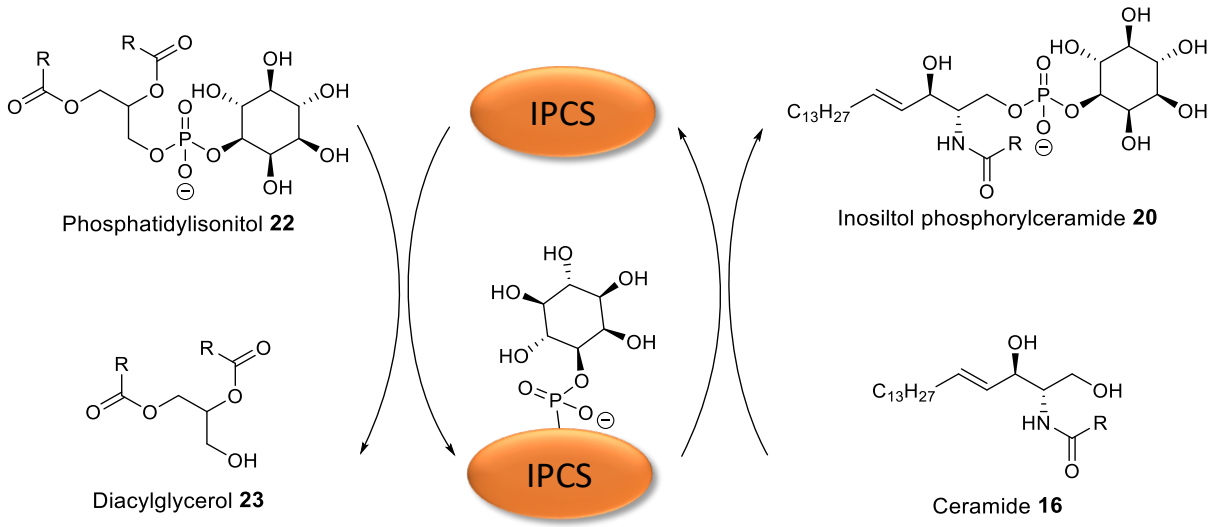

Figure 1.11. Mechanism of action of IPCS in *Leishmania spp*

The catalytic triad is responsible for the nucleophilic attack on the lipid phosphate ester, transferring the phosphoinositol group from PI **22** to ceramide **16**, thus producing IPC **20** and DAG **23** (Figure 1.10) [95]. The enzymatic activity modulates the intracellular levels of both ceramide **16** and DAG **23**, which display antagonistic effects. Ceramide **12** is classically known as a pro-apoptotic cell signal, whilst DAG **23** displays functions as a mitogenic second messenger [95].

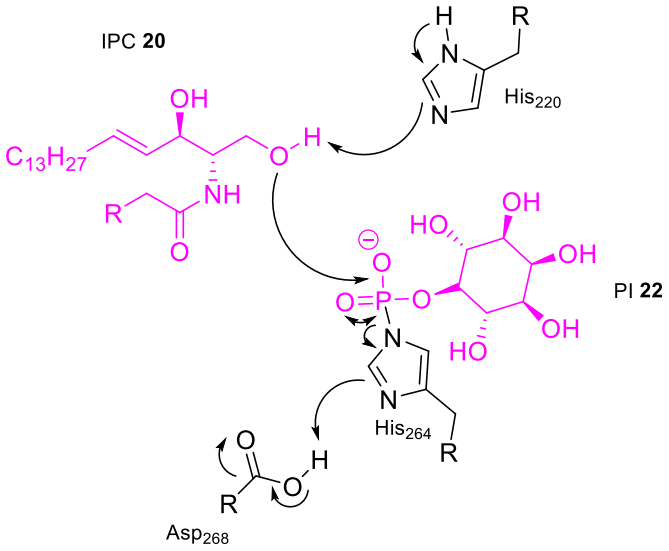

Figure 1.12. Mechanism of action of the IPCS catalytic triad in kinetoplastids. Pink, enzyme substrates; black, amino acids of the catalytic triad.

1.5.3. Drug target in Leishmania

Denny *et al* characterised and first proposed *Lmj*IPCS as a potential drug target showing that the enzyme activity could be inhibited by aureobasidin A [88]. Later, with the Steel group, a high-throughput phenotypic screen of 1.8 million compounds was performed using a *Lmj*IPCS dependent *S. cerevisiae* strain [96]. As a result, 5 hit compounds were found, of which 2 were confirmed to have IPCS as their molecular target. Hit-to-lead optimisation of these molecules represents ongoing work in the group. This work suggested that *Lmj*IPCS is a promising antileishmanial drug target.

In parallel to this program, a library comprising 1040 pharmacologically active compounds from the National Institute of Neurological Disorders and Stroke (NINDS) was screened against *Lmj*IPCS-enriched microsomes, using the yeast-based cell-free assay mentioned previously [97]. As a result, clemastine fumarate **27** (Figure 1.11), a first-generation antihistamine used to treat allergy symptoms, was identified as the most potent inhibitor of IPCS, with an IC_{50} of 3.06 µM. Further studies showed it to be pan-active across species against both promastigotes and intracellular amastigotes.

Subsequently, *in vivo* activity was assessed in BALB/c mice infected with *L. amazonensis.* Treatment was effective when clemastine fumarate **27** was administered intralesionally or intraperitoneally. Polypharmacology was later confirmed after *in vivo* and *in vitro* assays, which confirmed that clemastine **27** can sensitise immune cells to a more pro-inflammatory state, potentially enhancing parasite clearing. A library of analogues was synthesised by Brown and Charlton [98,99]. Amongst the compounds prepared was (S, R)-157 (Figure 1.11), which showed comparable activity *in vitro* and efficacious activity *in vivo* when compared to clemastine **27**. Further optimisation and biological characterisation of this structure represents ongoing activity in the group.

On a second independent project, Uliana and co-workers showed the antileishmanial potential of tamoxifen **28** (Figure 1.11), a selective estrogen receptor modulator (SERM) used in the treatment and prevention of estrogen-dependent breast cancer since the 1970s [100–103]. Tamoxifen **28** displays single digit-micromolar activity against intramacrophage amastigotes of several *Leishmania* species and cleared infections *in vivo* [104]. In promastigotes, tamoxifen **28** acts in the sphingolipid biosynthetic pathway, reducing intracellular content of PI **22** and IPC **20**. After these findings, subsequent work has shown that tamoxifen inhibits IPCS with an IC_{50} of 8.5 µM [105].

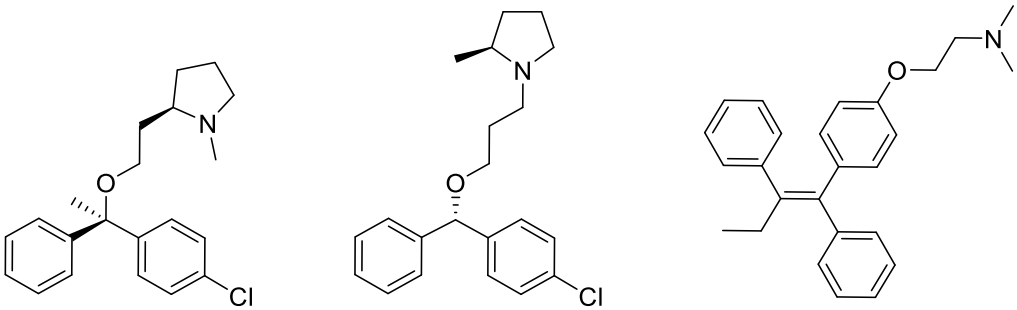

Clemastine **27** (*S, R*)-157 Tamoxifen **28**

Figure 1.13. Clemastine and its analogue (*S, R*)-157, and tamoxifen.

Although these data support the premise that IPCS is a promising drug target for the development of antileishmanials, recent findings by Kuhlmann *et al* suggest the opposite [89]. In their work, an *Lmj*IPCS null mutant line obtained by homologous recombination was not only viable but also more virulent in animal infections than the parental strain. Notably, intramacrophage amastigotes were able to scavenge sphingomyelin from the host, the synthesis of which remained unaltered. Thus, Kuhlmann proposed that incorporation of sphingomyelin by the parasite renders *Lmj*IPCS and IPC production redundant [89].

However, previously, Denny showed that SPT activity was absent in metacyclic promastigotes and amastigotes, suggesting that *de novo* sphingolipid synthesis is a stage-regulated process and present mostly in procyclic promastigotes [85]. For that reason, the scavenging of host ceramides (via sphingomyelin degradation for example) was proposed as a source for the parasite to produce IPC via *Lmj*IPCS independently of *de novo* ceramide synthesis. Recently, Denny's group has been able to generate an *L. mexicana* IPCS knockout line using CRISPR/Cas9 strategy (*Lmx*IPCS-/-, data unpublished). Preliminary data indicated that parasites can be normally cultured as promastigotes, but transformation into axenic amastigotes is impaired. *In vivo* infections by mutant lines led to smaller lesions but most importantly to lower parasite burden, indicating the importance of *Lmx*IPCS for parasite virulence.

Altogether, these recent findings raise a debate on whether IPCS is a tractable drug target or not. Genetic approaches used both by Denny's and Beverley's groups strongly suggest IPCS as non-essential. However, drug discovery programs selecting for IPCS inhibitors have so far successfully resulted in molecules with promising antileishmanial activity.

Kuhlmann's findings, for instance, lacks comparative genomic sequencing between the parental and mutant lines, which could provide insights on potential compensatory mechanisms by the parasite. When using homologous recombination to knockout the catalytic LCB2 subunit of SPT in *L. major* (*Lmj*LCB2), Denny concluded that the gene was non-essential considering that cells lacking this enzyme were viable both *in vitro* and *in vivo* [85]. However, it was later found that other areas of the parasite genome were also disrupted in a non-targeted way [106]. Further investigations using CRISPR/Cas9 technology in *L. mexicana* showed that mutation of LCB2 alone could not be achieved, suggesting its essentiality. Interestingly, viable parasites could only be selected when a putative ABC3A transporter, shown to be lost in the *Lmj*LCB2 knockout, was simultaneously knocked out [106]. Like the *Lmj*IPCS knockout line obtained by Kuhlmann, this *Lmj*ILCB2 ablated line was produced using a homologous recombination methodology relying on two rounds of drug selections of 4-6 weeks each. It was then hypothesized that loss of the putative ABC3A transporter represented a compensatory gene deletion, selected for in an *in vitro* environment and leading to a parasite that was sphingolipid-free but not singularly deficient in LCB2 expression. More refined technology, such as CRISPR/Cas9 and next-generation sequencing has allowed for in depth analysis of *Leishmania* mutant lines generated using classic techniques, revealing flaws that could mislead conclusions. For that reason, more in depth genomic analysis of the lines used by Kuhlmann is recommended.

Finally, enzyme essentiality does not always translate into druggability, and *vice-versa*. Compensatory mechanisms will unlikely take place in a drug treatment context, where conditions for parasite survival are harsher and selective pressure is higher. Thus, inhibition of IPCS in *Leishmania* could still represent a promising drug

target as well as an alternative approach for safe chemotherapies, considering its absence in the host.

2. Hypothesis and project aims

Analysis of the structure of clemastine and tamoxifen highlighted two chemical features that are shared between these molecules: an aminoalkoxy side chain (head group) and a diaryl system (scaffold) (Figure 2.1). It was hypothesised that these features contribute to their antileishmanial activity. The overall aim of this project was to exploit the similarities between clemastine and tamoxifen, and improve their antileishmanial activity by combining them in hybrid molecules.

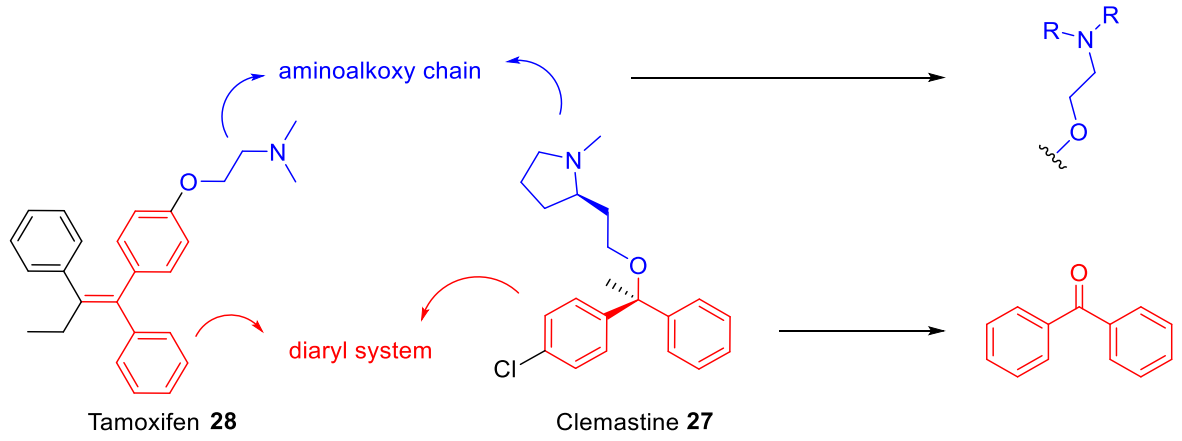

Figure 2.1. Highlight of clemastine and tamoxifen common structural features.

Together, the diaryl ethene from tamoxifen and the diaryl carbinol from clemastine give a benzophenone. Besides being commonly used as a drug scaffold, benzophenones are applied in photoaffinity labelling experiments, which are important for the investigation of the mechanism of action by chemical proteomics. Combining these ideas led to the specific aims listed below:

- To design and synthesise a library of clemastine/tamoxifen hybrid molecules;
- To evaluate antileishmanial activity *in vitro* against promastigotes and intracellular amastigotes;
- To determine cytotoxicity *in vitro* of molecules against relevant cell lines and primary cells;

- To establish the structure-activity relationship (SAR) of hybrid compounds against *Leishmania*;
- To design and synthesise a chemical probe for the investigation of molecular targets by chemical proteomics.

3. Clemastine/tamoxifen hybrids

3.1. Introduction

This section will describe the synthesis of a library of clemastine/tamoxifen hybrid molecules, as well as their antileishmanial testing. For simplification, both parent and chimera molecules generated will be divided into two parts: the scaffold, formed by the diaryl system, and the head group, composed by the aminoalkoxy chain. Once synthesised, the library underwent preliminary *in vitro* screening against *L. major* promastigotes, which was used to guide the synthesis of the library.

3.2. Primary design and synthesis

The first series of molecules addressed were based on the clemastine structure (Figure 3.1), in which the aminoalkoxy chain is a benzyl ether. Clemastine shows the highest antileishmanial activity of the two parent molecules, hence the choice. Analysis of a clemastine-like hybrid led to two derivatives varying in the position of the aminoalkoxy chain. Derivative B was more synthetically accessible due to having two di-substituted aromatic rings, against a tri-substituted aromatic ring in derivative A. For that reason, efforts were focused on synthesising derivative B.

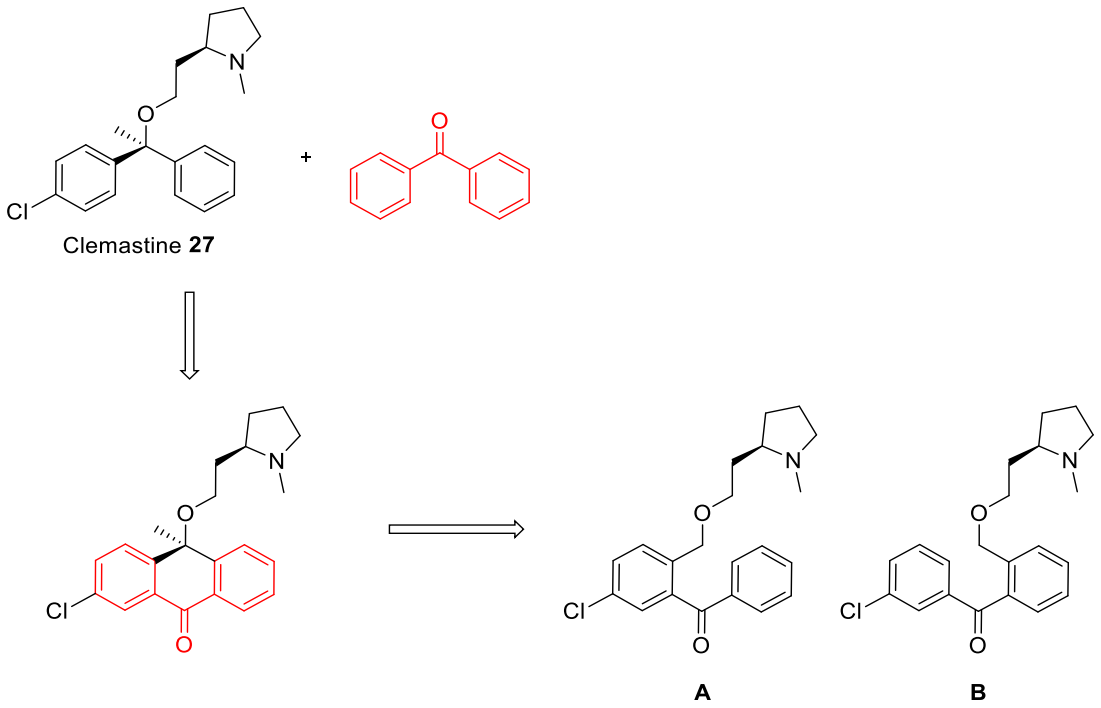

Figure 3.1. Clemastine-derived hybrids.

Retrosynthetic analysis of derivative B identified commercially available 3-chlorobenzaldehyde **29** as the precursor for ring A (Figure 2.2). To form ring B, the key elements are a coupling between the alcohol head group and 2-bromobenzyl bromide **30**.

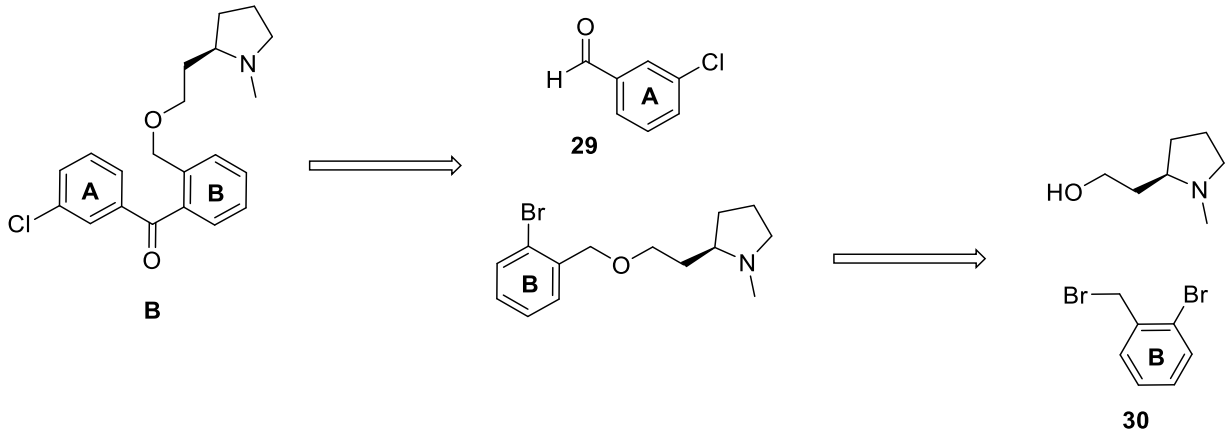

Figure 3.2. Retrosynthetic analysis of derivative B.

Given that the clemastine head group is a more expensive molecule with a laborious synthesis, it was decided that the synthetic route and reaction conditions would be tested with dimethylaminoethanol **31** instead. This is a commercially available molecule that has interesting relevance, considering it composes tamoxifen's head group.

After deprotonation with NaH, dimethylaminoethanol **31** was reacted with 2-bromobenzyl bromide **30** in the presence of catalytic amount of tert-butylammonium iodide (TBAI) (Figure 3.3). As purification by column chromatography led to low yields, purification by acid/base extraction was used. Amine **32** was obtained in good purity in a final yield of 55%. Formation of **32** was confirmed by LCMS analysis which showed the expected bromine isotope pattern in a 1:1 ratio (m/z = 258 [M(^{79}Br)+H] and m/z = 260 [M(^{81}Br)+H]), consistent with the loss of one bromine atom during the reaction.

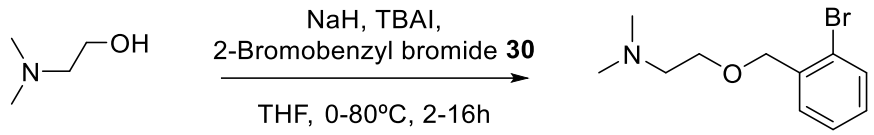

31 **32** (55%)

Figure 3.3. Synthesis of amine **30**.

Initial attempts to generate **33** involved lithiatiation of the amine **32** using n-BuLi, followed by reaction with 3-chlorobenzaldehyde **29** (Figure 3.4). However, LCMS analysis indicated that the expected product mass ([M+H]$^+$=320 m/z) was not formed. Instead, major peak showed a 1:1 ratio of 258 and 260 m/z, suggesting that the starting material was not consumed.

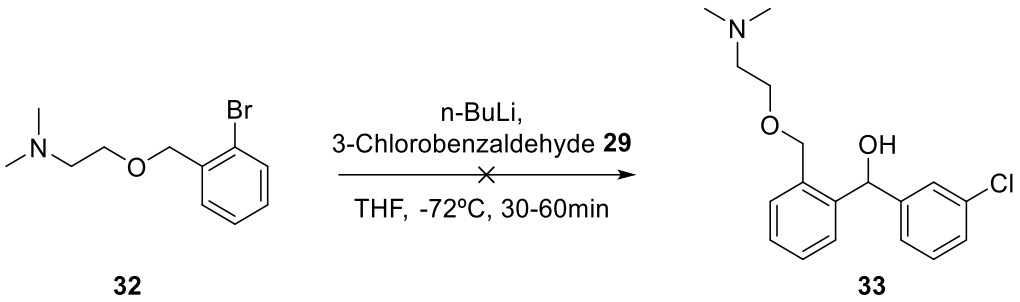

32 **33**

Figure 3.4. Lithiation of amine **32** and synthesis of ether **33**

As all attempts to address this problem were not successful, an alternative strategy to build the benzophenone component that could be coupled with different head groups was designed. Using disconnection analysis, 2-bromobenzyl alcohol **34** and 3-chlorobenzaldehyde **29** were identified as suitable starting materials (Figure 3.5).

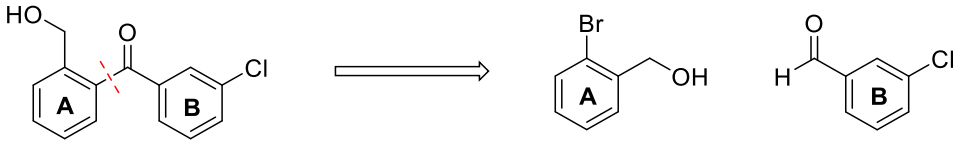

34 **29**

Figure 3.5. Retrosynthetic analysis of benzophenone scaffold.

First, the alcohol **34** was protected with TBDMS-chloride, successfully affording silylether **35** in 93% yield (Figure 3.6). However, all attempts to react this with 3-chlorobenzaldehyde **29** following lithiation by nBuLi failed and **36** could not be obtained (Figure 3.7). This reaction was repeated several times, using different batches of nBuLi, but none succeeded in forming alcohol **36**.

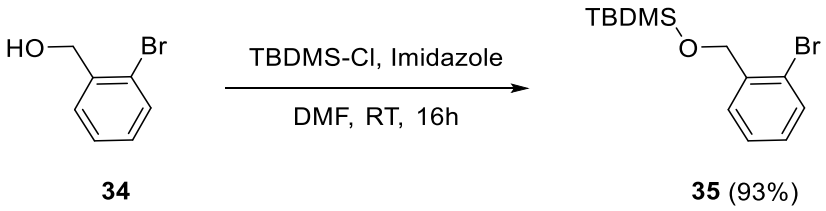

Figure 3.6. Protection of alcohol **34** with TBDMS.

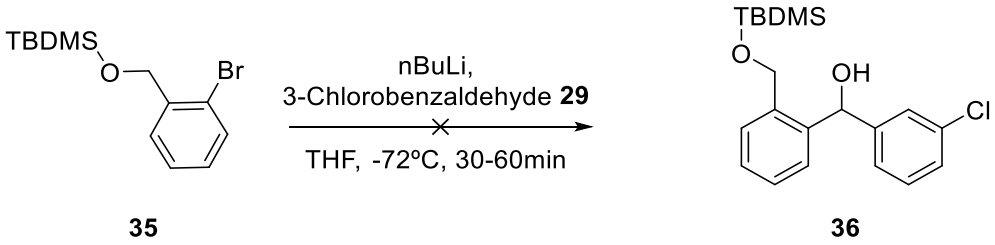

Figure 3.7. Lithiation of **35** and synthesis of alcohol **36**.

Given the difficulties with this strategy, a different approach explored the disconnection between the ketone and ring B in which aldehyde **37** could be combined with the Grignard reagent **38** to form ring B (Figure 3.8). Aldehyde **37** was identified as coming from phthalyl alcohol **39** after selective mono protection as described by Bouton [107] (Figure 3.9). However, whilst the expected mass for the mono-TBDMS-protected diol **40** could be identified by LCMS analysis (m/z = 253 [M+H]), most of the product degraded during workup and purification.

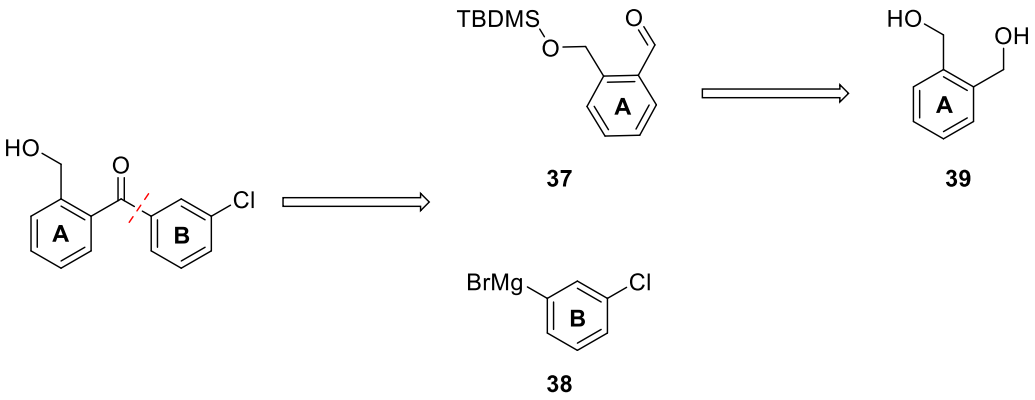

Figure 3.8. Retrosynthetic analysis of benzophenone scaffold.

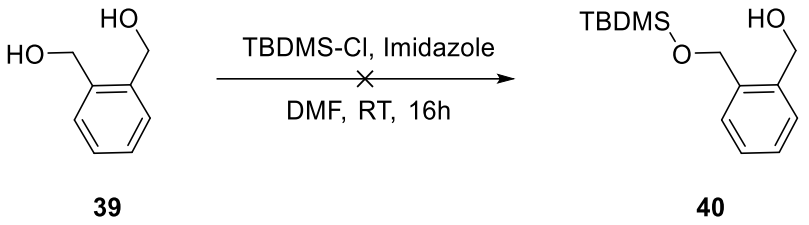

39 **40**

Figure 3.9. Mono-protection of diol **39** with TBDMS.

The reasons why the synthesis of these could not be achieved were not immediately obvious and remain unsolved. Ultimately, given the lack of success, this series was abandoned and other strategies for generating hybrids were explored.

3.3. *Ortho*-phenol ether benzophenones

3.3.1. Synthesis

Analysis of tamoxifen revealed that the head group is a phenol ether instead of a benzylic one (Figure 3.1), which allowed for the design of compound **41**. Retrosynthesis led to commercially available 2-hydroxybenzophenone **42** (Figure 3.10). For simplification, this series of molecules will be referred to as *ortho*-phenol ether benzophenones or *ortho*-BP.

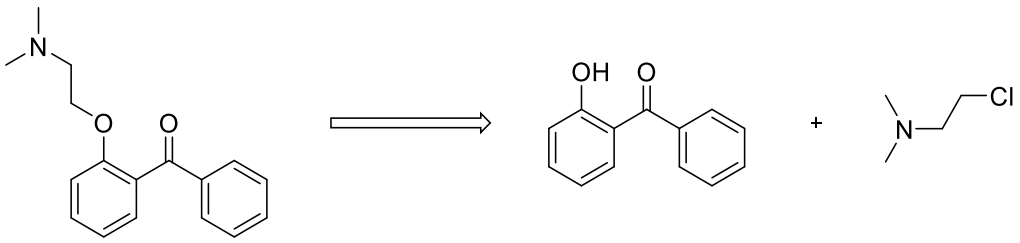

41 **42** **43**

Figure 3.10. Retrosynthetic analysis of analogues **41**.

Using NaH, the phenol was deprotonated and an excess of dimethylaminoethyl chloride hydrochloride **43** added (Figure 3.11). However, after 24 hours, starting materials had not been consumed. Consequently, the reaction was repeated replacing

the solvent by acetone, as well as using catalytic amounts of potassium iodide (KI) and potassium carbonate (K_2CO_3) as the base, as described previously by Santos *et al* [108] (Figure 3.12). Ether **44** was successfully obtained in 32% yield in sufficient purity for biological testing. Confirmation of the structure was obtained from the LCMS analysis, which showed the expected molecular ion (m/z 270 $[M+H]^+$). Further supporting evidence was gained from analysis at the ^1H NMR which confirmed loss of characteristic phenol peak at δ 12 ppm.

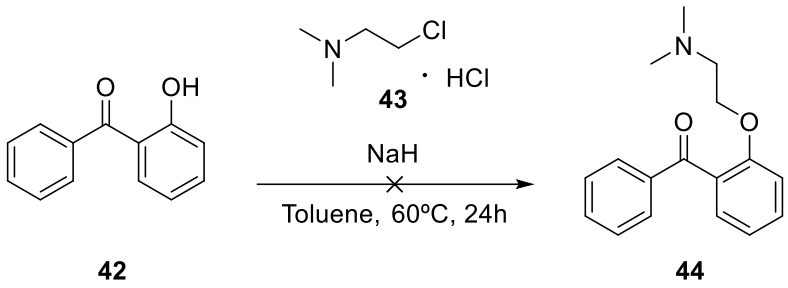

Figure 3.11. Synthesis of ether **44**.

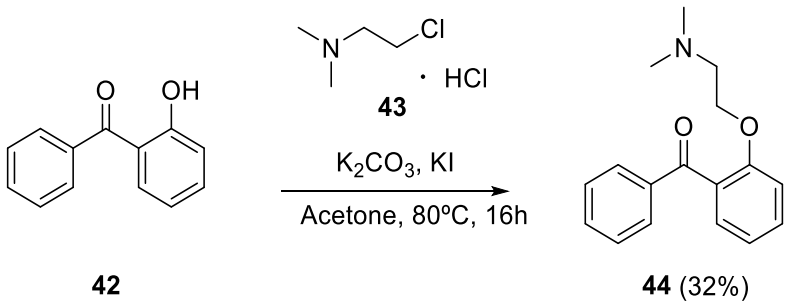

Figure 3.12. Synthesis of ether **44** following protocol described by Santos *et al* [108].

Further optimisation replacing the acetone solvent for DMF, and using a more soluble base (Cs_2CO_3) and catalyst (TBAI) allowed for an improved yield of 71% to be obtained using dimethylaminopropyl chloride hydrochloride **45** (Figure 3.13).

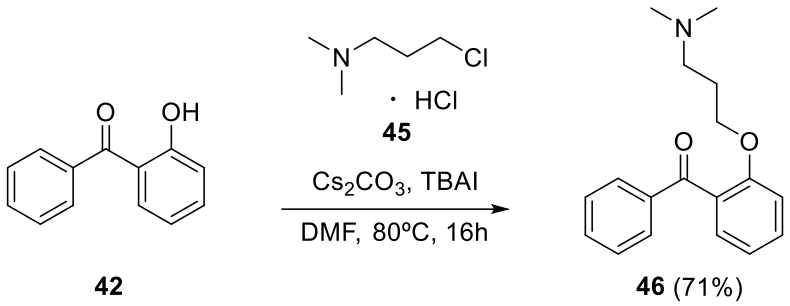

Figure 3.13. Synthesis of **46** using optimised protocol.

As final compounds were formed after a one-step route, in a state pure enough for biological testing, further optimisation of reaction conditions was not explored. These conditions were then applied to further combinations between 2-hydroxy-5-chlorobenzophenone **47** and dimethylamine head groups that were 2 and 3 carbon-long (Figure 3.14).

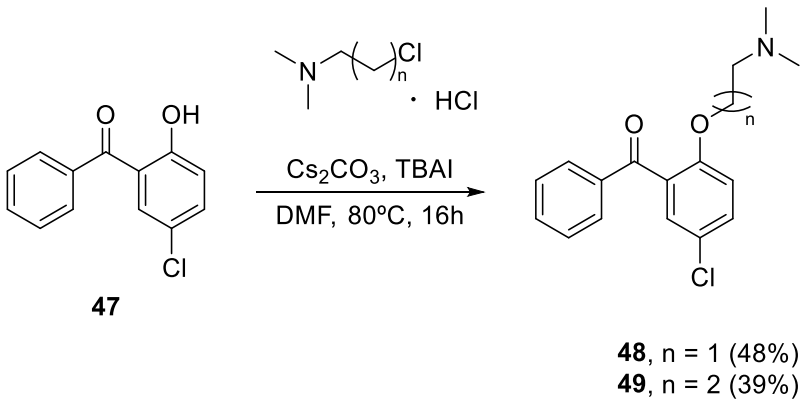

Figure 3.14. Synthesis of analogues **48** and **49**.

To obtain analogue **50**, clemastine head group was first synthesised following the procedure described by Fournier *et al* [109](Figure 3.15). The first steps involved the protection of D-proline **51** with benzyl chloroformate (Cbz). The carboxylic acid **52a/52b** was then converted into a diazoketone **53a/53b**, which was verified by the presence of a signal for the *C**H**N*$_2$ proton in the ^{1}H NMR spectrum at δ 5.47 ppm and δ 5.25 ppm, characteristic of rotamer mixture. The diazoketone **53a/53b** underwent

Wolff-rearrangement after treatment with silver benzoate, leading to homologation of the carbon chain. This rearrangement afforded the methyl ester **54a/54b** which was characterized by the appearance of a signal for *CH₃* group at ^{1}H NMR spectrum at δ 3.64 ppm.

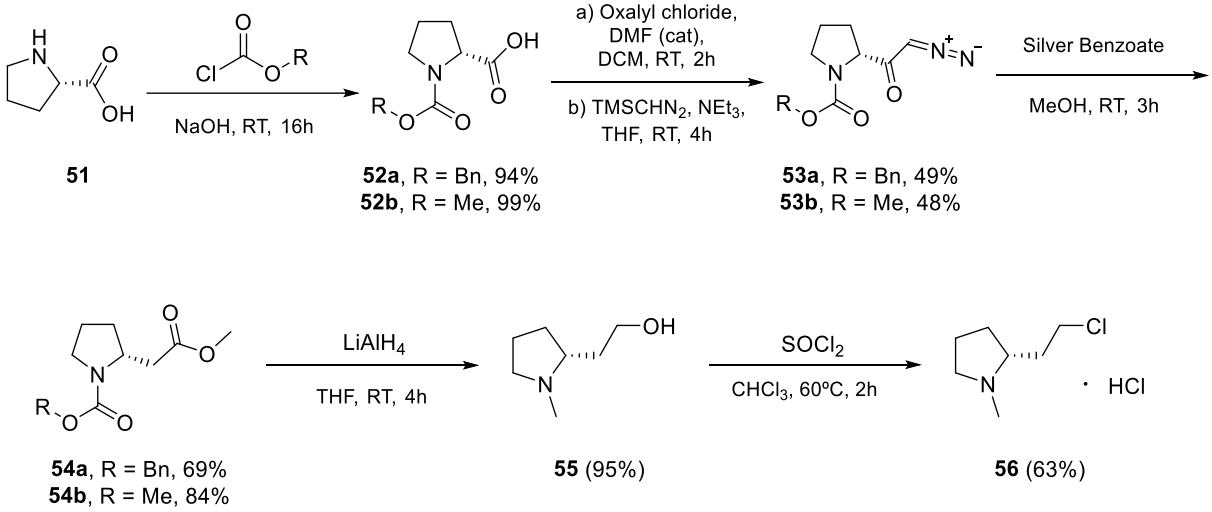

Figure 3.15. Synthesis of clemastine headgroup following Fournier *et al* [109] protocol.

Attempts to reduce the ester **54a** with $LiAlH_4$ afforded benzyl alcohol **57** as a by-product as well as the desired alcohol **55** in a 1:1 ratio, according to ^{1}H NMR analysis (Figure 3.16). Due to difficulties in separating these two compounds, the alternative ester **54b** was prepared using methyl chloroformate when protecting amine **51**. This procedure benefits from production of methanol **58** following reduction of methyl ester **54b**, cleanly affording alcohol **55** in 95% yield (Figure 3.16). The structure of the alcohol **55** was confirmed at ^{1}H NMR analysis by the appearance of a methyl group at δ 2.38 ppm, and the loss of carbonyl signals in ^{13}C NMR at δ 171.8 (**C**O_2CH_3) and δ 155.34 (N**C**O_2). The alcohol **55** was then treated with thionyl chloride to afford the head group **56** with an overall yield of 26% (Figure 3.15). LCMS analysis confirmed the chlorination by expected chlorine isotope pattern in a 3:1 ratio (m/z = 148 [M(^{35}Cl)+H] and m/z = 150 [M(^{37}Cl)+H]).

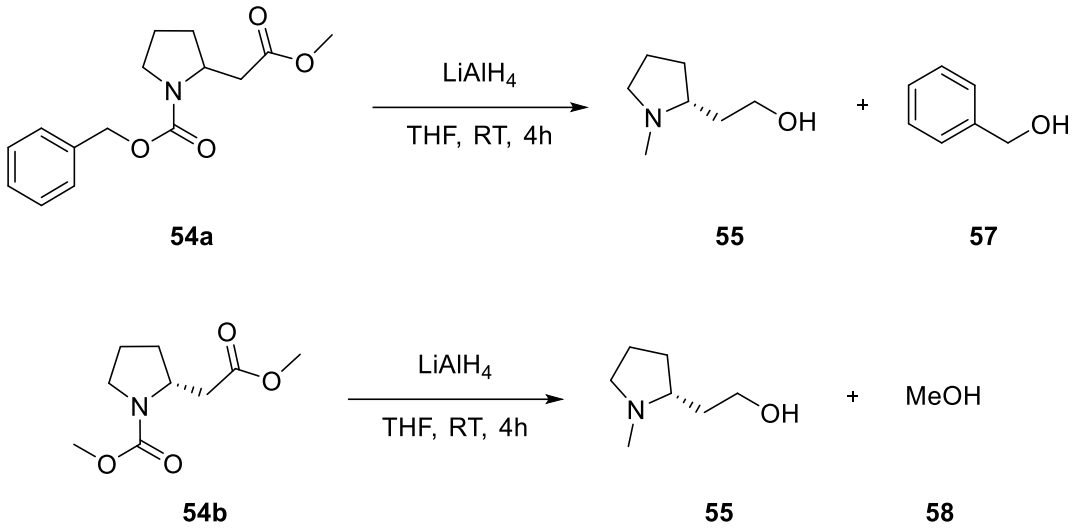

Figure 3.16. Reduction of methyl ester **54a/54b** with $LiAlH_4$ to obtain alcohol **55**.

Reaction of head group **56** with 2-hydroxybenzophenone **42** afforded an azepane isomer by-product that was inseparable by both normal- and reversed-phase chromatography. This has been reported by Fournier et al [109] and is hypothesized to be formed through an intramolecular S_N2 reaction that leads to the formation of a reactive bicyclic cation (Figure 3.17). For that reason, the alcohol **55** was alternatively reacted with 2-fluorobenzophenone **59** in a S_NAr fashion to afford analogue **60** in 26% (Figure 3.18).

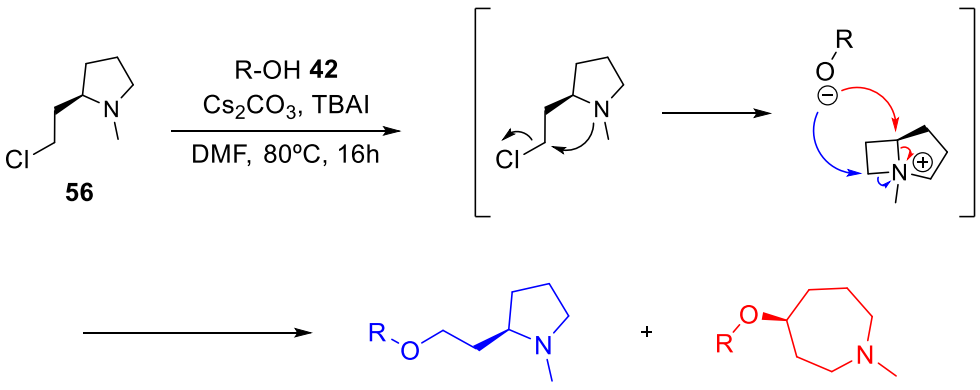

Figure 3.17. Bicyclic cation as the intermediate of etherification. Colours indicate the products generated upon each nucleophilic attack.

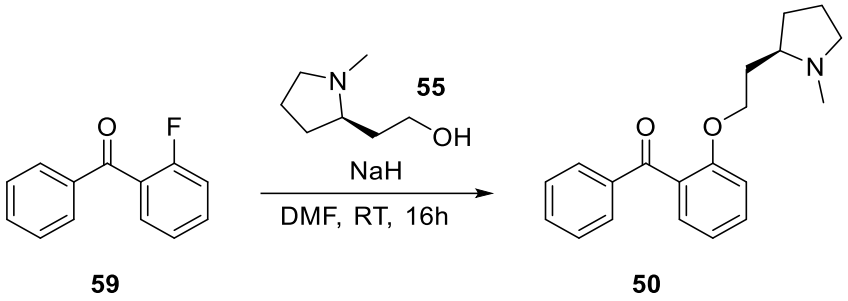

Figure 3.18. Synthesis of analogue **50**.

Considering the time-consuming synthesis and costs of making the clemastine head group, together with the low antileishmanial activity of analogue **50** (see section 3.3.2), the synthesis of more variants using this head group was discouraged. In our group, Charlton had generated several clemastine analogues of which compound (S, R)-157 was the most promising one [98]. This analogue contained an *N*-linked 2R-methylpyrrolidine group instead of the C-linked pyrrolidine present in Clemastine (Figure 1.13). This head group is more easily accessible synthetically, and analogue (S, R)-157 showed promising antileishmanial activity [98]. This group is also a hybrid between the head group of clemastine and tamoxifen, considering the combination of tamoxifen's *N*-linked alkoxy chain with clemastine's methyl-pyrrolidine ring, which fits the concept of this project. Therefore, analogues containing this group were targeted instead of clemastine's head group.

The route chosen was slightly different to account for the cost of the required reagent (2*R*)-methylpyrrolidine hydrochloride. Firstly, 2-hydroxy-5-chlorobenzophenone **47** was coupled with excess 1,3-Dibromopropane **48** to give bromoether **61e** (Figure 3.19). The latter was identified by LCMS analysis, which presented a 3:4:1 isotope pattern (m/z = 353 [M(^{79}Br, ^{35}Cl)+H], 355 [M(^{79}Br, ^{37}Cl) + M(^{81}Br, ^{35}Cl)+H], 357 [M(^{81}Br, ^{37}Cl)+H]) corresponding to the presence of both bromine and chlorine atoms. Subsequently, combination with (2*R*)-methylpyrrolidine

hydrochloride **62** afforded target compound **67** in 66% yield (Figure 3.19). This was characterized by LCMS analysis (m/z = 358 [M(^{35}Cl)+H] and m/z = 360 [M(^{37}Cl)+H]), which showed an expected chlorine isotope pattern in a 3:1 ratio, and the loss of the bromine isotope pattern. These conditions were then applied to obtain analogues **63**-**68** (Figure 3.19).

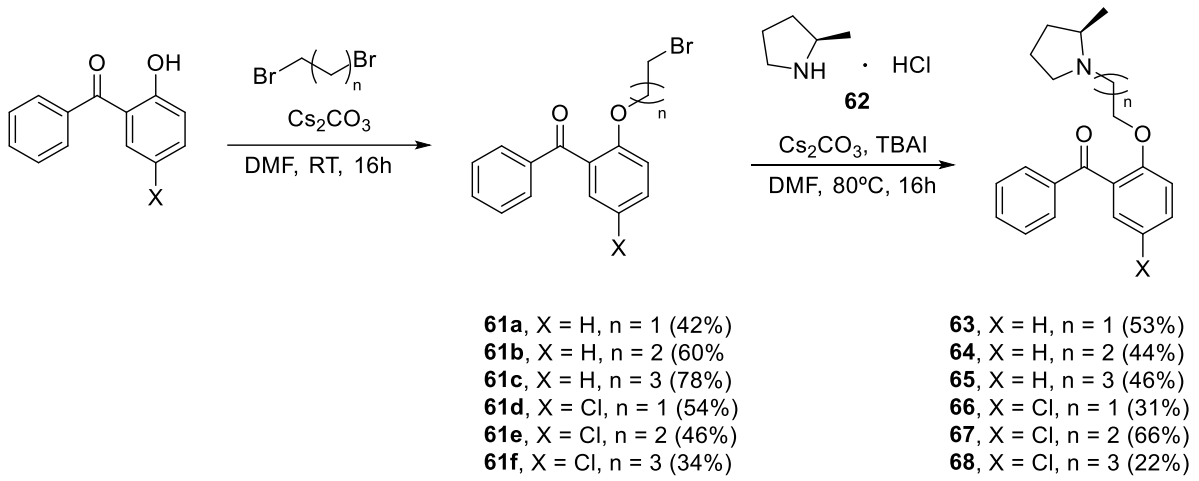

61a, X = H, n = 1 (42%)
61b, X = H, n = 2 (60%
61c, X = H, n = 3 (78%)
61d, X = Cl, n = 1 (54%)
61e, X = Cl, n = 2 (46%)
61f, X = Cl, n = 3 (34%)

63, X = H, n = 1 (53%)
64, X = H, n = 2 (44%)
65, X = H, n = 3 (46%)
66, X = Cl, n = 1 (31%)
67, X = Cl, n = 2 (66%)
68, X = Cl, n = 3 (22%)

Figure 3.19. Synthesis of analogues **63** to **68**.

3.3.2. Screening of ortho-*BP series against* L. major *promastigotes*

This first generation of 11 compounds was tested against *L. major* promastigotes in a dose-response resazurin assay regarding their growth inhibition potential (Figure 3.20). Their EC_{50} values were acquired and used for a preliminary structure-activity relationship (SAR) study. Compounds with EC_{50} > 100 µM were considered inactive.

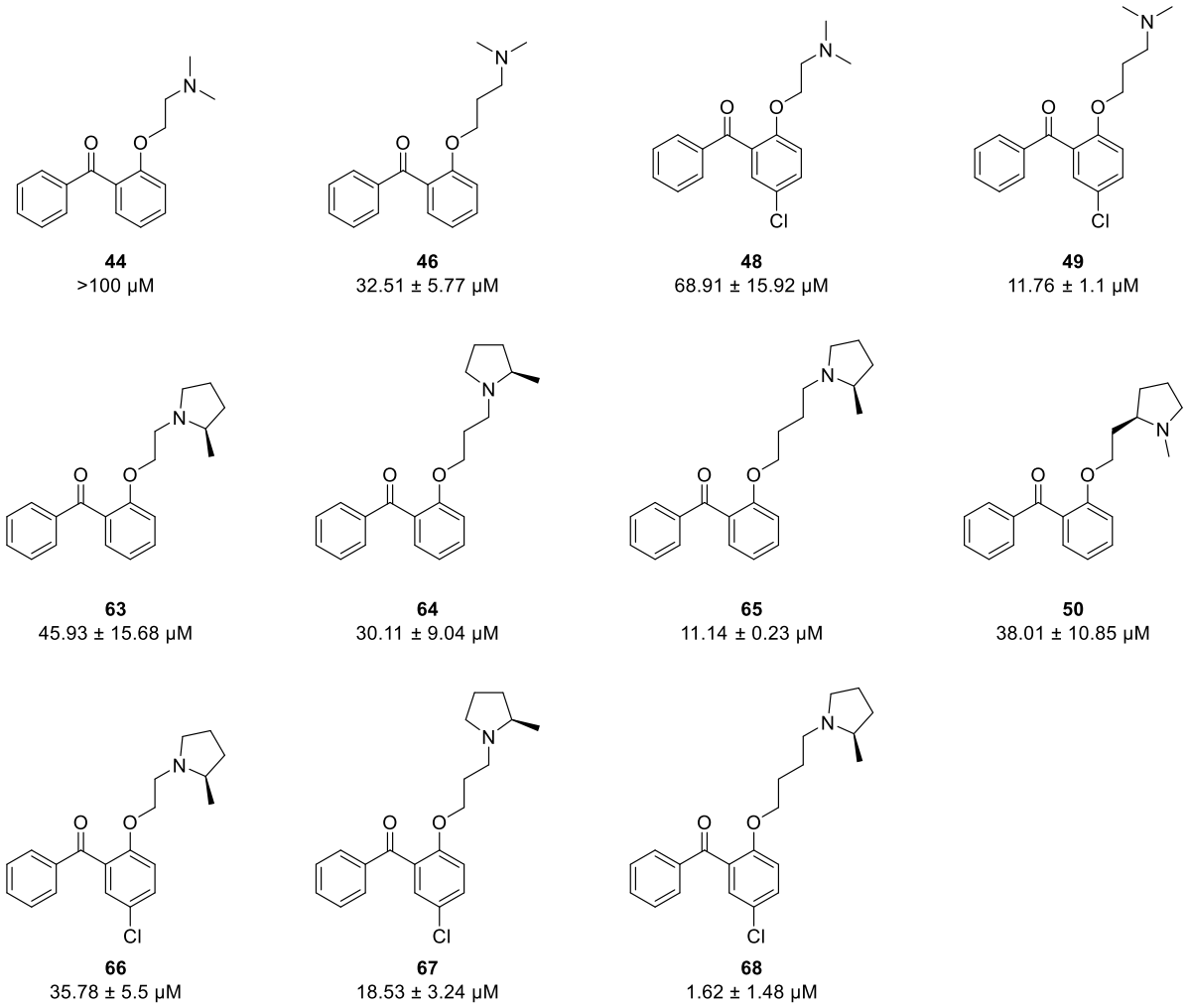

Figure 3.20. EC_{50} values of first generation of clemastine/tamoxifen hybrids against *L. major* promastigotes.

Overall, the antipromastigote activity of *ortho*-BP series was low. Out of 11 compounds, only 4 displayed an EC_{50} below 20 μM. A longer carbon length improved the activity, which was further enhanced in the presence of a chlorine substituent. For example, compound **68** containing a 4-carbon linker unit and a chlorine substituent displayed EC_{50} below 2 μM, and was the most active compound of the series. Analogue **50** displayed activity comparable to analogues **63** and **64**, suggesting that there was no difference in activity between the C-linked and N-linked pyrrolidine-containing analogues. Considering that the synthesis of C-linked analogues required

considerable synthetic effort, hybrids containing this head group were not further explored. Instead, the N-linked pyrrolidine group was selected for further studies. Finally, in the *ortho*-BP series no significant difference in activity was observed between compounds containing pyrrolidine or dimethylamine head groups.

3.4. *Para*-phenol ether benzophenones

3.4.1. Synthesis

In order to access *para*-phenol ether benzophenones and further expand the clemastine/tamoxifen hybrid library, retrosynthetic analysis suggested commercially available starting materials 4-hydroxybenzophenone **69** and 4-chloro-4'-hydroxybenzophenone **70** as suitable (Figure 3.21). The same conditions as described previously were used for the synthesis of ether **71** combining phenol **69** with 2-dimethylaminoethyl chloride hydrochloride **43** (Figure 3.22). The formation of the ether **71** was verified by LCMS analysis, which identified the expected mass (m/z 270 $[M+H]^+$). Analogue **72** was also obtained by applying the same conditions.

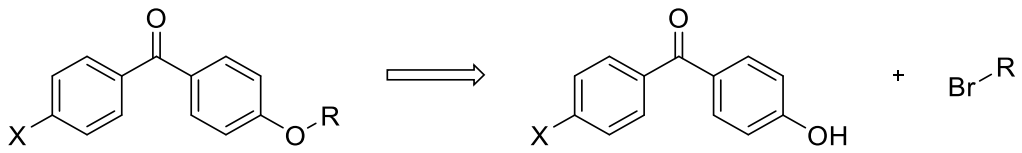

X = H (**69**), Cl (**70**)

Figure 3.21. Retrosynthetic analysis of *para*-phenol ether benzophenones.

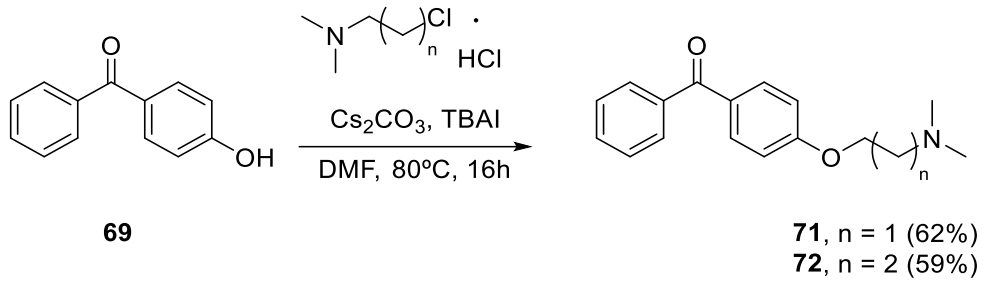

Figure 3.22. Synthesis of analogues **71** and **72**.

To obtain analogue **73**, 4-hydroxybenzophenone **69** was firstly coupled with 1,4-dibromobutane **74** to yield ether **75**. This was followed by reaction with dimethylamine hydrochloride **76** (Figure 3.23). Compound **73** was confirmed by LCMS analysis which identified expected mass (m/z 314 $[M+H]^+$).

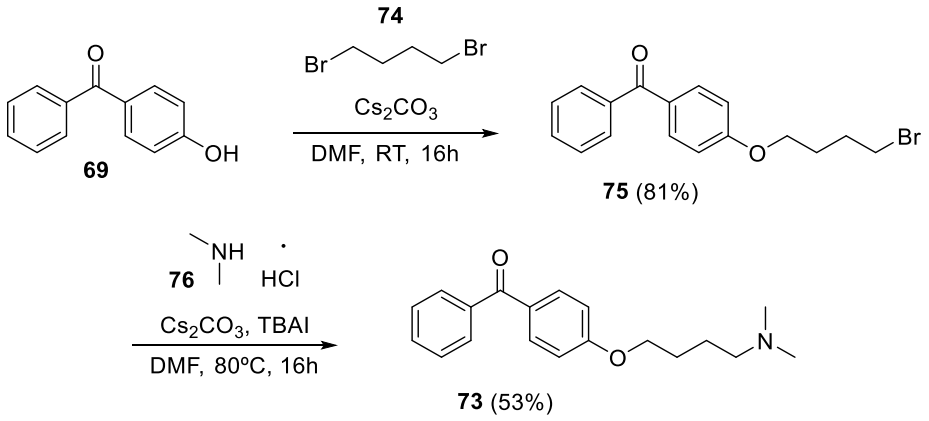

Figure 3.23. Synthesis of analogue **73**.

To obtain analogues **78**-**83**, benzophenones **69** and **70** were combined with a dibromoalkane to form ethers **77**a-f, which were further reacted with (2*R*)-methylpyrrolidine hydrochloride **62** (Figure 3.24). Formation of analogues **78**-**83** were evidenced by LCMS analysis which revealed the loss of bromine isotope pattern.

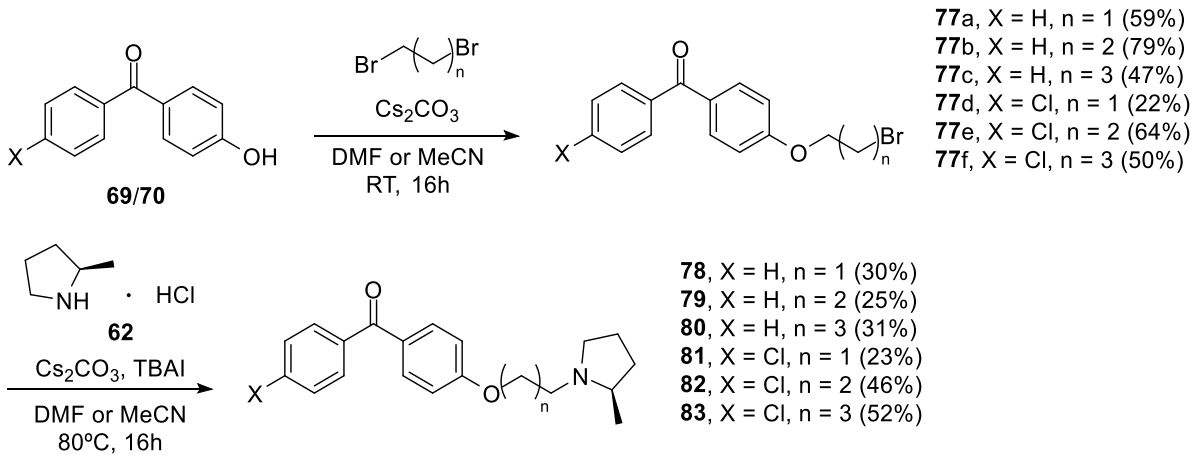

Figure 3.24. Synthesis of analogues **78** to **83**.

To explore the impact of chlorine position on ring A on antileishmanial activity, hydroxybenzophenones **84** and **85** were designed (Figure 3.25). Retrosynthetic analysis gave a chlorobenzoic acid and anisole for starting materials, which would yield the desired product by Friedel-Crafts acylation (Figure 3.25).

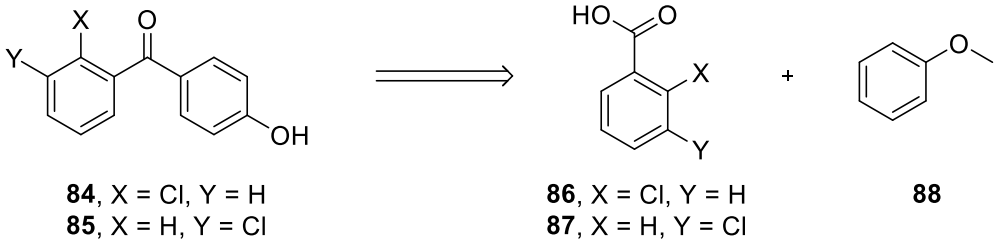

Figure **3.25.** Retrosynthetic analysis of hydroxybenzophenones **84** and **85**.

Firstly, the relevant chlorobenzoic acid was refluxed in thionyl chloride to form an acid chloride, which was reacted with anisole **88** upon the addition of aluminium trichloride to facilitate the Friedel-Crafts acylation and demethylation (Figure 3.26). This reaction yielded the hydroxybenzophenones **84**/**85** in one step. These were confirmed by LCMS spectra, in which the 3:1 isotope pattern for chlorine was observed for the expected mass (m/z 233/235 $[M+H]^+$) for both phenol **84** and phenol **85**. Once obtained, phenols **84** and **85** were reacted with 1,3-dibromopropane **48** to form ethers

89 and **90**, which were further reacted with (R)-2-methylpyrrolidine hydrochloride **62** to afford analogues **91** and **92** (Figure 3.27).

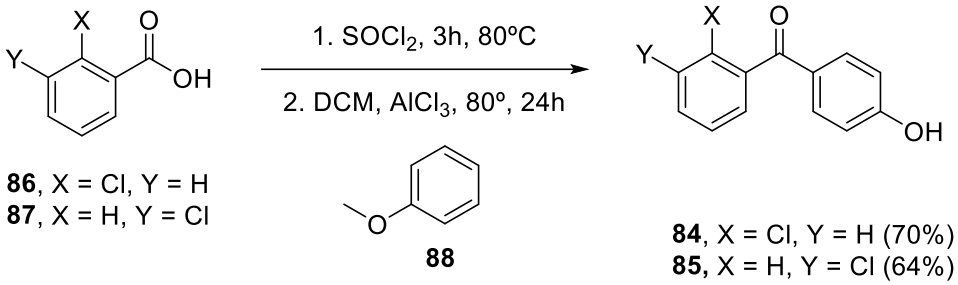

Figure 3.26. Synthesis of hydroxybenzophenones **84** and **85**.

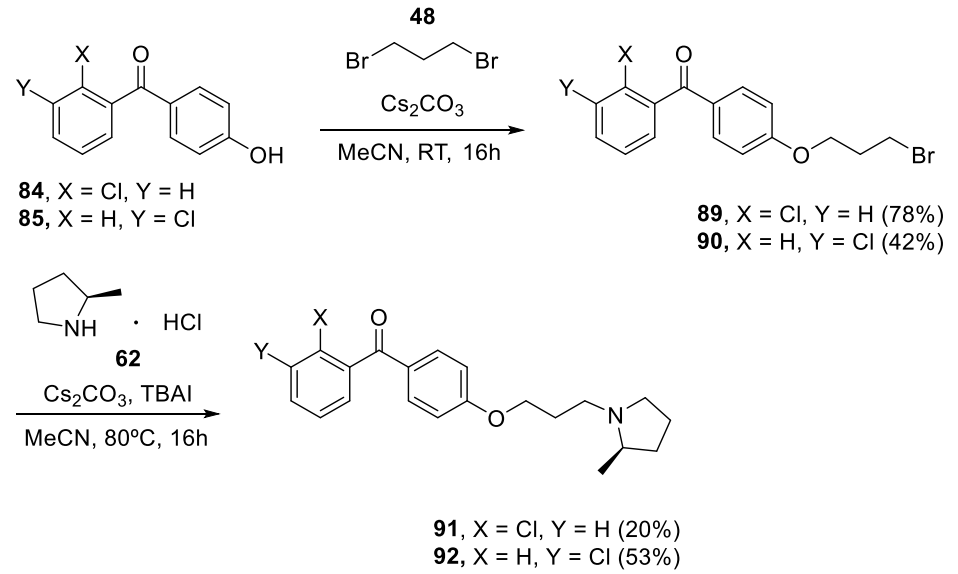

Figure 3.27. Synthesis of analogues **91** and **92**.

3.4.2. Screening of para-*BP series against* L. major *promastigotes*

This second generation of compounds consisting of 11 compounds were screened against *L. major* promastigotes using the same protocols as described for the *ortho*-BP series (Figure 3.28). Compared to the first generation of hybrids, the *para*-BP series showed overall higher activity, with 9 compounds displaying $EC_{50} \leq 5$ µM, which was seen for only compound **68** in the *ortho*-BP series.

For compounds **71**-**73** containing dimethylamine head group, the increase in the carbon linker unit translated to higher activity. However, this was not seen for compounds containing a pyrrolidine head group (**78**-**83**), in which the activity remained the same regardless of carbon chain length. In addition, there was a slight difference of 1.6-2.5x between compounds containing dimethylamine and methylpyrrolidine head groups; compounds **78** and **79** performed better than compounds **71** and **72**, respectively.

The chlorine substituent in compounds **81**-**83** improved the activity approximately 2-fold in relation to their respective analogues **78**-**80**, suggesting that the chlorine substituent contributes to higher antileishmanial activity. Furthermore, the position of the chlorine substituent around ring A also impacted the activity. EC_{50} values against *L. major* were similar when chlorine was in *meta* (**92**) or *para* (**82**) positions, however there was an improvement in activity of 4-5-fold when the substituent was in the *ortho* (**91**) position. Interestingly, when assessed against a second species (*L. amazonensis*), compound **91** showed EC_{50} of 6.77 ± 0.93 μM, suggesting this analogue has no consistent activity across species. In comparison, compounds **82** and **92** were equipotent or slightly more potent against *L. amazonensis* (EC_{50} of 1.56 ± 0.59 μM and 1.14 ± 0.39 μM respectively) compared to *L. major*. For that reason, *ortho*-chlorine-containing hybrids were not further explored.

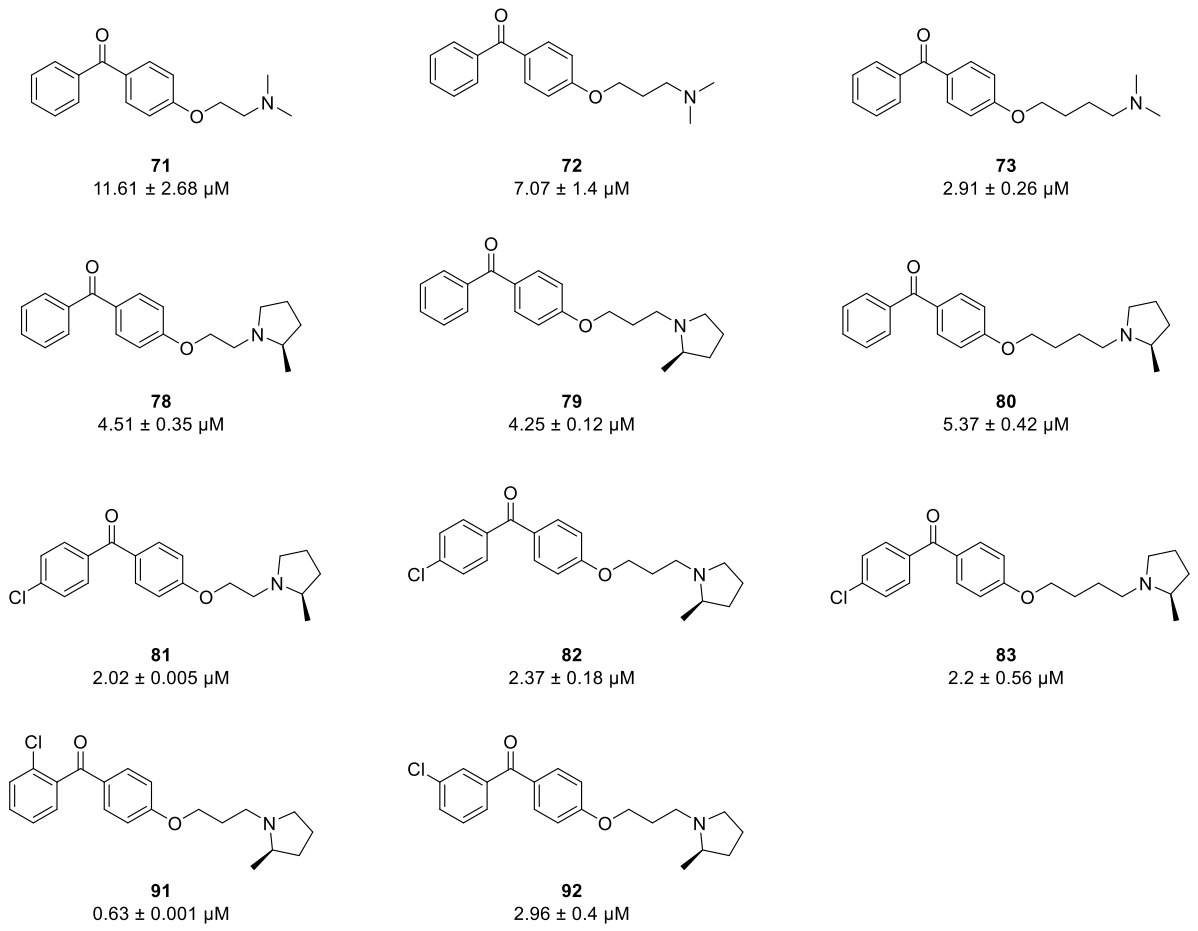

Figure 3.28. EC_{50} values of second generation of clemastine/tamoxifen hybrids against *L. major* promastigotes.

3.5. *Meta*-phenol ether benzophenones

3.5.1. Synthesis

The *para*-BP series displayed an improvement in activity compared to the *ortho*-BP series. In order to explore the library further, a *meta*-phenol ether benzophenone series (*meta*-BP) was synthesised. Given that, overall, methylpyrrolidine-containing analogues displayed higher activity, dimethylamine-containing molecules were not explored in this series. In addition, both analogues **82** and **92** displayed similar

activities against both species of promastigotes, suggesting that the chlorine substituent is tolerated in both *meta* and *para* positions. Considering the better synthetic accessibility of *para* position, substituents were used only in that position.

Commercially available 3-hydroxybenzophenone **93** was used to synthesise hybrids **95**-**97** applying similar conditions to those described above (Figure 3.29). Analogues **98** and **99** were designed to assess simple variations on the pyrrolidine head group. For this, 3-hydroxybenzophenone **93** was combined with either (2*S*)-methylpyrrolidine or 2,2-dimethylpyrrolidine head groups to afford final compounds **95-99** (Figure 3.30).

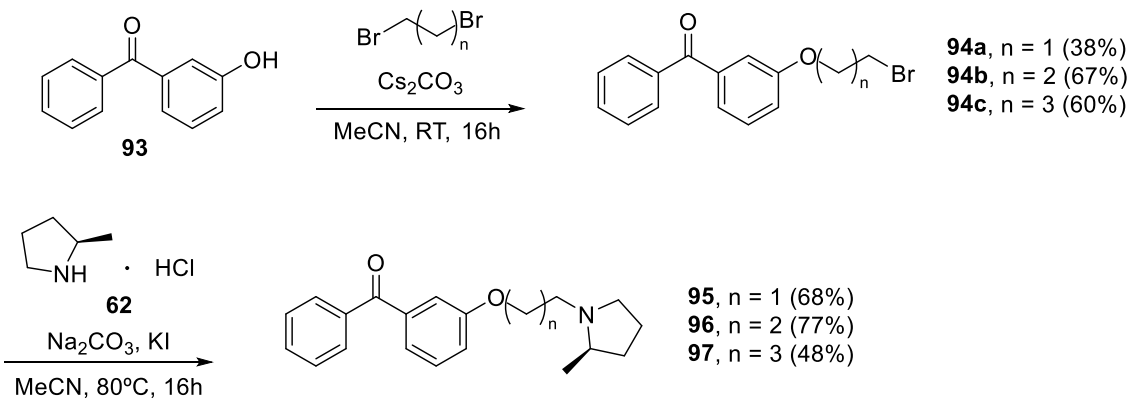

Figure 3.29. Synthesis of analogues **95**-**97**.

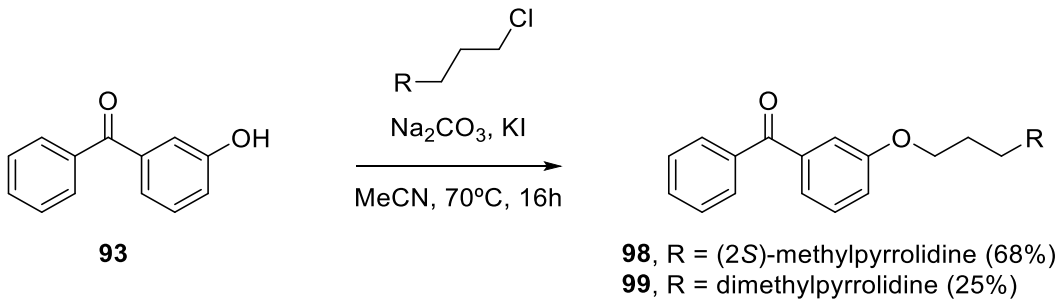

Figure 3.30. Synthesis of analogues **98** and **99**[a].

The proposed chlorine-containing analogues (**109-113**) required access to 4'-chloro-3-hydroxybenzophenone **100**. This could be synthesised using commercially

[a] These analogues were synthesised by Spencer Knight making use of starting materials previously made by the group.

available 3-methoxybenzoic acid **101** and chlorobenzene **102** using similar Friedel-Crafts acylation conditions as described previously (Figure 3.31). In a similar fashion, two other scaffolds were designed replacing the chlorine group with methyl (**112**) and isopropyl (**113**) groups using toluene and cumene instead, respectively (Figure 3.31). A methyl group was chosen to mimic the steric bulk of the chlorine substituent, and the isopropyl was chosen to assess the tolerance of additional steric bulk. These hydroxybenzophenone scaffolds were then used in the synthesis of analogues **109**-**113** (Figure 3.32).

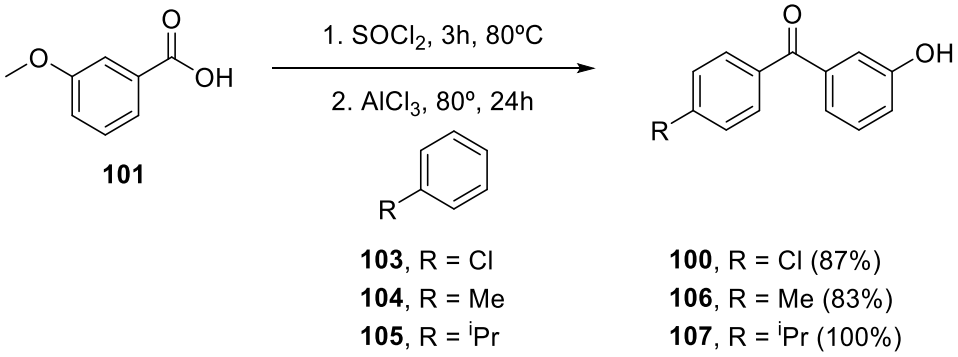

Figure 3.31. Synthesis of hydroxybenzophenones **100**, **106** and **107**.

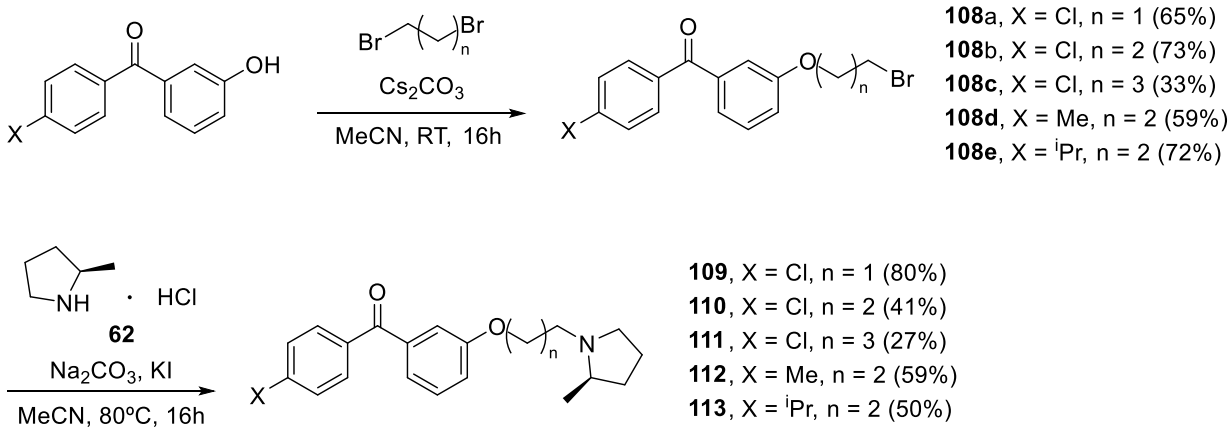

Figure 3.32. Synthesis of analogues **109**-**113**.

3.5.2. Screening of meta-*BP series against* L. major *promastigotes*

The *meta*-BP series of hybrids were assayed against *L. major* promastigotes and were found to be the most active series (Figure 3.33). 6 compounds had EC_{50} ≤ 1 μM and none of the compounds showed EC_{50} above 5 μM. Once again, compounds containing a 3- or 4-carbon linker unit were more active than the respective analogues with a 2-carbon linker.

Interestingly, even though the chlorine substituent improved the activity by approximately 3 to 5-fold (comparing analogue **96** to **110**, and **97** to **111**), molecules **96** and **97** still retained promising activity with an EC_{50} ≤ 2 μM. Substitution of (2*R*)-methylpyrrolidine by its enantiomer (2*S*)-methylpyrrolidine led to loss in activity, however when 2,2-dimethylpyrrolidine was used, the activity was retained.

Replacing the chlorine substituent with a methyl group was tolerated, indicating that small substituents could be further explored. However, a bulkier isopropyl group led to activity loss when compared to compound **110**, in addition to being cytotoxic to human cells (see section 4.2).

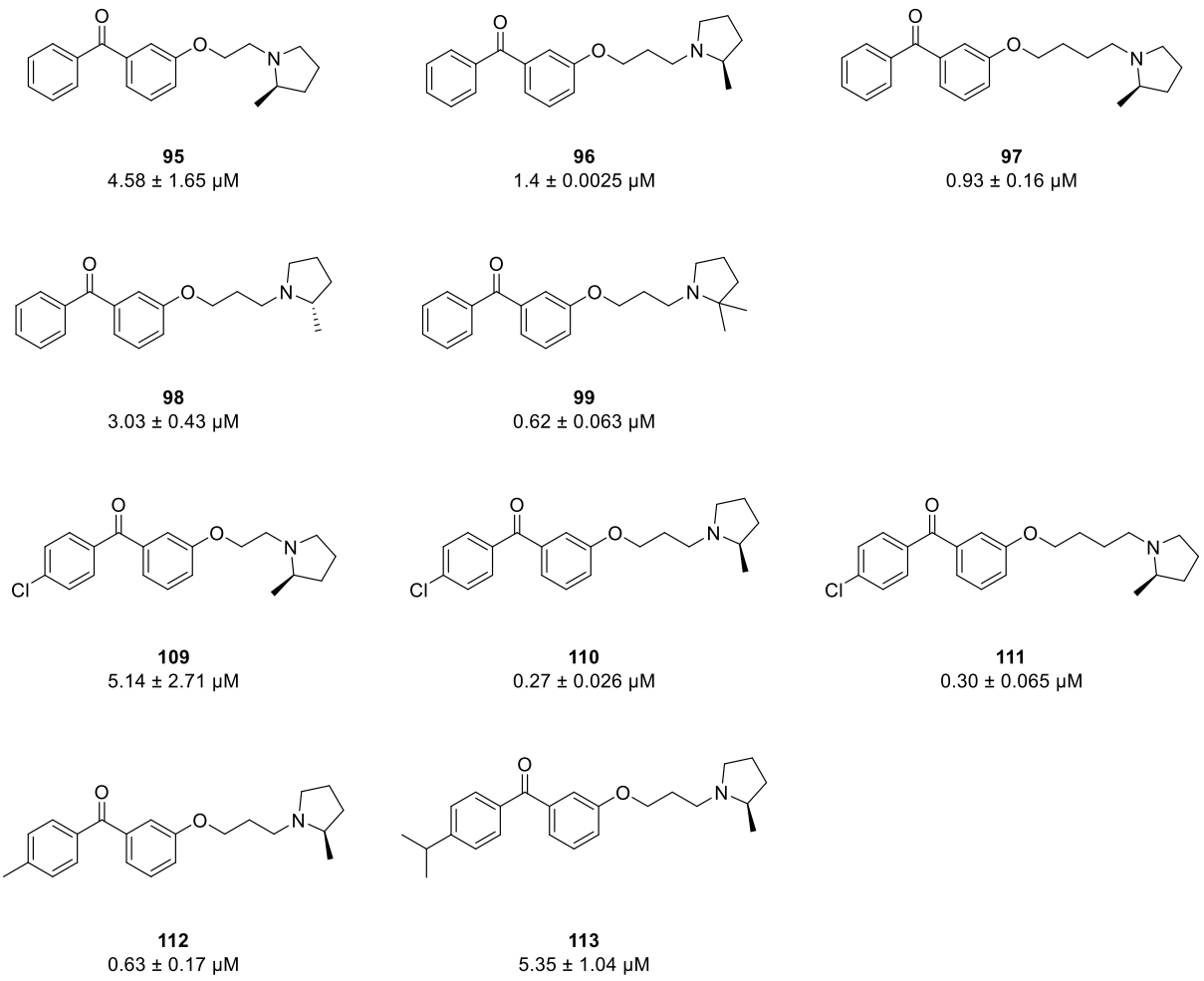

Figure 3.33. EC_{50} values of third generation of clemastine/tamoxifen hybrids against *L. major* promastigotes.

After assaying these three series against *L. major* and establishing their preliminary SAR, a selection of these molecules was further characterised following a screening workflow. The details regarding more in-depth biological characterisation are presented and discussed in section 4.2.

3.6. *Para*-benzylether benzophenones

After assaying the phenol ether benzophenones against *Leishmania* promastigotes, the design and synthesis of benzyl ether benzophenones (benzyl-BP) were revisited. Considering the better activity of *para*- and *meta*-BP over the *ortho*-BP primarily designed, commercially available 4-bromomethyl benzophenone **113** was explored to access the *para*-benzylether benzophenone series. Analogue **115** was obtained combining benzophenone **113** with 3-dimethylamino-1-propanol **114** using similar conditions to those described previously (Figure 3.34). This head group was chosen because of easier availability and cost compared to pyrrolidine head group. However, instead of desired hybrid **115**, the quaternary ammonium salt **116** was obtained (Figure 3.34). Considering the use of a relatively weak base in this reaction, the nucleophilic attack by the tertiary amine was favoured in relation to the primary alcohol. To overcome this issue, NaH was used instead and analogue **115** was successfully afforded with 15% yield. The improved conditions were applied to afford analogue **118** in 39 % yield using 2-dimethylamino-1-ethanol **117** (Figure 3.35). The antileishmanial activity of this series will be discussed in section 4.2.

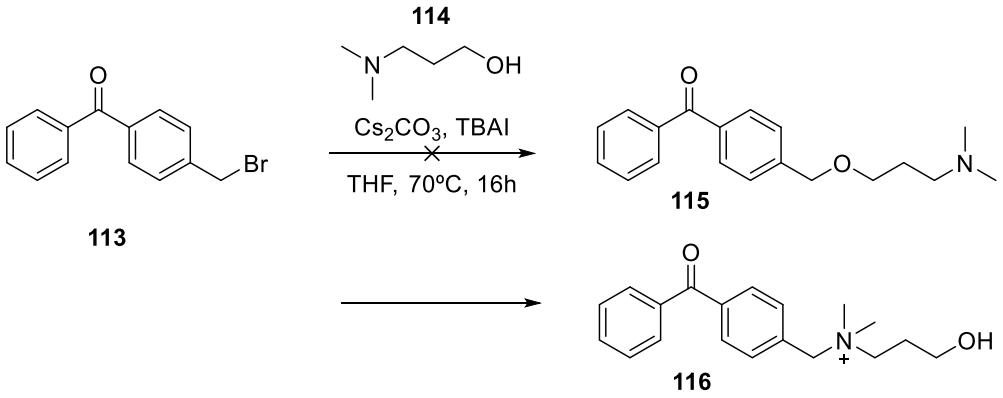

Figure 3.34. Synthesis of analogue **116**.

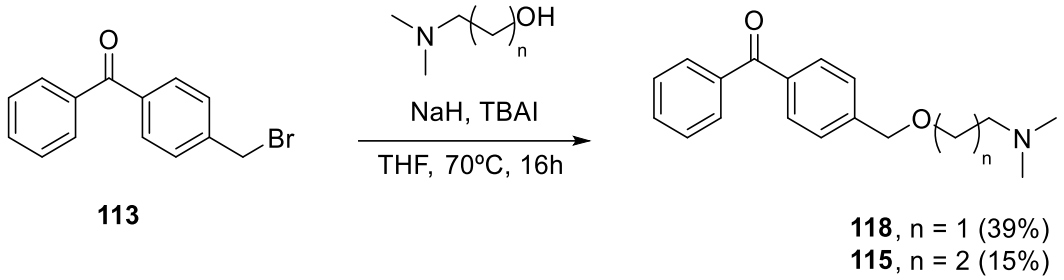

Figure 3.35. Synthesis of analogues **115** and **118**.

The same conditions were then applied to synthesise analogue **120** containing a pyrrolidine head group, however this reaction was repeatedly unsuccessful. Unexpectedly, several unidentified side products were formed and analogue **120** was never obtained.

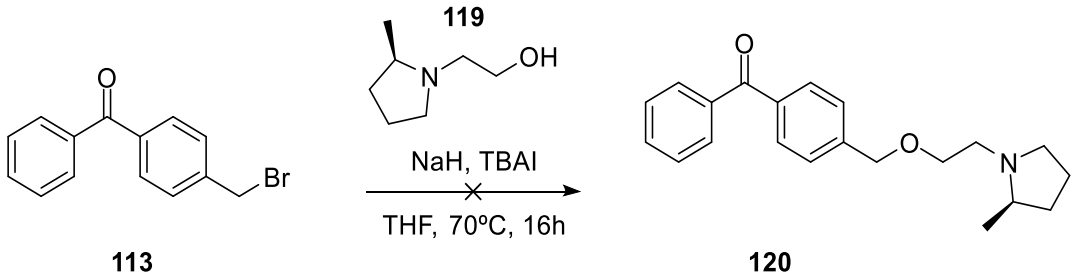

Figure 3.36. Attempt on the synthesis of analogue **120**.

3.7. Non-benzophenone analogues (non-BP)

3.7.1. Synthesis

In the previous sections, variations around the head group and its position were explored, as well as substituents on the aromatic rings. To explore the essentiality of the biaryl system, two mono-aromatic analogues were synthesised. Starting from phenol **121** or *p*-hydroxyacetophenone **122**, reaction with 1,3-dibromopropane **48** followed by (2*R*)-methylpyrrolidine hydrochloride **62** afforded analogues **124** and **125** (Figure 3.37).

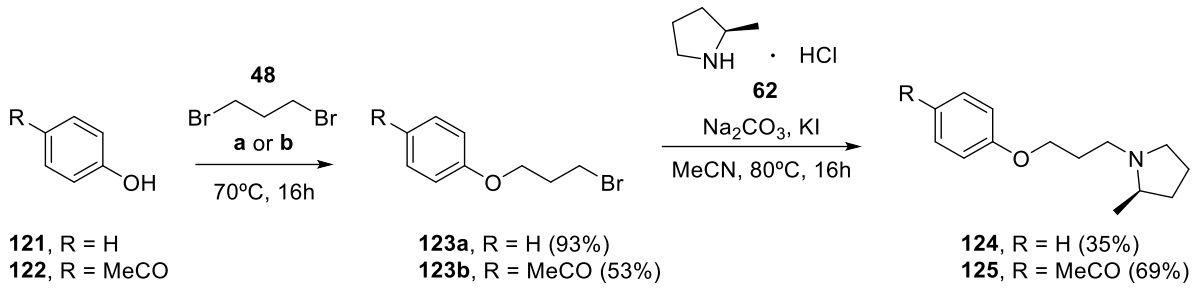

Figure 3.37. Synthesis of analogues **124** and **125**. a) K_2CO_3, TEBA-Cl, EtOAc; b) K_2CO_3, MeCN.

Other core scaffolds retaining the biaryl system were explored by replacing the ketone component for an alkene (diphenylethylene, **137**), an oxygen (diphenyl ether, **130**) or a carbon (diphenylmethane, **129** and **133**). Analogues were designed based on compound **96** due to its high activity and synthetic accessibility.

Using similar conditions to those described above, 3-benzylphenol **126** and 3-phenoxyphenol **127** were combined with 1,3-dibromopropane **48** (Figure 3.38). Ether **128a/b** were then reacted with (2*R*)-methylpyrrolidine hydrochloride to afford analogues **129** and **130**. 4-benzylphenol was also commercially available, therefore compound **133** was synthesised as an analogue of compound **79** (Figure 3.39).

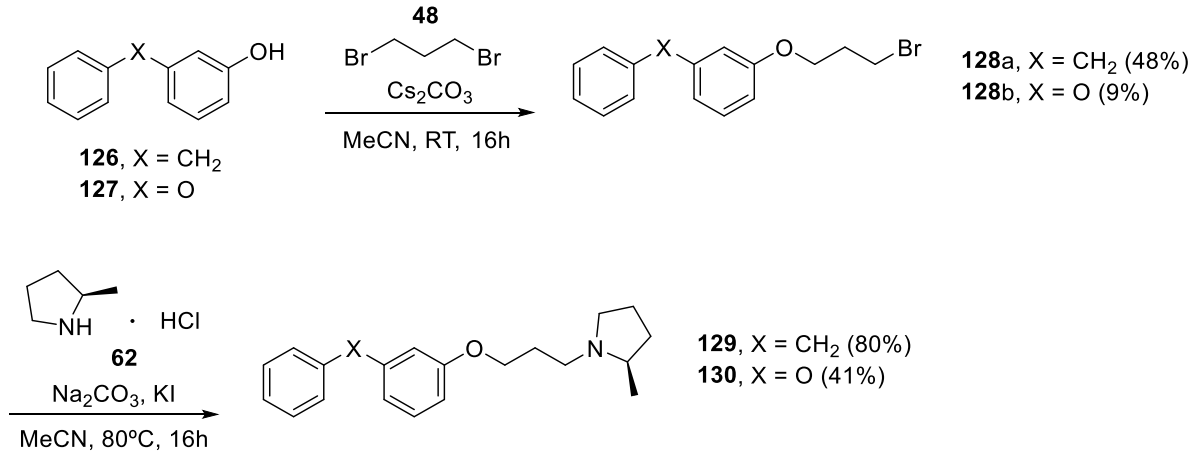

Figure 3.38. Synthesis of analogues **129** and **130**[b].

[b] Synthesis of non-BP analogues was achieved by Dr. Michaela Buerdsell.

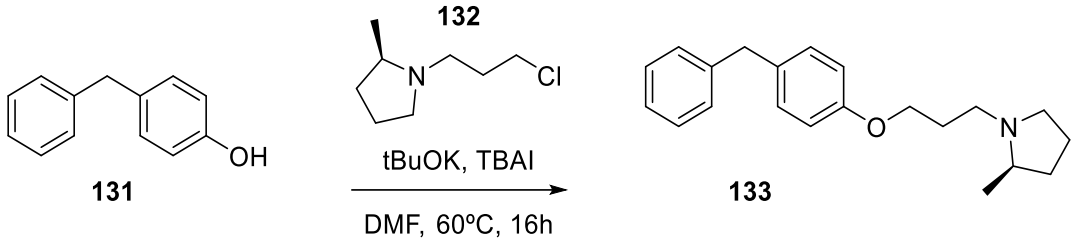

Figure 3.39. Synthesis of analogue **133**[b].

For the synthesis of analogue **137**, in which the ketone is replaced by an alkene, phenylmagnesium bromide **134** was combined with 3-hydroxyacetophenone **135** to form the phenol **136**. Reaction with head group **132** affordedanalogue **137** in 18% yield.

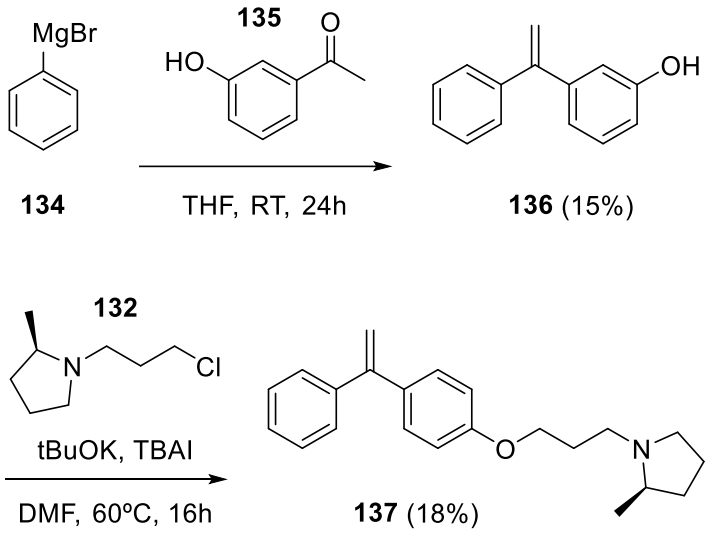

Figure 3.40. Synthesis of analogue **137**[b].

3.7.2. Screening of non-BP series against L. major *promastigotes*

An observed reduction in potency for compounds **124** and **125** against *L. major* promastigotes successfully confirmed that the biaryl system was essential for antileishmanial activity (Figure 3.41).

Overall, the antipromastigote activity of this series indicated that the benzophenone core is not required for activity if the biaryl system is present (Figure

3.41). All 4 compounds displayed comparable EC_{50} values to compound **96** from *meta*-BP series, suggesting that the ketone is not essential for activity and connecting substituents are tolerated. Compound **137** was surprisingly active with an EC_{50} value of 62 nM. It was hypothesised that the terminal alkene may contribute to potential polypharmacology not explored further in this work.

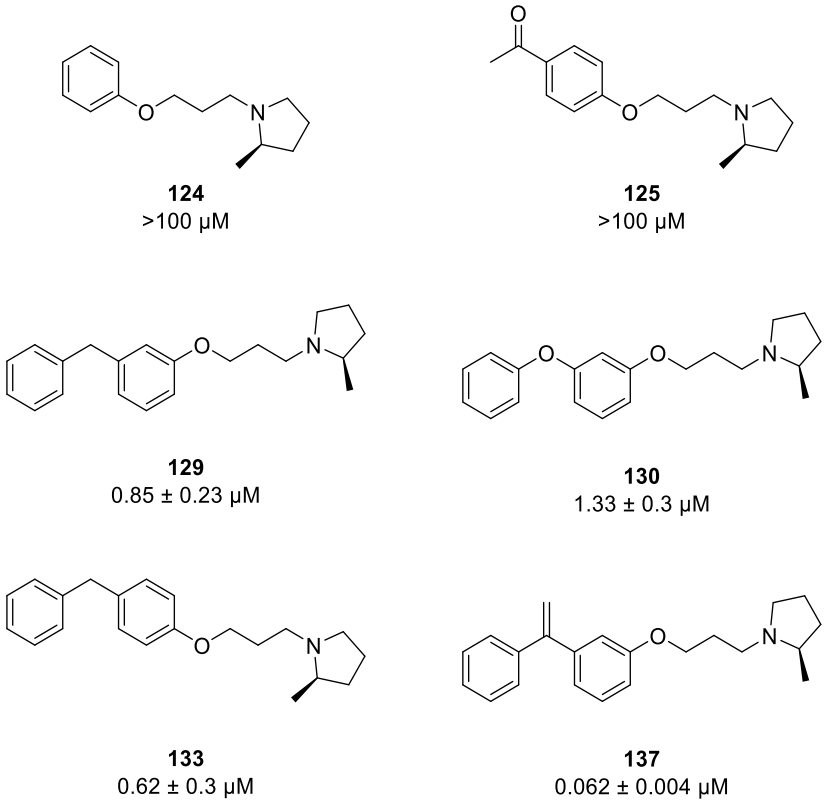

Figure 3.41. EC_{50} values of non-benzophenone analogues against *L. major* promastigotes.

4. Biological characterisation of the hybrids

4.1. Introduction

A library of 40 clemastine/tamoxifen hybrids were built based on the hypothesis that combining features of these two drugs would generate chemically optimised molecules with higher antileishmanial activity and selectivity than parent molecules. Once obtained, the next step was to assess the chemotherapeutic potential of this library. For that reason, a screening workflow was established with the aim of selecting the hybrids with the most promising therapeutic properties (Figure 4.1). Among these properties, a potential drug candidate displays an EC_{50} ≤ 2 μM against intracellular amastigotes and promastigotes as well as a selectivity index (SI) above 10 before being submitted to pre-clinical assays in animal models. These cut off values have been frequently used as standards in drug discovery programs, especially the ones led by the Drugs for Neglected Diseases initiative (DNDi) [68].

Firstly, the library was screened against *L. major* promastigotes, as discussed in the previous section. This species was chosen as an Old World model for cutaneous leishmaniasis. The compounds with an EC_{50} > 10 μM were discarded, and the remaining analogues were assayed against *L. amazonensis* promastigotes, which is the causative agent of cutaneous leishmaniasis in the New World. These hybrids were also assayed against HepG2 cells, a human liver cancer cell line commonly used for cytotoxicity evaluation [110]. Those that had an EC_{50} ≤ 2 μM against both promastigote species as well as a SI > 10 were singled out for further characterisation. This included assays against promastigotes of other two species (*L. braziliensis* and *L. infantum*) as well as anti-intracellular amastigote assays against *L. amazonensis* and *L. infantum*. The species selected for this final step of the screening workflow represented the most epidemiologically relevant species in South America, allowing for the evaluation of

activity of the clemastine/tamoxifen hybrids across species. Finally, the hybrids were assayed against bone-marrow derived macrophages (BMDM) for cytotoxicity evaluation of the most promising compounds. This is a relevant model for cytotoxicity considering it is a standard cell for *in vitro* infection studies. The assays of this final step of the screening workflow were performed during a research visit at the laboratory of Prof. Adriano Cappellazzo Coelho (Unicamp, Brazil)

Two methods were used for the screening of this library. For the anti-promastigote and cytotoxicity assays, cells were incubated with resazurin after treatment, which was metabolized by live cells generating fluorescence. The second method was a bioluminescence assay used for the anti-intracellular amastigote evaluation. This used luciferase-expressing parasites, which are able to metabolize luciferin, generating light. Both assays took place in a 96-well plate system and had a dose-response curve as an outcome used for the calculation of the EC_{50} values.

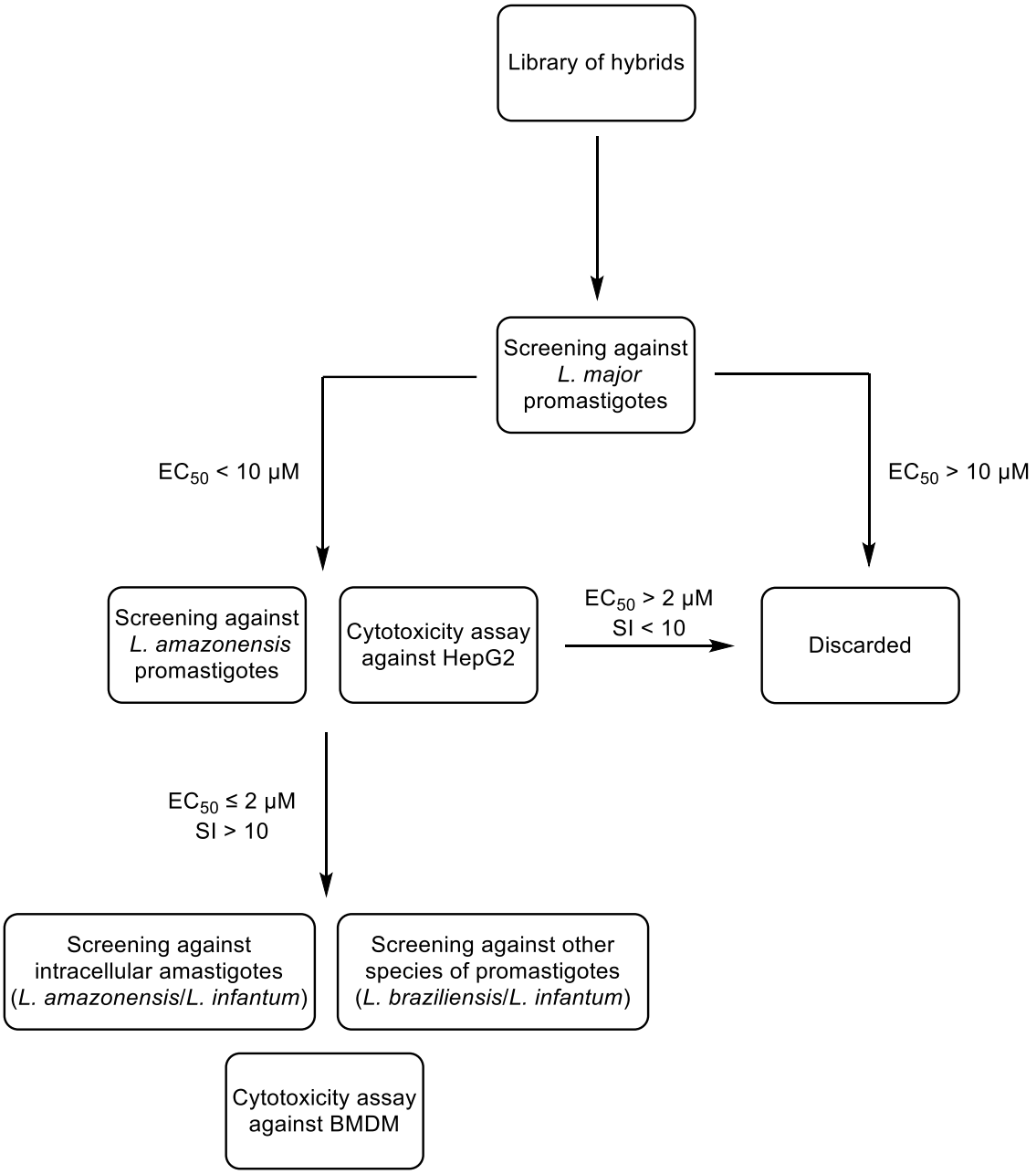

Figure 4.1. Screening workflow for selection of most promising clemastine/tamoxifen hybrids.

4.2. Anti-promastigote and cytotoxicity assays

The anti-promastigote assays against *L. major* and *L. amazonensis* comprise the first steps of the screening workflow established previously (Figure 4.1). These assays contributed to the structure-activity relationship (SAR) study of these compounds, which will be discussed in depth in this section.

Table 4.1. Tamoxifen/clemastine hybrid molecules primary screening against promastigotes of *L. major* and *L. amazonensis* and cytotoxicity screening against HepG2 cells.

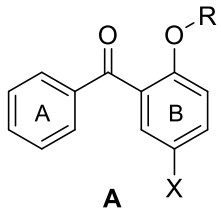

A

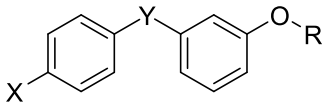

B

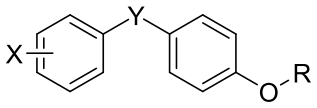

C

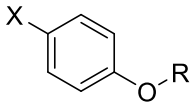

D

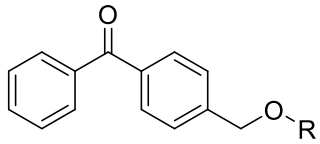

E

R =

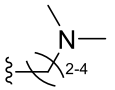

F

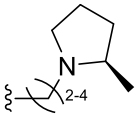

G

Compounds	Scaffold	X	Y	Carbon chain	R	EC_{50} *L. major*	EC_{50} *L. amazonensis*	CC_{50} HepG2	SI (*L. major*)	SI (*L. amazonensis*)
44	A	H	-	2	F	>100	ND	ND	ND	ND
46	A	H	-	3	F	32.51 ± 5.77	ND	ND	ND	ND
48	A	Cl	-	2	F	68.91 ± 15.92	ND	ND	ND	ND
49	A	Cl	-	3	F	11.76 ± 1.1	ND	ND	ND	ND
63	A	H	-	2	G	45.93 ± 15.68	ND	ND	ND	ND
64	A	H	-	3	G	30.11 ± 9.04	ND	ND	ND	ND
65	A	H	-	4	G	11.14 ± 0.23	ND	ND	ND	ND
66	A	Cl	-	2	G	35.78 ± 5.5	ND	ND	ND	ND
67	A	Cl	-	3	G	18.53 ± 3.24	ND	ND	ND	ND
68	A	Cl	-	4	G	1.62 ± 1.48	3.07 ± 0.92	>100	>61	>32
95	B	H	C=O	2	G	4.58 ± 1.65	>100	>100	>22	-
96	B	H	C=O	3	G	1.4 ± 0.0025	0.74 ± 0.13	>100	>71	>135
97	B	H	C=O	4	G	0.93 ± 0.16	3.51 ± 1.44	>100	>107	>48
109	B	Cl	C=O	2	G	5.14 ± 2.71	24.8 ± 10.51	>100	>19	>4
110	B	Cl	C=O	3	G	0.27 ± 0.026	0.37 ± 0.14	>100	>370	>270
111	B	Cl	C=O	4	G	0.30 ± 0.065	0.85 ± 0.46	25.64 ± 0.94	85	30

112	B	Methyl	C=O	3	G	0.63 ± 0.17	1.44 ± 0.44	>100	>158	>69
113	B	Isopropyl	C=O	3	G	5.35 ± 1.04	8.49 ± 2.64	16.45 ± 3.99	3	2
129	B	H	CH_2	3	G	0.85 ± 0.23	3.07 ± 0.19	>100	>117	>32
130	B	H	O	3	G	1.33 ± 0.3	1.77 ± 0.30	22.71 ± 3.50	17.07	12.83
137	B	H	$C=CH_2$	3	G	0.062 ± 0.004	-	16.44 ± 2.17	265	-
71	C	H	C=O	2	F	11.61 ± 2.68	ND	ND	ND	ND
72	C	H	C=O	3	F	7.07 ± 1.4	4.69 ± 1.38	ND	ND	ND
73	C	H	C=O	4	F	2.91 ± 0.26	1.58 ± 0.25	>100	>34	>63
78	C	H	C=O	2	G	4.51 ± 0.35	1.2 ± 0.35	>100	>22	>83
79	C	H	C=O	3	G	4.25 ± 0.12	3.69 ± 1.51	>100	>23	>27
80	C	H	C=O	4	G	5.37 ± 0.42	2.56 ± 0.84	>100	>18	>39
81	C	p-Cl	C=O	2	G	2.02 ± 0.005	0.8 ± 0.27	>100	>49	>125
82	C	p-Cl	C=O	3	G	2.37 ± 0.18	1.56 ± 0.59	31.07 ± 11.04	13	19
83	C	p-Cl	C=O	4	G	2.2 ± 0.56	1.42± 0.52	16.05 ± 2.13	7	11
92	C	m-Cl	C=O	3	G	2.96 ± 0.4	1.14 ± 0.39	25.11 ± 2.03	8	22
91	C	o-Cl	C=O	3	G	0.63 ± 0.001	6.77 ± 0.93	>100	>158	>15
133	C	H	CH_2	3	G	0.62 ± 0.3	7.25 ± 0.61	27.06 ± 6.67	44	3.73
124	D	H	-	3	G	>100	>100	>100	ND	ND
125	D	MeC=O	-	3	G	>100	>100	>100	ND	ND
118	E	-	-	2	F	8.01 ± 2.39	10.27 ± 2.9	ND	ND	ND
115	E	-	-	3	F	>10	>10	ND	ND	ND
Clemastine	-	-	-	-	-	0.035 ± 0.012	0.038 ± 0.003	25.57 ± 1.76	730	673
Tamoxifen	-	-	-	-	-	4.03 ± 0.33	2.39 ± 0.17	31.32 ± 1.91	8	13

Firstly, there was a notable difference in activity dependent on the position of the aminoalkoxy side chain around ring B in relation to the central ketone. The *ortho*-BP series (**46**-**49**, **63**-**68**) contained the least active molecules, which was attributed to a lower flexibility of the headgroup. It was hypothesised that the parallel oxygens from the ether and the ketone could form a six-membered ring when hydrogen bonding to amino acids in a putative binding pocket, thus decreasing their flexibility. The *para*-BP group (**71**-**73**, **78**-**83**, **91**-**92**) showed satisfactory activity, as well as easier chemical accessibility due to commercially available hydroxybenzophenones. The most active molecules, however, belonged to the *meta*-BP group (**95**-**97**, **109**-**113**); both compounds **110** and **111**, for example, had activity below 1 µM against both species tested, and promising selectivity index. Besides the flexibility of the head group, these three groups are electronically different; the ether in the *meta*-BP series does not participate on the aromatic resonance structure, which happens in both *ortho*- and *para*-BP series and could potentially impact on their activity.

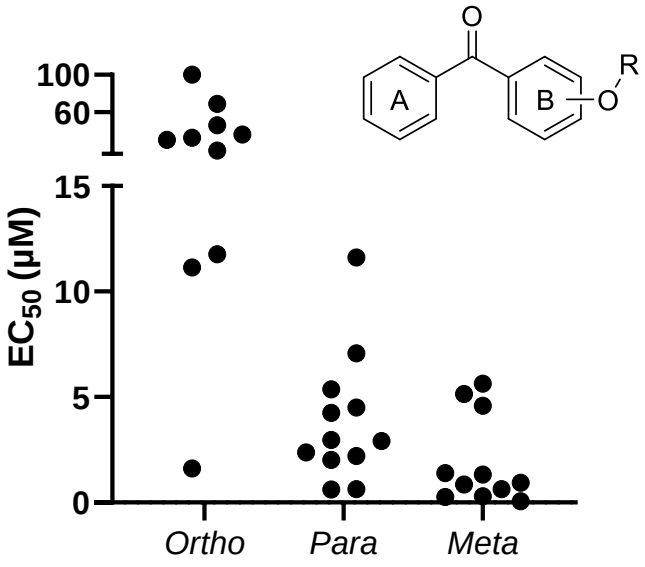

Figure 4.2. EC_{50} values of phenol ether benzophenones against *L. major* promastigotes. *Ortho*, *meta* and *para* represent the position of the head group around the ring. Each point represents the average of at least three independent experiments.

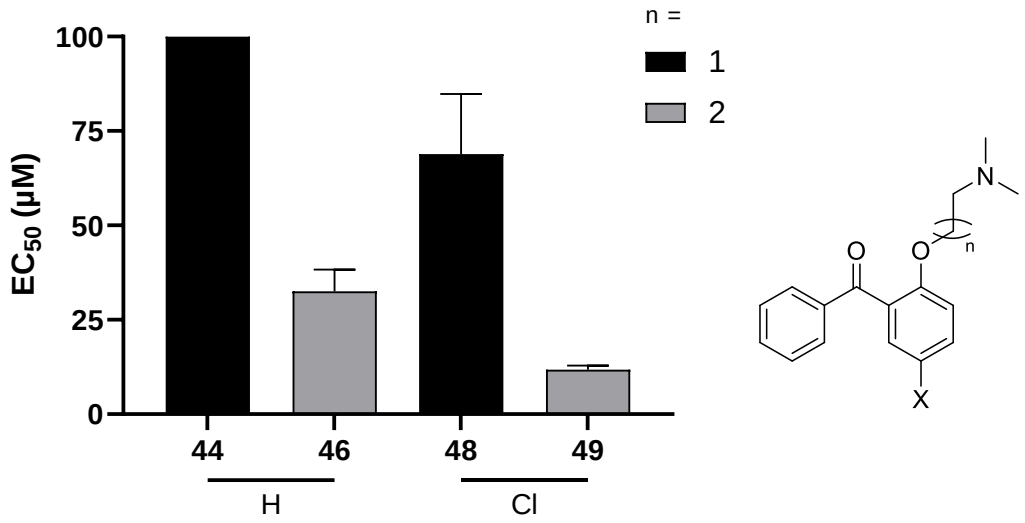

Figure 4.3. EC_{50} values of *ortho*-BP analogues with a dimethylamine headgroup against *L. major* promastigotes. Shading represent the size of the carbon chain in the head group. Each point represents the average of at least three independent experiments.

A difference in activity according to the size of the side chain was first observed in the *ortho*-BP series in analogues **44**-**46** and **48**-**49**, which contain a dimethylamine head group (Figure 4.3). The increase to a 3-carbon chain translated into enhanced activity. The same pattern was seen for pyrrolidine-containing analogues **63**-**68** (Figure 4.4). Analogues **65** and **68** containing 4-carbon chains had the highest activities. Analogues containing a 2-carbon chain displayed low or no activity against at least one of the two species tested in several examples. In the *meta*-BP series, analogues with a 2-carbon chain had the lowest activity, however no significant difference was observed between compounds with a 3- or 4-carbon chain. In contrast, in the *para*-BP series, a change in the linker length had no impact on antileishmanial activity. For analogues **83** and **111**, an increase in linker length led to an increase in cytotoxicity as well (Table 4.1). Based on these results, it was hypothesised that the length of the head group side chain could contribute to the flexibility of the molecule and its accessibility to protein binding sites.

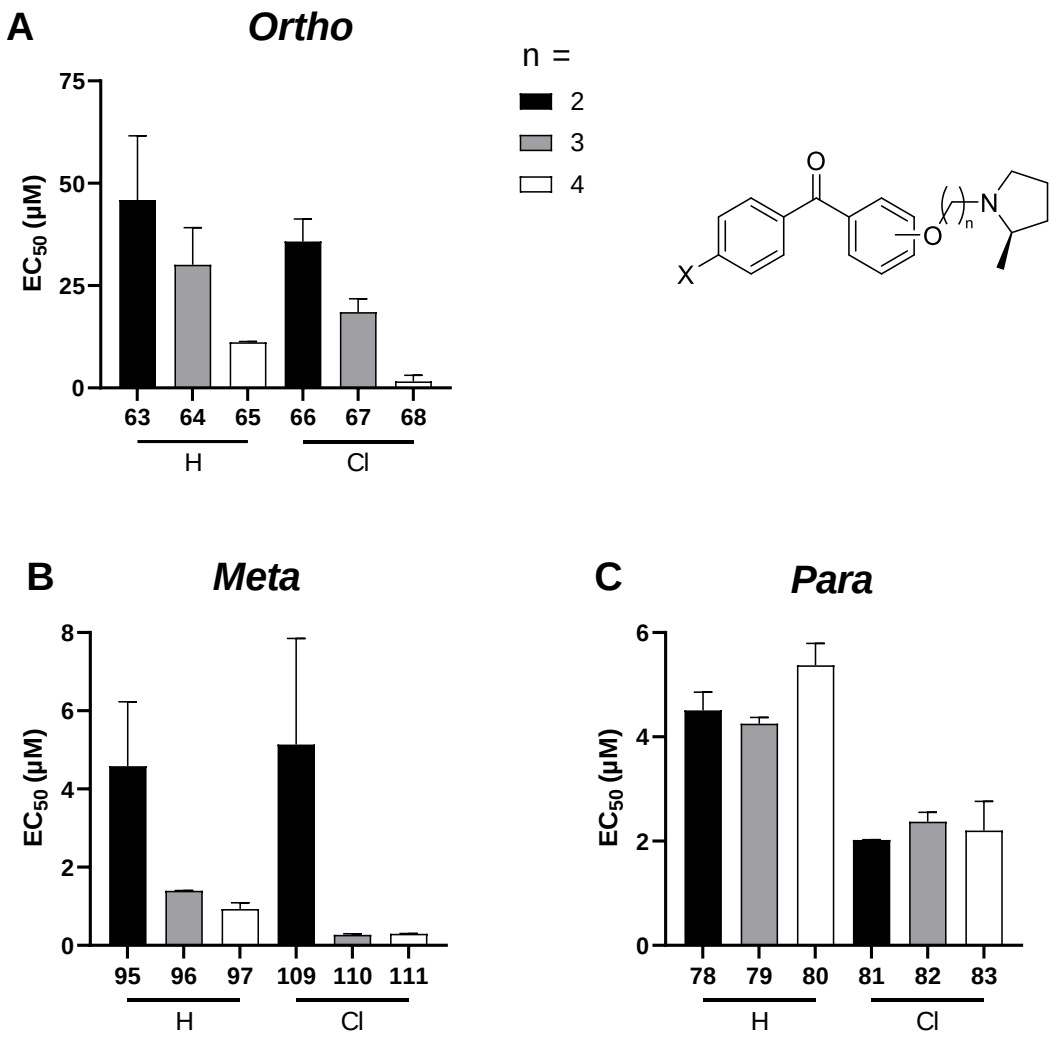

Figure 4.4. EC_{50} values of *ortho*-BP analogues with a pyrrolidine headgroup against *L. major* promastigotes. Shading represent the size of the carbon chain in the head group. Each bar is the mean and standard error of the mean of at least three independent experiments.

The chlorine substituent improved the activity significantly in all three series (Figure 4.4). When variation of the position of the chlorine was explored on the *para*-BP series, the *ortho* position was the least well-tolerated (Figure 4.5). Although compound **91** was the most active against *L. major*, it was 10x less active against *L. amazonensis* than *meta*- and *para*-substituted analogues **92** and **82**, respectively. In comparison, both compounds **92** and **82** displayed similar activity between both species, indicating that both positions are equally tolerated (Figure 4.5). With that in

mind, the *para*-chlorine was selected the preferred substituent due to easier chemical accessibility.

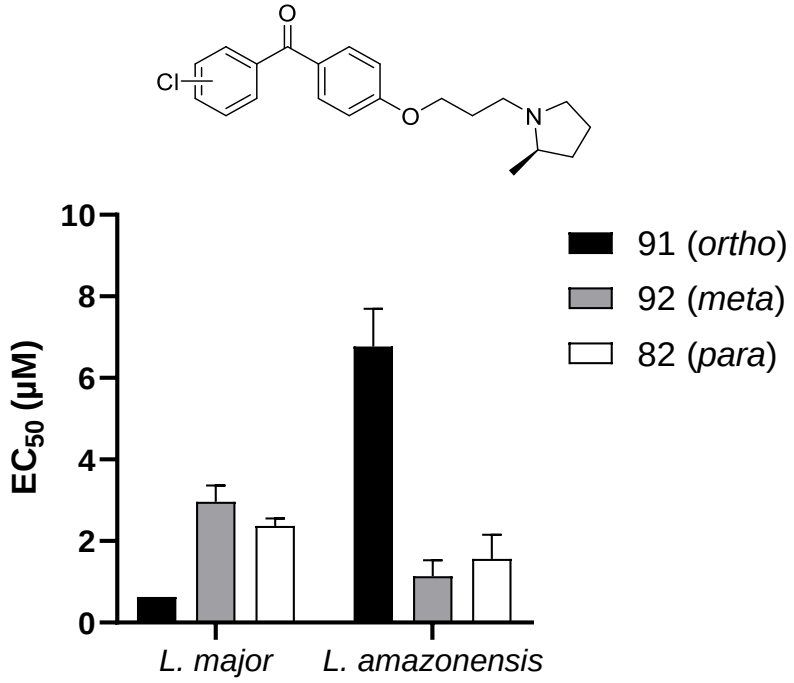

Figure 4.5. EC_{50} values of analogues **91**, **92** and **82** against *L. major* and *L. amazonensis* promastigotes. Each bar is the mean and standard error of the mean of at least three independent experiments.

When the chlorine substituent was replaced by a methyl group (**112**), the antileishmanial activity was retained (Figure 4.6). However, a bulkier substituent such as the isopropyl group caused loss in activity and increased cytotoxicity (Figure 4.6). Bulkier substituents could potentially impair the molecule's binding to its target, suggesting that other small substituents in that position could be explored, such as halogens and nitrile groups. The methyl group has an A-value (difference in energy in kcal/mol between a cyclohexane bearing the group in the equatorial position versus the axial position) of 1.70, while the A-value for the isopropyl group is 2.15. The value for the methyl group was then established as the highest A-value possible for a substituent on ring A. As described previously, changes in the position of the phenol-

ether side chain on ring B affected the activity drastically, which was attributed to the electronic contribution of the ether to the ring aromaticity. Therefore, another property that could be further explored on ring A is the electronic environment of its substituents. This could be achieved by attaching a stronger electron-donating group (EDG) than alkyl groups previously used (methoxy, phenol, amines) as well as electron-withdrawing groups (EWG) stronger than chlorine (nitro and acyl groups, sulfonic acids). Considering that both the chlorine and alkyl groups used (methyl and isopropyl) are weak EDG and EWGs, respectively, their electronic effect on the activity was considered minimal.

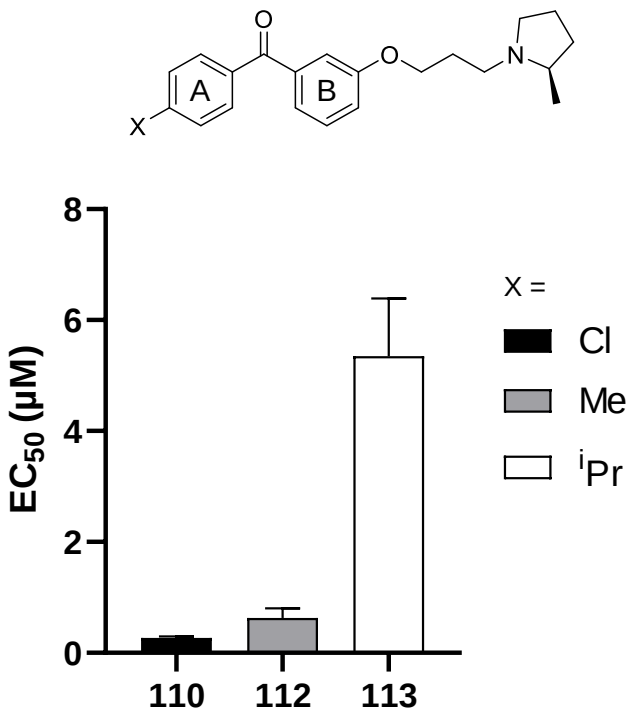

Figure 4.6. EC_{50} values of analogues **110**, **112** and **113** against *L. major* promastigotes. Each bar is the mean and standard error of the mean of at least three independent experiments.

The pyrrolidine-containing hybrids performed slightly better than the molecules containing a dimethylamine head group (Figure 4.3 and 4.4). When the (2*R*)-methylpyrrolidine was replaced by its enantiomer (2*S*)-methylpyrrolidine (**98**), the

activity dropped approximately 4x against *L. amazonensis*, suggesting that specific chirality is important to achieve higher activity. However, a 2,2-dimethylpyrrolidine group in analogue **99** was tolerated.

The mono-aromatic compounds **124** and **125** tested were inactive against both promastigote species, suggesting that the diaryl system was essential for activity (Table 4.1). Likewise, the benzyl-BP series (**115** and **118**) had low activity and were more chemically challenging, which contributed to the abandonment of this series (Table 4.1).

Although a ketone replacement was shown to be tolerated, the ketone-containing analogues remained as having the highest activities overall (Figure 4.8). The exception was for molecule **137** which had the ketone replaced by a terminal alkene, and activity was 62 nM against *L. major* – 22-fold difference from analogue **96**.

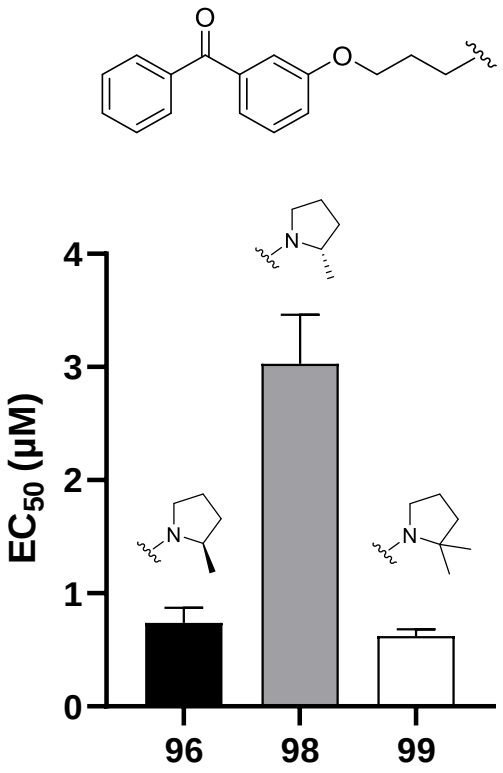

Figure 4.7. EC_{50} values of analogues **96**, **98** and **99** against and *L. amazonensis* promastigotes. Each bar is the mean and standard error of the mean of at least three independent experiments.

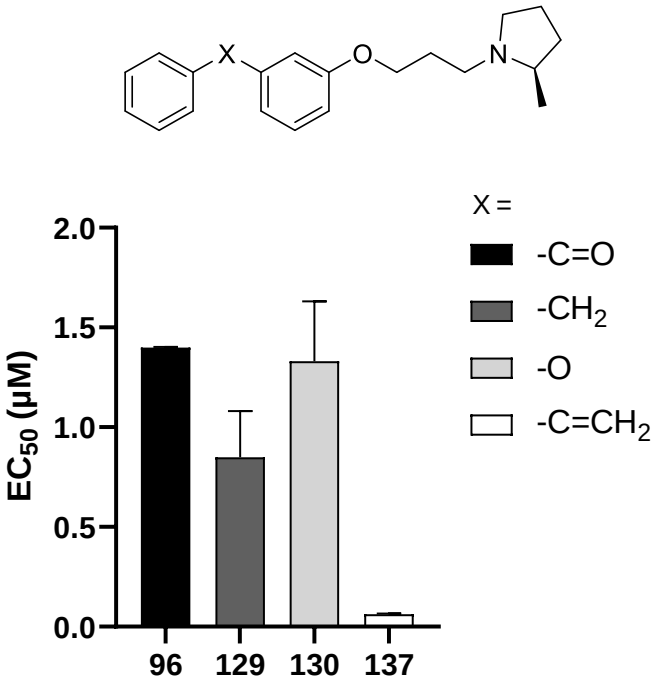

Figure 4.8. EC_{50} values of analogues **96**, **129**, **130**, and **137** against and *L. major* promastigotes. Each bar is the mean and standard error of the mean of at least three independent experiments.

Following the workflow described in section 4.1 (Figure 4.1), 7 compounds were singled out as having $EC_{50} \leq 2$ µM against both *L. major* and *L. amazonensis*, as well as a SI > 10 for both species against HepG2 cells. Therefore, these were submitted to activity evaluation against *L. braziliensis* and *L. infantum*. This is part of the final step of the screening workflow established (Figure 4.1), together with anti-intracellular amastigote assays (discussed in the next section). All compounds successfully showed EC_{50} below 1 µM against *L. braziliensis* and 6/7 compounds had EC_{50} approximate to 2 µM against *L. infantum* (Table 4.2). These results confirm that the hit molecules selected by this screening workflow were highly active against all four species of promastigotes tested, especially against *L. braziliensis*.

Table 4.2. Activity evaluation of most promising compounds against promastigotes of *L. braziliensis* and *L. infantum* and selectivity index in HepG2 cells.

Compounds	EC_{50} *L. braziliensis*	EC_{50} *L. infantum*	SI (*L. braziliensis*)	SI (*L. infantum*)
81	0.41 ± 0.091	2.32 ± 0.091	>243	>43
82	0.084 ± 0.015	1.25 ± 0.11	369	25
96	0.53 ± 0.14	4.42 ± 0.27	>189	>23
110	0.38 ± 0.054	1.32 ± 0.12	>263	>76
111	0.21 ± 0.044	1.00 ± 0.14	124	26
112	0.65 ± 0.12	2.93 ± 0.11	>154	>34
130	0.26 ± 0.10	2.84 ± 0.16	88	8
Clemastine	0.14 ± 0.002	0.71 ± 0.043	186	36
Tamoxifen	9.55 ± 2.045	4.97 ± 0.49	3	6

4.3. Anti-amastigote assays

As discussed in section 4.1, the final step of biological characterisation of the library was composed of two parts. The first was to assay the hit molecules against the other two species of promastigotes, which was described in the previous section, and the second was to assess the anti-intracellular amastigote activity of these molecules, described in this section.

For that, BMDM were extracted from BALB/c mice and infected with either *L. amazonensis* or *L. infantum* luciferase-expressing parasites. These cells were then treated with increasing concentrations of the 7 compounds identified from promastigotes. In parallel, cytotoxicity against the macrophages was determined using a standard resazurin assay, and used to determine the SI against each amastigote species (Table 4.3).

Whilst all analogues exhibited good activity against *L. infantum* amastigotes (EC_{50} ≤ 2 μM), only 4 analogues showed equivalent efficacy against the *L.*

amazonensis amastigotes. Importantly, with the exception of **110**, all compounds displayed SI > 10 for both species. Compounds **81**, **111** and **112** were highly active against both species tested and displayed promising SI and are among the most promising hit molecules of this library. However, compound **130** was the most active hit molecule of this series with an $EC_{50} \leq 1$ μM against both species, and a SI > 40.

Table 4.3. Activity evaluation of most promising compounds against intramacrophage amastigotes of *L. amazonensis* and *L. infantum*, and cytotoxicity against BMDM.

Compounds	EC_{50} *L. amazonensis*	EC_{50} *L. infantum*	CC_{50} BMDM	SI* (*L. amazonensis*)	SI* (*L. infantum*)
81	2.27 ± 0.26	1.72 ± 0.44	>100	44	58
82	3.89 ± 0.70	0.86 ± 0.17	43.13 ± 2.30	11	50
96	3.95 ± 0.38	1.30 ± 0.35	>100	25	77
110	5.35 ± 1.055	0.69 ± 0.18	36.38 ± 6.25	7	53
111	2.11 ± 0.43	2.43 ± 0.58	32.48 ± 5.01	15	13
112	2.44 ± 0.59	1.19 ± 0.29	48.73 ± 9.77	20	41
130	0.80 ± 0.096	1.076 ± 0.14	49.46 ± 0.36	62	46
Clemastine	0.46 ± 0.10	ND	22.35 ± 3.78	49	ND
Tamoxifen	4.90 ± 0.69	2.4 ± 0.3	52.44 ± 2.34	10	22

*Values calculated considering the CC50 against BMDM and EC50 against intracellular amastigotes.

4.4. Conclusion

The work described in this chapter involved the design and implementation of a screening workflow for the activity evaluation of the clemastine/tamoxifen library generated. The workflow included preliminary antipromastigote activity evaluation against *L. major*, followed by screen against a second species, *L. amazonensis*, as well as cytotoxicity determination using HepG2 cells. With these results, it was possible to explore the SAR of this library in relation to its antileishmanial potential. First, it was established that the biaryl system is essential for activity. In addition, the

most active molecules contained a chlorine substituent, a linker unit of 3 or 4 carbons and/or a pyrrolidine moiety composing the head group.

Using the workflow and cut off points established, a selection of seven molecules were assessed against two other species of promastigotes, *L. braziliensis* and *L. infantum*. All compounds were especially active against *L. braziliensis*. Compounds **110** and **111** were the most active analogues across the four species of promastigotes tested. However, compound **130** had the highest efficacy against intracellular amastigotes with good selectivity over BMDM. The next steps were to explore the mechanism of action of most active molecules, which is discussed in chapter 5.

5. Mechanism of action studies

5.1. Introduction

The screening of the library of clemastine/tamoxifen hybrids identified 7 compounds with high activity across species of promastigotes and intracellular amastigotes. Considering that both clemastine **27** and tamoxifen **28** target IPCS, it was hypothesised that the shared chemical features were responsible for that activity and, therefore, that the hybrids retained parental targets. To assess that hypothesis, preliminary dose-response assay of compounds **110** and **111** using an *L. mexicana* $^{IPCS\ -/-}$ line [c] (data not published) showed activity loss against this line when compared to the WT. This decrease in sensitivity supports the hypothesis that the hybrids target IPCS. To confirm this and further investigate other potential targets, two methods were selected; chemical proteomics, making use of synthetic probes based on the hit molecule **110** (section 5.2), and generation of *in vitro* resistance to this molecule, followed by genome sequencing (section 5.3).

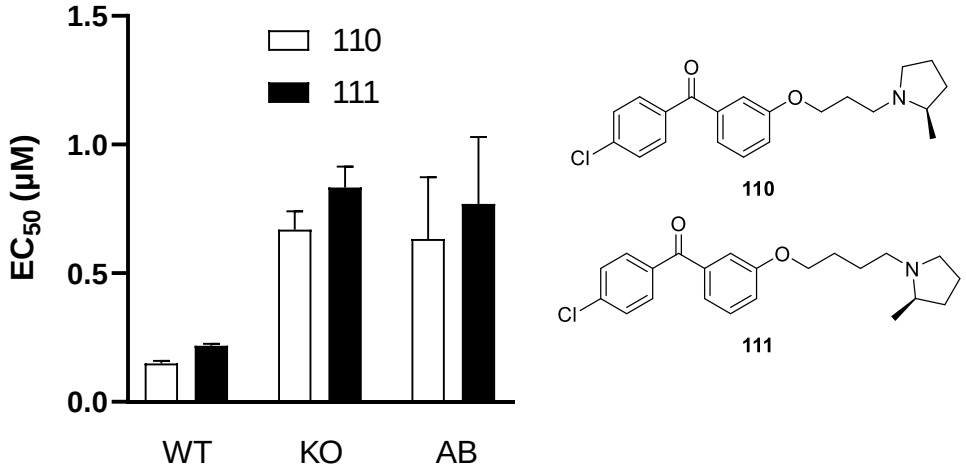

Figure 5.1. EC_{50} values of compounds **110** and **111** against three strains of *L. mexicana*: WT, KO (IPCS knockout line) and AB (add back line). Bars are the mean and standard error of the mean of three independent experiments.

[c] The *L. mexicana* $^{IPCS\ -/-}$ mutant and add back line were obtained by Prof. Paul Denny's group and data is in preparation for publication.

5.2. Chemical proteomics

5.2.1. Introduction

Chemical proteomics is a strategy that uses synthetic probes to deconvolute the protein interactions with a compound of interest by applying MS-based approaches [111]. The first step is to design the probe, which is composed of three parts (Figure 5.2); (1) the biological moiety responsible for binding to the target protein, (2) a reactive handle group responsible to covalently stabilise the molecule to the target, and (3) a tag necessary for pull-down assay and purification of bound proteins. The reactive handle can be either a photoreactive group, such as a benzophenone, a diazirine and an aryl azide, or an intrinsically reactive group, depending on the molecule's electrophilic nature. The use of a photoreactive group is known as photoaffinity labelling (PAL) [112–114].

The tag could be composed by a fluorophore or biotin. However, these modifications can impair protein binding because of the high molecular weight and bulkiness of the added structures. Instead, the use of a smaller tag, such as an alkyne or an azide, minimises alterations. These two examples are particularly used for bioorthogonal ligations in a reaction known as CuAAC (copper-catalysed azide-alkyne cycloaddition), which is highly selective and allows addition of the labelling partner later in the process.

Once the chemical probe is synthesised, the experimental pipeline (Figure 5.2) starts with the treatment of live cells (or cell lysates) followed, in case of PAL, by irradiation for covalent linking. The cells are then lysed and coupled with the complementary azide/alkyne labelled tag (fluorophore or biotin), which allows for in-gel analysis and/or MS-based approaches. These approaches are divided between gel-based and gel-free proteomics. In the first, after separation of enriched samples in

a gel, selected bands are removed, digested, and analysed by standard LC-MS/MS. This strategy has been widely used in the past, however problems with environmental contamination, bias, and lack of reliable quantification currently render gel-free approaches the favoured choice. With this method, sample handling is reduced, decreasing contamination while also avoiding bias, considering it covers the whole proteome.

Most quantification methods rely on isotope labelling that allow the quantification of the same protein across different samples. The most commonly used isotope labelling methods are the stable isotope labelling by amino acids in culture (SILAC), isobaric tag for relative and absolute quantitation (iTRAQ), and tandem mass tag (TMT). Such methods benefit from the combination of different biological samples on the same run, allowing quantitative analysis not only within the replicate's proteome but also between samples. Label-free methods analyse samples from different runs, and have been increasingly implemented in the recent years with the improved sensitivity and resolution of LC-MS/MS [115].

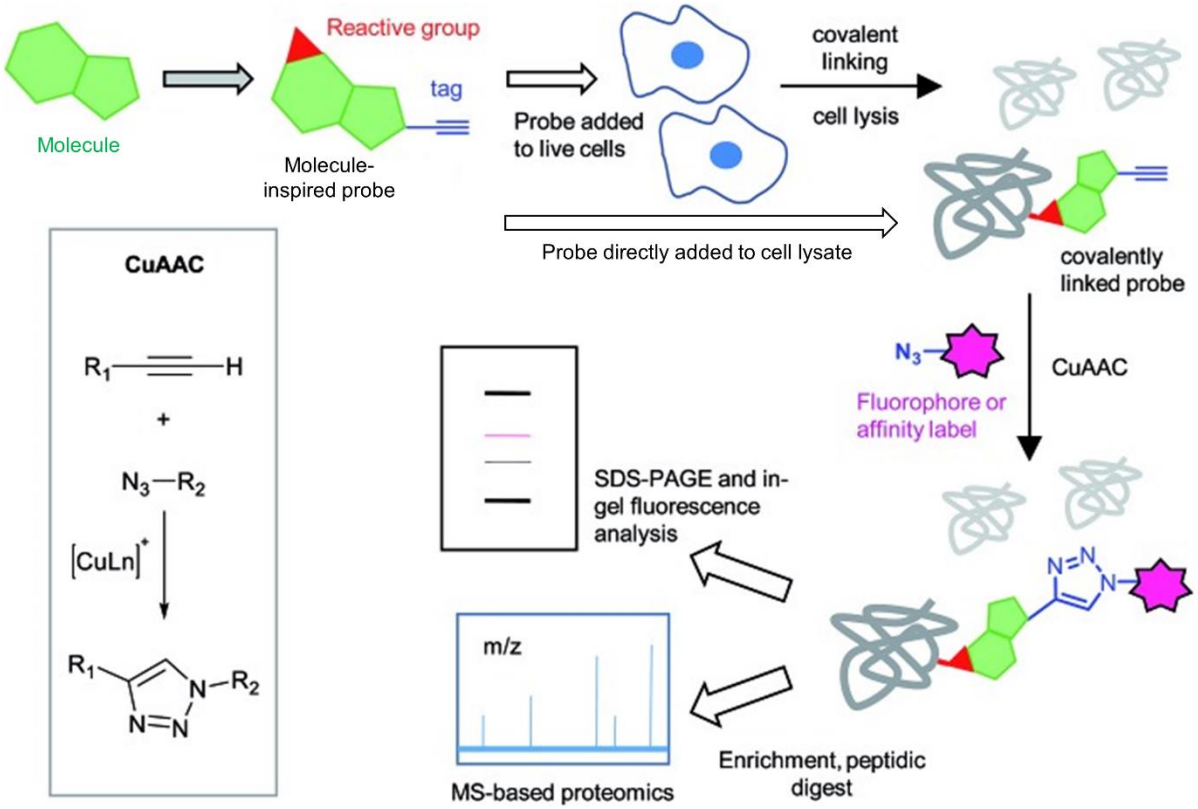

Figure. 5.2. Experimental pipeline for chemical proteomics, from probe synthesis to final analysis. The probe synthesis is inspired on the molecule of interested and contains a reactive group as well as a tag. Live cells or cell lysate is treated with the probe followed by covalent linking. Samples are subjected to copper-catalysed azide-alkyne cycloaddition (CuAAC) reaction for the attachment of fluorophore or biotin, allowing in-gel analysis and/or MS-based approaches. Modified from Wright and Sieber, 2016[111].

5.2.2. Design and synthesis of the chemical probe

Based on its high antipromastigote activity, analogue **110** was selected as the basis for the probe. This hybrid was consistently active against all species of promastigotes tested, especially *L. major* and *L. amazonensis* which are the species for which the biochemical assay conditions were optimised in the group. Significantly, **110** contains a benzophenone scaffold, a well-known PAL moiety. Therefore, the only remaining addition to the molecule needed to form a probe was the alkyne tag. The SAR studies described in chapter 4 revealed that bulky substituents on ring A impairs the activity drastically, and suggested ring B as the optimal site for modification. Within

this ring, the position that is mutually *meta* to the other two substituents was selected as anchor point of tag attachment, therefore reducing potential steric cluster and other binding issues (Figure 5.3). Considering the time restraints caused by the COVID-19 pandemics, efforts focused only on the synthesis of probe **138**, which was designed by adding an alkyne linker in that position (Figure 5.3).

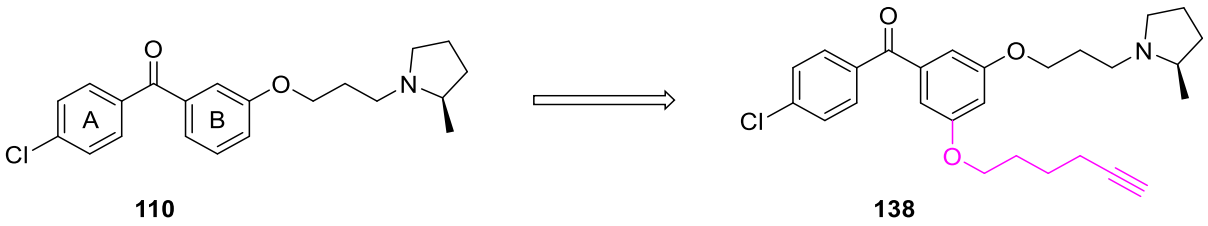

Figure 5.3. Design of chemical probe **138** based on compound **110**.

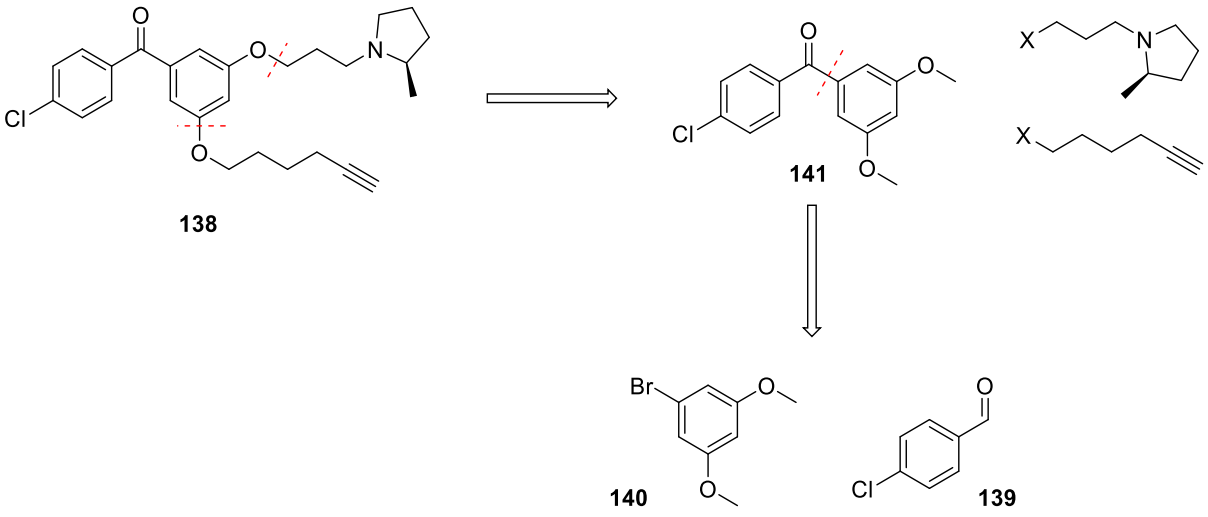

Figure 5.4. Retrosynthetic analysis of chemical probe **138**.

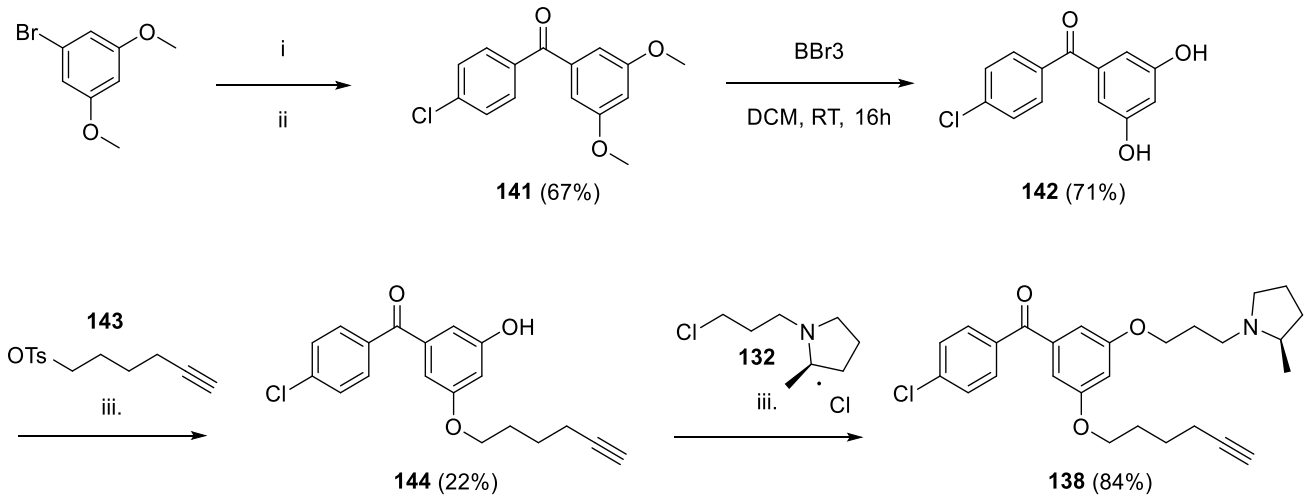

Figure 5.5. Synthesis of chemical probe **138**. i, nBuLi, THF, 30 min at -78ºC, then p-chlorobenzaldehyde **139**, 1h, RT; ii, $NaHCO_3$, DMP, DCM, RT, 16h; iii, K_2CO_3, KI, MeCN, RT, 16h;

Retrosynthetic analysis revealed benzophenone **141** as an intermediate, which could be synthesised using commercially available *para*-chlorobenzaldehyde **139** and 1-bromo-3,5-dimethoxybenzene **140** (Figure 5.4). The latter was lithiated with nBuLi, followed by reaction with the aldehyde **139** (Figure 5.5). The reaction mixture was washed with 1M HCl and the crude product extracted was directly submitted to oxidation by DMP to afford benzophenone **141** with 67% yield. This was demethylated using BBr_3, resulting in diphenol **142**, which was then mono-alkylated with tosylate **143**. Finally, alkylation with head group **132** afforded probe **138** in 84% yield (Figure 5.5).

5.2.3. Preliminary assays

The probe **138** was first assayed against *L. amazonensis* to evaluate if it retained activity when compared to analogue **110** (Figure 5.6). The addition of such linker adds on to the lipophilicity of the molecule and might change its uptake, however EC_{50} value remained below 2 µM. The drop of 7.5-fold in the EC_{50} value is within an

expected range of up to 10-fold difference, considering examples in the literature [114,116], and therefore was not considered a red flag to future experiments.

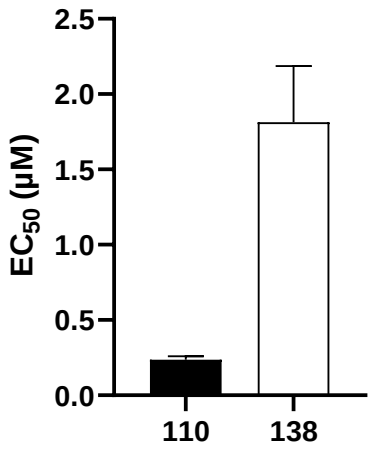

Figure 5.6. EC_{50} values of compounds **110** and **138** against *L. amazonensis*. Bars represent the mean and standard error of the mean of three independent experiments.

To evaluate if the probe **138** was functioning, a preliminary assay was performed (Figure 5.7). Live cells were incubated with the probe, followed by irradiation to activate the PAL by the benzophenone. Once lysates were produced, samples were submitted to the click chemistry reaction (CuAAC) with the fluorophore rhodamine azide and run in an SDS-PAGE gel. After fluorescence detection, strong bands at 25, 50 and 100 kDa were visible, together with other more weakly labelled bands throughout the lanes (Figure 5.7, Lanes 2 and 3), which were not seen in the negative control (Figure 5.7, Lane 1). This indicated that the probe **138** was functional. Current efforts in partnership with Dr. Exequiel Porta (Durham University) are towards further optimising this labelling and performing proteomic analysis that will identify the bound proteins.

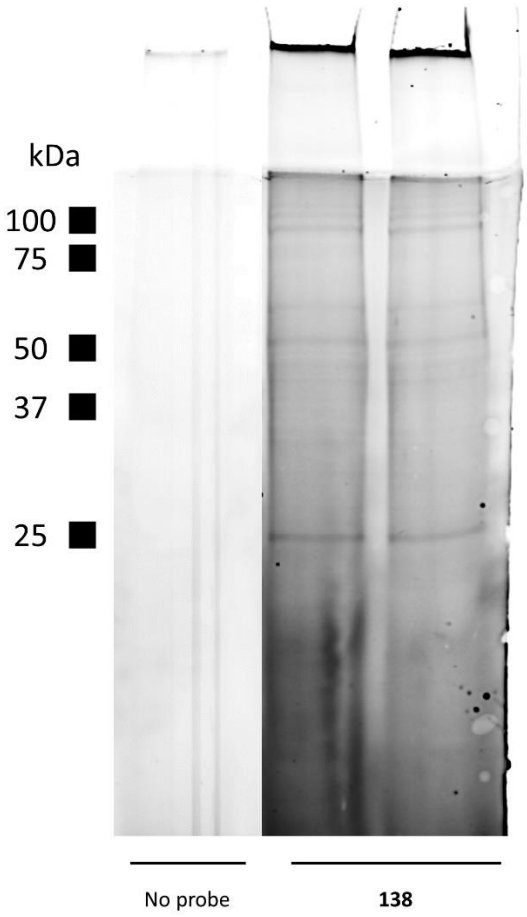

Figure 5.7. In-gel labelling of *L. mexicana* promastigotes with probe **138**. *Log*-phase promastigotes were incubated on ice with 100 uM of **138** for 30 min. After, a UV lamp (30 W, λmax 350 nm) was positioned 5cm above and used to irradiate the solutions for 1h. Cells were lysed and submitted to click chemistry with rhodamine azide fluorophore that allowed for fluorescence detection (emission at 560 nm) in an SDS-page gel. The first lane represents the negative control in which no probe was used, and the remaining two lanes represent biological replicates of the treatment with probe **138**.

5.3. Drug resistance and genomics

5.3.1. Introduction

Evaluation of drug resistant parasites has been a widely used strategy to deconvolute unexplored molecular targets and mechanisms of action of antimalarial and antitrypanosomatid chemotherapies [117]. By making use of resistant lines, next

generation sequencing (NGS) techniques are applied to find differentially expressed genes responsible for the resistance phenotype. For example, this approach was especially important in identifying the miltefosine transporter (MT), a phospholipid transporter responsible for the influx of miltefosine and, therefore, essential for its antileishmanial activity [118].

When studying novel compounds, resistant lines generated/selected in-house are more accessed by applying various techniques of drug pressure to wild type lines. One strategy first requires the overexpression of genomic libraries by a population of parasites in what is called Cos-Seq [119,120]. Another requires pre-treatment with a mutagen, such as MNNG (methylnitronitrosoguanidine), which causes random point mutations [121]. These populations undergo drug pressure, potentially selecting a pool of resistant parasites. When Cos-Seq is used, the resistant population is sequenced and the overexpressed chromosome regions responsible for the resistance phenotype are identified. MNNG-treated populations, however, undergo cloning for the isolation of potentially different mutations responsible for the phenotype before sequencing. Once genes are identified, they must be genetically validated, by CRISPR/Cas9 or homologous recombination. Besides these two techniques of resistance selection, the step-wise selection is the gold standard for the generation of resistant lines. This involves constant drug pressure of wild type lines under increasing concentrations of a compound over time [121]. Different kinds of mutations can take place, such as amplification of genes and/or chromosomes, deletions, and point mutations, and might require long periods of time to successfully select a resistant line. The successful selection of resistant lines by step-wise selection is a lengthy process when compared to the other techniques, taking up to 6 months depending on the compound.

The study of resistant lines generated in-house are most commonly, but not exclusively, used to explore potential molecular targets. The resistance mechanisms found may sometimes be extrapolated to the ones found in the field, however in most cases mutations are not always of clinical relevance. For instance, in the case of miltefosine resistance, mutations on MT are rarely found in clinical isolates, meaning that other resistance mechanisms take place .

In summary, the evaluation of drug resistant parasites is a hypothesis-free and unbiased method widely used for target deconvolution in drug discovery programs. The combination of NGS with other omics, such as transcriptomics and proteomics, allow for the selection of single genes that participate on the mechanism of action of a compound of interest. Although general genetic plasticity of parasites might lead to compensatory changes in gene expression that may hide the real molecular targets, this strategy is a reliable way of, at the very least, providing insights into the pathways involved in the compound activity.

5.3.2. Selection of L. amazonensis *lines resistant to 110*

Firstly, compound **110** was selected as the most active compound against *Leishmania* promastigotes, for resistance induction *in vitro*. Between the two parent molecules, tamoxifen has proven impossible to select for resistance *in vitro* [122]. Step-wise drug pressure with increasing concentrations of clemastine, however, was able to select resistant *L. major* promastigotes in a recent study by our group [97]. Sequencing of these lines revealed mutations within genes in the sphingolipid biosynthetic pathway. Knowing the potential mutations that lead to resistance to clemastine rendered this compound a good experimental control. In parallel, miltefosine was also used, considering that resistance selection for this compound is well established with a known phenotype.

The step-wise selection was discarded as the method of choice due to time limitations. Instead, *L. amazonensis* promastigotes were treated with the methylating agent MNNG before selection with the compounds of interest, following pipeline outlined in Figure 5.8. Once the cultures reached a density above $2x10^7$ cells/mL after treatment with MNNG, promastigote cultures were exposed to 2 µM of **110**, 0.2 µM of clemastine and 75 µM of miltefosine. The starting concentrations selected for clemastine and **110** were four times the EC_{90} values against *L. amazonensis* for each compound (0.5 µM for **110** and 0.05 µM for clemastine), while the concentration of miltefosine is based on previous established experiments by the group [122]. Concentrations of drugs were progressively increased until WT cultures revealed no viable parasites whereas MNNG-treated parasites survived. After 20 days, MNNG-treated cultures exposed to both clemastine and **110** were growing at a concentration of 10 µM. These cultures were cloned in agar/M199 plates, from which ten colonies were selected at random and grown in 24-well plates. Five colonies were selected at random from this set and grown into culture flasks for activity evaluation (Figure 5.9).

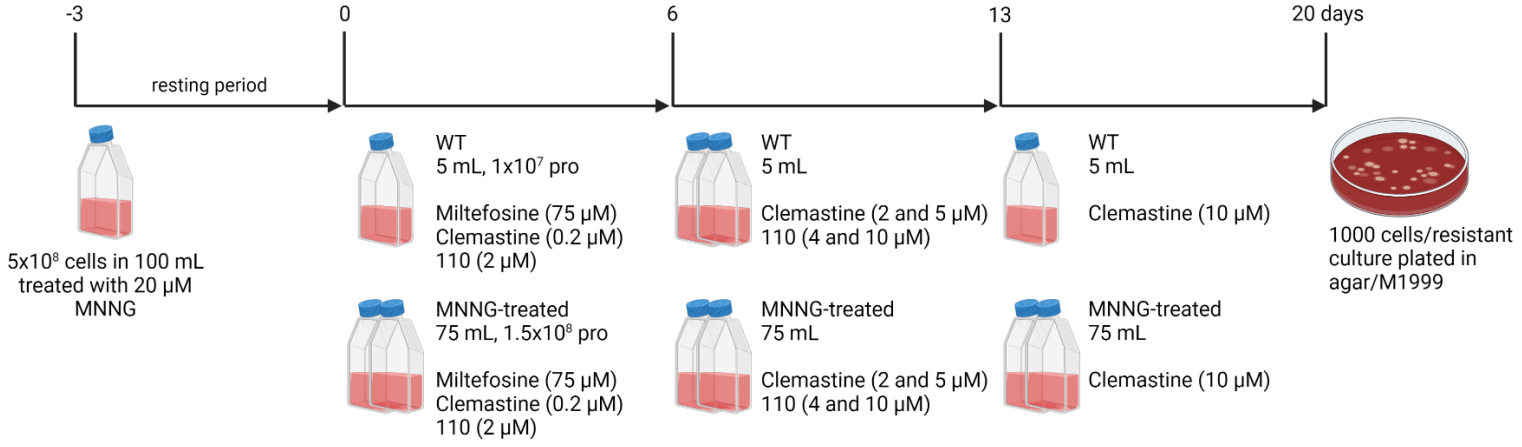

Figure 5.8. Timeline for selecting resistant lines of *L. amazonensis* to compound **110** and clemastine. $5x10^8$ stationary-phase promastigotes were treated for 4h with MNNG. Cells were washed with PBS and were resuspended in 100mL before resting under 25ºC for 3 days. During this time, culture was quantified daily and, once it reached a density above $2x10^7$ promastigotes/mL, selection pressure with

miltefosine, clemastine and compound **110** started. Two culture flasks containing 1.5x10^8 MNNG-treated promastigotes were prepared for treatment with each compound. In parallel, one bottle with WT cells was also treated with the compounds. Drug concentration was increased after 6 and 13 days. Finally, after 20 days, once it was clear that drug concentration was enough to clear WT cultures, 1000 cells of each resistant culture was plated in agar/M199 for selection of clones.

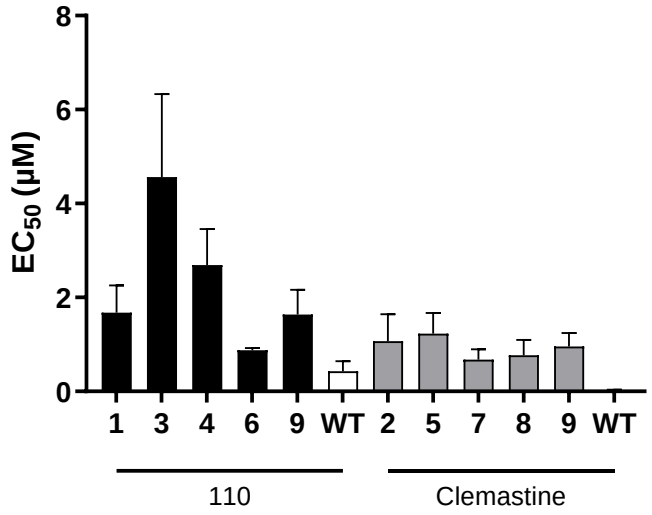

Figure 5.9. EC_{50} values of compounds **110** and clemastine against *L. amazonensis* resistant clones and WT lines. Bars represent the mean and standard error of the mean of three independent experiments.

There was an increase in the EC_{50} values against all the selected clones when compared to the WT. These ranged from a 2- to a 10-fold difference for compound **110**, and a surprisingly high 21- to 38-fold difference for clemastine, confirming that resistance to both compounds was successfully achieved.

Although not possible in the timeframe available, the next steps would be to evaluate cross-resistance of these clones to other hybrid compounds. This would be important to guarantee that results gathered from these lines could be extrapolated to other compounds of the library, including compound **130** which had the highest activity against intracellular amastigotes. In parallel, the maintenance of resistant phenotype will be assessed in intracellular amastigotes. Once this is confirmed, these lines will

be submitted for NGS which will allow for the comparative evaluation of resistant and WT lines and consequent identification of potential genes involved in the resistance phenotype. These will be validated genetically by generating mutant lines using CRISPR/Cas9 technology.

6. Conclusions and Future Work

6.1. Conclusions

In the recent years, two different drug discovery projects applying repurposing strategies found clemastine **27** and tamoxifen **28** as potent alternative chemotherapeutics for the treatment of leishmaniasis. Although it was found that these drugs share IPCS as their common target, this is a membrane-bound protein, and its crystal structure has not yet been solved due to experimental limitations. Therefore, chemoinformatic strategies relying on the target proteins were not applied for the chemical optimisation of these drugs against *Leishmania*. Thus, the initial hypothesis of this project was that the similar chemical features between clemastine **27** and tamoxifen **28** could be exploited for the improvement of their antileishmanial activity. To test that, a series of chimeric molecules was designed, synthesised, and tested against both promastigote and amastigote forms of several species of *Leishmania*. For the synthesis, a benzophenone scaffold was used as a result of the combination of the diaryl ethene from tamoxifen **28** and diaryl carbinol from clemastine **27**. The biological screening of this library led to a structure-activity relationship investigation against the parasite, and the conclusions are summarized in Figure 6.1.

The chlorine substituent present in clemastine **27** majorly improved the activity, however the isopropyl group was not tolerated. This was associated to a steric effect of this group that impaired protein binding. Knowing that a bulky group was not tolerated, this finding opens room for the investigation of other small substituents, including ones of varied electronic environments that may influence the aromaticity of the ring. This effect could not be explored in the present studies considering that analogues with a methyl and a chlorine substituent, which are respectively weak electron-donating and electron-withdrawing groups, displayed similar activity. It was

hypothesised that EDG may impact negatively the activity based on the fact that compounds with the phenol ether head group in *meta* were more active than the ones in *ortho* or *para*. This was potentially because the *meta*-phenol ether is electronically different considering that the oxygen does not participate on the aromaticity of the ring. The same effect was not observed when varying the position of the chlorine substituent around the ring, probably because it is a weak EWG. However, the presence of a small substituent (methyl or chlorine group) alone improved the activity overall.

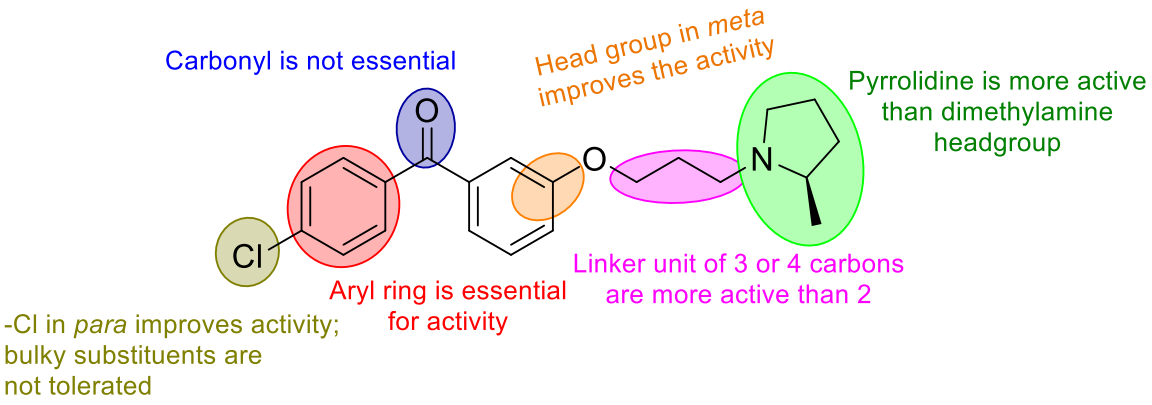

Figure 6.1. Structure-activity relationship of tamoxifen/clemastine hybrid molecules against *Leishmania* promastigotes.

In addition, it was found that molecules with a linker unit of 3 or 4 carbons were frequently more active than the ones with 2 carbons, which was previously seen in our group by Charlton [98]. This was interesting considering that both parent drugs have a linker unit of 2 carbons, suggesting a chemical improvement that could even be applied to their structures directly. A longer carbon linker unit is hypothesised to enhance the flexibility and, therefore, the accessibility of the head group to its binding pockets. This hypothesis is strengthened when analysing the more rigid molecules of the library, part of the *ortho*-BP series, in which the head group was locked in the *ortho*-position to the central ketone. This series contained the least active molecules

– a few were even considered inactive – when compared to the *para*-BP and *meta*-BP series, which had the head group in a more available position. When analysing the parent molecules, it is possible to conclude that, in both cases, the head group is spatially available, either being in the *para*-position, like in tamoxifen **28**, or as a central alkyl ether, like in clemastine **28**.

The diaryl system present in both parent molecules was confirmed to be essential for the activity. In this study, the diaryl system was mainly explored in the form of a benzophenone. However, when the central ketone was replaced by other groups, the antileishmanial activity remained similar. This suggests that flexibility around the rings may also impact the activity. Considering that clemastine **27** is composed of a flexible diaryl carbinol as opposed to the less active tamoxifen **28**, more flexibility between the rings may result in higher activity. For instance, compound **130**, which contained a diphenyl ether scaffold instead of a benzophenone, had the highest activity against intracellular amastigotes. Therefore, investigating other diaryl-containing scaffolds could represent further optimisation of the chimeric molecules.

Hybrids containing a pyrrolidine moiety like in clemastine **27** displayed higher activity than the dimethylamine group from tamoxifen **28**. This could be another chemical feature of tamoxifen **28** responsible for its lower antileishmanial activity when compared to clemastine **27**. When substituting clemastine's **27** head group by the dimethylamine group, Charlton demonstrated a huge loss in activity against both *L. major* (from EC_{50} = 0.17 µM to 70 µM) and *L. amazonensis* (from EC_{50} = 0.020 µM to 51 µM) promastigotes [98]. A molecule in which tamoxifen's **28** head group is replaced by a pyrrolidine-containing head group has not been obtained, however it could help address the essentiality of the pyrrolidine for the antileishmanial efficacy, together with the SAR insights raised in the present study.

The screening workflow established led to the identification of 7 hit molecules with an overall high activity over all promastigote and intracellular amastigote species tested, in addition to desired selectivity. In special, analogues **110** and **111** had the highest activities against the promastigotes, whilst analogue **130** was the most active against intracellular amastigotes. The hybrids demonstrated a drastic improvement in activity from tamoxifen **28** in all species tested, however their efficacy was never superior to clemastine **27**. On the other hand, both parent molecules have challenging chemistry; clemastine **27** displays a chiral carbinol and a head group with a lengthy synthetic route [98,109], whilst tamoxifen **28** is composed of a challenging tri-aryl scaffold with a specific *trans* conformation [123,124]. By exploiting the similarities between these two drugs, the hybrids obtained were of easier and accessible chemistry, making use of cheap commercially available starting materials without challenging chiral centres or isomerism. Overall, although clemastine **27** remained the most active compound tested so far, the hybrids successfully displayed a desired submicromolar activity together with an easy synthesis, which are attractive components to drug discovery for NTDs.

Altogether, this confirms the initial hypothesis that exploring chemical similarities between two molecules can be a successful strategy of chemical optimisation in drug discovery programs. This can be used in particular with repositioned drugs, in which chemical optimisation is not often applied to enhance their efficacy against their new targets or to find easier synthetic routes that may cheapen the production costs. Although repositioning drugs benefit from identifying approved molecules with known safety profiles, it is common that when applied to another disease they may not be as active or selective as a NCE fully developed for that purpose. By using chimeric molecules inspired by repurposed drugs, the time spent

with the design and synthesis of a library may be reduced by focusing on the similarities between two – or more – drugs. However, in this context, chimeric molecules are NCE that are designed based on repurposed drugs, which makes their safety profiling a requirement and, therefore, a disadvantage in relation to applying repurposed drugs directly.

After identifying the hit molecules within the clemastine/tamoxifen hybrid library, the next hypothesis was if these compounds had the same targets as their parent drugs – especially IPCS. A preliminary assay of compounds **110** and **111** against an *L. mexicana* $^{IPCS\ -/-}$ line revealed that this line was less sensitive to both compounds when compared to the WT. This supported the initial hypothesis that the similar chemical features shared by clemastine **27** and tamoxifen **28** were responsible for targeting IPCS. Two techniques were chosen to explore this and other potential molecular targets: chemical proteomics with the use of chemical probes, and the generation of resistance *in vitro* followed by genome sequencing. A chemical probe based on analogue **110** was successfully synthesised and preliminary data indicates that the probe is functional, however experimental conditions still require optimisation. The strongest band labelled was at 25 kDa, which is a lower weight than IPCS (38 kDa), suggesting that other proteins are targeted by the hybrids. This encourages the hypothesis that the hybrids may have retained the known polypharmacology of the parent molecules. In addition, resistant lines to analogue **110** and clemastine were generated and are in the process of characterisation against intracellular amastigotes. Unfortunately, due to time limitations, these studies were not completed.

6.2. Future work

Although the hybrids produced had higher antileishmanial activity *in vitro* than tamoxifen **28**, their activity was never superior to clemastine **27**. The SAR studies described here highlighted potential areas for further investigation that could improve the antileishmanial efficacy of the hybrid molecules. For instance, knowing that the chlorine substituent improves the activity, the immediate suggestion is to add it to analogue **130**, which could potentially lead to an optimal compound with an even higher activity against intracellular amastigotes. The scaffold **147** could be obtained by an Ullman condensation between 3-methoxyphenol **145** and *p*-chloroiodobenzene **146**. The scaffold **147** would then undergo previously described steps of demethylation and alkylation to afford analogue **148**.

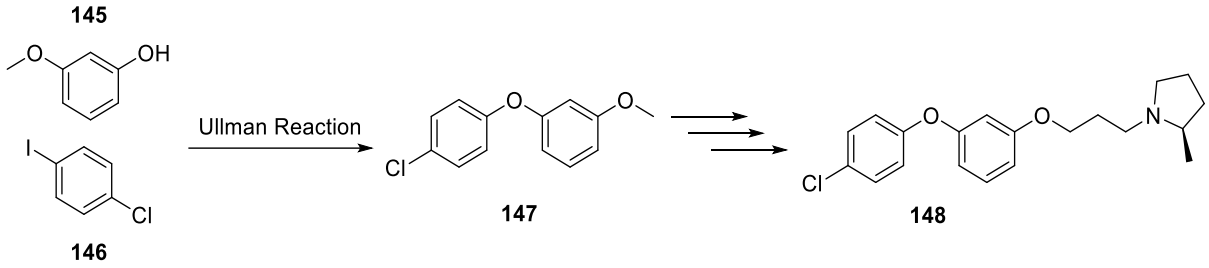

Figure 6.2. Scheme for the synthesis of scaffold **147** and analogue **148**.

In addition, other substituents besides chlorine could be explored, especially strong EWG and EDG, to investigate the impact of electronically different groups on the activity. Likewise, more variations on the pyrrolidine head group, such as removal of the methyl group, would be important to strengthen the insights regarding the essentiality of the chiral methyl group in that ring for activity.

The biological activity of analogue **137** was not sufficiently explored in this work, considering it had the highest activity against *L. major* promastigotes (EC_{50} = 62 nM). Analogue **137** was the only compound with an activity in the nanomolar range. Having

its activity against both promastigote and intracellular amastigotes species would open room to exploring the central alkyne as an important moiety for antileishmanial activity.

The hit molecules identified were highly active against all models tested and portray desirable EC_{50} and SI values in a drug candidate. The next steps are the evaluation of their metabolic stability *in vitro* using hepatic microsomes of humans and mice, as well as their solubility in gastrointestinal fluids. These would be essential to predict the drug-like properties of the hit molecules, which could support pre-clinical studies in mice models.

Regarding the chemical proteomics, preliminary data has shown that the chemical probe **138** was able to bind to low molecular weight proteins that remain unidentified. The next steps are to optimise the labelling conditions and perform the quantitative proteomics that will reveal the bound proteins. In parallel, the *L. amazonensis* lines resistant to **110** and clemastine will be prepared for genomic sequencing and bioinformatic analysis after phenotype characterisation in intracellular amastigotes. Together, these two methods will overlap in identifying the molecular targets of compound **110**. Competition assays between the chemical probe and the parent drugs or other hit molecules would allow identification of targets that are shared by them. Likewise, testing these molecules against the resistant lines obtained for cross-resistance would also hint on the shared targets. These studies could raise insights on the molecular features necessary to hit certain targets and help the design of future molecules.

7. Experimental details

7.1. Biological experimental

7.1.1. Leishmania *culture*

Leishmania amazonensis (MHOM/BR/1975/JOSEFA), *Leishmania major* (FV1), *Leishmania braziliensis* (MHOM/BR/1994/H3227) and *Leishmania infantum* (MHOM/BR/1972/LD) were cultivated at 25ºC in one of two media: (a) Schneider's insect medium at pH 7, supplemented with 15% FBS and 1% PenStrep; (b) 199 culture medium (Sigma-Aldrich, St. Louis, MO, USA), complemented with HEPES 40 mM, pH 7.4, adenine 0.1 mM, hemin 0.005% and supplemented with bovine fetal serum 10% (Gibco®), inactivated and sterile, and penicillin/streptomycin 100µg/ml. Parasites were subcultured every 4 days.

7.1.2. HepG2 cell culture

HepG2 cells were cultivated at 37ºC in a 5% CO_2 atmosphere in DMEM supplemented with 10% FBS and 1% PenStrep. Cells were split every 3 days by removing the media and adding trypsin, which incubated for 10 min at 37ºC in a 5% CO_2 atmosphere. Trypsin was deactivated by adding 20 mL fresh media, which was homogenised and added to a new culture flask in a 1:4 proportion.

7.1.3. Antipromastigote dose-response assay

Log-phase promastigotes were quantified using a Neubauer chamber and suspended in fresh medium to a density of 1 x 10^6 parasites/ml. In a 96-well plate, 1x10^5 parasites were applied per well and the parasites were incubated at 25ºC in increasing concentrations of each compound for 44 hours. Then, either 10 µL of 0.1

mg/mL Resazurin solution (Fisher Scientific, Leicestershire, UK) or 50 µL of 5 mg/mL MTT (Sigma-Aldrich, St. Louis, MO, USA) were added per well and the plate was incubated for 4 hours at 25ºC. For the plates in which resazurin was added, fluorescence was excited at 555 nm and read at 585 nm using the PolarStar Omega luminometer (BMGLabTech). In the cases where MTT was used, 50 µL of 20% SDS was added to lyse the cells, followed by absorbance reading using the same plate reader at 595 nm and a reference reading at 690 nm, which was subtracted from the first. EC_{50} values were obtained by GraphPad Prism 6, after determination of sigmoidal regression curves. At least three independent experiments were performed for each molecule with all samples in triplicates. Every plate had tamoxifen and/or clemastine as the control.

7.1.4. Anti-intramacrophage amastigote dose-response assay

Firstly, BMDM were generated at 37ºC in a 5% CO_2 atmosphere, after extraction of the bone marrow from BALC/c male mice. The extraction was followed by incubation for seven days in Petri dishes in RPMI medium containing 20% FBS and 30% L929 cells supernatant. This long incubation period is important for the differentiation of the bone marrow cells into macrophages. On the fourth day, supernatant is transferred into a new Petri dish and fresh media is added to all cultures. The cells were then detached with a scraper, quantified by Neubauer chamber, and plated in 96-well plates with a density of $8x10^4$ cells/well in 100 µL/well. After incubation for 24 hours at 37ºC in a 5% CO_2 atmosphere, cells were infected with stationary phase promastigotes (fourth day of culture) in a proportion of 20:1 for both *L. amazonensis* and *L. infantum*, and 30:1 for *L. braziliensis* (parasite:macrophage). After 4 hours of incubation at 34ºC, 200 µL of fresh medium containing several concentrations of the compounds tested was added to the wells, and the plates were

incubated for 72 hours at 34ºC. The supernatant was discarded, and 15 µL of luciferin (One-Glo Luciferase Assay System, Promega) was added to the 96-well. After homogenization, light production was detected in a PolarStar Omega luminometer (BMGLabTech). Parasite survival in treated samples was determined based on the ratio of treated/untreated cells. EC_{50} values were obtained by GraphPad Prism 6, after determination of sigmoidal regression curves. At least three independent experiments were performed for each molecule with all samples in triplicates.

7.1.5. Cytotoxicity assay

The cytotoxicity effect of compounds was evaluated against both a human liver cancer cell line (HepG2) and a primary cell (BMDM) using the resazurin assay previously described (section 7.1.3) in a 96-well plate system. When HepG2 cell culture was approximately 80% confluent, cells were detached with a scraper and quantified using Neubauer chamber. After, they were resuspended in fresh DMEM medium to a density of 0.5 x 10^5 cells/mL, from which 200 µL were added to each well (1x10^4 cells) of a 96-well plateand incubated overnight at 37ºC in a 5% CO_2 atmosphere. In the case of BMDM, the cells were extracted, differentiated, and plated as described in the section 7.1.4. In both cases, after cells were plated, supernatant was removed and fresh media containing several concentrations of compounds was added and plates incubated at 37ºC on a 5% CO_2 atmosphere for 44 hours. 10 µL of 0.1 mg/mL resazurin solution (Fisher Scientific, Leicestershire, UK) were added to each well and incubated for 4h before fluorescence intensity was determined using a plate reader (excitation at 555 nm and emission at 585 nm). At least three independent experiments were performed for each molecule with all samples in triplicates. Every plate had tamoxifen or clemastine as the control. EC_{50} values were obtained by

GraphPad Prism 6, after determination of sigmoidal regression curves. At least three independent experiments were performed for each molecule with all samples in triplicates.

7.1.6. Selection of resistance in vitro *and cloning*

Log-phase promastigotes were quantified by Neubauer chamber and $5x10^8$ cells were treated for 4h at 25ºC with 20 µM of MNNG (methylnitronitrosoguanidine). After, promastigotes were centrifuged (1000 × g, 10 min) and resuspended in 20 mL of PBS. This process was repeated twice and, after one more centrifugation step, cells were finally resuspended in 100 mL of fresh M199. The culture was quantified daily and, when it reached a density above $2x10^7$ cells/mL, promastigotes were distributed into five culture flasks ($1.5x10^8$/75 mL per flask); two flasks were designated for exposure to each compound of interest (clemastine and **110**), and the last was exposed to 75 µM of miltefosine, as the experimental control. In parallel, one culture flask containing untreated promastigotes ($1x10^7$ cells/5 mL per flask) was exposed to each one of the three compounds, which was used as the control for the lethal dose of the drug in question. These cultures were here referred to as WT. Starting concentration in both flasks for clemastine was 0.2 µM and for **110** was 2 µM. After a week, when it was confirmed that these doses were not lethal to WT cultures, promastigotes were washed as described previously and submitted to increased concentrations of clemastine (2 µM and 5 µM) and **110** (4 µM and 10 µM). This time, each one of the flasks had a different concentration, which allowed for “step-wise”-like selection in case the highest concentration was too lethal. After six days, the concentrations of clemastine in both flasks were increased to 10 µM, which finally proved to be the ideal dose to clear WT cultures of viable promastigotes.

The next step was to isolate clones of the resistant population. Initially, 2% sterile agar was heated to about 60ºC. 12.5 mL 2% agar were added to a tube containing 12.5 mL of medium 199 2x supplemented with biopterin 1.2 µg/mL heated in a water bath at 42ºC. The mixture was poured into a Petri dish. The final composition of the medium on the plate will be 1x medium 199, 1% agar and 0.6 µg/mL biopterin. The cultures were then quantified by Neubauer chamber and 1000 promastigotes were collected and diluted in medium 199 to a final volume of 200 µL, which were plated carefully with a Drigalski loop. Plates were incubated at 25ºC for at least one week, when the colonies started to be visible. 10 colonies were picked and transferred to a 24-well plate with 2 mL of fresh medium. After 72h, 5 clones were then randomly selected, and an anti-promastigote assay was performed to evaluate the resistance of each clone.

7.1.7. Probe labelling and lysate production

L. mexicana log-phase promastigote culture was centrifuged (1000 × g, 10 min) and resuspended in 100 µL of Schneider media containing 100 µM of probe **110** in a PCR microtube covered with aluminium foil for incubation on ice for 30 min. After, a transilluminator with an UV lamp (30 W, λmax 350 nm) was positioned at 5 cm directly above the open tubes. Tubes were irradiated for 1h before promastigotes were harvested (1000 × g, 5 min, 4°C), washed three times with cold PBS, and lysed with Pierce IP ThermoFisher lysis buffer (25 mM Tris HCl, pH 7.4, 150 mM NaCl, 1% NP-40, 1 mM EDTA, 5% glycerol). The resulting lysates were centrifuged (13,000 × g, 10 min, 4 °C) to remove insoluble material. The protein concentration in each sample was quantified using Pierce Rapid Gold BCA Protein Assay Kit (ThermoFisher) according

to the manufacturers' protocol and homogenates were adjusted to a concentration of 2 mg/mL.

7.1.8. SDS-PAGE Protein gels

Protein samples obtained following general procedure 7.1.7 were mixed with Laemmli 4X sample loading buffer and incubated at 95 °C for 10 min. 10-15 µL were loaded on 12% polyacrylamide-SDS gels. Samples were separated at 200 V for 1 hour in a MiniProtean system (BioRad) containing 1x running buffer, obtained by dilution a 10x running buffer (25 mM Trist, pH 8.3, 250 mM glycine and 0.1% SDS). Protein ladders (BioRad) were loaded onto gels as a molecular weight standard. At the end of each run, gel images were taken to detect fluorescent bands using the procedure 7.1.10. Subsequently, gels were stained with Quick Coomassie Brilliant Blue G-250 (Bio- Rad) to detect all protein bands, following the manufacturer instructions.

7.1.9. Biorthogonal Cu catalysed click chemistry

Leishmania lysates obtained following the general procedure 5.2.1.5 were incubated with the probe in the stated concentrations at rt for 1 h. After this period, TAG-N3, NaAsc (1 mM), TBTA (0.1 mM) and $CuSO_4$ (1 mM) were added respectively, and the mixture was incubated for a further 1 h with periodic mixing. The reaction was then stopped by addition of 4X LDS sample buffer and samples were analysed by in-gel analysis following procedure 7.1.8.

7.1.10. Fluorescent Imaging

At the end of each SDS-PAGE run, fluorescent bands were detected, and images were taken using a Typhoon 9400 Variable Mode Imager. Emission filter: 580 BP 30 Cy3, TAMRA, AlexaFluor546; Laser: green (532 nm).

7.1.11. Statistical analysis

All statistical analyses were performed by GraphPad Prisma 6 (CA, USA), using ANOVA *one-way* test and multiple comparisons Dunnett's test. *P* value < 0.05 was considered as statistically significant.

7.2. Chemistry experimental

7.2.1. General Conditions

All solvents and reagents were purchased from commercial suppliers. NMR spectra were recorded on the following instruments: Bruker Neo 700 MHz spectrometer with operating frequencies of 699.73 MHz for 1H, 175.95 MHz for 13C, 658.41 MHz for 19F, and 283.25 MHz for 31P; Varian VNMRS-600 spectrometer with operating frequencies of 599.42 MHz for 1H, 150.72 MHz for 13C, 564.02 MHz for 19F, 242.65 MHz for 31P; Bruker Neo-400 spectrometer with operating frequencies of 400.20 MHz for 1H, 100.63 MHz for 13C, 376.57 MHz for 19F, 162.00 MHz for 31P; Bruker Avance III-HD400 spectrometer with operating frequencies of 399.95 MHz for 1H, 100.57 MHz for 13C, 376.33 MHz for 19F, 161.90 MHz for 31P; Bruker Avance III-HD-400 spectrometer with operating frequencies of 400.07 MHz for 1H, 100.60 MHz for 13C, 376.45 MHz for 19F, 161.95 MHz for 31P. Spectra were referenced relative to CDCl3 (δH 7.26 ppm, δC 77.16 ppm), DMSO-d6 (δH 2.50 ppm, δC 39.52 ppm) or CD3OD (δH 4.87 ppm, δC 49.00 ppm), D2O (δH 4.79 ppm) Chemical shifts are reported in parts per million (ppm), coupling constants (J) in hertz (Hz) and multiplicity as singlet (s), doublet (d), triplet (t), quartet (q), multiplet (m) or a combination thereof. All 1H NMR and 13C NMR spectral assignments were made with the aid of 1H1H COSY, 1H13C HSQC and 1H13C HMBC NMR experiments. Infra-red spectra were recorded on a PerkinElmer Frontier FTIR spectrometer equipped with a

Specac Quest ATR accessory with extended range diamond puck. IR assignments are reported in wavenumbers (cm-1). Thin layer chromatography was performed using Merck F254 silica gel 60 aluminium sheets pre-coated with silica gel. High resolution mass spectrometry (HRMS) and liquid chromatography mass spectrometry (LCMS) were recorded on a 164 Waters TQD mass spectrometer ESI-LC water (0.1 % formic acid): MeCN, flow rate 0.6 mL min-1 with a UPLC BEH C18 1.7 µm (2.1 mm × 50 mm) column.

7.2.2. Experimental procedures and compound characterisation

General procedure A: S_N2 reaction

Cs_2CO_3 (4.7 equiv.) was added to a solution of hydroxybenzophenone (1 equiv.) in anhydrous DMF or MeCN (0.03 M), and the resulting suspension stirred at RT for 30 min. Dibromoalkyl (5 equiv.) was then added and the solution stirred overnight at RT. The reaction mixture was diluted in water (X mL) and extracted with EtOAc (3 x X mL). The combined organic extracts were washed with brine, dried over $MgSO_4$, and concentrated under reduced pressure.

General procedure B: S_N2 reaction

To a solution of hydroxybenzophenone (1 equiv.) in anhydrous DMF (0.3 M), caesium carbonate (3.5 equiv.) and TBAI (0.1 equiv.) were added. The mixture was heated to 60ºC and stirred for 15 min. Alkyl chloride (2 equiv.) was then added and the resultant solution heated under reflux overnight. After cooling to room temperature, sat. $Na_2CO_{3(aq)}$ was added (X mL) and the products were extracted with EtOAc (3 x X mL). The combined organic layers were washed with sat. $NaCO_{3(aq)}$ (4 x 2X mL), dried over $MgSO_4$, filtered, and concentrated *in vacuo*.

(2'''*R*)-1-[(benzyloxy)carbonyl]pyrrolidine-2-carboxylic acid 52a [109]

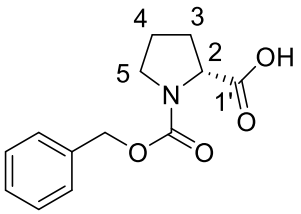

(D)-proline **26** (1 g, 8.62 mmol) in 2M $NaOH_{(aq)}$ (4.3mL) was added to a two-neck round-bottom flask and cooled to 0ºC. CbzCl (1.3 mL, 8.6 mmol) in 4M $NaOH_{(aq)}$ (2.1 mL) was added dropwise over 10 min while stirring. The solution was allowed to warm to RT and left to stir overnight. The mixture was acidified to pH 2 by a dropwise addition of 3M HCl(aq) and product was extracted with EtOAc (3 x 50 mL). The combined organic layers were dried over $MgSO_4$ and the volatiles removed under reduced pressure to afford the title compound **27a** as a colourless oil (2 g, 93%), which was used without further purification.

δ_H (400 MHz, $CDCl_3$) 11.14 (s, 1H, -COO***H***), 7.43 – 7.27 (m, 5H, Ar***H***), 5.30 – 5.05 (m, 2H, ArC***H₂***), 4.48 – 4.30 (m, 1H, 2-***H***), 3.70 – 3.39 (m, 2H, 5-***H₂***), 2.37 – 1.78 (m, 4H, 3-***H₂***, 4-***H₂***); δ_C (101 MHz, $CDCl_3$) 178.2 (***C***-1'), 176.9 (***C***-1'), 155.6 (N***C***O_2), 154.5 (N***C***O_2), 136.4 (Ar***C***), 136.5 (Ar***C***), 128.5 (Ar***C***), 128.4 (Ar***C***), 128.1 (Ar***C***), 127.9 (Ar***C***), 127.9 (Ar***C***), 127.6 (Ar***C***), 67.5 (Ar***C***H_2), 59.3 (***C***-2), 58.7 (***C***-2), 46.9 (***C***-5), 46.6 (***C***-5), 30.9 (***C***-3), 29.6 (***C***-3), 24.3 (***C***-4), 23.5 (***C***-4); *m/z* (LC-MS, ESI^+) 250 [$M+H^+$]. All data agrees with literature.

(2*R*)-1-(methoxycarbonyl)pyrrolidine-2-carboxylic acid 52b [98]

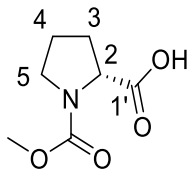

Methyl chloroformate (5 mL, 65.14 mmol) was added dropwise to a solution of (D)-proline (5.00g, 43.43 mmol) in THF (40 mL) and sat. $NaHCO_{3(aq)}$ (40 mL) at 0 °C. The mixture was let stirring overnight at RT. After, solution was acidified with 3M HCl to pH 2 and extracted with CH_2Cl_2 (3 x 30 mL). The combined organic layers were dried over $MgSO_4$ and volatiles were removed to afford the title compound **27b** (7.5g, 99%) as a colourless oil which was used without further purification.

δ_H (400 MHz, $CDCl_3$) 11.08 (s, 1H, -COO***H***), 4.40 – 4.19 (m, 1H, 2-***H***), 3.65 (d, *J* = 16.1 Hz, 3H, C***H₃***), 3.58 – 3.28 (m, 2H, 5-***H₂***), 2.27 – 1.99 (m, 2H, 3-***H₂***), 1.97 – 1.75 (m, 2H, 4-***H₂***); δ_C (101 MHz, $CDCl_3$, mixture of rotamers) 177.2 (***C***-1'), 176.6 (***C***-1'), 156.1 (N***C***O_2), 155.3 (N***C***O_2), 59.1 (***C***-2), 58.6 (***C***-2), 53.5 (***C***H_3), 52.9 (***C***H_3), 46.8 (***C***-5), 46.5 (***C***-5), 30.8 (***C***-3), 29.6 (***C***-3), 24.2 (***C***-4), 23.4 (***C***-4); *m/z* (LC-MS, ESI^+) 174 [$M+H^+$]. All data agrees with literature.

Benzyl (2*R*)-2-(2-diazoacetyl)pyrrolidine-1-carboxylate 53a [109]

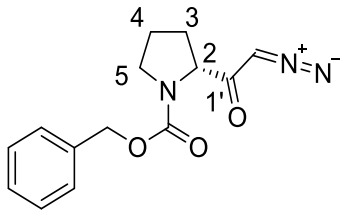

At 0ªC oxalyl chloride (0.2 mL, 2.28 mmol) was added dropwise to a solution of (2R)-1-[(benzyloxy)carbonyl]pyrrolidine-2-carboxylic acid **27a** (387 mg, 1.55 mmol) in DCM (5 mL), followed by DMF (3 drops). After 2 hours stirring, the volatiles were removed

under reduced pressure and a 1:1 mixture of THF (7 mL) and MeCN (7 mL) was added. After cooling the solution in an ice bath, NEt_3 (0.4 mL, 2.98 mmol) and $TMSCHN_2$ (2M solution in hexanes, 1.6 mL, 3.12 mmol) were added and stirred for 4h at RT. AcOH was then added to quench the reaction, which was diluted with H_2O, and stirred for 10 min before being concentrated under reduced pressure. The reaction mixture was diluted with EtOAc and washed with sat. $NaHCO_{3(aq)}$ (3 x 10 mL). The organic phase was then washed with brine (5 mL), dried over $MgSO_4$ and concentrated. Purification by column chromatography using 30% EtOAC in hexane afforded the diazoketone **28a** (206 mg, 49%) as a yellow oil.

δ_H (400 MHz, $CDCl_3$) 7.40 – 7.29 (m, 5H, Ar***H***), 5.49 (s, 1H, C***H***N_2), 5.21 – 5.07 (m, 2H, ArC***H₂***), 4.43 – 4.19 (m, 1H, 2-***H***), 3.64 – 3.42 (m, 2H, 5-***H₂***), 2.12 – 1.99 (m, 2H, 33-***H₂***), 1.99 – 1.82 (m, 2H, 4-***H₂***); δ_C (101 MHz, $CDCl_3$, mixture of rotamers) 195.3 (***C***-1'), 194.5 (***C***-1'), 155.2 (N***C***O_2), 154.6 (N***C***O_2), 136.5 (Ar***C***), 136.4 (Ar***C***), 128.6 (Ar***C***), 128.5 (Ar***C***), 128.5 (Ar***C***), 128.1 (Ar***C***), 128.0 (Ar***C***), 127.9 (Ar***C***), 67.2 (Ar***C***H_2), 64.1 (***C***-2), 53.8 (***C***HN_2), 47.4, 46.9 (***C***-5), 31.2 (***C***-3), 29.7 (***C***-3), 24.4 (***C***-4), 23.6 (***C***-4); *m/z* (LC-MS, ESI^+) 246 [$M-N_2+H^+$]. All data agrees with literature.

Methyl (2*R*)-2-(2-diazoacetyl)pyrrolidine-1-carboxylate 53b [98]

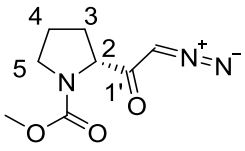

(2R)-1-(methoxycarbonyl)pyrrolidine-2-carboxylic acid **27b** (2g, 11.55 mmol) was reacted in the same fashion as the synthesis of Benzyl (2R)-2-(2-diazoacetyl)pyrrolidine-1-carboxylate. Title compound was obtained (1 g, 48%) as a yellow oil.

ν_{max} (ATR) 2105 (s, N_2), 1695 (s, C=O), 1643 (s, C=O) cm^{-1}; δ_H (400 MHz, $CDCl_3$, mixture of rotamers) 5.52 (s, 0.5H, C***H***N_2), 5.41 (s, 0.5H, C***H***N_2), 4.44 – 4.31 (m, 0.5H, 2-***H***), 4.32 – 4.20 (m, 0.5H, 2-***H***), 3.75 (s, 1.5H, C***H₃***), 3.72 (s, 1.5H, C***H₃***), 3.64 – 3.49 (m, 1.5H, 5-***H***H', 5-H***H'***), 3.49 – 3.40 (m, 0.5H, 5-H***H'***), 2.29 – 2.16 (m, 0.5H, 3-***H***H'), 2.16 – 2.02 (m, 1.5H, 3-***H***H', 3-***H'***), 2.02 – 1.84 (m, 2H, 4-***H₂***). δ_C (101 MHz, $CDCl_3$, mixture of rotamers) 195.5 (***C***-1'), 194.6 (***C***-1'), 155.9 (N***C***O_2Me), 154.9, 64.0(4) (***C***-2), 64.0(0) (***C***-2), 53.37 (***C***HN_2), 52.8 (***C***H_3), 52.7 (***C***H_3), 47.39 (***C***-5), 46.89 (***C***-5), 31.33 (***C***-3), 29.66 (***C***-3), 24.46 (***C***-4), 23.57 (***C***-4); *m/z* (LC-MS, ESI^+) 170 [M-N_2+H^+]. All data agrees with literature.

Benzyl-(2*R*)-2-(2-methoxy-2-oxoethyl)pyrrolidine-1-carboxylate 54a [109]

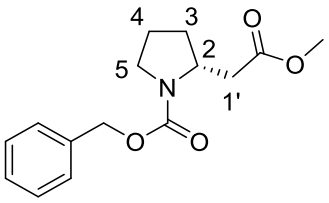

Silver benzoate (40 mg, 0.173 mmol) in NEt3 (0.7 mL, 5.27 mmol) was added to a solution of benzyl (2R)-2-(2-diazoacetyl)pyrrolidine-1-carboxylate **28a** (420 mg, 1.54 mmol) in dry MeOH (6.5 mL) and stirred at RT for 3h. The solution was then cooled in an ice bath and quenched by the dropwise addition of $Na_2S_2O_{5(aq.)}$ (20%, 4 mL) dropwise. The resulting mixture was filtered through Celite and washed with EtOAc (3 x 15 mL). The combined organic filtrate was washed once with brine (30 mL) and dried over $MgSO_4$. Volatiles were then removed under reduced pressure and crude product purified by flash column chromatography (20% EtOAC in hexane) to afford the title compound **29a** (292.6 mg, 69%) as a brown oil.

δ_H (400 MHz, $CDCl_3$, mixture of rotamers) 7.40 – 7.33 (m, 4H, Ar***H***), 7.33 – 7.27 (m, 1H, Ar***H***), 5.13 (s, 2H, ArC***H₂***), 4.35 – 4.15 (m, 1H, 2-***H***), 3.73 – 3.54 (m, 3H, C***H₃***),

3.52 – 3.32 (m, 2H, 5-***H₂***), 3.04 – 2.89 (m, 0.5H, 1-***H***H'), 2.88 – 2.70 (m, 0.5H, 1-***H***H'), 2.42 – 2.25 (m, 1H, 1-H***H'***), 2.14 – 2.01 (m, 1H, 3-***H***H'), 1.94 – 1.82 (m, 2H, 4-***H₂***), 1.81 – 1.63 (m, 1H, 3-H***H'***); δ_C (101 MHz, $CDCl_3$, mixture of rotamers) 171.9 (***C***O_2CH_3), 171.7 (***C***O_2CH_3), 154.7 (N***C***O_2), 136.9 (Ar***C***), 128.5 (Ar***C***), 127.9 (Ar***C***), 127.8 (Ar***C***), 66.8 (ArC***H₂***), 66.6 (ArC***H₂***), 54.6 (***C***-2), 53.9 (***C***-2), 51.6 (CO_2***C***H_3), 46.8 (***C***-5), 46.4 (***C***-5), 39.1 (***C***-1'), 38.2 (***C***-1'), 31.4 (***C***-3), 30.6 (***C***-3), 27.0, 23.6 (***C***-4), 22.7 (***C***-4); *m/z* (LC-MS, ESI^+) 278 [$M+H^+$]. All data agrees with literature.

Methyl (2*R*)-2-(2-methoxy-2-oxoethyl)pyrrolidine-1-carboxylate 54b [98]

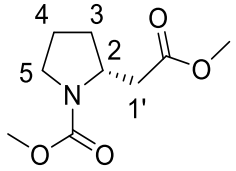

The title compound was prepared from methyl (2R)-2-(2-diazoacetyl)pyrrolidine-1-carboxylate **28b** (593 mg, 3.007 mmol) in the same fashion as the synthesis of Benzyl (2R)-2-(2-methoxy-2-oxoethyl)pyrrolidine-1-carboxylate **29a**. The methylester **29b** was obtained (507.6 mg, 84%) as a brown oil.

δ_H (400 MHz, $CDCl_3$, mixture of rotamers) 4.21 (s, 1H, 2-***H***), 3.76 – 3.65 (m, 6H, 2xCOOC***H₃***), 3.50 – 3.42 (m, 1H, 5-***H***H'), 3.41 – 3.30 (m, 1H, 5-H***H'***), 3.06 – 2.92 (m, 0.5H, 1'-***H***H'), 2.85 – 2.74 (m, 0.5H, 1'-***H***H'), 2.40 – 2.30 (m, 1H, 1'-H***H'***), 2.16 – 2.03 (m, 1H, 3-***H***H'), 1.94 – 1.83 (m, 2H, 4-***H₂***), 1.82 – 1.70 (m, 1H, 3-H***H'***); δ_C (101 MHz, $CDCl_3$, mixture of rotamers) 171.8 (***C***O_2CH_3), 171.7 (***C***O_2CH_3), 155.2 (N***C***O_2), 54.4 (***C***-2), 53.8 (***C***-2), 52.3 (CO_2***C***H_3), 52.1 (CO_2***C***H_3), 51.5 (CO_2***C***H_3), 46.7 (***C***-5), 46.3 (***C***-5), 39.0 (***C***-1'), 38.1 (***C***-1'), 31.3 (***C***-3'), 30.5 (***C***-3), 23.5 (***C***-4), 22.7 (***C***-4); *m/z* (LC-MS, ESI^+) 202 [$M+H^+$]. All data agrees with literature.

2-[(2*R*)-N-methylpyrrolidin-2'-yl]ethan-1'-ol 55 [109]

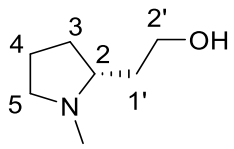

To a solution of $LiAlH_4$ (377.2 mg, 9.94 mmol) in anhydrous THF (5.5 mL) at 0ºC, methyl (2R)-2-(2-methoxy-2-oxoethyl)pyrrolidine-1-carboxylate **29b** (500 mg, 2.49 mmol) in anhydrous THF (6.5 mL) was added slowly. Mixture was refluxed for 4h and reaction was quenched with H_2O (1 mL) at 0ªC. A 3M NaOH(aq) solution (0.5 mL) was added and mixture was diluted with water until it became white, being left stirring for 10 min after. Solution was washed with EtOAc whilst being filtrated through Celite. Organic layer was dried over $MgSO_4$, filtered and volatiles were removed under reduced pressure, affording the title compound **30** (305 mg, 95%) as a colourless oil.

δ_H (400 MHz, $CDCl_3$, mixture of rotamers) 4.02 (td, *J* = 10.8, 2.9 Hz, 1H, 2'-***H***H'), 3.74 – 3.66 (m, 1H, 2-H***H'***), 3.14 – 2.99 (m, 1H, 5-***H***H'), 2.67 – 2.55 (m, 1H, 2-***H***), 2.38 (s, 3H, NC***H₃***), 2.23 – 2.13 (m, 1H, 5-H***H'***), 2.09 – 1.68 (m, 6H, 1'-***H₂***, 3- ***H₂***, 4- ***H₂***); δ_C (101 MHz, $CDCl_3$) 65.2 (***C***-2), 60.3 (***C***-2'), 57.0(***C***-5), 40.9 (N***C***H3), 31.2 (***C***-1'), 28.2 (***C***-3), 23.2 (***C***-4); *m/z* (LC-MS, ESI^+) 130 [$M+H^+$]. All data agrees with literature.

(2*R*)-2-(2-chloroethyl)-1-methylpyrrolidine hydrochloride 56 [109]

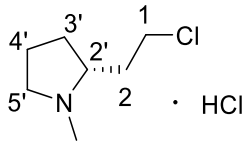

2-[(2*R*)-N-methylpyrrolidin-2'-yl]ethan-1'-ol **30** (215 mg, 1.66 mmol) in anhydrous chloroform (4 mL) was treated dropwise with thionyl chloride (0.45 mL, 6.20 mmol) at 0ºC. After refluxing for 2h, volatiles were removed under reduced pressure, affording

the crude chloride as a brown oil. Precipitation (cold ethanol-diethyl ether) afforded title compound **31** (193 mg, 63%) as a brown solid.

δ_H (400 MHz, $CDCl_3$, mixture of rotamers) 12.55 (s, 1H, N^+***H***), 3.97 – 3.87 (m, 2H, 5'-***H***H', 1-***H***H'), 3.63 – 3.55 (m, 1H, 1-H***H'***), 3.45 – 3.36 (m, 1H, 2'-***H***), 2.95 – 2.88 (m, 1H, 5'-H***H'***), 2.87 (d, *J* = 5.0 Hz, 3H, C***H₃***), 2.63 – 2.44 (m, 2H, 2-***H₂***), 2.42 – 2.26 (m, 2H, 3'-***H***H', 4'-***H***H'), 2.15 – 1.99 (m, 2H, 3'-H***H'***, 4'-H***H'***); δ_C (101 MHz, $CDCl_3$) 66.5 (***C***-2'), 56.3 (***C***-5'), 41.6 (***C***-1), 39.5 (***C***H_3), 32.4 (***C***-2), 29.3 (***C***-3'), 21.6 (***C***-4'); *m/z* (LC-MS, ESI^+) 148 [M(^{35}Cl)+H] and 150 [M(^{37}Cl)+H]) in a 3:1 ratio. All data agrees with literature.

2-benzoylphenyl trifluoromethanesulfonate

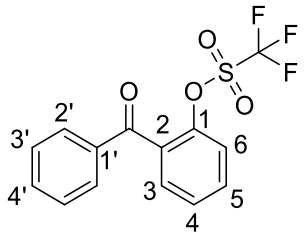

A solution of 2-hydroxybenzophenone (100mg) in dry pyridine (2.5 mL) was cooled down to 0ºC and stirred for 15 min. Trifluoromethylsulfonic anhydride (0.09 ml) was slowly added and mixture was stirred for a further 15 min. The solution was then allowed to warm up to RT and left to stir at this temperature overnight. The reaction mixture was then concentrated under reduced pressure, diluted in 1M HCl (aq) (25 mL), and were extracted with EtOAc. Combined organic extracts were washed with sat. Na_2CO_3 (aq), dried over $MgSO_4$ and concentrated under reduced pressure.

δ_H (700 MHz, $CDCl_3$) 7.83 – 7.80 (m, 2H, 2'-***H***), 7.65 – 7.61 (m, 2H, 4'-***H***, 5-***H***), 7.60 – 7.57 (m, 1H, 3-***H***), 7.52 – 7.47 (m, 3H, 3'-***H***, 4-***H***), 7.44 – 7.41 (m, 1H, 6-***H***); δ_C (176 MHz, $CDCl_3$) 192.6 (Ar_2***C***O), 146.8 (***C***-1), 136.5 (***C***-1'), 133.8 (***C***-4'), 132.6 (***C***-5), 132.5

(***C***-2), 131.2 (***C***-3), 130.1 (***C***-2'), 128.5 (***C***-3'), 128.0 (***C***-4), 122.4 (***C***-6); δ_F (376c MHz, $CDCl_3$) -73.44; Accurate mass: found [M+H] 331.0257, $C_{14}H_{10}F_3O_4S$ requires *M*, 331.0252.

(2'''*R*)-2'''-[2''-(2-benzoylphenoxy)ethyl]-1'''-methylpyrrolidine 60

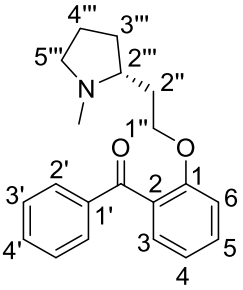

To a suspension of NaH (60% in mineral oil) (21 mg, 0.52 mmol) in anhydrous DMF (3.5 mL), 2-[(2*R*)-N-methylpyrrolidin-2'-yl]ethan-1'-ol **30** (70 mg, 0.54 mmol) was slowly added. After stirring for 1 hour, a solution of 2-fluorobenzophenone (70 mg, 0.35 mmol) was added slowly, and mixture stirred overnight. The reaction was then diluted with sat. $Na_2CO_{3(aq)}$ (15 mL) and products extracted with EtOAc (3 x 15 mL). The combined organic extracts were washed with sat. $Na_2CO_{3(aq)}$ (3 x 30 mL), dried over $MgSO_4$, filtered and concentrated under reduced. Sample was submitted to column chromatography (MeOH in DCM) to afford the ether (28.1 mg, 26%) as a yellow oil.

ν_{max} (ATR) 1662 (s, C=O), 1603 (s), 1455 (s), 1253 (s, C-O) cm^{-1}. δ_H (599 MHz, $CDCl_3$) 7.80 – 7.76 (m, 2H, 2'-***H***), 7.55 – 7.52 (m, 1H, 4'-***H***), 7.48 – 7.44 (m, 1H, 5-***H***), 7.44 – 7.40 (m, 3H, 3-***H***), 7.08 – 7.05 (m, 1H, 4-***H***), 6.97 – 6.93 (m, 1H, 6-***H***), 4.07 – 4.00 (m, 1H, 1''-***H***), 3.92 – 3.84 (m, 1H, 1''-***H***), 3.20 – 3.03 (m, 1H, 5'''-***H***), 2.17 (s, 3H, C***H₃***), 2.14 – 2.06 (m, 1H, 5'''-***H***), 1.94 – 1.82 (m, 2H, 2''-***H***, 2'''-***H***), 1.80 – 1.69 (m, 2H, 3'''-***H***, 4'''-***H***), 1.66 – 1.57 (m, 1H, 4'''-***H***), 1.56 – 1.46 (m, 1H, 2''-***H***), 1.42 – 1.31 (m, 1H,

3’’’-***H***); δ_C (151 MHz, $CDCl_3$) 196.7 (Ar_2***C***O), 156.5 (***C***-1), 138.4 (***C***-1’), 132.7 (***C***-4’), 132.1 (***C***-5), 129.7 (***C***-3), 129.5 (***C***-2’), 128.9 (***C***-2), 128.2 (***C***-3’), 120.8 (***C***-4), 111.9 (***C***-6), 65.7 (***C***-1’’), 63.9 – 62.8 (m, ***C***-2’’’), 56.7 (***C***-5’’’), 40.0 (***C***H_3), 33.0 – 31.4 (m, ***C***-2’’), 30.1 (***C***-3’’’), 21.7 (***C***-4’’’). Accurate mass: found [M+H] 310.1795, $C_{20}H_{24}NO_2$ requires *M*, 310.1807.

{2-[(2-bromophenyl)methoxy]ethyl}dimethylamine 32

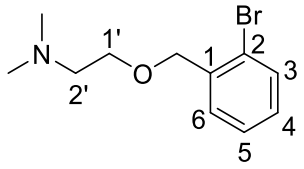

To a solution of NaH (384 mg, 16 mmol) in anhydrous THF (2 mL), 2-dimethylaminoethanol **34** (0.535 mL, 5.2 mmol) in anhydrous THF (4 mL) was slowly added. After heating under reflux for 1h, a solution of 2-bromobenzyl bromide **35** (1g, 4 mmol) and TBAI (148 mg, 0.4 mmol) in anhydrous THF (3 mL) was added dropwise, and mixture then heated under reflux overnight. The reaction was then diluted with water (10 mL) and products extracted with EtOAc (3 x 15 mL). The combined organic extracts were washed with 1M $HCl_{(aq)}$ (3 x 30 mL). The aqueous layers were then adjusted to pH 9 using 2M $NaOH_{(aq)}$ and product extracted with EtOAc (3 x 15 mL). The combined organic extracts were dried over $MgSO_4$, filtered and concentrated under reduced pressure to afford the title ether **36** (570 mg, 55%) as a colourless oil.

δ_H (700 MHz, $CDCl_3$) 7.52 (dd, *J* = 8.0 Hz, 1.2 Hz, 1H, 3-***H***), 7.49 (ddt, *J* = 7.7 Hz, 1.7 Hz, 0.8 Hz, 1H, 6-***H***), 7.13 (dd, *J* = 7.7, 1.7 Hz, 1H, 5-***H***), 7.31 (td, *J* = 7.5, 1.2 Hz, 1H, 4-***H***), 4.60 (s, 2H, ArC***H₂***), 3.65 (t, *J* = 5.8 Hz, 2H, 1’-***H₂***), 2.58 (t, *J* = 5.8 Hz, 2H, 2’-***H₂***), 2.29 (s, 6H, C***H₃*** x2); δ_C (176 MHz, $CDCl_3$) 137.7 (1-***C***), 132.4 (3-***C***), 129.0 (6-***C***), 128.8 (4-***C***), 127.3 (5-***C***), 122.6 (6-***C***), 72.3 (Ar***C***H_2), 68.9 (1’-***C***), 58.9 (2’-***C***), 45.9

(***C***H_3); *m/z* (LC-MS, ESI^+) 258 [M(^{79}Br)+H] and 260 [M(^{81}Br)+H]); Accurate mass: found [M+H] 258.0502, $C_{11}H_{17}NO^{79}Br$ requires *M*, 258.0494.

[(2-bromophenyl)methoxy](tert-butyl)dimethylsilane 35

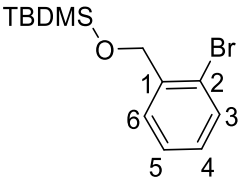

To a solution of 2-bromobenzyl alcohol (1 g, 5.35 mmol) in anhydrous DMF (8 mL) at RT, a mixture of tert-butyldimethylsilyl (TBDMS) chloride (1.2 g, 8 mmol) and imidazole (737 mg, 10.7 mmol) in anhydrous DMF (10 mL) was slowly added. After stirring overnight, the reaction mixture was diluted in ether (30 mL) and washed with water (4 x 100 mL). Organic phase was washed once with brine, dried over $MgSO_4$ and concentrated under reduced pressure. Purification by column chromatography (10% chloroform in petroleum ether 60-80ºC) afforded the title ether **40** (1.5 g, 93%) as a colourless oil.

δ_H (700 MHz, $CDCl_3$) 7.58 – 7.55 (m, 1H, 3-***H***), 7.50 (dt, *J* = 8.0, 1.3 Hz, 1H, 6-***H***), 7.33 (tt, *J* = 7.4, 1.2 Hz, 1H, 5-***H***), 7.14 – 7.10 (m, 1H, 4-***H***), 4.75 (s, 2H, ArC***H₂***), 0.98 (s, 9H, -C(C***H₃***)$_3$), 0.14 (s, 6H, -Si(C***H₃***)$_2$); δ_C (176 MHz, $CDCl_3$) 140.3 (***C***-1), 131.9 (***C***-3), 128.1 (***C***-4), 127.5 (***C***-6), 127.3 (***C***-5), 121.0 (***C***-2), 64.6 (Ar***C***H_2), 25.9 (C(***C***H_3)$_3$), 18.4 (***C***$(CH_3)_3$), -5.3 (Si(***C***H_3)$_2$).

{2-[2''-(dimethylamino)ethoxy]phenyl}(phenyl)methanol

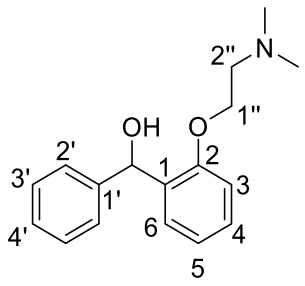

To a suspension of NaH (60% in mineral oil) (60 mg, 1.49 mmol) in anhydrous DMF (3 mL), 2-dimethylamino ethanol (0.08 mL, 0.77 mmol) was added. After stirring for 1 hour, a solution of 2-fluorobenzophenone (0.08 mL, 0.49 mmol) in anhydrous DMF (2 mL) was added dropwise, and mixture stirred overnight. The reaction mixture was then diluted with sat. $Na_2CO_{3(aq)}$ (15 mL) and extracted with EtOAc (3 x 15 mL). The combined organic extracts were washed with sat. $Na_2CO_{3(aq)}$ (3 x 30 mL), dried over $MgSO_4$, filtered and concentrated under reduced. Purification by column chromatography (MeOH in DCM) to afford title product (95 mg, 70%) as a white solid.

ν_{max} (ATR) 3000 (b, OH), 1455 (s), 1242 (s), 1035 (s). δ_H (700 MHz, $CDCl_3$) 7.43 – 7.39 (m, 2H, 2'-***H***), 7.32 (dd, *J* = 8.5, 7.0 Hz, 2H, 3'-***H***), 7.26 – 7.21 (m, 2H, 4-***H***, 4'-***H***), 7.07 – 7.03 (m, 1H, 6-***H***), 6.94 – 6.89 (m, 2H, 3-***H***, 5-***H***), 6.00 (s, 1H, $Ar_2C\boldsymbol{H}OH$), 4.15 – 4.10 (m, 2H, 1''-$\boldsymbol{H_2}$), 2.65 – 2.56 (m, 2H, 2''-$\boldsymbol{H_2}$), 2.28 (s, 6H, $C\boldsymbol{H_3}$); δ_C (176 MHz, $CDCl_3$) 156.7 (***C***-2), 143.6 (***C***-1'), 134.5 (***C***-1), 128.9 (***C***-6), 128.6 (***C***-4), 127.9 (***C***-3'), 126.6 (***C***-4'), 126.4 (***C***-2'), 121.4 (***C***-5), 113.8 (***C***-3), 72.4 ($Ar_2\boldsymbol{C}OH$), 66.0 (***C***-1''), 58.1 (***C***-2''), 45.0 ($\boldsymbol{C}H_3$).

[2''-(2-benzoylphenoxy)ethyl]dimethylamine 44

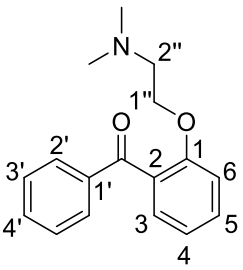

A solution of 2-hydroxybenzophenone (100 mg, 0.5 mmol) in anhydrous acetone (2 mL) was stirred with potassium carbonate (209 mg, 1.5 mmol) and potassium iodide (92 mg, 0.5 mmol) for 20 min when 2-dimethylamine ethylchloride hydrochloride (106 mg, 0.74 mmol) in anhydrous acetone (2 mL) was slowly added to the mixture. The reaction was then heated to 40ºC and stirred for 72 hours. After cooling, the reaction mixture was diluted with water and the products extracted with EtOAc (3 x 20 mL). The combined organic phases were washed with brine (20 mL), dried over $MgSO_4$ and concentrated under reduced pressure. Purification by column chromatography (10% MeOH in DCM) to afford the title compound **47** (43 mg, 32%) as a yellow oil.

ν_{max} (ATR) 1666 (s, C=O), 1298 (s, C-O), 1034 (w, C-N) cm^{-1}. δ_H (700 MHz, $CDCl_3$) 7.77 (dd, *J* = 7.1, 1.2 Hz, 2H, 2'-***H***), 7.55 – 7.51 (m, 1H, 4'-***H***), 7.47 – 7.44 (m, 1H, 5-***H***), 7.43 – 7.39 (m, 3H, 3'-***H***, 3-***H***), 7.05 (dt, *J* = 7.4, 0.9 Hz, 1H, 4-***H***), 6.97 (dd, *J* = 8.4, 0.9 Hz, 1H, 6-***H***), 4.00 (t, *J* = 5.8 Hz, 2H, 1''-C***H₂***), 2.37 (t, *J* = 5.8 Hz, 2H, 2''-C***H₂***), 2.10 (s, 6H, C***H₃*** x2); δ_C (176 MHz, $CDCl_3$) 196.7 (Ar_2***C***O), 156.7 (***C***-1), 138.3 (***C***-1'), 132.7 (***C***-4'), 132.0 (***C***-5), 129.7 (***C***-3), 129.6 (***C***-2'), 129.2 (***C***-2), 128.1 (***C***-3'), 120.8 (***C***-4), 112.6 (***C***-6), 67.3 (***C***-1''), 57.6 (***C***-2''), 45.8 (***C***H_3); Accurate mass: found [M+H] 270.1507, $C_{17}H_{20}NO_2$ requires *M,* 270.1494.

[3''-(2-benzoylphenoxy)propyl]dimethylamine 46

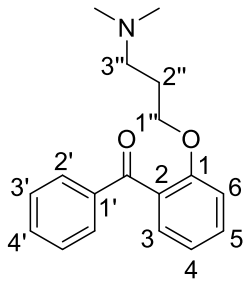

2-hydroxybenzophenone (70 mg, 0.35 mmol) was reacted with 3-dimethylaminopropylchloride hydrochloride (84 mg, 0.53 mmol) following general procedure B. Purification by column chromatography (10% MeOH in DCM) afforded the title compound **49** (71 mg, 71%) as a yellow oil.

ν_{max} (ATR) 1663 (s, C=O), 1246 (s, C-O), 1052 (m, C-N) cm^{-1}. δ_H (700 MHz, $CDCl_3$) 7.79 – 7.75 (m, 2H, 2'-***H***), 7.55 – 7.50 (m, 1H, 4'-***H***), 7.46 – 7.39 (m, 4H, 3-***H***, 5-***H***, 3'-***H***), 7.04 (td, *J* = 7.5, 1.0 Hz, 1H, 4-***H***), 6.97 – 6.93 (m, 1H, 6-***H***), 3.92 (t, *J* = 6.1 Hz, 2H, 1''-$\boldsymbol{H_2}$), 2.05 (s, 6H, C$\boldsymbol{H_3}$ x2), 1.96 (t, *J* = 7.4 Hz, 2H, 3'' $\boldsymbol{H_2}$), 1.59 (m, 2H, 2''-$\boldsymbol{H_2}$); δ_C (176 MHz, $CDCl_3$), 196.9 (Ar_2***C***O), 156.7 (***C***-1), 138.5 (***C***-1'), 132.7 (***C***-4'), 132.0 (***C***-5), 129.7 (***C***-3), 129.5 (***C***-2'), 129.05 (***C***-2), 128.1 (***C***-3'), 120.6 (***C***-4), 112.1 (***C***-6), 66.4 (***C***-1''), 55.9 (***C***-3''), 45.3 (***C***H_3), 27.1 (***C***-2''); Accurate mass: found [M+H] 284.1658, $C_{18}H_{22}NO_2$ requires M, 284.1651.

[2''-(2-benzoyl-4-chlorophenoxy)ethyl]dimethylamine 48

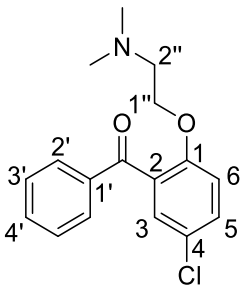

5-chloro-2-hydroxybenzophenone (100 mg, 0.43 mmol) was reacted with 2-dimethylamino-ethylchloride hydrochloride (490 mg, 1.5 mmol) following general procedure B. The product was purified by column chromatography (10% MeOH in DCM with 1% NEt_3) to afford the title compound **49** (63 mg, 48%) as a yellow oil.

ν_{max} (ATR) 1667 (s, C=O), 1271 (s, C-O), 1033 (w, C-N) 738 (s, C-Cl) cm^{-1}. δ_H (700 MHz, $CDCl_3$) 7.78 – 7.75 (m, 2H, 2'-***H***), 7.58 – 7.55 (m, 1H, 4'-***H***), 7.45 – 7.42 (m, 2H, 3'-***H***), 7.41 (dd, *J* = 8.8, 2.6 Hz, 1H, 5-***H***), 7.37 (d, *J* = 2.6 Hz, 1H, 3-***H***), 6.91 (d, *J* = 8.8 Hz, 1H, 6-***H***), 3.97 (t, *J* = 5.8 Hz, 2H, 1''-***H₂***), 2.35 (t, *J* = 5.8 Hz, 2H, 2''-***H₂***), 2.08 (s, 6H, C***H₃***); δ_C (176 MHz, $CDCl_3$) 195.0 (Ar_2***C***O), 155.2 (***C***-1), 137.6 (***C***-1'), 133.0 (***C***-4'), 131.6 (***C***-5), 130.5 (***C***-4), 129.6 (***C***-2'), 129.3 (***C***-3), 128.3 (***C***-3'), 126.0 (***C***-2), 113.9 (***C***-6), 67.9 (***C***-1''), 57.5 (***C***-2''), 45.8 (***C***H_3); Accurate mass: found [M+H] 304.1119, $C_{17}H_{19}N^{35}ClO_2$ requires *M*, 304.1104.

[3''-(2-benzoyl-4-chlorophenoxy)propyl]dimethylamine 49

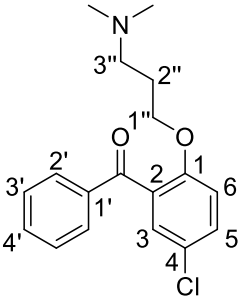

5-chloro-2-hydroxybenzophenone (100 mg, 0.43 mmol) was reacted with 3-dimethylaminepropylchloride hydrochloride (136 mg, 0.86 mmol) following general procedure B. The product was purified by column chromatography (10% MeOH in DCM with 1% NEt_3) to afford the title compound **49** (53 mg, 39%) as a yellow oil.

ν_{max} (ATR) 1665 (s, C=O), 1244 (s, C-O), 1128 (m, C-N), 708 (C-Cl) cm^{-1}; δ_H (700 MHz, $CDCl_3$) 7.79 – 7.76 (m, 2H, 2'-***H***), 7.60 – 7.56 (m, 1H, 4'-***H***), 7.48 – 7.45 (m, 2H, 3'-***H***), 7.41 (dd, 1H, *J* = 8.8, 2.6 Hz, 5-***H***), 7.37 (d, 1H, *J* = 2.6, 3-***H***), 6.90 (d, 1H, *J* = 8.8, 6-***H***), 3.97 (t, 2H, *J* = 5.7, 1''-$\boldsymbol{H_2}$), 2.39 – 2.33 (m, 6H, C$\boldsymbol{H_3}$ x2), 2.32 – 2.24 (m, 2H, 3''-$\boldsymbol{H_2}$), 1.88 (m, 2H, 2''-$\boldsymbol{H_2}$); δ_C (176 MHz, $CDCl_3$) 194.8 ($Ar_2\boldsymbol{C}O$), 154.8 (***C***-1), 137.8 (***C***-1'), 133.2 (***C***-4'), 131.8 (***C***-5), 130.1 (***C***-4), 129.6 (***C***-2'), 129.5 (***C***-3), 128.5 (***C***-3'), 126.3 (***C***-2), 113.6 (***C***-6), 66.0 (***C***-1''), 55.4 (***C***-3''), 43.9 (***C***H_3), 25.5 (***C***-2''); Accurate mass: found [M+H] 318.1261, $C_{18}H_{21}N^{35}ClO_2$ requires *M*, 318.1261.

[2''-(4-benzoylphenoxy)ethyl]dimethylamine 71

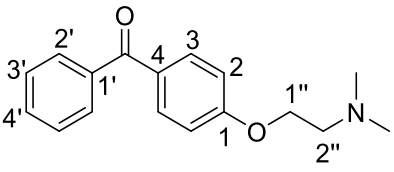

4-hydroxybenzophenone (70 mg, 0.35 mmol) was reacted with 2-dimethylamino-ethylchloride hydrochloride (76 mg, 0.53 mmol) following general procedure B. The

product was purified by column chromatography (10% MeOH in DCM with 1% NEt_3) to afford the title compound **61** (59 mg, 62%) as a yellow oil.

ν_{max} (ATR) 1600 (s, C=O) cm^{-1}. δ_H (700 MHz, $CDCl_3$) 7.83 – 7.80 (m, 2H, 3-***H***), 7.76 – 7.73 (m, 2H, 2'-***H***), 7.58 – 7.54 (m, 1H, 4'-***H***), 7.49 – 7.45 (m, 2H, 3'-***H***), 7.00 – 6.96 (m, 2H, 2-***H***), 4.21 (t, *J* = 5.6 Hz, 2H, 1''-***H₂***), 2.87 (t, *J* = 5.6 Hz, 2H, 2''-***H₂***), 2.43 (s, 6H, C***H₃***); δ_C (176 MHz, $CDCl_3$) 195.5 (Ar_2***C***O), 162.2 (***C***-1), 138.2 (***C***-1'), 132.5 (***C***-3), 131.9 (***C***-4'), 130.3 (***C***-4), 129.7 (***C***-2'), 128.2 (***C***-3'), 114.1 (***C***-2), 65.8 (***C***-1''), 57.9 (***C***-2''), 45.6 (***C***H_3); Accurate mass: found [M+H] 270.1481, $C_{17}H_{20}NO_2$ requires *M*, 270.1494.

[3''-(4-benzoylphenoxy)propyl]dimethylamine 72

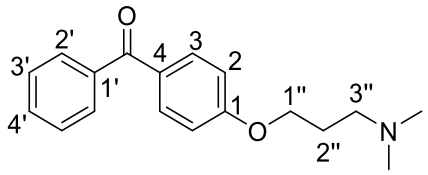

4-hydroxybenzophenone (100 mg, 0.50 mmol) was reacted with 3-dimethylamino-propylchloride hydrochloride (159.5 mg, 1 mmol) following general procedure B. The product was purified by column chromatography (10% MeOH in DCM) to afford the title compound (84 mg, 59%) as a colourless oil.

ν_{max} (ATR) 1603 (s, C=O), 1264 (s) cm^{-1}. δ_H (700 MHz, $CDCl_3$) 7.83 – 7.80 (m, 2H, 3-***H***), 7.76 – 7.74 (m, 2H, 2'-***H***), 7.58 – 7.54 (m, 1H, 4'-***H***), 7.49 – 7.45 (m, 2H, 3'-***H***), 6.97 – 6.94 (m, 2H, 2-***H***), 4.12 (t, *J* = 6.3 Hz, 2H, 1''-***H₂***), 2.62 – 2.54 (m, 2H, 3''-***H₂***), 2.35 (s, 6H, C***H₃***), 2.09 – 2.03 (m, 2H, 2''-***H₂***); δ_C (176 MHz, $CDCl_3$) 195.5 (Ar_2***C***O), 162.6 (***C***-1), 138.3 (***C***-1'), 132.5 (***C***-3), 131.8 (***C***-4'), 130.1 (***C***-4), 129.7 (***C***-2'), 128.1 (***C***-3'), 114.0 (***C***-2), 66.3 (***C***-1''), 56.1 (***C***-3''), 45.2 (***C***H_3), 27.1 (***C***-2''). Accurate mass: found [M+H] 284.1644, $C_{18}H_{22}NO_2$ requires *M*, 284.1651.

{2''-[(4-benzoylphenyl)methoxy]ethyl}dimethylamine 118

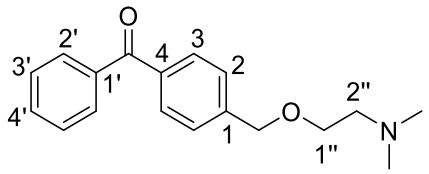

To a suspension of NaH (60% in mineral oil) (40 mg, 1 mmol) in anhydrous THF (1 mL), 2-dimethylaminoethanol **34** (0.05 mL, 0.48 mmol) was slowly added. After heating under reflux for 1h, a solution of 4-bromomethyl benzophenone (50 mg, 0.18 mmol) and TBAI (6 mg, 0.02 mmol) in anhydrous THF (1 mL) was added dropwise, and mixture then heated under reflux overnight. The reaction was then diluted with sat. $NaCO_{3(aq)}$ (15 mL) and products extracted with EtOAc (3 x 15 mL). The combined organic extracts were washed with sat. $Na_2CO_{3(aq)}$ (3 x 30 mL), dried over $MgSO_4$, filtered and concentrated under reduced pressure to afford the title ether (20 mg, 39%) as a yellow oil.

ν_{max} (ATR) 1662 (s, C=O), 1286 (s) cm^{-1}. δ_H (599 MHz, $CDCl_3$) 7.81 – 7.77 (m, 4H, 3-***H***, 2'-***H***), 7.60 – 7.56 (m, 1H, 4'-***H***), 7.50 – 7.44 (m, 4H, 2-***H***, 3'-***H***), 4.63 (s, 2H, ArC***H₂***), 3.66 (t, 2H, *J* = 5.6 Hz, 1''-***H₂***), 2.67 (t, 2H, *J* = 5.6 Hz, 2''-***H₂***), 2.37 (s, 6H, C***H₃***); δ_C (151 MHz, $CDCl_3$) 196.4 (Ar_2***C***O), 142.9 (***C***-1), 137.6 (***C***-1'), 136.8 (***C***-4), 132.3 (***C***-4'), 130.2 (***C***-3), 129.9 (***C***-2'), 128.2 (***C***-3'), 127.2 (***C***-2), 72.6 (Ar***C***H_2), 68.1 (***C***-1''), 58.6 (***C***-2''), 45.6 (***C***H_3). Accurate mass: found [M+H] 284.1646, $C_{18}H_{22}NO_2$ requires *M*, 284.1651.

{3''-[(4-benzoylphenyl)methoxy]propyl}dimethylamine 115

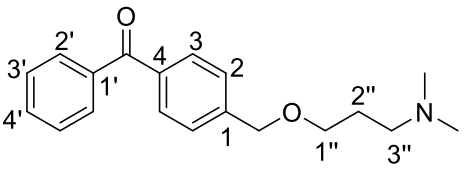

To a suspension of NaH (60% in mineral oil) (22 mg, 0.545 mmol) in anhydrous DMF (1.5 mL), 2-dimethylaminoethanol **34** (0.073 mL, 0.612 mmol) was slowly added and let stir for 1 hour at RT. After, a solution of 4-bromomethyl benzophenone (100 mg, 0.363 mmol) and TBAI (13 mg, 0.036 mmol) in anhydrous DMF (2 mL) was added dropwise, and the mixture stirred overnight at RT. The reaction was then diluted with sat. $Na_2CO_{3(aq)}$ (15 mL) and products extracted with EtOAc (3 x 15 mL). The combined organic extracts were washed with sat. $Na_2CO_{3(aq)}$ (3 x 30 mL), dried over $MgSO_4$, filtered and concentrated under reduced pressure. The product was purified by column chromatography (20% MeOH in DCM) to afford the title compound (16 mg, 15%) as a colourless oil.

ν_{max} (ATR) 1661 (s, C=O), 1282 (s) cm^{-1}. δ_H (599 MHz, $CDCl_3$) 7.80 – 7.77 (m, 4H, 2'-***H***, 3-***H***), 7.60 – 7.57 (m, 1H, 4'-***H***), 7.50 – 7.46 (m, 2H, 3'-***H***), 7.45 – 7.42 (m, 2H, 2-***H***), 4.59 (s, 2H, ArC***H₂***), 3.59 (t, *J* = 6.3 Hz, 2H, 1''-***H₂***), 2.61 – 2.54 (m, 2H, 3''-***H₂***), 2.41 – 2.34 (m, 6H, C***H₃***), 1.95 – 1.88 (m, 2H, 2''-***H₂***); δ_C (151 MHz, $CDCl_3$) 196.4 (Ar_2***C***O), 143.2 (***C***-1), 137.6 (***C***-1'), 136.8 (***C***-4), 132.3 (***C***-4'), 130.2 (***C***-4), 129.9 (***C***-2'), 128.2 (***C***-3'), 127.1 (***C***-2), 72.4 (Ar***C***H_2), 68.6 (***C***-1''), 56.4 (***C***-3''), 44.8 (***C***H_3), 27.2 (***C***-2''). Accurate mass: found [M+H] 298.1800, $C_{19}H_{24}NO_2$ requires *M*, 298.1807.

[(4-benzoylphenyl)methyl](3''-hydroxypropyl)dimethylazanium chloride 116

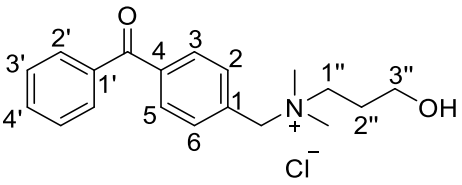

4-bromomethyl benzophenone (70 mg, 0.25 mmol) was reacted with 3-dimethylamino-propan-1-ol (0.04 mL, 0.38 mmol) following general procedure B. The product was purified by reverse-phase column chromatography (0 -> 100% Water in Acetonitrile) to afford the title compound (30 mg, 40%) as a colourless oil.

ν_{max} (ATR) 3390 (b, OH), 2984 (s), 1659 (s), 1285 (s) cm^{-1}. δ_H (700 MHz, $CDCl_3$) 7.85 (d, 2H, *J* = 8.0 Hz, 2-***H***), 7.75 (d, 2H, *J* = 8.0, 3-***H***), 7.70 (d, 2H, *J* = 7.7 Hz, 2'-***H***), 7.55 (t, 1H, *J* = 7.7 Hz, 4'-***H***), 7.43 (t, 2H, *J* = 7.7, 3'-***H***), 4.99 (s, 2H, ArC***H₂***), 3.85 – 3.79 (m, 2H, 1''-***H₂***), 3.74 (t, 2H, *J* = 5.6, 3''-***H₂***), 3.25 (s, 6H, C***H₃*** x2), 2.24 – 2.17 (m, 2H, 2''-***H₂***); δ_C (176 MHz, $CDCl_3$) 195.8 (Ar_2***C***O), 139.4 (***C***-4), 136.5 (***C***-1'), 133.4 (***C***-2), 133.1 (***C***-4'), 131.4 (***C***-1), 130.3 (***C***-3), 130.1 (***C***-2'), 128.5 (***C***-3'), 66.6 (Ar***C***H_2), 63.2 (***C***-1''), 58.4 (***C***-3''), 50.0 (***C***H_3), 26.2 (***C***-2''); Accurate mass: found [M+H] 298.1820, $C_{19}H_{23}NO_2$ requires *M*, 298.1807.

2-(2''-bromoethoxy)phenyl](phenyl)methanone 61a

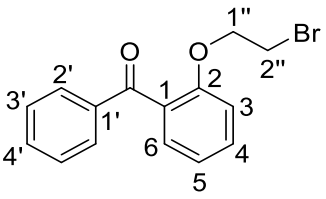

1,2-dibromoethane (0.262 mL, 3.027 mmol) was reacted with 2-hydroxybenzophenone (150 mg, 0.757 mmol) in anhydrous DMF (3 mL) following

general procedure A. Purification by column chromatography (0 to 100% Chloroform in Chloroform) afforded the title compound (82.5 mg, 36%) as a colourless oil.

δ_H (599 MHz, $CDCl_3$) 7.83 – 7.79 (m, 2H, 2'-***H***), 7.61 – 7.56 (m, 1H, 4'-***H***), 7.51 – 7.43 (m, 4H, 4-***H***, 6-***H***, 3'-***H***), 7.10 – 7.06 (m, 1H, 5-***H***), 7.02 – 6.99 (m, 1H, 3-***H***), 4.09 – 4.05 (m, 2H, 1''-$\boldsymbol{H_2}$), 3.68 – 3.64 (m, 2H, 2''-$\boldsymbol{H_2}$); δ_C (151 MHz, $CDCl_3$) 196.5 ($Ar_2\boldsymbol{C}O$), 156.9 (***C***-2), 138.4 (***C***-1'), 132.9 (***C***-4'), 132.5 (***C***-4), 130.3 (***C***-6), 129.5 (***C***-2'), 128.8 (***C***-1), 128.4 (***C***-3'), 121.1 (***C***-5), 113.4 (***C***-3), 70.5 (***C***-1''), 61.1 (***C***-2''). Accurate mass: found [M+H] 305.0193, $C_{15}H_{14}{}^{79}BrO_2$ requires *M*, 305.0177.

(2'''*R*)-*N*-[2''-(2-benzoylphenoxy)ethyl]-2'''-methylpyrrolidine 63

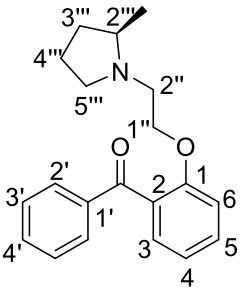

2-(2''-Bromoethoxy)phenyl](phenyl)methanone (82 mg, 0.27 mmol) was reacted with (2R)-methylpyrrolidine hydrochloride (37 mg, 0.303 mmol) in anhydrous DMF following general procedure B. Product was purified by column chromatography (10% MeOH in DCM) to afford the title compound (45 mg, 53%) as a yellow oil.

ν_{max} (ATR) 1600 (s, C=O), 1453 (s). δ_H (599 MHz, $CDCl_3$) 7.80 – 7.75 (m, 2H, 2'-***H***), 7.56 – 7.52 (m, 1H, 4'-***H***), 7.48 – 7.44 (m, 1H, 5-***H***), 7.44 – 7.38 (m, 3H, 3'-***H***, 3-***H***), 7.05 (td, *J* = 7.5, 0.9 Hz, 1H, 4-***H***), 6.98 (dd, *J* = 8.4, 0.9 Hz, 1H, 6-***H***), 4.24 – 3.97 (m, 2H, 1''-$\boldsymbol{H_2}$), 3.01 – 2.92 (m, 1H, 5'''-***H***), 2.92 – 2.81 (m, 1H, 2''-***H***), 2.37 – 2.29 (m, 1H, 2''-***H***), 2.30 – 2.22 (m, 1H, 2'''-***H***), 2.06 – 1.05 (m, 1H, 5'''-***H***), 1.88 – 1.78 (m, 1H, 3'''-***H***), 1.73 – 1.62 (m, 1H, 4'''-***H***), 1.61 – 1.51 (m, 1H, 4'''-***H***), 1.42 – 1.31 (m, 1H, 3'''-***H***),

1.01 (d, *J* = 6.1 Hz, 3H, C***H₃***); δ_C (151 MHz, $CDCl_3$) 196.7 (Ar_2***C***O), 156.5 (***C***-1), 138.2 (***C***-1'), 132.7 (***C***-4'), 132.0 (***C***-5), 129.6 (***C***-2', ***C***-3), 129.0 (***C***-2), 128.1 (***C***-3'), 120.8 (***C***-4), 112.4 (***C***-6), 67.5 (***C***-1''), 60.4 (***C***-2''') 54.4 (***C***-5'''), 51.9 (***C***-2''), 32.1 (***C***-3'''), 21.7 (***C***-4'''), 18.5 (***C***H_3). Accurate mass: found [M+H] 310.1820, $C_{20}H_{24}NO_2$ requires *M*, 310.1807.

[2-(3''-bromopropoxy)phenyl](phenyl)methanone 61b

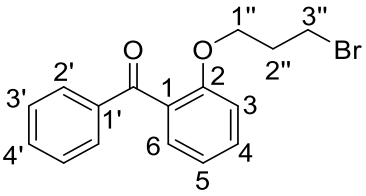

2-hydroxybenzophenone (70 mg, 0.35 mmol) was reacted with 1,3-dibromopropane (0.12 mL, 1.41 mmol) in anhydrous DMF (1.2 mL) following general procedure A. Purification by column chromatography (10% MeOH in DCM) afforded the title compound (45 mg, 42%) as a colourless oil.

δ_H (599 MHz, $CDCl_3$) 7.79 – 7.76 (m, 2H, 2'-***H***), 7.57 – 7.53 (m, 1H, 4'-***H***), 7.50 – 7.43 (m, 4H, 4-***H***, 6-***H***, 3'-***H***), 7.10 – 7.06 (m, 1H, 5-***H***), 6.99 – 6.96 (m, 1H, 3-***H***), 4.02 (t, *J* = 5.6 Hz, 2H, 1''-***H₂***), 2.97 (t, *J* = 6.3 Hz, 2H, 3''-***H₂***), 1.97 (tt, *J* = 6.3, 5.6 Hz, 2H, 2''-***H₂***); δ_C (151 MHz, $CDCl_3$) 196.7 (Ar_2***C***O), 156.4 (***C***-2), 138.4 (***C***-1'), 132.7 (***C***-4'), 132.1 (***C***-4), 129.9 (***C***-6), 129.3 (***C***-2'), 128.9 (***C***-1), 128.3 (***C***-3'), 120.9 (***C***-5), 111.9 (***C***-3), 65.2 (***C***-1''), 31.9 (***C***-3''), 29.7 (***C***-2''). Accurate mass: found [M+H] 319.0324, $C_{16}H_{15}{}^{79}BrO_2$ requires *M*, 319.0334.

(2’’’*R*)-*N* -[3’’-(2-benzoylphenoxy)propyl]-2’’’-methylpyrrolidine 64

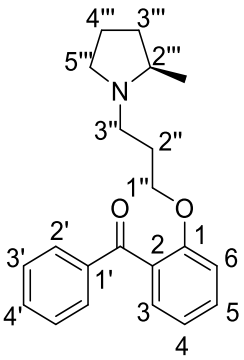

[2-(3’’-bromopropoxy)phenyl](phenyl)methanone (106 mg, 0.332 mmol) was reacted with (2*R*)-Methylpyrrolidine hydrochloride (44 mg, 0.362 mmol) following general procedure B. Product was purified by column chromatography (10% MeOH in DCM with 1% NEt_3) to afford the title compound (40 mg, 66%) as a yellow oil.

ν_{max} (ATR) 1669 (s, C=O), 1607 (s), 1453 (s). δ_H (599 MHz, $CDCl_3$) 7.81 – 7.76 (m, 2H, 2’-***H***), 7.55 – 7.51 (m, 1H, 4’-***H***), 7.45 (ddd, *J* = 8.4, 7.5, 1.8 Hz, 1H, 5-***H***), 7.43 – 7.39 (m, 3H, 3’-***H***, 3-***H***), 7.05 (td, *J* = 7.5, 0.9 Hz, 1H, 4-***H***), 6.96 (dd, *J* = 8.4, 0.9 Hz, 1H, 6-***H***), 4.02 – 3.89 (m, 2H, 1’’-***H₂***), 3.06 (s, 1H, 5’’’-***H***), 2.64 – 2.54 (m, 1H, 3’’-***H***), 2.33 – 2.17 (m, 1H, 2’’’-***H***), 2.05 – 1.95 (m, 1H, 5’’’-***H***), 1.93 – 1.81 (m, 2H, 3’’-***H***, 3’’’-***H***), 1.80 – 1.60 (m, 4H, 2’’-***H₂***, 4’’’-***H₂***), 1.44 (s, 1H, 3’’’-***H***), 1.08 – 0.94 (m, 3H, C***H₃***); δ_C (151 MHz, $CDCl_3$) 196.8 (Ar_2***C***O), 156.6 (***C***-1), 138.3 (***C***-1’), 132.7 (***C***-4’), 132.1 (***C***-5), 129.7 (***C***-3), 129.6 (***C***-2’), 129.0 (***C***-2), 128.2, 120.7 (***C***-4), 112.1 (***C***-6), 66.6 (***C***-1’’), 60.5 (***C***-2’’’), 53.6 (***C***-5’’’), 50.5 (***C***-3’’), 32.4 (***C***-3’’’), 27.7 (***C***-2’’), 21.5 (***C***-4’’’), 18.3 (***C***H_3). Accurate mass: found [M+H] 324.1963, $C_{21}H_{26}NO_2$ requires *M*, 324.1964.

[2-(4''-bromobutoxy)phenyl](phenyl)methanone 61c

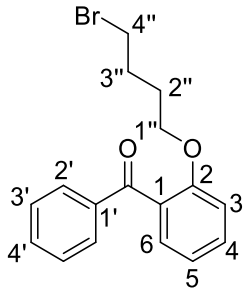

1,4-dibromobutane (0.36 mL, 3.023 mmol) was reacted with 2-hydroxybenzophenone (156 mg, 0.79 mmol) in anhydrous DMF (8 mL) following general procedure B. Product was purified by column chromatography (0-100% DCM in Hexane) to afford title product (203.4 mg, 78%) as a white solid.

δ_H (599 MHz, $CDCl_3$) 7.76 (d, *J* = 7.4 Hz, 2H, 2'-***H***), 7.54 (t, *J* = 7.6 Hz, 1H, 4'-***H***), 7.50 – 7.36 (m, 4H, 4- ***H***, 6- ***H***, 3'-***H***), 7.06 (t, *J* = 7.4 Hz, 1H, 5-***H***), 6.94 (d, *J* = 8.3 Hz, 1H, 3-***H***), 3.90 (t, *J* = 5.8 Hz, 2H, 1''-$\boldsymbol{H_2}$), 3.17 (t, *J* = 6.5 Hz, 2H, 4''- $\boldsymbol{H_2}$), 1.69 – 1.56 (m, 2H, 2''-$\boldsymbol{H_2}$), 1.52 (m, 2H, 3''-$\boldsymbol{H_2}$); δ_C (151 MHz, $CDCl_3$) 196.8 ($Ar_2\boldsymbol{C}O$), 156.6 (***C***-2), 138.5 (***C***-1'), 132.7 (***C***-4'), 132.1 (***C***-4), 129.8 (***C***-6), 129.4 (***C***-2'), 129.0 (***C***-1), 128.2 (***C***-3'), 120.8 (***C***-5), 112.0 (***C***-3), 66.9 (***C***-1''), 33.3 (***C***-4''), 28.7 (***C***-2''), 27.4 (***C***-3''). Accurate mass: found [M+H] 333.0476, $C_{17}H_{18}{}^{79}BrO_2$ requires *M*, 333.0490.

(2’’’*R*)- *N* -[4’’-(2-benzoylphenoxy)butyl]-2’’’-methylpyrrolidine 65

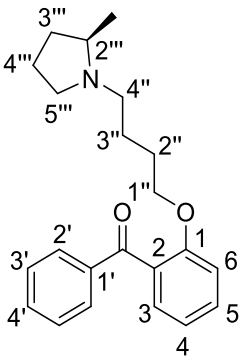

[2-(4’’-bromobutoxy)phenyl](phenyl)methanone (150 mg, 0.45 mmol) was reacted with (2*R*)-methylpyrrolidine hydrochloride (57.5 mg, 0.47 mmol) in anhydrous DMF (2.5 mL) following general procedure B. Product was purified by column chromatography (10% MeOH in DCM) to afford the title compound (70.7 mg, 46%) as a yellow oil.

ν_{max} (ATR) 1669 (s), 1602 (s, C=O), 1457 (s). δ_H (599 MHz, $CDCl_3$) 7.80 – 7.76 (m, 2H, 2’-***H***), 7.55 – 7.51 (m, 1H, 4’-***H***), 7.45 (td, *J* = 8.5, 7.5 Hz, 1H, 5-***H***), 7.43 – 7.37 (m, 3H, 3-***H***, 3’-***H***), 7.03 (td, *J* = 7.5, 0.9 Hz, 1H, 4-***H***), 6.95 (d, *J* = 8.5 Hz, 1H, 6-***H***), 3.98 – 3.84 (m, 2H, 1’’-***H₂***), 3.11 – 2.99 (m, 1H, 5’’’-***H***), 2.72 – 2.61 (m, 1H, 4’’-***H***), 2.42 – 2.22 (m, 1H, 2’’’-***H***), 2.14 – 1.95 (m, 2H, 4’’-***H***, 5’’’-***H***), 1.96 – 1.85 (m, 1H, 3’’’-***H***), 1.85 – 1.72 (m, 1H, 4’’’-***H***), 1.72 – 1.62 (m, 1H, 4’’’-***H***), 1.61 – 1.50 (m, 1H, 2’’-***H***), 1.52 – 1.31 (m, 4H, 2’’-***H***, 3’’-***H₂***, 3’’’-***H***), 1.10 (d, *J* = 6.2 Hz, 3H, C***H₃***); δ_C (151 MHz, $CDCl_3$) 196.7 (Ar_2***C***O), 156.7 (***C***-1), 138.2 (***C***-1’), 132.7 (***C***-4’), 131.9 (***C***-5), 129.6 (***C***-3), 129.6 (***C***-2’), 129.0 (***C***-2), 128.1 (***C***-3’), 120.5 (***C***-4), 112.2 (***C***-6), 68.1 (***C***-1’’), 60.6 (***C***-2’’’), 53.4 (***C***-5’’’), 53.3 (***C***-4’’), 32.4 (***C***-3’’’), 26.9 (***C***-2’’), 24.4 (***C***-3’’), 21.5 (***C***-4’’’), 18.2 (***C***H_3). Accurate mass: found [M+H] 338.2133, $C_{22}H_{28}NO_2$ requires *M*, 338.2120.

[2-(2''-bromopropoxy)-5-chlorophenyl](phenyl)methanone 61d

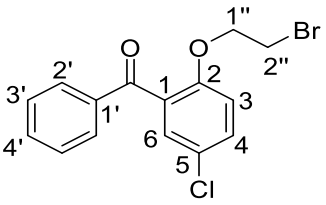

5-chloro-2-hydroxybenzophenone (100 mg, 0.43 mmol) was reacted with 2-bromoethane (0.15 mL, 1.72 mmol) in anhydrous DMF (1.4 mL) following general procedure A. Purification by column chromatography (100% Chloroform) afforded the title compound (78.5 mg, 54%) as a colourless oil.

δ_H (599 MHz, $CDCl_3$) 7.79 – 7.75 (m, 2H, 2'-***H***), 7.60 – 7.55 (m, 1H, 4'-***H***), 7.47 – 7.43 (m, 2H, 3'-***H***), 7.43 – 7.40 (m, 1H, 4-***H***), 7.40 – 7.38 (m, 1H, 3-***H***), 6.93 – 6.89 (m, 1H, 6-***H***), 4.20 – 4.15 (m, 2H, 1''-$\boldsymbol{H_2}$), 3.28 – 3.23 (m, 2H, 2''-$\boldsymbol{H_2}$); δ_C (151 MHz, $CDCl_3$) 194.7 ($Ar_2\boldsymbol{C}O$) 154.3 (***C***-1), 137.5 (***C***-1'), 133.2 (***C***-4'), 131.5 (***C***-5), 130.9 (***C***-4), 129.6 (***C***-2'), 129.5 (***C***-3), 128.3 (***C***-3'), 126.8 (***C***-2), 114.4 (***C***-6), 68.8 (***C***-1''), 27.8 (***C***-2''); Accurate mass: found [M+H] 338.9784, $C_{15}H_{13}{}^{35}Cl^{79}BrO_2$ requires *M*, 338.9787.

(2'''*R*)-*N* -[2-(2''-benzoyl-4-chlorophenoxy)ethyl]-2'''-methylpyrrolidine 66

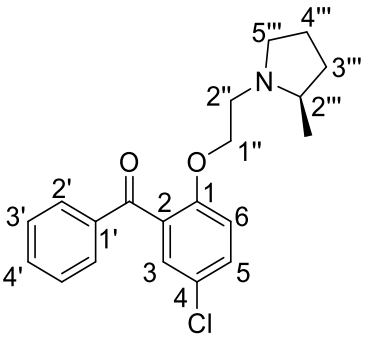

(2*R*)-methylpyrrolidine hydrochloride (22.6 mg, 0.18 mmol) was reacted with [2-(2-bromoethoxy)-5-chlorophenyl](phenyl)methanone (60 mg, 0.18 mmol) in dry DMF (2

mL) following general procedure B. Product was purified by column chromatography to afford the title product (18.6 mg, 31%) as a yellow oil.

ν_{max} (ATR) 1669 (s, C=O), 1475 (s), 1237 (s). δ_H (599 MHz, $CDCl_3$) 7.78 – 7.74 (m, 2H, 2'-***H***), 7.57 – 7.53 (m, 1H, 4'-***H***), 7.44 – 7.41 (m, 2H, 3'-***H***), 7.39 (dd, *J* = 8.8, 2.6 Hz, 1H, 5-***H***), 7.35 (d, *J* = 2.6 Hz, 1H, 3-***H***), 6.91 (d, *J* = 8.8 Hz, 1H, 6-***H***), 4.07 – 3.95 (m, 2H, 1''-$\boldsymbol{H_2}$), 2.87 (ddd, *J* = 9.3, 8.2, 2.9 Hz, 1H, 5'''-***H***), 2.84 – 2.78 (m, 1H, 2''-***H***), 2.25 – 2.15 (m, 2H, 2''-***H***, 2'''-***H***), 1.91 (q, *J* = 8.9 Hz, 1H, 5'''-***H***), 1.84 – 1.76 (m, 1H, 3'''-***H***), 1.68 – 1.59 (m, 1H, 4'''-***H***), 1.59 – 1.49 (m, 1H, 4'''-***H***), 1.35 – 1.26 (m, 1H, 3'''-***H***), 0.95 (d, *J* = 6.0 Hz, 3H, C$\boldsymbol{H_3}$); δ_C (151 MHz, $CDCl_3$) 195.1 (Ar_2***C***O), 155.2 (***C***-1), 137.6 (***C***-1'), 133.1 (***C***-4'), 131.5 (***C***-5), 130.4 (***C***-2), 129.63 (***C***-2'), 129.2 (***C***-3), 128.3 (***C***-3'), 125.9 (***C***-4), 113.7 (***C***-6), 68.4 (***C***-1''), 60.1 (***C***-2'''), 54.6 (***C***-5'''), 51.9 (***C***-2''), 32.2 (***C***-3'''), 21.7 (***C***-4'''), 18.8 (***C***H_3). Accurate mass: found [M+H] 344.1430, $C_{20}H2_3{}^{35}ClNO_2$ requires *M*, 344.1417.

[2-(3''-bromopropoxy)-5-chlorophenyl](phenyl)methanone 61e

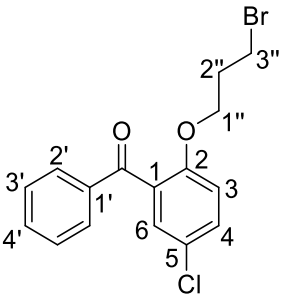

5-chloro-2-hydroxybenzophenone (100 mg, 0.43 mmol) was reacted with 1,3-dibromopropane (0.220 mL, 2.15 mmol) in anhydrous DMF (1.4 mL) following general procedure A. Purification by column chromatography (75% EtOAc in Hexane) afforded the title compound **56b** (70 mg, 46%) as a white solid.

ν_{max} (ATR) 1670 (s, C=O), 1244 (s, C-O), 703 (w, C-Br) cm^{-1}. δ_H (700 MHz, $CDCl_3$) 7.78 – 7.75 (m, 2H, 2'-***H***), 7.59 – 7.56 (m, 1H, 4'-***H***), 7.48 – 7.44 (m, 2H, 3'-***H***), 7.43 – 7.41 (m, 1H, 4-***H***), 7.40 (d, *J* = 2.6 Hz, 1H, 6-***H***), 6.92 (d, *J* = 8.8 Hz, 1H, 3-***H***), 4.00 (t, *J* = 5.6 Hz, 2H, 1''-$\boldsymbol{H_2}$), 2.96 (t, *J* = 6.3 Hz, 2H, 3''-$\boldsymbol{H_2}$), 1.99 – 1.94 (m, 2H, 2''-$\boldsymbol{H_2}$); δ_C (176 MHz, $CDCl_3$) 195.0 (Ar_2***C***O), 154.9 (***C***-2), 137.7 (***C***-1'), 133.1 (***C***-4'), 131.7 (***C***-4), 130.3 (***C***-1), 129.5 (***C***-6), 129.3 (***C***-2'), 128.4 (***C***-3'), 126.2 (***C***-5), 113.4 (***C***-3), 65.7 (***C***-1''), 31.8 (***C***-2''), 29.5 (***C***-3''); Accurate mass: found [M+H] 352.9937, $C_{16}H_{16}N^{35}Cl^{79}BrO_2$ requires *M*, 352.9944.

(2'''*R*)-*N*-[3''-(2-benzoyl-4-chlorophenoxy)propyl]-2'''-methylpyrrolidine 67

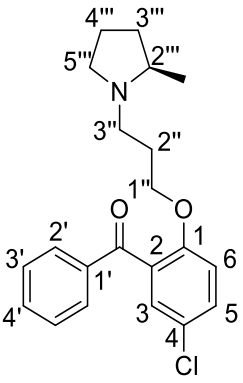

56b (60 mg, 0.17 mmol) was reacted with (2*R*)-Methylpyrrolidine hydrochloride (21.7 mg, 0.178 mmol) following general procedure B. The product was purified by column chromatography (10% MeOH in DCM with 1% NEt_3) to afford the title compound **59** (40 mg, 66%) as a yellow oil.

δ_H (599 MHz, $CDCl_3$) 7.80 – 7.74 (m, 2H, 2'-***H***), 7.59 – 7.54 (m, 1H, 4'-***H***), 7.47 – 7.43 (m, 2H, 3'-***H***), 7.41 (dd, *J* = 8.8, 2.6 Hz, 1H, 5-***H***), 7.36 (d, *J* = 2.6 Hz, 1H, 3-***H***), 6.91 (d, *J* = 8.8 Hz, 1H, 6-***H***), 4.01 – 3.91 (m, 2H, 1''-$\boldsymbol{H_2}$), 3.29 – 3.10 (m, 1H, 5'''-***H***), 2.74 – 2.63 (m, 1H, 3''-***H***), 2.57 – 2.40 (m, 1H, 2'''-***H***), 2.26 – 2.10 (m, 1H, 5'''-***H***), 2.06 – 1.92 (m, 3H, 2''-***H***, 3''-***H***, 3'''-***H***), 1.92 – 1.83 (m, 1H, 4'''-***H***), 1.83 – 1.69 (m, 2H, 2''-***H***, 4'''-

H), 1.65 – 1.51 (m, 1H, 3’’’-***H***), 1.18 – 1.09 (m, 3H, C***H₃***); δ_C (151 MHz, $CDCl_3$) 194.9 (Ar_2***C***O), 154.9 (***C***-1), 137.7 (***C***-1’), 133.2 (***C***-4’), 131.7 (***C***-5), 130.2 (***C***-4), 129.6 (***C***-2’), 129.4 (***C***-3), 128.4 (***C***-3’), 126.1 (***C***-2), 113.6 (***C***-6), 66.6 (***C***-1’’), 61.7 (***C***-2’’’), 53.3 (***C***-5’’’) 50.2 (***C***-3’’), 31.9 (***C***-3’’’), 26.8 (***C***-2’’), 21.4 (***C***-4’’’), 17.3 (***C***H_3); Accurate mass: found [M+H] 358.1582, $C_{21}H_{25}N^{35}ClO_2$ requires 358.1574.

[2-(4’’-bromobutoxy)-5-chlorophenyl](phenyl)methanone 61f

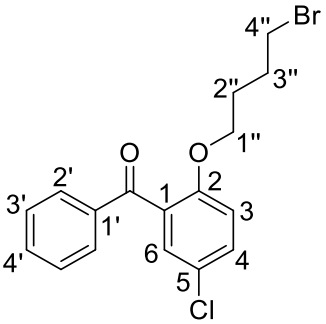

Na_2CO_3 (2.3 g, 21.7 mmol) was added to a solution of 1,4-dibromobutane (0.1.3 mL, 10.74 mmol) in anhydrous acetonitrile (20 mL). A solution 5-chloro-2-hydroxybenzophenone (500 mg, 2.15 mmol) in anhydrous acetonitrile (23 mL) was slowly added and stirred overnight at 70ºC. Once full conversion was achieved, the reaction mixture was concentrated under reduced pressure and product was purified by column chromatography (0-100% DCM in Hexane) to afford the title compound (269.1 mg, 34%) as a colourless oil.

δ_H (400 MHz, $CDCl_3$) 7.78 – 7.73 (m, 2H, 2’-***H***), 7.60 – 7.54 (m, 1H, 4’-***H***), 7.47 – 7.37 (m, 4H, 3’-***H***, 4-***H***, 6-***H***), 6.90 – 6.85 (m, 1H, 3-***H***), 3.88 (t, *J* = 5.7 Hz, 2H, 1’’-***H₂***), 3.16 (t, *J* = 6.4 Hz, 2H, 4’’-***H₂***), 1.65 – 1.55 (m, 2H, 2’’-***H₂***), 1.55 – 1.43 (m, 2H, 3’’- ***H₂***); δ_C (101 MHz, $CDCl_3$) 195.2 (Ar_2***C***O), 155.2 (***C***-2), 137.8 (***C***-1’), 133.2 (***C***-4’), 131.7 (***C***-4), 130.3 (***C***-1), 129.4 (***C***-6), 129.4 (***C***-2’), 128.4 (***C***-3’), 125.9 (***C***-5’), 113.4 (***C***-3), 67.4 (***C***-

1''), 33.2 (***C***-4''), 28.6 (***C***-2''), 27.4 (***C***-3''). Accurate mass: found [M+H] 367.0094, $C_{17}H_{17}{}^{79}Br^{35}ClO_2$ requires *M*, 367.0100.

(2'''*R*)-*N*-[4''-(2-benzoyl-4-chlorophenoxy)butyl]-2'''-methylpyrrolidine 68

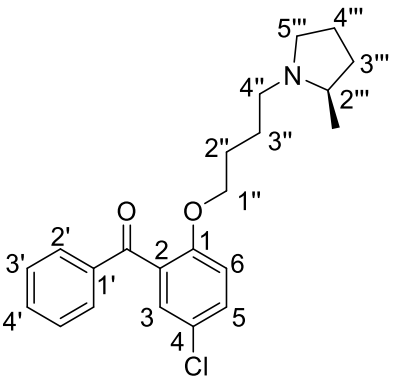

To a solution of (2*R*)-Methylpyrrolidine hydrochloride (50 mg, 0.41 mmol), KI (4.5 mg, 0.027 mmol) and Na_2CO_3 (132.6 mg, 1.25 mmol) in dry acetonitrile (7 mL) at 70ºC, [2-(4-bromobutoxy)-5-chlorophenyl](phenyl)methanone (100 mg, 0.27 mmol) in dry acetonitrile (7 mL) was slowly added. Mixture stirred overnight under nitrogen atmosphere. Solution was cooled down to RT, filtered and concentrated under reduced pressure. Crude mixture was submitted to column chromatography (10% MeOH in DCM) to afford the title compound (22.3 mg, 22%) as a brown oil.

ν_{max} (ATR) 1669 (s, C=O) cm^{-1}. δ_H (599 MHz, $CDCl_3$) δ 7.80 – 7.73 (m, 2H, 2'-***H***), 7.58 – 7.52 (m, 1H, 4'-***H***), 7.45 – 7.40 (m, 2H, 3'-***H***), 7.39 (dd, *J* = 8.8, 2.6 Hz, 1H, 5-***H***), 7.34 (d, *J* = 2.6 Hz, 1H, 3-***H***), 6.88 (d, *J* = 8.8 Hz, 1H, 6-***H***), 3.94 – 3.84 (m, 2H, 1''-***H₂***), 3.10 – 2.98 (m, 1H, 5'''-***H***), 2.72 – 2.60 (m, 1H, 4''-***H***), 2.40 – 2.24 (m, 1H, 2'''-***H***), 2.09 – 1.95 (m, 2H, 4''-***H***, 5'''-***H***), 1.95 – 1.87 (m, 1H, 3'''-***H***), 1.84 – 1.72 (m, 1H, 4'''-***H***), 1.71 – 1.63 (m, 1H, 4'''-***H***), 1.59 – 1.51 (m, 1H, 2''-***H***), 1.51 – 1.43 (m, 2H, 2''-***H***, 3'''-***H***), 1.43 – 1.38 (m, 1H, 3''-***H***), 1.38 – 1.30 (m, 1H, 3''-***H***), 1.09 (d, *J* = 6.1 Hz, 3H, C***H₃***); δ_C (151 MHz, $CDCl_3$) 195.1 (Ar_2***C***O), 155.3 (***C***-1), 137.5 (***C***-1'), 133.1 (***C***-4'), 131.5 (***C***-5), 130.3

(***C***-2), 129.6 (***C***-2'), 129.2 (***C***-3), 128.3 (***C***-3'), 125.7 (***C***-4), 113.6 (***C***-6), 68.6 (***C***-1''), 60.7 (***C***-2'''), 53.5 (***C***-5'''), 53.3 (***C***-4''), 32.4 (***C***-3'''), 26.9 (***C***-2''), 24.4 (***C***-3''), 21.5 (***C***-4'''), 18.3 (***C***H_3). Accurate mass: found [M+H] 372.1738, $C_{22}H_{27}{}^{35}ClNO_2$ requires *M*, 372.1730.

[3-(2''-bromoethoxy)phenyl](phenyl)methanone 94a

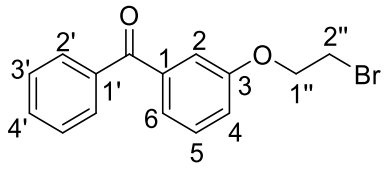

Cs_2CO_3 (986 g, 3.03 mmol) was added to a solution of 1,2-dibromoethane (0.35 mL, 4.04 mmol) in anhydrous acetonitrile (5 mL). A solution of 3-hydroxybenzophenone (200 mg, 1.01 mmol) in anhydrous acetonitrile (5 mL) was slowly added and stirred overnight at 70ºC. Once full conversion was achieved, the reaction mixture was concentrated under reduced pressure and product was purified by column chromatography (0-100% Chloroform in Hexane) to afford the title compound (116 mg, 38%) as a colourless oil.

δ_H (599 MHz, $CDCl_3$) 7.82 – 7.78 (m, 2H, 2'-***H***), 7.61 – 7.57 (m, 1H, 4'-***H***), 7.52 – 7.46 (m, 2H, 3'-***H***), 7.42 – 7.35 (m, 3H, 2-***H***, 5-***H***, 6-***H***), 7.18 – 7.14 (m, 1H, 4-***H***), 4.35 (t, *J* = 6.1 Hz, 2H, 1''-***H*****$_2$**), 3.66 (t, *J* = 6.1 Hz, 2H, 2''-***H*****$_2$**); δ_C (151 MHz, $CDCl_3$) 196.2 (Ar_2***C***O), 158.1 (***C***-3), 139.0 (***C***-1), 137.5 (***C***-1'), 132.5 (***C***-4'), 130.0 (***C***-2'), 129.4 (***C***-5), 128.3 (***C***-3'), 123.5 (***C***-6), 119.5 (***C***-4), 115.1 (***C***-2), 68.0 (***C***-1''), 28.9 (***C***-2''). Accurate mass: found [M+H] 305.0184, $C_{15}H_{14}{}^{79}BrO_2$ requires *M*, 305.0177.

(2'''*R*)- *N* -[2''-(3-benzoylphenoxy)ethyl]-2'''-methylpyrrolidine 95

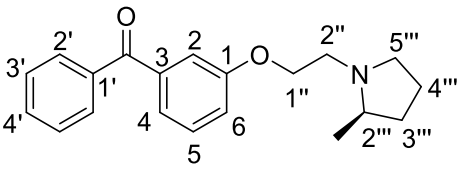

To a solution of (2*R*)-methylpyrrolidine hydrochloride (48 mg, 0.39 mmol), KI (5.4 mg, 0.033 mmol) and Na_2CO_3 (105 mg, 1.64 mmol) in dry acetonitrile (10 mL) at 70ºC, [3-(2-bromoethoxy)phenyl](phenyl)methanone (100 mg, 0.33 mmol) in dry acetonitrile (6 mL) was slowly added. Mixture stirred overnight under nitrogen atmosphere. The solution was cooled down to RT, filtered and concentrated under reduced pressure. The crude mixture was submitted to column chromatography (10% MeOH in DCM) to afford the title compound (69.1 mg, 68%) as a yellow solid.

ν_{max} (ATR) 1663 (s, C=O), 1286 (s) cm^{-1}. δ_H (599 MHz, $CDCl_3$) 7.80 – 7.75 (m, 2H, 2'-***H***), 7.58 – 7.54 (m, 1H, 4'-***H***), 7.48 – 7.43 (m, 2H, 3'-***H***), 7.37 – 7.30 (m, 3H, 2-***H***, 4-***H***, 5-***H***), 7.15 – 7.10 (m, 1H, 6-***H***), 4.19 (t, *J* = 6.0 Hz, 2H, 1''-***H₂***), 3.30 (ddd, *J* = 9.5, 8.9, 3.1 Hz, 1H, 5'''-***H***), 3.25 (dt, *J* = 12.5, 6.0 Hz, 1H, 2''-***H***), 2.64 (dt, *J* = 12.5, 6.0 Hz, 1H, 2''-***H***), 2.60 – 2.51 (m, 1H, 2'''-***H***), 2.38 (q, *J* = 8.9 Hz, 1H, 5'''-***H***), 2.00 – 1.90 (m, 1H, 3'''-***H***), 1.90 – 1.79 (m, 1H, 4'''-***H***), 1.79 – 1.69 (m, 1H, 4'''-***H***), 1.55 – 1.43 (m, 1H, 3'''-***H***), 1.18 (d, *J* = 6.1 Hz, 3H, C***H₃***); δ_C (151 MHz, $CDCl_3$) 196.4 (Ar_2***C***O), 158.6 (***C***-1), 138.9 (***C***-3), 137.5 (***C***-1'), 132.4 (***C***-4'), 129.9 (***C***-2'), 129.2 (***C***-5), 128.2 (***C***-3'), 122.9 (***C***-4), 119.2 (***C***-6), 115.2 (***C***-2), 66.9 (***C***-1''), 60.9 (***C***-2'''), 54.7 (***C***-5'''), 52.5 (***C***-2''), 32.2 (***C***-3'''), 21.8 (***C***-4'''), 18.6 (***C***H_3). Accurate mass: found [M+H] 310.1819, $C_{20}H_{24}NO_2$ requires *M*, 310.1807.

(2’’’*R*)-*N* -[3’’-(3-benzoylphenoxy)propyl]-2’’’-methylpyrrolidine 96

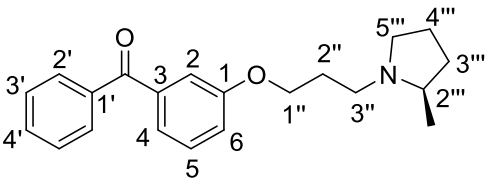

To a solution of (2*R*)-methylpyrrolidine hydrochloride (45.7 mg, 0.37 mmol), KI (0.5 mg, 0.003 mmol) and Na_2CO_3 (152.7 mg, 1.44 mmol) in dry acetonitrile (10 mL) at 70ºC, [3-(3-bromopropoxy)phenyl](phenyl)methanone (100 mg, 0.31 mmol) in dry acetonitrile (6 mL) was slowly added. Mixture stirred overnight under nitrogen atmosphere. The solution was cooled down to RT, filtered and concentrated under reduced pressure. The crude mixture was submitted to column chromatography (10% MeOH in DCM) to afford the title compound (77.7 mg, 77%) as a yellow solid.

ν_{max} (ATR) 1663 (s, C=O), 1281 (s) cm^{-1}. δ_H (599 MHz, $CDCl_3$) 7.82 – 7.78 (m, 2H, 2’-***H***), 7.59 (ddt, *J* = 8.7, 7.0, 1.3 Hz, 1H, 4’-***H***), 7.51 – 7.46 (m, 2H, 3’-***H***), 7.39 – 7.31 (m, 3H, 2-***H***, 4-***H***, 5-***H***), 7.13 (ddd, *J* = 8.1, 2.6, 1.2 Hz, 1H, 6-***H***), 4.13 – 4.04 (m, 2H, 1’’-***H₂***), 3.32 – 3.18 (m, 1H, 5’’’-***H***), 3.04 (q, *J* = 8.8 Hz, 1H, 3’’-***H***), 2.50 – 2.37 (m, 1H, 2’’’-***H***), 2.37 – 2.26 (m, 1H, 3’’-***H***), 2.26 – 2.14 (m, 1H, 5’’’-***H***), 2.13 – 2.01 (m, 2H, 2’’-***H₂***), 2.01 – 1.90 (m, 1H, 3’’’-***H***), 1.90 – 1.79 (m, 1H, 4’’’-***H***), 1.79 – 1.68 (m, 1H, 4’’’-***H***), 1.56 – 1.42 (m, 1H, 3’’’-***H***), 1.15 (d, *J* = 6.0 Hz, 3H, C***H₃***); δ_C (151 MHz, $CDCl_3$) 196.5 (Ar_2***C***O), 158.9 (***C***-1), 138.8 (***C***-3), 137.6 (***C***-1’), 132.4 (***C***-4’), 130.0 (***C***-2’), 129.2 (***C***-5), 128.2 (***C***-3’), 122.8 (***C***-4), 119.2 (***C***-6), 115.1 (***C***-2), 66.5 (***C***-1’’), 60.6 (***C***-2’’’), 53.9 (***C***-5’’’), 50.7 (***C***-3’’), 32.6 (***C***-3’’’), 28.1 (***C***-2’’), 21.6 (***C***-4’’’), 18.6 (***C***H_3). Accurate mass: found [M+H] 324.1971, $C_{21}H_{26}NO_2$ requires *M*, 324.1964.

[3-(4''-bromobutoxy)phenyl](phenyl)methanone 94c

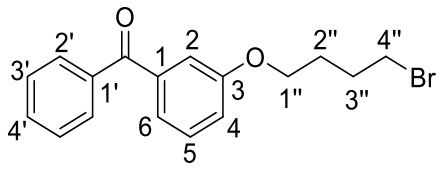

Cs_2CO_3 (986 g, 3.03 mmol) was added to a solution of 1,4-dibromobutane (0.48 mL, 4.04 mmol) in anhydrous acetonitrile (5 mL). A solution of 3-hydroxybenzophenone (200 mg, 1.01 mmol) in anhydrous acetonitrile (5 mL) was slowly added and stirred overnight at 70ºC. Once full conversion was achieved, the reaction mixture was concentrated under reduced pressure and product was purified by column chromatography (0-100% DCM in Hexane) to afford the title compound (201 mg, 60%) as a colourless oil.

δ_H (599 MHz, $CDCl_3$) 7.82 – 7.79 (m, 2H, 2'-***H***), 7.61 – 7.57 (m, 1H, 4'-***H***), 7.51 – 7.46 (m, 2H, 3'-***H***), 7.37 (t, *J* = 7.7 Hz, 1H, 5-***H***), 7.35 – 7.32 (m, 2H, 2-***H***, 6-***H***), 7.13 – 7.10 (m, 1H, 4-***H***), 4.05 (t, *J* = 6.1 Hz, 2H, 1''-$\boldsymbol{H_2}$), 3.49 (t, *J* = 6.1 Hz, 2H, 4''-$\boldsymbol{H_2}$), 2.11 – 2.04 (m, 2H, 2''-$\boldsymbol{H_2}$), 2.01 – 1.93 (m, 2H, 3''-$\boldsymbol{H_2}$); δ_C (151 MHz, $CDCl_3$) 196.5 (Ar_2***C***O), 158.8 (***C***-3), 138.9 (***C***-1), 137.6 (***C***-1'), 132.4 (***C***-4'), 130.0 (***C***-2'), 129.2 (***C***-5), 128.2 (***C***-3'), 122.9 (***C***-6), 119.2 (***C***-4), 114.9 (***C***-2), 67.1 (***C***-1''), 33.3 (***C***-4''), 29.4 (***C***-2''), 27.8 (***C***-3''). Accurate mass: found [M+H] 333.0490, $C_{17}H_{18}{}^{79}BrO_2$ requires *M*, 333.0490.

(2'''*R*)-*N*-[4''-(3-benzoylphenoxy)butyl]-2'''-methylpyrrolidine 97

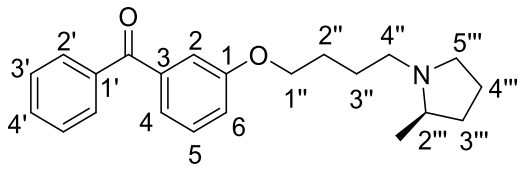

To a solution of (2*R*)-methylpyrrolidine hydrochloride (73 mg, 0.6 mmol), KI (5 mg, 0.03 mmol) and Na_2CO_3 (159 mg, 1.5 mmol) in dry acetonitrile (7 mL) at 70ºC, [3-(4-

bromobutoxy)phenyl](phenyl)methanone (100 mg, 0.3 mmol) in dry acetonitrile (8 mL) was slowly added. Mixture stirred overnight under nitrogen atmosphere. The solution was cooled down to RT, filtered and concentrated under reduced pressure. The crude mixture was submitted to column chromatography (10% MeOH in DCM) to afford the title compound (48.4 mg, 48%) as a brown oil.

ν_{max} (ATR) 1663 (s, C=O), 1286 (s) cm^{-1}. δ_H (599 MHz, $CDCl_3$) 7.83 – 7.77 (m, 2H, 2'-***H***), 7.61 – 7.55 (m, 1H, 4'-***H***), 7.48 (t, *J* = 7.7 Hz, 2H, 3'-***H***), 7.36 (t, *J* = 8.0 Hz, 1H, 5-***H***), 7.34 – 7.30 (m, 2H, 2-***H***, 4-***H***), 7.13 – 7.07 (m, 1H, 6-***H***), 4.09 – 3.98 (m, 2H, 1''-***H₂***), 3.49 – 3.26 (m, 1H, 5'''-***H***), 3.07 – 2.90 (m, 1H, 4''-***H***), 2.71 – 2.51 (m, 1H, 2'''-***H***), 2.47 – 2.24 (m, 2H, 1''-***H***, 5'''-***H***), 2.08 – 1.98 (m, 1H, 3'''-***H***), 1.98 – 1.73 (m, 6H, 2''-***H₂***, 3''-***H₂***, 4'''-***H₂***), 1.68 – 1.56 (m, 1H, 3'''-***H***), 1.35 – 1.14 (m, 3H, C***H₃***); δ_C (151 MHz, $CDCl_3$) 196.5 (Ar_2***C***O), 158.8 (***C***-1), 138.9 (***C***-3), 137.6 (***C***-1'), 132.4 (***C***-4'), 130.0 (***C***-2'), 129.2 (***C***-5), 128.2 (***C***-3'), 122.8 (***C***-4), 119.2 (***C***-6), 115.0 (***C***-2), 67.7 (***C***-1''), 61.4 (***C***-2'''), 53.5 (***C***-5'''), 53.4 (***C***-4''), 32.2 (***C***-3'''), 24.3 (***C***-3''), 21.5 (***C***-4'''), 17.7 (***C***H_3). Accurate mass: found [M+H] 338.2130, $C_{22}H_{28}NO_2$ requires *M*, 338.2120.

3-(4'-methylbenzoyl)phenol 106 [125]

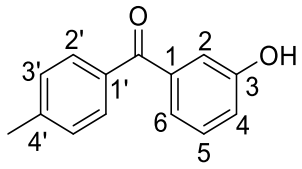

3-methoxybenzoic acid (1 g, 6.57 mmol) was dissolved in thionyl chloride (3 mL) and heated under reflux for 2h. After cooling down to RT, the volatiles were removed under reduced pressure and the products redissolved in anhydrous toluene (10 mL). $AlCl_3$ (2.63 g, 19.72 mmol) was added in portions over 20 minutes and the mixture stirred for 24h at 70ºC. After cooling to room temperature, the reaction mixture was added to

3M HCl (aq.) (10 mL) in a separating funnel and extracted with DCM (3x10 mL). The combined organic layers were washed with brine, dried over $MgSO_4$, filtered, and concentrated under reduced solid. The crude product was submitted to column chromatography (0-100% EtOAc in Hexane) to afford the title product (1.16 g, 83%) as a brown solid.

δ_H (400 MHz, $CDCl_3$) 7.73 (d, *J* = 8.2 Hz, 2H, 2'-***H₂***), 7.37 – 7.26 (m, 5H, 2-***H***, 5-***H***, 6-***H***, 3'-***H₂***), 7.09 – 7.06 (m, 1H, 4-***H***), 2.44 (s, 3H, -C***H₃***); δ_C (101 MHz, $CDCl_3$) 196.5 (Ar_2***C***O), 155.7 (***C***-3), 143.5 (***C***-4'), 139.3 (***C***-1), 134.7 (***C***-1'), 130.4 (***C***-2'), 129.5 (***C***-5), 129.0 (***C***-3'), 122.7 (***C***-6), 119.5 (***C***-4), 116.4 (***C***-2), 21.7 (-***C***H_3). *m/z* (LC-MS, ESI^+) 213.25 [M+H]. All data agrees with literature.

(2'''*R*)-*N*-{3''-[3-(4'-methylbenzoyl)phenoxy]propyl}2'''-methylpyrrolidine 112

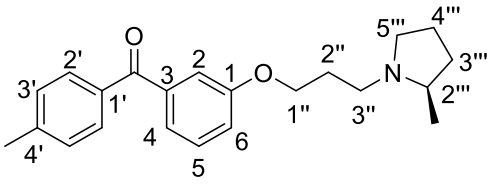

Cs_2CO_3 (2.2 g, 6.75 mmol) was added to a solution of 1,3-dibromopropane (0.72 mL, 7.07 mmol) in anhydrous acetonitrile (20 mL). A solution of 3-(4-methylbenzoyl)phenol (300 mg, 1.41 mmol) in anhydrous acetonitrile (27 mL) was slowly added and stirred overnight at 70ºC. Once full conversion was achieved, the reaction mixture was concentrated under reduced pressure and crude product was submitted to column chromatography (0-100% DCM in Hexane) to remove inorganic salts. Resultant product (200 mg) in dry acetonitrile (15 mL) was then slowly added to a stirring solution of (2*R*)-Methylpyrrolidine hydrochloride (87.6 mg, 0.72 mmol), KI (10 mg, 0.06 mmol) and Na_2CO_3 (292.6 mg, 2.76 mmol) in dry acetonitrile (15 mL) at 70ºC. Mixture stirred overnight under nitrogen atmosphere. Solution was cooled down to RT,

filtered and concentrated under reduced pressure. Crude mixture was submitted to column chromatography (10% MeOH in DCM) to afford the title compound (119.8 mg, 59%) as a brown oil.

ν_{max} (ATR) 1663 (s, C=O), 1590 (s), 1292 (s) cm^{-1}. δ_H (599 MHz, $CDCl_3$) 7.74 – 7.70 (m, 2H, 2'-***H*₂**), 7.38 – 7.34 (m, 1H, 5-***H***), 7.33 – 7.30 (m, 2H, 2-***H***, 4-***H***), 7.29 – 7.27 (m, 2H, 3'-***H*₂**), 7.12 – 7.09 (m, 1H, 6-***H***), 4.15 – 4.02 (m, 2H, 1''-***H*₂**), 3.46 – 3.30 (m, 1H, 5'''-***H***), 3.19 – 3.06 (m, 1H, 3''-***H***), 2.75 – 2.55 (m, 1H, 2'''-***H***), 2.53 – 2.45 (m, 1H, 3''-***H***), 2.44 (s, 3H, ArC***H*₃**), 2.43 – 2.36 (m, 1H, 5'''-***H***), 2.27 – 2.16 (m, 1H, 2''-***H***), 2.16 – 2.08 (m, 1H, 2''-***H***), 2.08 – 1.99 (m, 1H, 3'''-***H***), 1.98 – 1.87 (m, 1H, 4'''-***H***), 1.87 – 1.76 (m, 1H, 4'''-***H***), 1.66 – 1.59 (m, 1H, 3-***H***), 1.32 – 1.20 (m, 3H, C***H*₃**); δ_C (151 MHz, $CDCl_3$) 196.2 (Ar_2***C***O), 158.7 (***C***-1), 143.3 (***C***-4'), 139.3 (***C***-3), 134.8 (***C***-1'), 130.3 (***C***-2'), 129.2 (***C***-5), 128.9 (***C***-3'), 122.7 (***C***-4), 118.8 (***C***-6), 115.1 (***C***-2), 66.2 (***C***-1''), 61.4 (***C***-2'''), 53.6 (***C***-5'''), 50.7 (***C***-3''), 32.3 (***C***-3'''), 27.5 (***C***-2''), 21.6 (Ar***C***H_3), 21.5 (***C***-4'''), 17.8 (***C***H_3). Accurate mass: found [M+H] 338.2116, $C_{22}H_{28}NO_2$ requires *M*, 338.2120

3-[4'-(isopropanyl)benzoyl]phenol 107

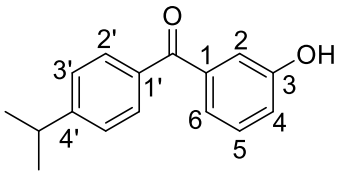

3-methoxybenzoic acid (1 g, 6.57 mmol) was dissolved in thionyl chloride (3 mL) and refluxed for 2h. After cooling down to RT, volatiles were removed under reduced pressure and products redissolved in anhydrous cumene (10 mL). $AlCl_3$ (2.63 g, 19.72 mmol) was added in portions over 20 minutes and mixture stirred for 24h at 70ºC. After cooling down to room temperature, reaction mixture was added to 3M HCl (aq.) (10 mL) in a separating funnel and extracted with DCM (3x10 mL). Combined organic

layers were washed with brine, dried over $MgSO_4$, filtered, and concentrated under reduced solid. Crude was submitted to column chromatography (0-100% EtOAc in Hexane) to afford de title product (1.58 g, 100%) as a light brown solid.

ν_{max} (ATR) 3369 (b, OH), 1642 (s, C=O), 1596 (s), 1315 (s), 1296 (s) cm^{-1}. δ_H (400 MHz, $CDCl_3$) 7.80 – 7.71 (m, 2H, 2'-***H***), 7.38 – 7.29 (m, 5H, 2-***H***, 5-***H***, 6-***H***, 3'-$\boldsymbol{H_2}$), 7.11 – 7.05 (m, 1H,), (h, *J* = 7.0 Hz, 1H, C***H***), 1.29 (d, *J* = 7.0 Hz, 6H, 2xC$\boldsymbol{H_3}$); δ_C (151 MHz, $CDCl_3$) 196.0 (Ar_2***C***O), 155.5 (***C***-3), 154.1 (***C***-4'), 139.5 (***C***-1), 135.1 (***C***-1'), 130.4 (***C***-2'), 129.5 (***C***-5), 126.4 (***C***-3'), 122.7 (***C***-6), 119.3 (***C***-4), 116.4 (***C***-2), 34.3 (***C***H), 23.7 (2x***C***H_3). Accurate mass: found [M+H] 241.1236, $C_{16}H_{17}O_2$ requires *M*, 241.1229

(2'''*R*)-*N*-(3''-{3-[4'-(propan-2''''-yl)benzoyl]phenoxy}propyl)-2'''-methylpyrrolidine 113

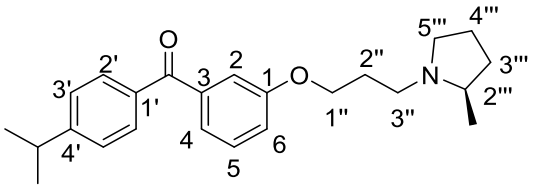

Cs_2CO_3 (1.25 g, 3.83 mmol) was added to a solution of 1,3-dibromopropane (0.42 mL, 4.16 mmol) in anhydrous acetonitrile (10 mL). A solution 3-[4-(propan-2-yl)benzoyl]phenol (200 mg, 0.83 mmol) in anhydrous acetonitrile (17 mL) was slowly added and stirred overnight at 70ºC. Once full conversion was achieved, the reaction mixture was concentrated under reduced pressure and crude product was submitted to column chromatography (0-100% DCM in Hexane) to to remove inorganic salts. Resultant product (150 mg) in dry acetonitrile (15 mL) was then slowly added to a stirring solution of (2*R*)-Methylpyrrolidine hydrochloride (60.6 mg, 0.49 mmol), KI (7 mg, 0.042 mmol) and Na_2CO_3 (202.4 mg, 1.91 mmol) in dry acetonitrile (11 mL) at 70ºC. Mixture stirred overnight under nitrogen atmosphere. Solution was cooled down

to RT, filtered and concentrated under reduced pressure. Crude mixture was submitted to column chromatography (10% MeOH in DCM) to afford the title compound (76 mg, 50%) as a brown oil.

ν_{max} (ATR) 1663 (s, C=O), 1590 (s), 1292 (s) cm^{-1}. δ_H (400 MHz, $CDCl_3$) 7.78 – 7.70 (m, 2H, 2'-***H₂***), 7.38 – 7.28 (m, 5H, 2-***H***, 4-***H***, 5-***H***, 3'-***H₂***), 7.13 – 7.08 (m, 1H, 6-***H***), 4.12 – 4.02 (m, 2H, 1''-***H₂***), 3.26 – 3.18 (m, 1H, 3''-***H***), 3.07 – 2.93 (m, 2H, C***H***, 5'''-***H***), 2.42 – 2.32 (m, 1H, 2'''-***H***), 2.30 – 2.21 (m, 1H, 3''-***H***), 2.21 – 2.13 (m, 1H, 5'''-***H***), 2.08 – 1.99 (m, 2H, 2''-***H₂***), 1.99 – 1.88 (m, 1H, 3'''-***H***), 1.88 – 1.65 (m, 2H, 4'''-***H₂***), 1.51 – 1.40 (m, 1H, 3'''-***H***), 1.26 (d, *J* = 7.0 Hz, 6H, 2xC***H₃***), 1.10 (d, *J* = 6.0 Hz, 3H, C***H₃***); δ_C (101 MHz, $CDCl_3$) 196.3 (Ar_2***C***O), 158.9 (***C***-3), 153.9 (***C***-4'), 139.2 (***C***-1), 135.2 (***C***-1'), 130.4 (***C***-2'), 129.1 (***C***-5), 126.4 (***C***-3'), 122.7 (***C***-6), 118.9 (***C***-4), 115.1 (***C***-2), 66.6 (***C***-1''), 60.5 (***C***-2'''), 53.9 (***C***-5'''), 50.8 (***C***-3''), 34.3 (***C***H), 32.6 (***C***-3'''), 28.3 (***C***-2''), 23.7 (2x***C***H_3), 21.6 (***C***-4'''), 18.7 (***C***H_3). Accurate mass: found [M+H] 366.2446, $C_{24}H_{34}NO_2$ requires *M*, 366.2433

3-(4'-chlorobenzoyl)phenol 100 [126]

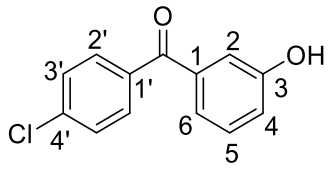

3-methoxybenzoic acid (500 mg, 3.28 mmol) was dissolved in thionyl chloride (3 mL) and heated under reflux for 2h. After cooling to RT, the volatiles were removed under reduced pressure and the products redissolved in anhydrous chlorobenzene (10 mL). $AlCl_3$ (1.31 g, 9.86 mmol) was added in portions over 20 minutes and the mixture stirred for 24h at 70ºC. After cooling to room temperature, the reaction mixture was added to 3M HCl (aq.) (10 mL) in a separating funnel and extracted with DCM (3x10

mL). The combined organic layers were washed with brine, dried over $MgSO_4$, filtered, and concentrated under reduced solid. The crude product was submitted to column chromatography (0-100% DCM in Hexane) to afford the title product (670.5 mg, 87%) as a brown solid.

δ_H (400 MHz, $CDCl_3$) 7.79 – 7.73 (m, 2H, 2'-***H***), 7.48 – 7.43 (m, 2H, 3'-***H***), 7.39 – 7.33 (m, 1H, 5-***H***), 7.33 – 7.26 (m, 2H, 2-***H***, 6-***H***), 7.12 – 7.07 (m, 1H, 4-***H***), 5.76 (s, 1H, O***H***); δ_C (101 MHz, $CDCl_3$) 195.6 (Ar_2***C***O), 155.9 (***C***-3), 139.2 (***C***-4'), 138.6 (***C***-1), 135.6 (***C***-1'), 131.5 (***C***-2'), 129.7 (***C***-5), 128.7 (***C***-3'), 122.7 (***C***-6), 120.1 (***C***-4), 116.4 (***C***-2); *m/z* (LC-MS, ESI^+) 233 [M(^{35}Cl)+H] and 235 [M(^{37}Cl)+H]) in a 3:1 ratio. All data agrees with literature.

[3-(2''-bromoethoxy)phenyl](4'-chlorophenyl)methanone 108a

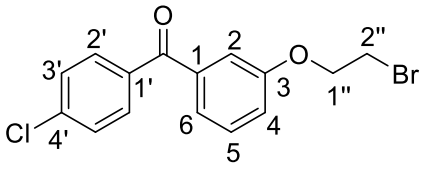

Cs_2CO_3 (420 mg, 1.28 mmol) was added to a solution of 1,2-dibromoethane (0.15 mL, 1.72 mmol) in anhydrous acetonitrile (5 mL). A solution of 4'-chloro-3-hydroxybenzophenone (100 mg, 0.43 mmol) in anhydrous acetonitrile (5 mL) was slowly added and stirred overnight at 70ºC. Once full conversion was achieved, the reaction mixture was concentrated under reduced pressure and product purified by column chromatography (0-100% DCM in Hexane) to afford the title compound (94.5 mg, 65%) as a yellow oil.

ν_{max} (ATR) 1669 (s, C=O), 1592 (s), 1270 (s) cm^{-1}. δ_H (599 MHz, $CDCl_3$) 7.75 (d, *J* = 8.4 Hz, 2H, 2'-***H***), 7.46 (d, *J* = 8.4 Hz, 2H, 3'-***H***), 7.42 – 7.38 (m, 1H, 5-***H***), 7.35 – 7.32 (m, 2H, 2-***H***, 6-***H***), 7.18 – 7.15 (m, 1H, 4-***H***), 4.35 (t, *J* = 6.1 Hz, 2H, 1''-***H₂***), 3.66 (t, *J*

= 6.1 Hz, 2H, 2''-***H₂***); δ_C (151 MHz, $CDCl_3$) 195.0 (Ar_2***C***O), 158.2 (***C***-3), 138.9 (***C***-4'), 138.6 (***C***-1), 135.7 (***C***-1'), 131.4 (***C***-2'), 129.5 (***C***-5), 128.6 (***C***-3'), 123.3 (***C***-6), 119.6 (***C***-4), 115.1 (***C***-2), 68.0 (***C***-1''), 28.9 (***C***-2''). Accurate mass: found [M+H] 338.9789, $C_{15}H_{13}N^{35}Cl^{79}BrO_2$ requires *M*, 338.9787.

(2'''*R*)-*N*-{2''-[3-(4'-chlorobenzoyl)phenoxy]ethyl}-2'''-methylpyrrolidine 109

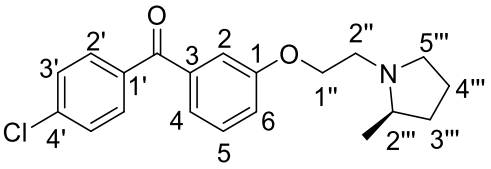

To a solution of (2*R*)-Methylpyrrolidine hydrochloride (50.1 mg, 0.41 mmol), KI (3.4 mg, 0.021 mmol) and Na_2CO_3 (110 mg, 1.038 mmol) in dry acetonitrile (5 mL) at 70ºC, [3-(2-bromoethoxy)phenyl](4-chlorophenyl)methanone (70 mg, 0.41 mmol) in dry acetonitrile (5 mL) was slowly added. Mixture stirred overnight under nitrogen atmosphere. Solution was cooled down to RT, filtered and concentrated under reduced pressure. Crude mixture was submitted to column chromatography (10% MeOH in DCM) to afford the title compound (56.5 mg, 80%) as a brown oil.

ν_{max} (ATR) 1663 (s, C=O), 1590 (s), 1292 (s) cm^{-1}. δ_H (599 MHz, $CDCl_3$) 7.76 – 7.71 (m, 2H, 2'-***H₂***), 7.46 – 7.42 (m, 2H, 3'-***H₂***), 7.39 – 7.35 (m, 1H, 5-***H***), 7.32 – 7.28 (m, 2H, 2-***H***, 4-***H***), 7.18 – 7.12 (m, 1H, 6-***H***), 4.38 – 4.30 (m, 1H, 1''-***H***), 4.30 – 4.21 (m, 1H, 1''-***H***), 3.49 – 3.41 (m, 1H, 5'''-***H***), 3.41 – 3.32 (m, 1H, 2''-***H***), 2.88 – 2.76 (m, 2H, 2''-***H***, 2'''-***H***), 2.64 – 2.52 (m, 1H, 5'''-***H***), 2.09 – 2.00 (m, 1H, 3'''-***H***), 2.00 – 1.89 (m, 1H, 4'''-***H***), 1.89 – 1.78 (m, 1H, 4'''-***H***), 1.66 – 1.57 (m, 1H, 3'''-***H***), 1.29 (d, *J* = 6.2 Hz, 3H, C***H₃***); δ_C (151 MHz, $CDCl_3$) 195.1 (Ar_2***C***O), 158.3 (***C***-1), 138.9 (***C***-4'), 138.6 (***C***-3), 135.7 (***C***-1'), 131.4 (***C***-2'), 129.5 (***C***-5), 128.63 (***C***-3'), 122.9 (***C***-4), 119.3 (***C***-6), 115.2 (***C***-2), 66.0 (***C***-1''), 61.8 (***C***-2'''), 54.6 (***C***-5'''), 52.3 (***C***-2''), 31.9 (***C***-3'''), 21.7 (***C***-4'''),

17.9 (***C***H_3). Accurate mass: found [M+H] 344.1427, $C_{20}H_{23}N^{35}ClO_2$ requires *M*, 344.1417.

[3-(3''-bromopropoxy)phenyl](4'-chlorophenyl)methanone 108b

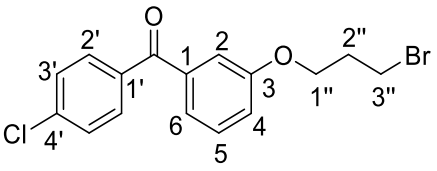

Cs_2CO_3 (630 mg, 1.93 mmol) was added to a solution of 1,3-dibromopropane (0.33 mL, 3.22 mmol) in anhydrous acetonitrile (6 mL). A solution of 4'-chloro-3-hydroxybenzophenone (150 mg, 0.64 mmol) in anhydrous acetonitrile (7 mL) was slowly added and stirred overnight at 70ºC. Once full conversion was achieved, the reaction mixture was concentrated under reduced pressure and product submitted to column chromatography (0-100% DCM in Hexane) to afford the title compound contaminated with 32% (4-chlorophenyl) [3-(prop-2-en-1-yloxy)phenyl] methanone (166.5 mg, 73%) as a white solid.

δ_H (400 MHz, $CDCl_3$) 7.79 – 7.73 (m, 2H, 2'-***H***), 7.49 – 7.43 (m, 2H, 3'-***H***), 7.42 – 7.36 (m, 1H, 5-***H***), 7.34 – 7.29 (m, 2H, 2-***H***, 6-***H***), 7.16 – 7.11 (m, 1H, 4-***H***), 4.16 (t, *J* = 5.8 Hz, 2H, 1''-***H₂***), 3.61 (t, *J* = 6.4 Hz, 2H, 3''-***H₂***), 2.38 – 2.29 (m, 2H, 2''-***H₂***); δ_C (101 MHz, $CDCl_3$) 195.2 (Ar_2***C***O), 158.8 (***C***-3), 138.9 (***C***-4'), 138.6 (***C***-1), 135.8 (***C***-1'), 131.5 (***C***-2'), 129.4 (***C***-5), 128.7 (***C***-3'), 122.9 (***C***-6), 119.4 (***C***-4), 115.0 (***C***-4), 65.5 (***C***-1''), 32.2 (***C***-3''), 29.8 (***C***-2''). Accurate mass: found [M+H] 352.9951, $C_{16}H_{15}N^{35}Cl^{79}BrO_2$ requires *M*, 352.9944.

(2’’’R)-*N*-{3’’-[3-(4’-chlorobenzoyl)phenoxy]propyl}-2’’’-methylpyrrolidine 110

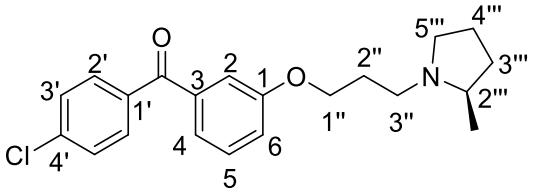

To a solution of (2*R*)-Methylpyrrolidine hydrochloride (68.8 mg, 0.56 mmol), KI (4.7 mg, 0.028 mmol) and Na_2CO_3 (150 mg, 1.41 mmol) in dry acetonitrile (5 mL) at 70ºC, [3-(3-bromopropoxy)phenyl](4-chlorophenyl)methanone (100 mg, 0.28 mmol) in dry acetonitrile (5 mL) was slowly added. Mixture stirred overnight under nitrogen atmosphere. Solution was cooled down to RT, filtered and concentrated under reduced pressure. Crude mixture was submitted to column chromatography (10% MeOH in DCM) to afford the title compound (41.5 mg, 41%) as a brown oil.

ν_{max} (ATR) 1663 (s, C=O), 1585 (s), 1292 (s) cm^{-1}. δ_H (599 MHz, $CDCl_3$) 7.76 – 7.72 (m, 2H, 2-***H*₂**), 7.46 – 7.43 (m, 2H, 3’-***H***), 7.36 (t, *J* = 8.0 Hz, 1H, 5-***H***), 7.31 – 7.26 (m, 2H, 2-***H***, 4-***H***), 7.15 – 7.10 (m, 1H, 6-***H***), 4.12 – 4.03 (m, 2H, 1’’-***H*₂**), 3.30 – 3.21 (m, 1H, 5’’’-***H***), 3.09 – 2.99 (m, 1H, 3’’-***H***), 2.50 – 2.41 (m, 1H, 2’’’-***H***), 2.37 – 2.28 (m, 1H, 3’’-***H***), 2.28 – 2.19 (m, 1H, 5’’’-***H***), 2.13 – 2.02 (m, 2H, 2’’-***H*₂**), 2.02 – 1.93 (m, 1H, 3’’’-***H***), 1.89 – 1.79 (m, 1H, 4’’’-***H***), 1.79 – 1.69 (m, 1H, 4’’’-***H***), 1.55 – 1.46 (m, 1H, 3’’’-***H***), 1.16 (d, *J* = 6.2 Hz, 3H, C***H*₃**); δ_C (151 MHz, $CDCl_3$) 195.2 (Ar_2***C***O), 158.9 (***C***-1), 138.8 (***C***-4’), 138.5 (***C***-3), 135.8 (***C***-1’), 131.4 (***C***-2’), 129.3 (***C***-5), 128.6 (***C***-3’), 122.5 (***C***-4), 119.3 (***C***-6), 115.0 (***C***-2), 66.5 (***C***-1’’), 60.8 (***C***-2’’’), 53.8 (***C***-5’’’), 50.7 (***C***-3’’), 32.5 (***C***-3’’’), 28.0 (***C***-2’’), 21.6 (***C***-4’’’), 18.4 (***C***H_3). Accurate mass: found [M+H] 358.1579, $C_{21}H_{25}N^{35}ClO_2$ requires *M*, 358.1574.

(2'''*R*)-*N*-{4''-[3-(4'-chlorobenzoyl)phenoxy]butyl}-2'''-methylpyrrolidine 111

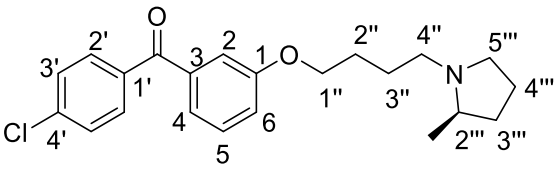

Cs_2CO_3 (630 mg, 1.93 mmol) was added to a solution of 1,4-dibromobutane (0.385 mL, 3.22 mmol) in anhydrous acetonitrile (16 mL). A solution 4'-chloro-3-hydroxybenzophenone (150 mg, 0.64 mmol) in anhydrous acetonitrile (16 mL) was slowly added and stirred overnight at 70ºC. Once full conversion was achieved, the reaction mixture was concentrated under reduced pressure and crude product was submitted to column chromatography (0-100% DCM in Hexane) to remove inorganic salts. Resultant product (130 mg) in dry acetonitrile (10 mL) was slowly added to a stirring solution of (2*R*)-methylpyrrolidine hydrochloride (86 mg, 0.71 mmol), KI (6 mg, 0.035 mmol) and Na_2CO_3 (187.4 mg, 1.77 mmol) in dry acetonitrile (8 mL) at 70ºC. Mixture stirred overnight under nitrogen atmosphere. Solution was cooled down to RT, filtered and concentrated under reduced pressure. The crude mixture was submitted to column chromatography (10% MeOH in DCM) to afford the title compound (35.3 mg, 27%) as a brown oil.

ν_{max} (ATR) 1662 (s, C=O), 1585 (s), 1289 (s) cm^{-1}. δ_H (599 MHz, $CDCl_3$) 7.77 – 7.73 (m, 2H, 2'-***H*₂**), 7.47 – 7.43 (m, 2H, 3'-***H*₂**), 7.39 – 7.35 (m, 1H, 5), 7.30 – 7.27 (m, 2H, 2-***H***, 4-***H***), 7.13 – 7.10 (m, 1H, 6-***H***), 4.09 – 3.97 (m, 2H, 1''-***H*₂**), 3.35 – 3.23 (m, 1H, 5'''-***H***), 3.00 – 2.88 (m, 1H, 4''-***H***), 2.61 – 2.40 (m, 1H, 2'''-***H***), 2.37 – 2.20 (m, 2H, 4''-***H***, 5'''-***H***), 2.07 – 1.94 (m, 1H, 3'''-***H***), 1.92 – 1.84 (m, 2H, 2''-***H***, 4'''-***H***), 1.83 – 1.71 (m, 4H, 2''-***H***, 3''-***H*₂**, 4'''-***H***), 1.62 – 1.48 (m, 1H, 3'''-***H***), 1.20 (d, *J* = 6.2 Hz, 3H, ***C***H_3); δ_C (151 MHz, $CDCl_3$) 195.3 (Ar_2***C***O), 159.0 (***C***-1), 138.9 (***C***-4'), 138.5 (***C***-3), 135.9 (***C***-1'),

131.4 (***C***-2'), 129.3 (***C***-5), 128.6 (***C***-3'), 122.5 (***C***-4), 119.4 (***C***-6), 114.9 (***C***-2), 67.8 (***C***-1''), 61.0 (***C***-2'''), 53.6 (***C***-4''), 53.5 (***C***-5'''), 32.3 (***C***-3'''), 27.2 (***C***-2''), 24.6 (***C***-3''), 21.5 (***C***-4'''), 18.1 (***C***H_3). Accurate mass: found [M+H] 372.1716, $C_{22}H_{27}N^{35}ClO_2$ requires *M*, 372.1730.

[4-(2''-bromoethoxy)phenyl](phenyl)methanone 77a

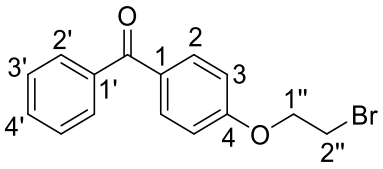

1,2-Dibromoethane (0.175 mL, 2.02 mmol) was reacted with 4-Hydroxybenzophenone (100 mg, 0.50 mmol) in anhydrous acetonitrile (5 mL) following general procedure A. Purification by column chromatography (100% Chloroform) afforded the title compound (90.3 mg, 58.7%) as a white solid.

ν_{max} (ATR) 1602 (s, C=O) cm^{-1}. δ_H (599 MHz, $CDCl_3$) 7.85 – 7.82 (m, 2H, 2-***H***), 7.78 – 7.74 (m, 2H, 2'-***H***), 7.59 – 7.55 (m, 1H, 4'-***H***), 7.50 – 7.46 (m, 2H, 3'-***H***), 7.00 – 6.96 (m, 2H, 3-***H***), 4.38 (t, *J* = 6.2 Hz, 2H, 1''-***H*₂**), 3.68 (t, *J* = 6.2 Hz, 2H, 2''-***H*₂**); δ_C (176 MHz, $CDCl_3$) 195.4 (Ar_2***C***O), 161.6 (***C***-4), 138.1 (***C***-1'), 132.6 (***C***-2), 131.9 (***C***-4'), 130.8 (***C***-1), 129.7 (***C***-2'), 128.2 (***C***-3'), 114.1 (***C***-3), 67.8 (***C***-1''), 28.5 (***C***-2''). Accurate mass: found [M+H] 305.0175, $C_{15}H_{14}{}^{79}BrO_2$ requires *M*, 305.0177.

(2'''*R*)-1'''-[2''-(4-benzoylphenoxy)ethyl]-2'''-methylpyrrolidine 78

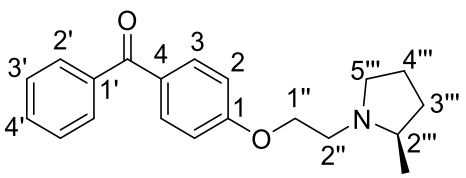

To a solution of (2*R*)-methylpyrrolidine hydrochloride (43 mg, 0.35 mmol), KI (5 mg, 0.033 mmol) and K_2CO_3 (208 mg, 1.51 mmol) in dry acetonitrile (30.5 mL) at 70ºC, [4-(2''-Bromoethoxy)phenyl](phenyl)methanone (100 mg, 0.33 mmol) in dry acetonitrile (30 mL) was slowly added. The mixture was then stirred overnight under a nitrogen atmosphere. The solution was then cooled to RT, filtered and concentrated. The crude mixture was submitted to column chromatography (10% MeOH in DCM) to afford the title compound (29 mg, 28%) as a yellow oil.

ν_{max} (ATR) 1669 (s, C=O), 1603 (s), 1456 (s) cm^{-1}. δ_H (599 MHz, $CDCl_3$) 7.83 – 7.78 (m, 2H, 3-***H***), 7.76 – 7.72 (m, 2H, 2'-***H***), 7.57 – 7.53 (m, 1H, 4'-***H***), 7.49 – 7.44 (m, 2H, 3'-***H***), 6.98 – 6.93 (m, 2H, 2-***H***), 4.20 (td, *J* = 6.1, 2.0 Hz, 2H, 1''-***H₂***), 3.32 – 3.20 (m, 2H, 2''-***H***, 5'''-***H***), 2.65 – 2.58 (m, 1H, 2''-***H***), 2.53 – 2.43 (m, 1H, 2'''-***H***), 2.38 – 2.30 (m, 1H, 5'''-***H***), 1.99 – 1.91 (m, 1H, 3'''-***H***), 1.89 – 1.78 (m, 1H, 4'''-***H***), 1.78 – 1.70 (m, 1H, 4'''-***H***), 1.52 – 1.41 (m, 1H, 3'''-***H***), 1.16 (d, *J* = 6.2 Hz, 3H, C***H₃***); δ_C (151 MHz, $CDCl_3$) 195.5 (Ar_2***C***O), 162.4 (***C***-1), 138.3 (***C***-1'), 132.5 (***C***-3), 131.8 (***C***-4'), 130.1 (***C***-4), 129.7 (***C***-2'), 128.1 (***C***-3'), 114.1 (***C***-2), 67.3 (***C***-1''), 60.6 (***C***-2'''), 54.8 (***C***-5'''), 52.5 (***C***-2''), 32.3 (***C***-3'''), 21.9 (***C***-4'''), 18.9 (***C***H_3). Accurate mass: found [M+H] 324.1976, $C_{21}H_{24}NO_2$ requires *M*, 324.1964.

[4-(3''-bromopropoxy)phenyl](phenyl)methanone 77b

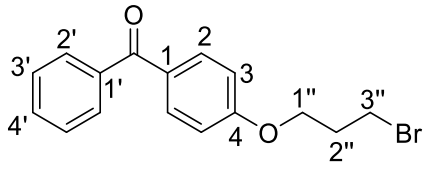

4-Hydroxybenzophenone (100 mg, 0.50 mmol) was reacted with 1,3-Dibromopropane (0.3 mL, 3.03 mmol) in anhydrous DMF (5 mL) following general procedure A. Purification by column chromatography (100% Chloroform) afforded the title

compound (128 mg, 79%) as a colourless oil.

ν_{max} (ATR) 1653 (s, C=O), 1601 (s), 1251 (s) cm^{-1}. δ_H (700 MHz, $CDCl_3$) 7.85 – 7.81 (m, 2H, 2-***H***), 7.77 – 7.74 (m, 2H, 2'-***H***), 7.58 (t, *J* = 7.5 Hz, 1H, 4'-***H***), 7.50 – 7.45 (m, 2H, 3'-***H***), 6.99 – 6.96 (m, 2H, 3-***H***), 4.20 (t, *J* = 5.8 Hz, 2H, 1''-***H₂***), 3.62 (t, *J* = 6.4 Hz, 2H, 3''-***H₂***), 2.36 (p, *J* = 6.1 Hz, 2H, 2''-***H₂***); δ_C (176 MHz, $CDCl_3$) 195.5 (Ar_2***C***O), 162.3 (***C***-4), 138.2 (***C***-1'), 132.5 (***C***-2), 131.90 (***C***-4'), 130.4 (***C***-1), 129.7 (***C***-2'), 128.2 (***C***-3'), 114.0 (***C***-3), 65.5 (***C***-1''), 32.1 (***C***-3''), 29.7 (***C***-2''). Accurate mass: found [M+H] 319.0332, $C_{16}H_{16}{}^{79}BrO_2$ requires *M*, 319.0334.

(2'''*R*)-1'''-[3''-(4-benzoylphenoxy)propyl]-2'''-methylpyrrolidine 79

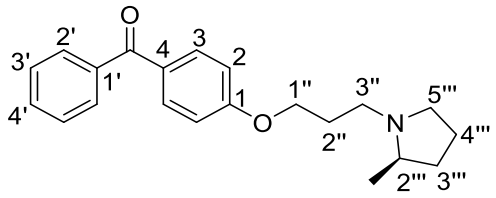

[4-(3''-Bromopropoxy)phenyl](phenyl)methanone (70 mg, 0.22 mmol) was reacted with (2*R*)-methylpyrrolidine hydrochloride (28 mg, 0.23 mmol) following general procedure B. The product was purified by column chromatography (10% MeOH in DCM) to afford the title compound (17.6 mg, 25%) as a brown solid.

ν_{max} (ATR) 1603 (s, C=O), 1259 (s) cm^{-1}. δ_H (599 MHz, $CDCl_3$) 7.83 – 7.79 (m, 2H, 3-***H***), 7.76 – 7.73 (m, 2H, 2'-***H***), 7.58 – 7.54 (m, 1H, 4'-***H***), 7.49 – 7.44 (m, 2H, 3'-***H***), 6.96 – 6.93 (m, 2H, 2-***H***), 4.18 – 4.09 (m, 2H, 1''-***H₂***), 3.43 – 3.32 (m, 1H, 5'''-***H***), 3.19 – 3.09 (m, 1H, 3''-***H***), 2.71 – 2.58 (m, 1H, 2'''-***H***), 2.54 – 2.45 (m, 1H, 3''-***H***), 2.45 – 2.35 (m, 1H, 5'''-***H***), 2.27 – 2.18 (m, 1H, 2''-***H***), 2.18 – 2.09 (m, 1H, 2''-***H***), 2.08 – 1.99 (m, 1H, 3'''-***H***), 1.98 – 1.88 (m, 1H, 4'''-***H***), 1.86 – 1.76 (m, 1H, 4'''-***H***), 1.67 – 1.57 (m, 1H, 3'''-***H***), 1.34 – 1.24 (m, 3H, C***H₃***); δ_C (151 MHz, $CDCl_3$) 195.5 (Ar_2***C***O), 162.4 (***C***-1), 138.2 (***C***-1'), 132.5 (***C***-3), 131.9 (***C***-4'), 130.2 (***C***-4), 129.7 (***C***-2'), 128.1 (***C***-3'), 113.9 (***C***-2),

66.2 (***C***-1''), 61.4 (***C***-2'''), 53.6 (***C***-5'''), 50.5 (***C***-3''), 32.2 (***C***-3'''), 27.4 (***C***-2''), 21.5 (***C***-4'''), 17.8 (***C***H_3). Accurate mass: found [M+H] 324.1959, $C_{21}H_{26}NO_2$ requires *M*, 324.1964.

[4-(4''-bromobutoxy)phenyl](phenyl)methanone 77c

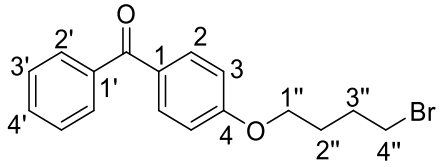

1,4-Dibromobutane (0.602 mL, 5.045 mmol) was reacted with 4-Hydroxybenzophenone (200 mg, 1.009 mmol) in anhydrous DMF (5 mL) following general procedure A. Purification by column chromatography (0 to 100% DCM in Hexane) afforded the title compound (159 mg, 47%) as a white solid.

ν_{max} (ATR) 1602 (s, C=O), 1264 (s) cm^{-1}. δ_H (599 MHz, $CDCl_3$) 7.84 – 7.80 (m, 2H, 2-***H***), 7.78 – 7.73 (m, 2H, 2'-***H***), 7.59 – 7.54 (m, 1H, 4'-***H***), 7.50 – 7.45 (m, 2H, 3'-***H***), 6.97 – 6.92 (m, 2H, 3-***H***), 4.09 (t, *J* = 6.1 Hz, 2H, 1''-***H*****2**), 3.50 (t, *J* = 6.6 Hz, 2H, 4''-***H*****2**), 2.13 – 2.06 (m, 2H, 2''-***H*****2**), 2.04 – 1.95 (m, 2H, 3''-***H*****2**); δ_C (151 MHz, $CDCl_3$) 195.5 (Ar_2***C***O), 162.5 (***C***-4), 138.3 (***C***-1'), 132.6 (***C***-2), 131.9 (***C***-4'), 130.2 (***C***-1), 129.7 (***C***-2'), 128.2 (***C***-3'), 113.9 (***C***-3), 67.1 (***C***-1''), 33.2 (***C***-4''), 29.3 (***C***-2''), 27.7 (***C***-3''). Accurate mass: found [M+H] 333.0493, $C_{17}H_{18}{}^{79}BrO_2$ requires *M*, 333.0490.

(2'''*R*)-1'''-[4''-(4-benzoylphenoxy)butyl]-2'''-methylpyrrolidine 80

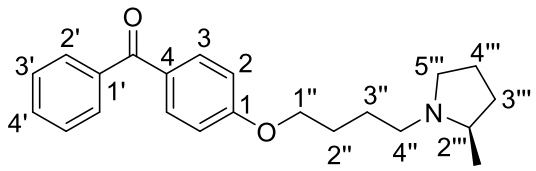

[4-(4’’-Bromobutoxy)phenyl](phenyl)methanone (100 mg, 0.300 mmol) was reacted with (2*R*)-methylpyrrolidine hydrochloride (38 mg, 0.312 mmol) in DMF following general procedure B. Product was purified by column chromatography (10% MeOH in DCM) to afford the title compound (31.3 mg, 31%) as a light brown solid.

ν_{max} (ATR) 1605 (s, C=O), 1260 (s) cm^{-1}. δ_H (599 MHz, $CDCl_3$) 7.84 – 7.77 (m, 2H, 3-***H***), 7.77 – 7.70 (m, 2H, 2’-***H***), 7.58 – 7.52 (m, 1H, 4’-***H***), 7.49 – 7.43 (m, 2H, 3’-***H***), 6.97 – 6.90 (m, 2H, 2-***H***), 4.06 (t, *J* = 6.4 Hz, 2H, 1’’-***H₂***), 3.28 – 3.18 (m, 1H, 5’’’-***H***), 2.93 – 2.84 (m, 1H, 4’’-***H***), 2.42 – 2.34 (m, 1H, 2’’’-***H***), 2.23 – 2.10 (m, 2H, 4’’-***H***, 5’’’-***H***), 1.99 – 1.91 (m, 1H, 3’’’-***H***), 1.91 – 1.85 (m, 1H, 2’’-***H***), 1.85 – 1.79 (m, 2H, 2’’-***H***, 4’’’-***H***), 1.78 – 1.66 (m, 3H, 3’’-***H₂***, 4’’’-***H***), 1.54 – 1.41 (m, 1H, 3’’’-***H***), 1.15 (d, *J* = 6.1 Hz, 3H, C***H₃***); δ_C (151 MHz, $CDCl_3$) 195.6 (Ar_2***C***O), 162.7 (***C***-1), 138.3 (***C***-1’), 132.5 (***C***-3), 131.8 (***C***-4’), 129.9 (***C***-4), 129.7 (***C***-2’), 128.1 (***C***-3’), 114.0 (***C***-2), 67.9 (***C***-1’’), 60.6 (***C***-2’’’), 53.7 (***C***-5’’’), 53.6 (***C***-4’’), 32.5 (***C***-3’’’), 27.2 (***C***-2’’), 24.9 (***C***-3’’), 21.6 (***C***-4’’’), 18.5 (***C***H_3). Accurate mass: found [M+H] 338.2139, $C_{22}H_{28}NO_2$ requires *M*, 338.2120.

[4-(2’’-bromoethoxy)phenyl](4’-chlorophenyl)methanone 77d

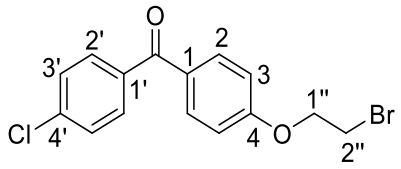

1,2-Dibromoethane (0.15 mL, 1.72 mmol) was reacted with 4-Chloro-4'-hydroxybenzophenone (100 mg, 0.43 mmol) in anhydrous DMF (4.5 mL) following general procedure A. Purification by column chromatography (100% DCM) afforded the title compound (32.6 mg, 22.3%) as a white solid.

ν_{max} (ATR) 1607 (s, C=O) cm^{-1}. δ_H (599 MHz, $CDCl_3$) 7.82 – 7.78 (m, 2H, 2-***H***), 7.73 – 7.69 (m, 2H, 2’-***H***), 7.47 – 7.44 (m, 2H, 3’-***H***), 7.00 – 6.96 (m, 2H, 3-***H***), 4.38 (t, *J* = 6.2

Hz, 2H, 1''-***H₂***), 3.68 (t, *J* = 6.2 Hz, 2H, 2''-***H₂***); δ_C (151 MHz, $CDCl_3$) 194.2 (Ar_2***C***O), 161.8 (***C***-4), 138.4 (***C***-1'), 136.4 (***C***-4'), 132.5 (***C***-2), 131.2 (***C***-2'), 130.5 (***C***-1), 128.6 (***C***-3'), 114.3 (***C***-3), 67.9 (***C***-1''), 28.5 (***C***-2''). Accurate mass: found [M+H] 338.9796, $C_{15}H_{13}N^{35}Cl^{79}BrO_2$ requires *M*, 338.9807.

(2'''*R*)-1'''-{2''-[4-(4'-chlorobenzoyl)phenoxy]ethyl}-2'''-methylpyrrolidine 81

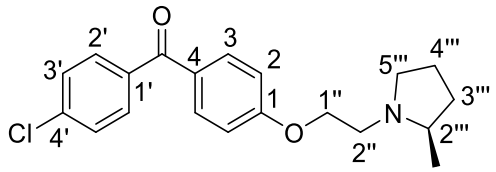

[4-(2''-Bromoethoxy)phenyl](4'-chlorophenyl)methanone (30 mg, 0.088 mmol) was reacted with (2*R*)-methylpyrrolidine hydrochloride (11.3 mg, 0.093 mmol) in anhydrous MeCN following general procedure B. Product was purified by column chromatography (10% MeOH in DCM) to afford the title compound (7 mg, 23%) as a brown solid.

ν_{max} (ATR) 1657 (s, C=O) cm^{-1}. δ_H (599 MHz, $CDCl_3$) 7.81 – 7.76 (m, 2H, 3-***H***), 7.72 – 7.68 (m, 2H, 2'-***H***), 7.47 – 7.43 (m, 2H, 3'-***H***), 6.99 – 6.95 (m, 2H, 2-***H***), 4.50 – 4.20 (m, 2H, 1''-***H₂***), 3.51 – 3.22 (m, 2H, 2''-***H***, 5'''-***H***), 2.87 – 2.61 (m, 2H, 2''-***H***, 2'''-***H***), 2.61 – 2.41 (m, 1H, 5'''-***H***), 2.10 – 1.98 (m, 1H, 3'''-***H***), 1.98 – 1.88 (m, 1H, 4'''-***H***), 1.88 – 1.77 (m, 1H, 4'''-***H***), 1.68 – 1.50 (m, 1H, 3'''-***H***), 1.34 – 1.25 (m, 3H, C***H₃***); δ_C (151 MHz, $CDCl_3$) 194.2 (Ar_2***C***O), 162.2 (***C***-1) 138.3 (***C***-1'), 136.5 (***C***-4'), 132.4 (***C***-3), 131.1 (***C***-2'), 130.1 (***C***-4), 128.5 (***C***-3'), 114.2 (***C***-2), 66.4 (***C***-1''), 61.4 (***C***-2'''), 54.4 (***C***-5'''), 52.2 (***C***-2''), 33.9 (***C***-3'''), 21.7 (***C***-4'''), 18.0 (***C***H_3). Accurate mass: found [M+H] 344.1425, $C_{20}H_{23}N^{35}ClO_2$ requires *M*, 344.1417.

[4-(3’’-bromopropoxy)phenyl](4’-chlorophenyl)methanone 77e

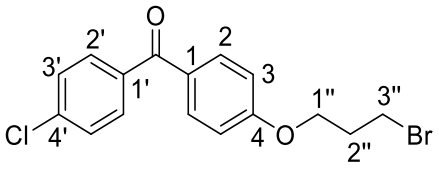

1,3-Dibromoproane (0.349 mL, 3.438 mmol) was reacted with 4-Hydroxybenzophenone (200 mg, 0.860 mmol) in anhydrous acetonitrile (4.5 mL) following general procedure A. Purification by column chromatography (50% Hexane in DCM) afforded the title compound (193.8 mg, 64%) as a white solid.

ν_{max} (ATR) 1607 (s, C=O) cm^{-1}. δ_H (599 MHz, $CDCl_3$) 7.81 – 7.77 (m, 2H, 2-***H***), 7.73 – 7.69 (m, 2H, 2’-***H***), 7.47 – 7.44 (m, 2H, 3’-***H***), 7.00 – 6.95 (m, 2H, 3-***H***), 4.20 (d, *J* = 5.9 Hz, 2H, 1’’-$\boldsymbol{H_2}$), 3.62 (t, *J* = 5.9 Hz, 2H, 3’’-$\boldsymbol{H_2}$), 2.36 (p, *J* = 5.9 Hz, 2H, 2’’-$\boldsymbol{H_2}$); δ_C (151 MHz, $CDCl_3$) 194.2 ($Ar_2\boldsymbol{C}O$), 162.5 (***C***-4), 138.3 (***C***-1’), 136.5 (***C***-4’), 132.5 (***C***-2), 131.1 (***C***-2’), 130.0 (***C***-1), 128.5 (***C***-3’), 114.1 (***C***-3), 65.5 (***C***-1’’), 32.1 (***C***-2’’), 29.6 (***C***-3’’). Accurate mass: found [M+H] 352.9944, $C_{16}H_{15}N^{35}Cl^{79}BrO_2$ requires *M*, 352.9944.

(2’’’*R*)-*N*-{3’’-[4-(4’-chlorobenzoyl)phenoxy]propyl}-2’’’-methylpyrrolidine 82

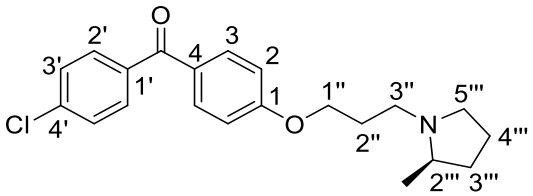

[4-(3-bromopropoxy)phenyl](4-chlorophenyl)methanone (106 mg, 0.300 mmol) was reacted with (2*R*)-Methylpyrrolidine hydrochloride (44 mg, 0.384 mmol) following general procedure B. Product was purified by column chromatography (10% MeOH in DCM) to afford the title compound (49.1 mg, 46%) as a brown solid.

ν_{max} (ATR) 1602 (s, C=O), 1264 (s) cm^{-1}. δ_H (400 MHz, $CDCl_3$) 7.87 – 7.77 (m, 2H, 3-***H₂***), 7.77 – 7.65 (m, 2H, 2'-***H₂***), 7.51 – 7.42 (m, 2H, 3'-***H₂***), 7.07 – 6.91 (m, 2H, 2-***H₂***), 4.24 – 4.05 (m, 2H, 1''-***H₂***), 3.34 – 3.18 (m, 1H, 5'''-***H***), 3.12 – 2.96 (m, 1H, 3''-***H***), 2.50 – 2.34 (m, 1H, 2'''-***H***), 2.34 – 2.25 (m, 1H, 3''-***H***), 2.25 – 2.15 (m, 1H, 5'''-***H***), 2.15 – 2.03 (m, 2H, 2''-***H₂***), 2.03 – 1.92 (m, 1H, 3'''-***H***), 1.92 – 1.68 (m, 2H, 4'''-***H₂***), 1.55 – 1.42 (m, 1H, 3'''-***H***), 1.22 – 1.08 (m, 3H, C***H₃***). δ_C (151 MHz, $CDCl_3$) 194.2 (Ar_2***C***O), 162.3 (***C***-1), 138.4 (***C***-1'), 136.4 (***C***-4'), 132.5 (***C***-3), 131.1 (***C***-2'), 130.1 (***C***-4), 128.5 (***C***-3'), 114.1 (***C***-2), 65.9 (***C***-1''), 64.3 (***C***-2'''), 53.3 (***C***-5'''), 50.5 (***C***-3''), 31.9 (***C***-3'''), 26.6 (***C***-2''') 21.4 (***C***-4'''), 17.9 (***C***H_3). Accurate mass: found [M+H] 358.1575, $C_{21}H_{25}N^{35}ClO_2$ requires *M*, 358.1574.

[4-(4''-bromobutoxy)phenyl](4'-chlorophenyl)methanone 77f

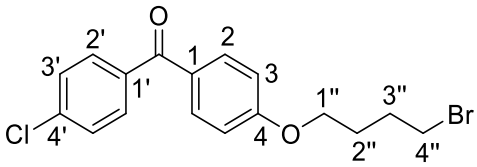

1,4-dibromobutane (0.411 mL, 3.428 mmol) was reacted with 4'-Chloro-4-hydroxybenzophenone (150 mg, 0.757 mmol) in anhydrous DMF (8.6 mL) following general procedure A. The product was precipitated overnight at -20ºC. Solvent was removed using a glass pipette and white solid left was washed with cold EtOAc to afford the title product (135.3mg, 41%).

ν_{max} (ATR) 1643 (s, C=O), 1607 (s), 1258 (s) cm^{-1}. δ_H (599 MHz, $CDCl_3$) 7.80 – 7.77 (m, 2H, 2-***H***), 7.72 – 7.69 (m, 2H, 2'-***H***), 7.47 – 7.44 (m, 2H, 3'-***H***), 6.97 – 6.93 (m, 2H, 3-***H***), 4.09 (t, *J* = 6.0 Hz, 2H, 1''-***H₂***), 3.50 (t, *J* = 6.6 Hz, 2H, 4''-***H₂***), 2.13 – 2.06 (m, 2H, 3''-***H₂***), 2.03 – 1.96 (m, 2H, 2''-***H₂***); δ_C (151 MHz, $CDCl_3$) 194.2 (Ar_2***C***O), 162.7 (***C***-4), 138.3 (***C***-1'), 136.5 (***C***-4'), 132.5 (***C***-2), 131.1 (***C***-2'), 129.83 (***C***-1), 128.5 (***C***-3'), 114.09 (***C***-3), 67.16 (***C***-1''), 33.21 (***C***-4''), 29.32 (***C***-3''), 27.73 (***C***-2''). Accurate mass: found [M+H] 367.0097, $C_{17}H_{17}N^{35}Cl^{79}BrO_2$ requires *M*, 367.367.0100.

(2'''*R*)-*N*-{4''-[4-(4'-chlorobenzoyl)phenoxy]butyl}-2'''-methylpyrrolidine 83

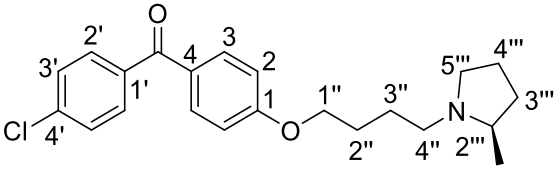

[4-(4-bromobutoxy)phenyl](4-chlorophenyl)methanone (92 mg, 0.25 mmol) was reacted with (2*R*)-Methylpyrrolidine hydrochloride (35 mg, 0.29 mmol) in dry DMF (2.5 mL) following general procedure B. Product was purified by column chromatography (10% MeOH in DCM) to afford the title compound (48.2 mg, 52%) as a yellow oil.

ν_{max} (ATR) 1603 (s, C=O), 1257 (s) cm^{-1}. δ_H (599 MHz, $CDCl_3$) 7.80 – 7.74 (m, 2H, 3-***H₂***), 7.72 – 7.66 (m, 2H, 2-***H₂***), 7.46 – 7.40 (m, 2H, 2'-***H₂***), 6.97 – 6.90 (m, 2H, 3'-***H₂***), 4.11 – 4.01 (m, 2H, 1''-***H₂***), 3.40 – 3.26 (m, 1H, 5'''-***H***), 3.03 – 2.91 (m, 1H, 4''-***H***), 2.67 – 2.47 (m, 1H, 2'''-***H***), 2.42 – 2.24 (m, 2H, 4''-***H***, 5'''-***H***), 2.06 – 1.96 (m, 1H, 3'''-***H***), 1.96 – 1.73 (m, 6H, 2''-***H₂***, 3''-***H₂***, 4'''-***H₂***), 1.64 – 1.55 (m, 1H, 3'''-***H₂***), 1.24 (d, *J* = 6.3 Hz, 3H, C***H₃***); δ_C (151 MHz, $CDCl_3$) 194.2 (Ar_2***C***O), 162.8 (***C***-1), 138.2 (***C***-1'), 136.5 (***C***-4'), 132.4 (***C***-3), 131.1 (***C***-2'), 129.7 (***C***-4), 128.5 (***C***-3'), 114.1 (***C***-2), 67.8 (***C***-1''), 61.2 (***C***-2'''), 53.5 (***C***-5'''), 53.4 (***C***-4''), 32.2 (***C***-3'''), 27.1 (***C***-2''), 24.4 (***C***-3''), 21.5 (***C***-4'''), 17.9 (***C***H_3). Accurate mass: found [M+H] 372.1736, $C_{22}H_{27}N^{35}ClO_2$ requires *M*, 372.1730.

(3'-chlorophenyl)(4-methoxyphenyl)methanone [127]

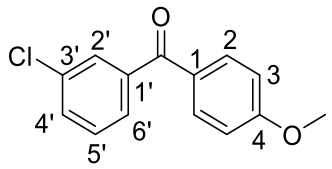

3-chlorobenzoate (1g, 6.39 mmol) was dissolved in thionyl chloride (3 mL) and refluxed for 3hours. After cooling down to RT, volatiles were removed under reduced pressure. 3-benzoyl chloride was then added to a solution of anisole (0.85 mL, 7.78 mmol) in anhydrous DCE (31 mL). $AlCl_3$ (1.04 g, 7.78 mmol) was added in portions over 20 minutes and mixture stirred for 24h at RT. In a separating funnel, the reaction mixture was added to 3M HCl (aq.) (30 mL) and extracted with DCM (3x20 mL). Combined organic layers were washed with brine, dried over $MgSO_4$, filtered, and concentrated under reduced solid. Crude was submitted to column chromatography (0-100% EtOAc in Hexane) to afford de title product (1.19 g, 77%) as a white solid.

ν_{max} (ATR) 1602 (s, C=O), 1259 (s) cm^{-1}. δ_H (400 MHz, $CDCl_3$) 7.84 – 7.79 (m, 2H, 2-***H*₂**), 7.75 – 7.71 (m, 1H, 2'-***H***), 7.64 – 7.60 (m, 1H, 6'-***H***), 7.56 – 7.52 (m, 1H, 4'-***H***), 7.44 – 7.39 (m, 1H, 5'-***H***), 7.00 – 6.96 (m, 2H, 3-***H*₂**), 3.90 (s, 3H, C***H*₃**); δ_C (101 MHz, $CDCl_3$) 194.1 (Ar_2***C***O), 163.5 (***C***-4), 139.9 (***C***-5), 134.4 (***C***-1'), 132.6 (***C***-2), 131.9 (***C***-3'), 129.6 (***C***-5'), 129.6 (***C***-6'), 129.5 (***C***-4'), 127.8 (***C***-2'), 113.8 (***C***-3), 55.6 (***C***H_3). *m/z*

(LC-MS, ESI^+) 247 [M(^{35}Cl)+H] and 249 [M(^{37}Cl)+H]) in a 3:1 ratio. All data agrees with literature.

4-(3'-chlorobenzoyl)phenol 84 [127]

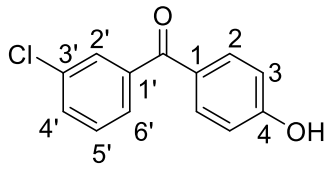

$AlCl_3$ (421.2 mg, 3.16 mmol) was added to a solution of (3-chlorophenyl)(4-methoxyphenyl)methanone (208 mg, 0.843 mmol) in dry toluene (5.6 mL) and mixture was heated under reflux for 2h. The mixture was cooled then poured into 3M HCl (aq.) (10 mL) in a separating funnel and extracted with EtOAc (3x15 mL). The organic layer was washed with brine, dried over $MgSO_4$, filtered, and concentrated under reduced pressure to afford the title product (196.17 mg, 99%) as a brown solid.

ν_{max} (ATR) 1740 (s, C=O), 1247 (s) cm^{-1}. δ_H (400 MHz, $CDCl_3$) 7.81 – 7.75 (m, 2H, 2-***H***), 7.75 – 7.70 (m, 1H, 2'-***H***), 7.62 (dt, *J* = 7.8, 1.4 Hz, 1H, 6'-***H***), 7.57 – 7.52 (m, 1H, 4'-***H***), 7.42 (t, *J* = 7.8 Hz, 1H, 5'-***H***), 6.96 – 6.89 (m, 2H, 3-***H***); δ_C (101 MHz, $CDCl_3$) 194.2 (Ar_2***C***O), 160.0 (***C***-4), 139.9 (***C***-3'), 134.5 (***C***-1'), 132.9 (***C***-2), 131.9 (***C***-4'), 129.7 (***C***-1'), 129.6 (***C***-2'), 129.6 (***C***-5'), 127.8 (***C***-6'), 115.3 (***C***-3). *m/z* (LC-MS, ESI^+) 233 [M(^{35}Cl)+H] and 235 [M(^{37}Cl)+H]) in a 3:1 ratio. All data agrees with literature.

[4-(3''-bromopropoxy)phenyl](3'-chlorophenyl)methanone 89

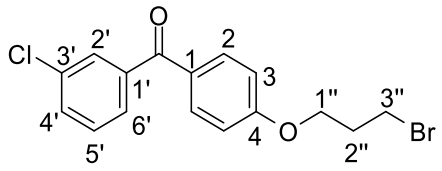

Na_2CO_3 (683.3 mg, 6.45 mmol) was added to a solution of 1,3-dibromopropane (0.327 mL, 3.22 mmol) in anhydrous acetonitrile (15.2 mL). A solution of 4-(3-chlorobenzoyl)phenol (150 mg, 0.645 mmol) in anhydrous acetonitrile (17 mL) was slowly added and stirred overnight at 70ºC. Once full conversion was achieved, the reaction mixture was concentrated under reduced pressure and product was purified by column chromatography (0-100% Chloroform) to afford the title compound (90.3 mg, 59%) as a yellow oil.

δ_H (400 MHz, $CDCl_3$) 7.84 – 7.78 (m, 2H, 2-***H***), 7.73 (t, *J* = 1.8 Hz, 1H, 2'-***H***), 7.62 (dt, *J* = 7.8, 1.4 Hz, 1H, 6'-***H***), 7.56 – 7.51 (m, 1H, 4'-***H***), 7.42 (t, *J* = 7.8 Hz, 1H, 5'-***H***), 7.01 – 6.95 (m, 2H, 3-***H***), 4.21 (t, *J* = 5.8 Hz, 2H, 1''-$\boldsymbol{H_2}$), 3.62 (t, *J* = 6.3 Hz, 2H, 3''-$\boldsymbol{H_2}$), 2.41 – 2.32 (m, 2H, 2''-$\boldsymbol{H_2}$); δ_C (101 MHz, $CDCl_3$) 194.0 ($Ar_2\boldsymbol{C}O$), 162.6 (***C***-4), 139.9 (***C***-3'), 134.4 (***C***-1'), 132.6 (***C***-2), 131.9 (***C***-4'), 129.7 (***C***-1), 129.6 (***C***-2'), 129.6 (***C***-5'), 127.8 (***C***-6'), 114.2 (***C***-3), 65.6 (***C***-1''), 32.1 (***C***-2''), 29.7 (***C***-3''). *m/z* (LC-MS, ESI^+) 353 [M($^{35}Cl^{79}Br$)+H], 355 [M($^{37}Cl^{79}Br$)+H]) and 357 [M($^{37}Cl^{81}Br$)+H]) in a 3:4:1 ratio.

(2'''*R*)-*N*-{3''-[4-(3'-chlorobenzoyl)phenoxy]propyl}-2'''-methylpyrrolidine 91

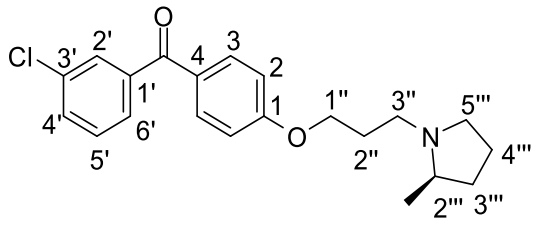

To a solution of (2*R*)-methylpyrrolidine hydrochloride (37.1 mg, 0.305 mmol), KI (4.2 mg, 0.025 mmol) and Na_2CO_3 (124 mg, 1.71 mmol) in dry acetonitrile (7 mL) at 70ºC,

[4-(3-Bromopropoxy)phenyl](3-chlorophenyl)methanone (96 mg, 0.27 mmol) in dry acetonitrile (5 mL) was slowly added. The mixture stirred overnight under nitrogen atmosphere. The solution was then cooled to RT, filtered, and concentrated under reduced pressure. The crude mixture was submitted to column chromatography (10% MeOH in DCM) to afford the title compound (51.3 mg, 53%) as a yellow oil.

ν_{max} (ATR) 1602 (s, C=O), 1270 (s) cm^{-1}. δ_H (599 MHz, $CDCl_3$) 7.82 – 7.78 (m, 2H, 3-***H***), 7.72 (t, *J* = 1.9 Hz, 1H, 2'-***H***), 7.61 (dt, *J* = 7.8, 1.3 Hz, 1H, 6'-***H***), 7.55 – 7.52 (m, 1H, 4'-***H***), 7.41 (t, *J* = 7.8 Hz, 1H, 5'-***H***), 6.99 – 6.95 (m, 2H, 2-***H***), 4.18 – 4.09 (m, 2H, 1''-$\boldsymbol{H_2}$), 3.35 – 3.21 (m, 1H, 5'''-***H***), 3.12 – 3.00 (m, 1H, 3''-***H***), 2.59 – 2.41 (m, 1H, 2'''-***H***), 2.42 – 2.30 (m, 1H, 3''-***H***), 2.30 – 2.19 (m, 1H, 5'''-***H***), 2.19 – 2.04 (m, 2H, 2''-$\boldsymbol{H_2}$), 2.04 – 1.92 (m, 1H, 3'''-***H***), 1.92 – 1.81 (m, 1H, 4'''-***H***), 1.81 – 1.71 (m, 1H, 4'''-***H***), 1.60 – 1.44 (m, 1H, 3'''-***H***), 1.18 (d, *J* = 6.0 Hz, 3H, C$\boldsymbol{H_3}$); δ_C (151 MHz, $CDCl_3$) 193.9 ($Ar_2\boldsymbol{C}O$), 162.9 (***C***-1), 139.9 (***C***-3'), 134.4 (***C***-1'), 132.5 (***C***-3), 131.8 (***C***-4'), 129.6 (***C***-2'), 129.5 (***C***-5'), 129.4 (***C***-4), 127.7 (***C***-6'), 114.2 (***C***-2), 66.5 (***C***-1''), 60.6 (***C***-2'''), 53.8 (***C***-5'''), 50.6 (***C***-3''), 32.5 (***C***-3'''), 27.9 (***C***-2''), 21.6 (***C***-4'''), 18.4 (***C***H_3). Accurate mass: found [M+H] 358.1584, $C_{21}H_{25}N^{35}ClO_2$ requires *M*, 358.1574.

4-(2'-chlorobenzoyl)phenol 85 [128]

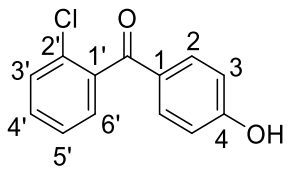

2-chlorobenzoic acid (1g, 6.39 mmol) was dissolved in thionyl chloride (3 mL) and refluxed for 3hours. After cooling down to RT, volatiles were removed under reduced pressure and a solution of anisole (0.85 mL, 7.78 mmol) in anhydrous DCE (31 mL) was added. $AlCl_3$ (1.04 g, 7.78 mmol) was added in portions over 20 minutes and

mixture stirred for 2h at RT and 2h at 80ºC. After cooling down to room temperature, reaction mixture was added to 3M HCl (aq.) (30 mL) in a separating funnel and extracted with DCM (3x20 mL). Combined organic layers were washed with brine, dried over $MgSO_4$, filtered, and concentrated under reduced solid. Crude was submitted to column chromatography (0-100% EtOAc in Hexane) to afford de title product (1.04 g, 70%) as a white solid.

ν_{max} (ATR) 3292 (b, OH), 1567 (s, C=O), 1289 (s), 1150 (s) cm^{-1}. δ_H (400 MHz, $CDCl_3$) 7.78 – 7.72 (m, 2H, 2-***H*₂**), 7.48 – 7.39 (m, 2H, 3'-***H***, 6'-***H***), 7.37 – 7.33 (m, 2H, 4'-***H***, 5'-***H***), 6.91 – 6.84 (m, 2H, 3-***H*₂**), 5.79 (s, 1H, OH); δ_C (101 MHz, $CDCl_3$) 194.1 (Ar_2***C***O), 160.7 (***C***-4), 138.8 (***C***-1), 132.9 (***C***-2), 131.1 (***C***-1'), 130.9 (***C***-2'), 130.0 (***C***-5'), 129.6 (***C***-4'), 128.9 (***C***-3'), 126.7 (***C***-6'), 115.5 (***C***-3). *m/z* (LC-MS, ESI^+) 233 [M(^{35}Cl)+H] and 235 [M(^{37}Cl)+H]) in a 3:1 ratio. All data agrees with literature.

(2'''*R*)-*N*-{3''-[4-(2'-chlorobenzoyl)phenoxy]propyl}-2''-methylpyrrolidine 92

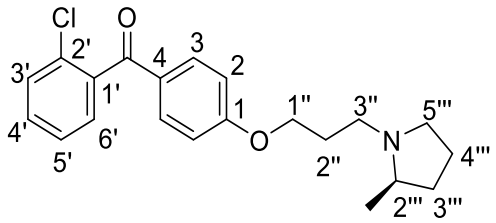

Cs_2CO_3 (1.93 g, 5.93 mmol) was added to a solution of 1,3-dibromopropane (0.65 mL, 6.45 mmol) in anhydrous acetonitrile (20 mL). A solution of 4-(2-chlorobenzoyl)phenol (300 mg, 1.29 mmol) in anhydrous acetonitrile (23 mL) was slowly added and stirred overnight at 70ºC. Once full conversion was achieved, the reaction mixture was concentrated under reduced pressure and product was submitted to column chromatography (0-100% DCM in Hexane) remove inorganic salts. Resultant product (100 mg) in dry acetonitrile (7 mL) was slowly added to a stirring solution of (2*R*)-

Methylpyrrolidine hydrochloride (41.3 mg, 0.34 mmol), KI (4.7 mg, 0.028 mmol) and Na_2CO_3 (138 mg, 1.30 mmol) in dry acetonitrile (7 mL) at 70ºC. Mixture stirred overnight under nitrogen atmosphere. Solution was cooled down to RT, filtered and concentrated under reduced pressure. Crude mixture was submitted to column chromatography (10% MeOH in DCM) to afford the title compound (20.4 mg, 20%) as a yellow solid.

ν_{max} (ATR) 1663 (s, C=O), 1590 (s), 1292 (s) cm^{-1}. δ_H (400 MHz, $CDCl_3$) 7.81 – 7.74 (m, 2H, 3'-***H₂***), 7.47 – 7.37 (m, 2H, 3'-***H***, 6'-***H***), 7.37 – 7.32 (m, 2H, 4'-***H***, 5'-***H***), 6.96 – 6.89 (m, 2H, 2-***H₂***), 4.19 – 4.01 (m, 2H, 1''-***H₂***), 3.36 – 3.12 (m, 1H, 5'''-***H***), 3.12 – 2.92 (m, 1H, 3''-***H***), 2.51 – 2.33 (m, 1H, 2''-***H***), 2.33 – 2.22 (m, 1H, 3''-***H***), 2.22 – 2.13 (m, 1H, 5'''-***H***), 2.13 – 2.00 (m, 2H, 2''-***H₂***), 2.00 – 1.90 (m, 1H, 3'''-***H***), 1.90 – 1.76 (m, 1H, 4'''-***H***), 1.77 – 1.66 (m, 1H, 4'''-***H***), 1.58 – 1.38 (m, 1H, 3'''-***H***), 1.22 – 1.01 (m, 3H, C***H₃***); δ_C (101 MHz, $CDCl_3$) 193.9 (Ar_2***C***O), 163.6 (***C***-1), 139.0 (***C***-2'), 132.5 (***C***-3), 131.1 (***C***-4), 130.8 (***C***-1'), 129.9 (***C***-5'), 129.3 (***C***-4'), 128.9 (***C***-6'), 126.7 (***C***-3'), 114.3 (***C***-2), 66.7 (***C***-1''), 60.7 (***C***-2'''), 53.9 (***C***-5'''), 50.6 (***C***-3''), 32.6 (***C***-3'''), 28.2 (***C***-2''), 21.6 (***C***-3'''), 18.7 (***C***H_3). Accurate mass: found [M+H] 344.1427, $C_{20}H_{23}N^{35}ClO_2$ requires *M*, 344.1417.

4-[1-(3'-bromopropoxy)phenyl]ethenone 123b

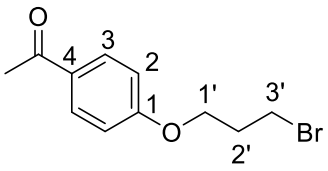

A solution of 4'-hydroxyacetophenone (200 mg, 1.47 mmol) in EtOAc (2.1 mL) was slowly added to a solution of 1,3-dibromopropane (1.1 mL, 11.018 mmol), potassium carbonate (710 mg, 5.14 mmol) and triethylbenzylammonium chloride (33 mg, 0.148

mmol) in EtOAc (2.1 mL). After refluxing overnight, reaction was cooled to room temperature, filtered, diluted with water (5 mL) and extracted with EtOAc (10 mL). Combined organic layers were washed with 1M NaOH (aq), brine and dried over $MgSO_4$. After filtration, volatiles were removed and crude mixture was submitted to column chromatography (0-100% EtOAc in Hexane) to afford title product (201 mg, 53%) as a colourless oil.

ν_{max} (ATR) 1679 (s, C=O), 1607 (s), 1253 (s) cm^{-1}. δ_H (400 MHz, $CDCl_3$) 7.96 – 7.90 (m, 2H, 3-***H*****$_2$**), 6.97 – 6.90 (m, 2H, 2-***H*****$_2$**), 4.17 (t, *J* = 6.0 Hz, 2H, 1'-***H*****$_2$**), 3.61 (t, *J* = 6.0 Hz, 2H, 3'-***H*****$_2$**), 2.56 (s, 3H, C***H*****$_3$**), 2.34 (p, *J* = 6.0 Hz, 2H, 2'-***H*****$_2$**); δ_C (101 MHz, $CDCl_3$) 196.8 (Ar_2***C***O), 162.6 (***C***-1), 130.6 (***C***-3), 130.5 (***C***-4), 114.2 (***C***-2), 65.5 (***C***-1'), 32.1 (***C***-3'), 29.7 (***C***-2'), 26.4 (***C***H_3). Accurate mass: found [M+H] 257.0193, $C_{11}H_{14}N^{79}BrO_2$ requires *M*, 257.0177.

4-(1-{3'-[(2''*R*)-2''-methylpyrrolidine]propoxy}phenyl)ethenone 125

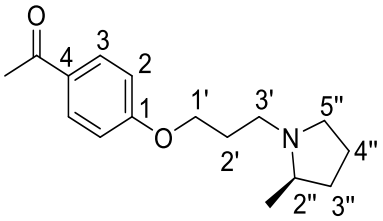

To a solution of (2*R*)-Methylpyrrolidine hydrochloride (56.8 mg, 0.46 mmol), KI (6.5 mg, 0.039 mmol) and Na_2CO_3 (189.6 mg, 1.79 mmol) in dry acetonitrile (10 mL) at 70ºC, 1-[4-(3-bromopropoxy)phenyl]ethan-1-one (100 mg, 0.39 mmol) in dry acetonitrile (10 mL) was slowly added. Mixture stirred overnight under nitrogen atmosphere. Solution was cooled down to RT, filtered and concentrated under reduced pressure. Crude mixture was submitted to column chromatography (10% MeOH in DCM) to afford the title compound (69.8 mg, 69%) as a brown oil.

ν_{max} (ATR) 1680 (s, C=O), 1607 (s), 1264 (s) cm^{-1}. δ_H (599 MHz, $CDCl_3$) 7.94 – 7.90 (m, 2H, 3-***H₂***), 6.95 – 6.90 (m, 2H, 2-***H₂***), 4.14 – 4.05 (m, 2H, 1'-***H₂***), 3.28 – 3.17 (m, 1H, 5''-***H***), 3.06 – 2.97 (m, 1H, 3'-***H***), 2.55 (s, 3H, COC***H₃***), 2.44 – 2.33 (m, 1H, 2''-***H***), 2.32 – 2.24 (m, 1H, 3'-***H***), 2.24 – 2.14 (m, 1H, 5''-***H***), 2.10 – 2.01 (m, 2H, 2'-***H₂***), 2.00 – 1.91 (m, 1H, 3''-***H***), 1.87 – 1.77 (m, 1H, 4''-***H***), 1.77 – 1.68 (m, 1H, 4''-***H***), 1.53 – 1.41 (m, 1H, 3''-***H***), 1.13 (d, *J* = 6.1 Hz, 3H, C***H₃***); δ_C (151 MHz, $CDCl_3$) 196.8 (Ar_2***C***O), 162.9 (***C***-1), 130.5 (***C***-3), 130.2 (***C***-4), 114.1 (***C***-2), 66.6 (***C***-1'), 60.5 (***C***-2''), 53.9 (***C***-5''), 50.6 (***C***-3'), 32.6 (***C***-3''), 28.2 (***C***-2'), 26.3 (CO***C***H_3), 21.6 (***C***-4''), 18.7 (***C***H_3). Accurate mass: found [M+H] 262.1809, $C_{16}H_{24}NO_2$ requires *M*, 262.1807.

(2'*R*)-2'-methyl-*N*-(3-phenoxypropyl)pyrrolidine 124

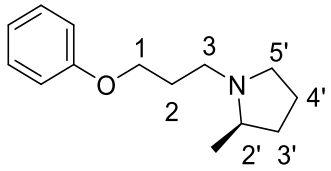

A solution of phenol (200 mg, 2.12 mmol) in acetonitrile (4 mL) was slowly added to a mixture of potassium carbonate (1.46 g, 10.63 mmol) and 1,3- dibromopropane (1.1 mL, 10.63 mmol) in dry acetonitrile (3 mL) at 70ºC. After stirring overnight, reaction mixture was cooled to room temperature and filtered. Volatiles were removed and crude mixture was submitted to column chromatography (0-100% EtOAc in Hexane) to remove inorganic salts. Resultant product (100 mg) in dry acetonitrile (13 mL) was slowly added to a stirring solution of (2*R*)-Methylpyrrolidine hydrochloride (67.8 mg, 0.56 mmol), KI (7.7 mg, 0.046 mmol) and Na_2CO_3 (226.7 mg, 2.14 mmol) in dry acetonitrile (10 mL) at 70ºC. Mixture stirred overnight under nitrogen atmosphere. Solution was cooled down to RT, filtered and concentrated under reduced pressure.

Crude mixture was submitted to column chromatography (10% MeOH in DCM) to afford the title compound (35.4 mg, 35%) as a brown oil.

ν_{max} (ATR) 1253 (s) cm^{-1}. δ_H (599 MHz, $CDCl_3$) 7.30 – 7.26 (m, 2H, 2xAr***H***), 6.95 – 6.92 (m, 1H, Ar***H***), 6.92 – 6.88 (m, 2H, 2xAr***H***), 4.10 – 3.97 (m, 2H, 1-***H₂***), 3.28 – 3.20 (m, 1H, 5'-***H***), 3.08 – 2.98 (m, 1H, 3-***H₂***), 2.47 – 2.34 (m, 1H, 2'-***H***), 2.34 – 2.25 (m, 1H, 3-***H***), 2.25 – 2.15 (m, 1H, 5'-***H***), 2.11 – 2.01 (m, 2H, 2-***H₂***), 2.01 – 1.91 (m, 1H, 3'-***H***), 1.87 – 1.78 (m, 1H, 4'-***H***), 1.78 – 1.68 (m, 1H, 4'-***H***), 1.53 – 1.44 (m, 1H, 3'-***H***), 1.15 (d, *J* = 6.1 Hz, 3H, C***H₃***). δ_C (151 MHz, $CDCl_3$) 158.9 (***C***-Ar), 129.4 (***C***-Ar), 120.6 (***C***-Ar), 114.5 (***C***-Ar), 66.2 (***C***-1), 60.6 (***C***-2'), 53.9 (***C***-5'), 50.8 (***C***-3), 32.6 (***C***-3'), 28.3 (***C***-2), 21.6 (***C***-4'), 18.7 (***C***H_3). Accurate mass: found [M+H] 220.1711, $C_{14}H_{22}NO_2$ requires *M*, 220.1701.

(4-chlorophenyl)(3',5'-dimethoxyphenyl)methanone 141

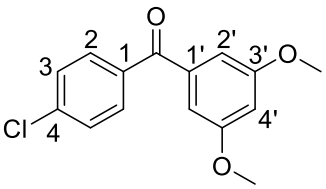

A solution of 1-Bromo-3,5-dimethoxybenzene (1 g, 4.61 mmol) in anhydrous THF (9 mL) was cooled to -78ºC in a cold bath of acetone and dry ice. nBuli (1.9 mL of 2.5M solution in THF, 4.84 mmol), was added slowly and solution stirred for 30 min before addition of *para*-chlorobenzaldehyde (712 mg, 5.07 mmol) in anhydrous THF. The reaction mixture stirred for 1h at RT. After, the mixture was diluted in 1M HCl (30 mL) and extracted with DCM (3x20 mL). The combined organic layers were dried over $MgSO_4$, filtered, and concentrated under reduced pressure. The resultant product (1.1 g) in dry DCM (6 mL) was slowly added to a stirring solution of DMP (3.45 g, 8.13 mmol) and $NaHCO_3$ (0.48 mg, 5.68 mmol) in dry DCM at RT. The reaction stirred

overnight before quenching with sat. $NaS_2O_{3(aq)}$. Organic layer was removed, and aqueous layer was washed with EtOAc (3x20 mL). The combined organic layers were dried over $MgSO_4$, filtered, and concentrated under reduced pressure. The crude product was submitted to column chromatography (0-100% EtOAc in Hexane) to afford the title product (737.5 mg, 67%) as a white solid.

δ_H (400 MHz, $CDCl_3$) 7.79 – 7.74 (m, 2H, 2-***H₂***), 7.48 – 7.43 (m, 2H, 3-***H₂***), 6.88 (d, *J* = 2.3 Hz, 2H, 2'-***H₂***), 6.68 (t, *J* = 2.3 Hz, 1H, 4'-***H***), 3.83 (s, 6H, 2xC***H₃***); δ_C (101 MHz, $CDCl_3$) 195.2 (Ar_2***C***O), 160.6 (***C***-3'), 139.1 (***C***-1'), 138.9 (***C***-1), 135.8 (***C***-4), 131.5 (***C***-2), 128.6 (***C***-3), 107.8 (***C***-2'), 104.9 (***C***-4'), 55.6 (2x***C***H_3).

3'-(4-chlorobenzoyl)-5'-(hex-5''-yn-1''-yloxy)phenol 144

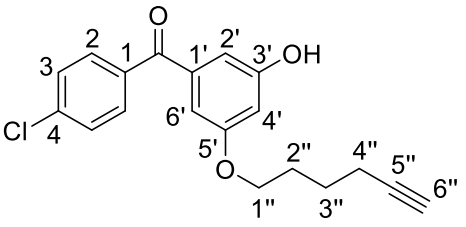

K_2CO_3 (333.5 mg, 2.41 mmol) and KI (1.3 mg, 0.008 mmol) were added to a solution of 5-hexynyl p-toluenesulfonate (274 mg, 0.84 mmol) and diol **142** (200 mg, 0.81 mmol) in anhydrous acetonitrile (8 mL). The reaction mixture stirred overnight at 80ºC. Once full conversion was achieved, the reaction mixture was concentrated under reduced pressure and product was submitted to column chromatography (0-100% DCM in Hexane) to afford title product (72.6 mg, 22%) as a yellow oil.

δ_H (400 MHz, $CDCl_3$) 7.79 – 7.72 (m, 2H, 2-***H₂***), 7.49 – 7.41 (m, 2H, 3-***H₂***), 6.87 – 6.79 (m, 2H, 2'-***H***, 6'-***H***), 6.66 – 6.60 (m, 1H, 4'-***H***), 5.49 (s, 1H, O***H***), 3.98 (t, *J* = 6.2 Hz, 2H, 1''-***H₂***), 2.27 (td, *J* = 7.0, 2.6 Hz, 2H, 4''-***H₂***), 1.97 (t, *J* = 2.7 Hz, 1H, C***H***), 1.95 – 1.85 (m, 2H, 2''-***H₂***), 1.75 – 1.67 (m, 2H, 3''-***H₂***); δ_C (101 MHz, $CDCl_3$) 195.3 (Ar_2***C***O), 160.2

(***C***-3'), 156.7 (***C***-5'), 139.2 (***C***-1'), 139.1 (***C***-1), 135.6 (***C***-4), 131.5 (***C***-2), 128.7 (***C***-3), 109.4 (***C***-6'), 108.6 (***C***-2'), 106.4 (***C***-4'), 83.9 (***C***-5''), 68.8 (***C***H), 67.7 (***C***-1''), 28.1 (***C***-2''), 24.9 (***C***-3''), 18.1 (***C***-4''). Accurate mass: found [M+H] 329.0963, $C_{19}H_{18}N^{35}ClO_3$ requires *M*, 329.0944.

(2'''*R*)-*N*-{3'''-[3'-(4-chlorobenzoyl)-5'-(hex-5''-yn-1''-yloxy)phenoxy]propyl}-2'''-methylpyrrolidine 138

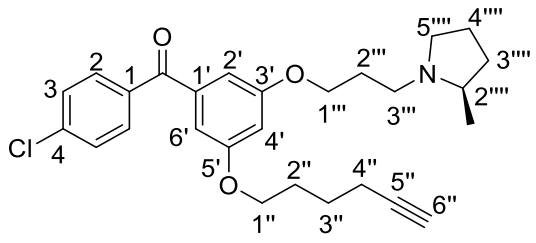

To a solution of the phenol **144** (50 mg, 0.15 mmol), K_2CO_3 (97 mg, 0.70 mmol) and TBAI (0.6 mg, 0.002 mmol) in dry acetonitrile (1 mL), a solution of **138** (36 mg, 0.18 mmol) in dry acetonitrile (1 mL) was added. The mixture stirred overnight at 70ºC under nitrogen atmosphere. The solution was then cooled down to RT, filtered and concentrated under reduced pressure. The crude mixture was submitted to column chromatography (10% MeOH in DCM) to afford the title compound (58 mg, 84%) as a yellow oil.

ν_{max} (ATR) 1590 (s, C=O), 1168 (s) cm^{-1}. δ_H (599 MHz, $CDCl_3$) 7.77 – 7.73 (m, 2H, 2-***H*₂**), 7.47 – 7.43 (m, 2H, 3-***H*₂**), 6.87 – 6.83 (m, 2H, 2'-***H***, 6'-***H***), 6.69 – 6.65 (m, 1H, 4'-***H***), 4.07 – 4.01 (m, 2H, 1'''-***H*₂**), 4.01 – 3.97 (m, 2H, 1''-***H*₂**), 3.26 – 3.15 (m, 1H, 5''''-

H), 3.04 – 2.93 (m, 1H, 3’’’-***H***), 2.43 – 2.30 (m, 1H, 2’’’’-***H***), 2.27 (td, *J* = 7.0, 2.7 Hz, 2H, 4’’-***H₂***), 2.25 – 2.20 (m, 1H, 3’’’-***H***), 2.20 – 2.11 (m, 1H, 5’’’-***H***), 2.06 – 1.98 (m, 2H, 2’’’-***H₂***), 1.96 (t, *J* = 2.6 Hz, 1H, C***H***), 1.96 – 1.87 (m, 3H, 3’’’’-***H***, 2’’-***H₂***), 1.85 – 1.75 (m, 1H, 4’’’’-***H***), 1.75 – 1.65 (m, 3H, 4’’’’-***H***, 3’’-***H₂***), 1.50 – 1.40 (m, 1H, 3’’’’-***H***), 1.12 (d, *J* = 6.1 Hz, 3H, C***H₃***); δ_C (151 MHz, $CDCl_3$) 195.2 (Ar_2***C***O), 160.0 (***C***-3’), 159.9 (***C***-5’), 138.9 (***C***-1’), 138.8 (***C***-1), 135.9 (***C***-4), 131.4 (***C***-2), 128.6 (***C***-3), 108.4 (***C***-6’), 108.2 (***C***-2’), 105.8 (***C***-4’), 83.9 (***C***-5’’), 68.7 (***C***H), 67.6 (***C***-1’’), 66.7 (***C***-1’’’), 60.4 (***C***-2’’’’), 53.9 (***C***-5’’’’), 50.7 (***C***-3’’’), 32.6 (***C***-3’’’’), 28.3 (***C***-2’’’), 28.1 (***C***-2’’), 24.9 (***C***-3’’), 21.6 (***C***-4’’’’), 18.8 (***C***H_3), 18.1 (***C***-4’’). Accurate mass: found [M+H] 454.2154, $C_{27}H_{33}N^{35}ClO_3$ requires *M*, 454.2149.

8. References

1. Burza, S., Croft, S. L. & Boelaert, M. Leishmaniasis. *Lancet* **392**, 951–970 (2018).

2. Lukeš, J., Hashimi, H. & Zíková, A. Unexplained complexity of the mitochondrial genome and transcriptome in kinetoplastid flagellates. *Curr. Genet.* **48**, 277–299 (2005).

3. Damasceno, J. D., Marques, C. A., Black, J., Briggs, E. & McCulloch, R. Read, Write, Adapt: Challenges and Opportunities during Kinetoplastid Genome Replication. *Trends Genet.* **37**, 21–34 (2021).

4. Poulaki, A., Piperaki, E. T. & Voulgarelis, M. Effects of visceralising leishmania on the spleen, liver, and bone marrow: A pathophysiological perspective. *Microorganisms* **9**, (2021).

5. Silva, T. F. *et al.* Phenotypical and genotypical differences among Leishmania (Leishmania) amazonensis isolates that caused different clinical frames in humans and dogs: A systematic review. *Acta Trop.* **221**, 106018 (2021).

6. Abadías-Granado, I., Diago, A., Cerro, P. A., Palma-Ruiz, A. M. & Gilaberte, Y. Cutaneous and Mucocutaneous Leishmaniasis. *Actas Dermo-Sifiliográficas (English Ed.* **112**, 601–618 (2021).

7. Volpedo, G. *et al.* Mechanisms of Immunopathogenesis in Cutaneous Leishmaniasis And Post Kala-azar Dermal Leishmaniasis (PKDL). *Front. Cell. Infect. Microbiol.* **11**, 1–16 (2021).

8. Pederiva, M. M. C. *et al.* Asymptomatic Leishmania infection in humans: A systematic review. *J. Infect. Public Health* **16**, 286–294 (2023).

9. Kantzanou, M. *et al.* Prevalence of visceral leishmaniasis among people with HIV: a systematic review and meta-analysis. *Eur. J. Clin. Microbiol. Infect. Dis.* 1–12 (2022). doi:10.1007/s10096-022-04530-4

10. Scarpini, S. *et al.* Visceral Leishmaniasis: Epidemiology, Diagnosis, and Treatment Regimens in Different Geographical Areas with a Focus on Pediatrics. *Microorganisms* **10**, (2022).

11. Bern, C., Desjeux, P., Cano, J. & Alvar, J. Leishmaniasis Worldwide and Global Estimates of Its Incidence. **7**, (2012).

12. Akhoundi, M. *et al.* A Historical Overview of the Classification, Evolution, and Dispersion of Leishmania Parasites and Sandflies. *PLoS Negl. Trop. Dis.* **10**, 1–40 (2016).

13. Cecílio, P., Cordeiro-da-Silva, A. & Oliveira, F. Sand flies: Basic information on the vectors of leishmaniasis and their interactions with Leishmania parasites. *Commun. Biol.* **5**, 305 (2022).

14. Alemayehu, B. & Alemayehu, M. Leishmaniasis: A Review on Parasite, Vector and Reservoir Host. *Heal. Sci. J.* **11**, 1–6 (2017).

15. Kupani, M., Pandey, R. K. & Mehrotra, S. Neutrophils and Visceral Leishmaniasis: Impact on innate immune response and cross-talks with macrophages and dendritic cells. *J. Cell. Physiol.* **236**, 2255–2267 (2021).

16. Passelli, K., Billion, O. & Tacchini-Cottier, F. The Impact of Neutrophil Recruitment to the Skin on the Pathology Induced by Leishmania Infection. *Front. Immunol.* **12**, 1–12 (2021).

17. Carneiro, M. B. & Peters, N. C. The Paradox of a Phagosomal Lifestyle: How Innate Host Cell-Leishmania amazonensis Interactions Lead to a Progressive Chronic Disease. *Front. Immunol.* **12**, 1–22 (2021).

18. Silveira, F. T., Lainson, R., De Castro Gomes, C. M., Laurenti, M. D. & Corbett, C. E. P. Immunopathogenic competences of Leishmania (V.) braziliensis and L. (L.) amazonensis in American cutaneous leishmaniasis. *Parasite Immunol.* **31**, 423–431 (2009).

19. Machado, G. U., Prates, F. V. & Machado, P. R. L. Disseminated leishmaniasis: clinical, pathogenic, and therapeutic aspects. *An. Bras. Dermatol.* **94**, 9–16 (2019).

20. Scorza, B., Carvalho, E. & Wilson, M. Cutaneous Manifestations of Human and Murine Leishmaniasis. *Int. J. Mol. Sci.* **18**, 1296 (2017).

21. Baileyid, F. *et al.* Cutaneous leishmaniasis and co-morbid major depressive disorder: A systematic review with burden estimates. *PLoS Negl. Trop. Dis.* **13**, 1–22 (2019).

22. Pires, M., Wright, B., Kaye, P. M., da Conceição, V. & Churchill, R. C. The impact of leishmaniasis on mental health and psychosocial well-being: A systematic review. *PLoS ONE* **14**, (2019).

23. Yanik, M., Gurel, M. S., Simsek, Z. & Kati, M. The psychological impact of cutaneous leishmaniasis. *Clin. Exp. Dermatol.* **29**, 464–467 (2004).

24. Grifferty, G. *et al.* Vulnerabilities to and the Socioeconomic and Psychosocial Impacts of the Leishmaniases: A Review. *Res. Rep. Trop. Med.* **Volume 12**, 135–151 (2021).

25. Bennis, I. *et al.* Psychosocial impact of scars due to cutaneous leishmaniasis on high school students in Errachidia province, Morocco. *Infect. Dis. Poverty* **6**, (2017).

26. Harhay, M. O. *et al.* Who is a typical patient with visceral leishmaniasis? Characterizing the demographic and nutritional profile of patients in Brazil, East Africa, and South Asia. *Am. J. Trop. Med. Hyg.* **84**, 543–550 (2011).

27. Russo, R. *et al.* Visceral leishmaniasis in those infected with HIV : **97**, (2002).

28. Uliana, S. R. B., Trinconi, C. T. & Coelho, A. C. Chemotherapy of leishmaniasis: present challenges. *Parasitology* 1–17 (2017). doi:10.1017/S0031182016002523

29. El-On, J., Livshin, R., Even-Paz, Z., Hamburger, D. & Weinrauch, L. Topical treatment of cutaneous leishmaniasis. *J. Invest. Dermatol.* **87**, 284–288 (1986).

30. Chakravarty, J. & Sundar, S. Current and emerging medications for the treatment of leishmaniasis. *Expert Opin. Pharmacother.* **20**, 1251–1265 (2019).

31. Marsden, P. D. Pentavalent antimonials: old drugs for new diseases. *Rev. Soc. Bras. Med. Trop.* **18**, 187–198 (1985).

32. Periferakis, A. *et al.* Availability, Toxicology and Medical Significance of Antimony. *Int. J. Environ. Res. Public Health* **19**, (2022).

33. Malafaia, G. Protein-energy malnutrition as a risk factor for visceral leishmaniasis: A review. *Parasite Immunol.* **31**, 587–596 (2009).

34. Olliaro, P., Guerrin, P. & Gerstl, S. Treatment options for visceral leishmaniasis: a systematic review of clinical studies done in India, 1980- 2014. *Lancet Infect. Dis.* **5 (12)**, 763–774 (2005).

35. Perry, M. R., Wyllie, S., Raab, A., Feldmann, J. & Fairlamb, A. H. Chronic exposure to arsenic in drinking water can lead to resistance to antimonial drugs in a mouse model of visceral leishmaniasis. *Proc. Natl. Acad. Sci. U. S. A.* **110**, 19932–19937 (2013).

36. Machado, P. R. *et al.* Miltefosine in the Treatment of Cutaneous Leishmaniasis Caused by Leishmania braziliensis in Brazil: A Randomized and Controlled Trial. *PLoS Negl. Trop. Dis.* **4**, e912 (2010).

37. Chrusciak-Talhari, A. *et al.* Randomized controlled clinical trial to access efficacy and safety of miltefosine in the treatment of cutaneous leishmaniasis caused by Leishmania (Viannia) guyanensis in Manaus, Brazil. *Am. J. Trop. Med. Hyg.* **84**, 255–260 (2011).

38. Balaña-Fouce, R., Reguera, R. M., Cubría, J. C. & Ordóñez, D. *The Pharmacology of Leishmaniasis*. *Gen. Pharmac* **30**, (1998).

39. Sampaio, S. A. P., Godoy, J. T., Paiva, L., Dillon, N. L. & Lacaz, C. D. S. The Treatment of American (Mucocutaneous) Leishmaniasis with Amphotericin B. *Arch. Dermatol.* **82**, 627–635 (1960).

40. Prata, A. Treatment of kala-azar with amphotericin B. *Trans. R. Soc. Trop. Med. Hyg.* **57**, 266–

268 (1963).

41. Kumari, S. *et al.* Amphotericin B: A drug of choice for Visceral Leishmaniasis. *Acta Tropica* **235**, (2022).

42. Neumann, A., Baginski, M. & Czub, J. How do sterols determine the antifungal activity of amphotericin B? Free energy of binding between the drug and its membrane targets. *J. Am. Chem. Soc.* **132**, 18266–18272 (2010).

43. Szoka, F. C., Milholland, D. & Barza, M. Effect of lipid composition and liposome size on toxicity and in vitro fungicidal activity of liposome-intercalated amphotericin B. *Antimicrob. Agents Chemother.* **31**, 421–429 (1987).

44. Botero Aguirre, J. & Restrepo Hamid, A. Amphotericin B deoxycholate versus liposomal amphotericin B : effects on kidney function (Review) SUMMARY OF FINDINGS FOR THE MAIN COMPARISON. (2015). doi:10.1002/14651858.CD010481.pub2.www.cochranelibrary.com

45. Lanza, J. S., Pomel, S., Loiseau, P. M. & Frézard, F. Recent advances in amphotericin B delivery strategies for the treatment of leishmaniases. *Expert Opin. Drug Deliv.* **16**, 1063–1079 (2019).

46. Sundar, S. & Olliaro, P. L. Miltefosine in the treatment of leishmaniasis: Clinical evidence for informed clinical risk management. *Ther. Clin. Risk Manag.* **3**, 733–40 (2007).

47. Sundar, S. *et al.* Oral Miltefosine for Indian Visceral Leishmaniasis. *N. Engl. J. Med.* **347**, 1739–1746 (2002).

48. Dorlo, T. P. C. *et al.* Pharmacokinetics of miltefosine in old world cutaneous leishmaniasis patients. *Antimicrob. Agents Chemother.* **52**, 2855–2860 (2008).

49. Machado, P. R. *et al.* Miltefosine in the treatment of cutaneous leishmaniasis caused by leishmania braziliensis in Brazil: A randomized and controlled trial. *PLoS Negl. Trop. Dis.* **4**, 1–6 (2010).

50. Dos Santos Nogueira, F. *et al.* Use of miltefosine to treat canine visceral leishmaniasis caused by Leishmania infantum in Brazil. *Parasites and Vectors* **12**, 1–11 (2019).

51. Andrade, H. M. *et al.* Evaluation of miltefosine for the treatment of dogs naturally infected with L. infantum (=L. chagasi) in Brazil. *Veterinary Parasitology* **181**, 83–90 (2011).

52. Neal, R. A. The effect of antibiotics of the neomycin group on experimental cutaneous leishmaniasis. *Ann. Trop. Med. Parasitol.* **62**, 54–62 (1968).

53. Musa, A. M. *et al.* Paromomycin for the treatment of visceral leishmaniasis in Sudan: A randomized, open-label, dose-finding study. *PLoS Negl. Trop. Dis.* **4**, 4–10 (2010).

54. Sundar, S., Jha, T. K., Thakur, C. P., Sinha, P. K. & Bhattacharya, S. K. Injectable Paromomycin for Visceral Leishmaniasis in India. *N. Engl. J. Med.* **356**, 2571–2581 (2007).

55. Hailu, A. *et al.* Geographical variation in the response of visceral leishmaniasis to paromomycin in East Africa: A multicentre, open-label, randomized trial. *PLoS Negl. Trop. Dis.* **4**, (2010).

56. Musa, A. *et al.* Sodium stibogluconate (ssg) & paromomycin combination compared to ssg for visceral leishmaniasis in east africa: A randomised controlled trial. *PLoS Negl. Trop. Dis.* **6**, (2012).

57. Bray, P. G., Barrett, M. P., Ward, S. A. & De Koning, H. P. Pentamidine uptake and resistance in pathogenic protozoa: Past, present and future. *Trends Parasitol.* **19**, 232–239 (2003).

58. Van Der Meide, W. F. *et al.* Evaluation of treatment with pentamidine for cutaneous leishmaniasis in Suriname. *Int. J. Dermatol.* **48**, 52–58 (2009).

59. Olliaro, P. L. Drug combinations for visceral leishmaniasis. *Curr. Opin. Infect. Dis.* **23**, 595–602 (2010).

60. Sundar, S. & Singh, A. Chemotherapeutics of Visceral Leishmaniasis: present and future developments. *Parasitology* **145**, 481–489 (2018).

61. Goswami, R. P., Rahman, M., Das, S., Tripathi, S. K. & Goswami, R. P. Combination therapy against Indian visceral leishmaniasis with liposomal amphotericin B (FungisomeTM) and short-course miltefosine in comparison to miltefosine monotherapy. *Am. J. Trop. Med. Hyg.* **103**, 308–314 (2020).

62. Madusanka, R. K., Silva, H. & Karunaweera, N. D. Treatment of Cutaneous Leishmaniasis and Insights into Species-Specific Responses: A Narrative Review. *Infect. Dis. Ther.* **11**, 695–711 (2022).

63. Salari, S., Bamorovat, M., Sharifi, I. & Almani, P. G. N. Global distribution of treatment resistance gene markers for leishmaniasis. *J. Clin. Lab. Anal.* **36**, 1–16 (2022).

64. Swinney, D. C. & Anthony, J. How were new medicines discovered? *Nat. Rev. Drug Discov.* **10**, 507–519 (2011).

65. Nunes-Alves, C. New tricks for old drugs. *Nat. Rev. Microbiol.* **13**, 68 (2015).

66. Sittampalam, G. *et al. Assay Guidance Manual*. *Assay Guidance Manual* (2016).

67. Strovel, J. *et al.* Early Drug Discovery and Development Guidelines: For Academic Researchers, Collaborators, and Start-up Companies. in *Assay Guidance Manual* 1–35 (2004).

68. Katsuno, K. *et al.* Hit and lead criteria in drug discovery for infectious diseases of the developing world. *Nat. Rev. Drug Discov.* **14**, 751–758 (2015).

69. Swinney, D. C. Phenotypic vs. Target-based drug discovery for first-in-class medicines. *Clin. Pharmacol. Ther.* **93**, 299–301 (2013).

70. Terstappen, G. C., Schlüpen, C., Raggiaschi, R. & Gaviraghi, G. Target deconvolution strategies in drug discovery. *Nat. Rev. Drug Discov.* **6**, 891–903 (2007).

71. Croston, G. E. The utility of target-based discovery. *Expert Opin. Drug Discov.* **12**, 427–429 (2017).

72. Gao, M. *et al.* Chemical genetics strategy identifies an HCV NS5A inhibitor with a potent clinical effect. *Nature* **465**, 96–100 (2010).

73. Petersen, D. N. *et al.* A Small-Molecule Anti-secretagogue of PCSK9 Targets the 80S Ribosome to Inhibit PCSK9 Protein Translation. *Cell Chem. Biol.* **23**, 1362–1371 (2016).

74. Lindsay, M. A. Target discovery. *Nat. Rev. Drug Discov.* **2**, 831–838 (2003).

75. Moffat, J. G., Vincent, F., Lee, J. A., Eder, J. & Prunotto, M. Opportunities and challenges in phenotypic drug discovery: an industry perspective. *Nat. Rev. Drug Discov.* **16**, 531–543 (2017).

76. Pushpakom, S. *et al.* Drug repurposing: Progress, challenges and recommendations. *Nat. Rev. Drug Discov.* **18**, 41–58 (2018).

77. Braga, S. S. Multi-target drugs active against leishmaniasis: A paradigm of drug repurposing. *European Journal of Medicinal Chemistry* **183**, (2019).

78. Cha, Y. *et al.* Drug repurposing from the perspective of pharmaceutical companies. *Br. J. Pharmacol.* **175**, 168–180 (2018).

79. Charlton, R. L., Rossi-Bergmann, B., Denny, P. W. & Steel, P. G. Repurposing as a strategy for the discovery of new anti-leishmanials: The-state-of-the-art. *Parasitology* **145**, 219–236 (2018).

80. Gault, C. R., Obeid, L. M. & Hannun, Y. A. An overview of sphingolipid metabolism: From synthesis to breakdown. *Adv. Exp. Med. Biol.* **688**, 1–23 (2010).

81. Lahiri, S. & Futerman, A. H. The metabolism and function of sphingolipids and

glycosphingolipids. *Cell. Mol. Life Sci.* **64**, 2270–2284 (2007).

82. Zhang, K. & Beverley, S. M. Phospholipid and sphingolipid metabolism in Leishmania. *Mol. Biochem. Parasitol.* **170**, 55–64 (2010).

83. Ikonen, E. Roles of lipid rafts in membrane transport. *Curr. Opin. Cell Biol.* **13**, 470–477 (2001).

84. Zhang, K., Bangs, J. D. & Beverley, S. M. Sphingolipids in parasitic protozoa. *Adv. Exp. Med. Biol.* **688**, 238–248 (2010).

85. Denny, P. W., Goulding, D., Ferguson, M. A. J. & Smith, D. F. Sphingolipid-free Leishmania are defective in membrane trafficking, differentiation and infectivity. *Mol. Microbiol.* **52**, 313–327 (2004).

86. Huitema, K., Van Den Dikkenberg, J., Brouwers, J. F. H. M. & Holthuis, J. C. M. Identification of a family of animal sphingomyelin synthases. *EMBO J.* **23**, 33–44 (2004).

87. Mina, J. G. *et al.* The Trypanosoma brucei sphingolipid synthase, an essential enzyme and drug target. *Mol. Biochem. Parasitol.* **168**, 16–23 (2009).

88. Denny, P. W., Shams-Eldin, H., Price, H. P., Smith, D. F. & Schwarz, R. T. The protozoan inositol phosphorylceramide synthase: A novel drug target that defines a new class of sphingolipid synthase. *J. Biol. Chem.* **281**, 28200–28209 (2006).

89. Kuhlmann, F. M. *et al.* Inositol phosphorylceramide synthase null Leishmania are viable and virulent in animal infections where salvage of host sphingomyelin predominates. *J. Biol. Chem.* **298**, 1–14 (2022).

90. Heidler, S. A. & Radding, J. A. The AUR1 gene in Saccharomyces cerevisiae encodes dominant resistance to the antifungal agent aureobasidin A (LY295337). *Antimicrob. Agents Chemother.* **39**, 2765–2769 (1995).

91. Rollin-Pinheiro, R., Singh, A., Barreto-Bergter, E. & Poeta, M. Del. Sphingolipids as targets for treatment of fungal infections Special Focus Issue – Antifungal Drug Discovery. *Futur. Med. Chem* **8**, 1469–1484 (2016).

92. Georgopapadakou, N. H. Antifungals targeted to sphingolipid synthesis: Focus on inositol phosphorylceramide synthase. *Expert Opin. Investig. Drugs* **9**, 1787–1796 (2000).

93. Mina, J. G. *et al.* A plate-based assay system for analyses and screening of the Leishmania major inositol phosphorylceramide synthase. *Int. J. Biochem. Cell Biol.* **42**, 1553–1561 (2010).

94. Mina, J. G. M. & Denny, P. W. Everybody needs sphingolipids, right! Mining for new drug targets in protozoan sphingolipid biosynthesis. *Parasitology* **145**, 134–147 (2018).

95. Mina, J. G., Mosely, J. A., Ali, H. Z., Denny, P. W. & Steel, P. G. Exploring Leishmania major Inositol Phosphorylceramide Synthase (LmjIPCS): Insights into the ceramide binding domain. *Org. Biomol. Chem.* **9**, 1823–1830 (2011).

96. Norcliffe, J. L. *et al.* Identifying inhibitors of the Leishmania inositol phosphorylceramide synthase with antiprotozoal activity using a yeast-based assay and ultra-high throughput screening platform. *Sci. Rep.* **8**, 1–10 (2018).

97. Mina, J. G. M. *et al.* Antileishmanial Chemotherapy through Clemastine Fumarate Mediated Inhibition of the Leishmania Inositol Phosphorylceramide Synthase. *ACS Infect. Dis.* **7**, 47–63 (2021).

98. Charlton, R. L. *Repurposing as a strategy for the discovery of new anti-leishmanials: The-state-of-the-art (PhD thesis, Durham University)*. *Parasitology* (2018).

99. Brown, C. *Inhibitors of Leishmania major Inositol Phosphorylceramide Synthase: New Therapies for Leishmaniasis (PhD thesis, Durham University)*. (2016).

100. Miguel, D. C., Yokoyama-Yasunaka, J. K. U. & Uliana, S. R. B. Tamoxifen is effective in the treatment of Leishmania amazonensis infections in mice. *PLoS Negl. Trop. Dis.* **2**, (2008).

101. Miguel, D. C., Yokoyama-Yasunaka, J. K. U., Andreoli, W. K., Mortara, R. A. & Uliana, S. R. B. Tamoxifen is effective against Leishmania and induces a rapid alkalinization of parasitophorous vacuoles harbouring Leishmania (Leishmania) amazonensis amastigotes. *J. Antimicrob. Chemother.* **60**, 526–534 (2007).

102. Miguel, D. C. *et al.* Tamoxifen as a potential antileishmanial agent: Efficacy in the treatment of Leishmania braziliensis and Leishmania chagasi infections. *J. Antimicrob. Chemother.* **63**, 365–368 (2009).

103. Trinconi, C. T. *et al.* Topical tamoxifen in the therapy of cutaneous leishmaniasis. *Parasitology* **145**, 490–496 (2018).

104. Miguel, D. C. *et al.* Clinical isolates of New World Leishmania from cutaneous and visceral leishmaniasis patients are uniformly sensitive to tamoxifen. *Int. J. Antimicrob. Agents* **38**, 93–94 (2011).

105. Trinconi, C. T. *et al.* Tamoxifen inhibits the biosynthesis of inositolphosphorylceramide in Leishmania. *Int. J. Parasitol. Drugs Drug Resist.* **8**, 475–487 (2018).

106. Alpizar-Sosa, E. A. *et al.* Genome deletions to overcome the directed loss of gene function in Leishmania. *Front. Cell. Infect. Microbiol.* **12**, 1–16 (2022).

107. Bouton, J., Van Hecke, K., Rasooly, R. & Van Calenbergh, S. Synthesis of pyrrolidine-based hamamelitannin analogues as quorum sensing inhibitors in staphylococcus aureus. *Beilstein J. Org. Chem.* **14**, 2822–2828 (2018).

108. Dos Santos, M. L. & De Magalhães, G. C. Utilisation of Cashew Nut Shell Liquid from Anacardium occidentale as Starting Material for Organic Synthesis: A Novel Route to Lasiodiplodin from Cardols. *J. Braz. Chem. Soc.* **10**, 13–20 (1999).

109. Fournier, A. M., Brown, R. A., Farnaby, W., Miyatake-Ondozabal, H. & Clayden, J. Synthesis of (-)-(S, S)-clemastine by invertive N → C aryl migration in a lithiated carbamate. *Org. Lett.* **12**, 2222–2225 (2010).

110. Brioschi, M. B. C., Coser, E. M., Coelho, A. C., Gadelha, F. R. & Miguel, D. C. Models for cytotoxicity screening of antileishmanial drugs: what has been done so far? *Int. J. Antimicrob. Agents* **60**, 106612 (2022).

111. Wright, M. H. & Sieber, S. A. Chemical proteomics approaches for identifying the cellular targets of natural products. *Nat. Prod. Rep.* **33**, 681–708 (2016).

112. Murale, D. P., Hong, S. C., Haque, M. M. & Lee, J. S. Photo-affinity labeling (PAL) in chemical proteomics: A handy tool to investigate protein-protein interactions (PPIs). *Proteome Sci.* **15**, 1–34 (2017).

113. Smith, E. & Collins, I. Photoaffinity labeling in target- and binding-site identification. *Future Med. Chem.* **7**, 159–183 (2015).

114. Hill, J. R. & Robertson, A. A. B. Fishing for Drug Targets: A Focus on Diazirine Photoaffinity Probe Synthesis. *J. Med. Chem.* **61**, 6945–6963 (2018).

115. Feng, F., Zhang, W., Chai, Y., Guo, D. & Chen, X. Label-free target protein characterization for small molecule drugs: recent advances in methods and applications. *J. Pharm. Biomed. Anal.* **223**, 115107 (2023).

116. Pala, N. *et al.* Development of a Raltegravir-based Photoaffinity-Labeled Probe for Human Immunodeficiency Virus-1 Integrase Capture. *ACS Med. Chem. Lett.* **11**, 1986–1992 (2020).

117. Leprohon, P., Fernandez-Prada, C., Gazanion, É., Monte-Neto, R. & Ouellette, M. Drug resistance analysis by next generation sequencing in Leishmania. *Int. J. Parasitol. Drugs Drug Resist.* **5**, 26–35 (2015).

118. Pérez-Victoria, F. J., Sánchez-Cañete, M. P., Castanys, S. & Gamarro, F. Phospholipid translocation and miltefosine potency require both L. donovani miltefosine transporter and the new protein LdRos3 in Leishmania parasites. *J. Biol. Chem.* **281**, 23766–23775 (2006).

119. Fernandez-Prada, C. *et al.* High-throughput Cos-Seq screen with intracellular Leishmania infantum for the discovery of novel drug-resistance mechanisms. *Int. J. Parasitol. Drugs Drug Resist.* **8**, 165–173 (2018).

120. Gazanion, É., Fernández-Prada, C., Papadopoulou, B., Leprohon, P. & Ouellette, M. Cos-Seq for high-throughput identification of drug target and resistance mechanisms in the protozoan parasite Leishmania. *Proc. Natl. Acad. Sci. U. S. A.* **113**, E3012–E3021 (2016).

121. Beilstein, S. *et al.* Laboratory Selection of Trypanosomatid Pathogens for Drug Resistance. *Pharmaceuticals* **15**, 1–12 (2022).

122. Coelho, A. C., Trinconi, C. T., Senra, L., Yokoyama-Yasunaka, J. K. U. & Uliana, S. R. B. Leishmania is not prone to develop resistance to tamoxifen. *Int. J. Parasitol. Drugs Drug Resist.* **5**, 77–83 (2015).

123. Shiina, I. *et al.* An expeditious synthesis of tamoxifen, a representative SERM (selective estrogen receptor modulator), via the three-component coupling reaction among aromatic aldehyde, cinnamyltrimethylsilane, and β-chlorophenetole. *Bioorganic Med. Chem.* **15**, 7599–7617 (2007).

124. M. Kasiotis, K. & A. Haroutounian, S. Tamoxifen: A Synthetic Overview. *Curr. Org. Chem.* **16**, 335–352 (2012).

125. Zhang, Z., Lindale, M. G. & Liebeskind, L. S. Mobilizing Cu(I) for carbon-carbon bond forming catalysis in the presence of thiolate. Chemical mimicking of metallothioneins. *J. Am. Chem. Soc.* **133**, 6403–6410 (2011).

126. Debnath, J. *et al.* Discovery of selective menaquinone biosynthesis inhibitors against Mycobacterium tuberculosis. *J. Med. Chem.* **55**, 3739–3755 (2012).

127. Sultan, S., Bhat, M. U. S., Rizvi, M. A. & Shah, B. A. Visible Light-Mediated [2 + 2] Cycloaddition Reactions of 1,4-Quinones and Terminal Alkynes. *J. Org. Chem.* **84**, 8948–8958 (2019).

128. Liu, W., Guo, J., Xing, S. & Lu, Z. Highly Enantioselective Cobalt-Catalyzed Hydroboration of Diaryl Ketones. *Org. Lett.* **22**, 2532–2536 (2020).

Appendix

NMR Spectra

(2*R*)-1-[(benzyloxy)carbonyl]pyrrolidine-2-carboxylic acid 52a

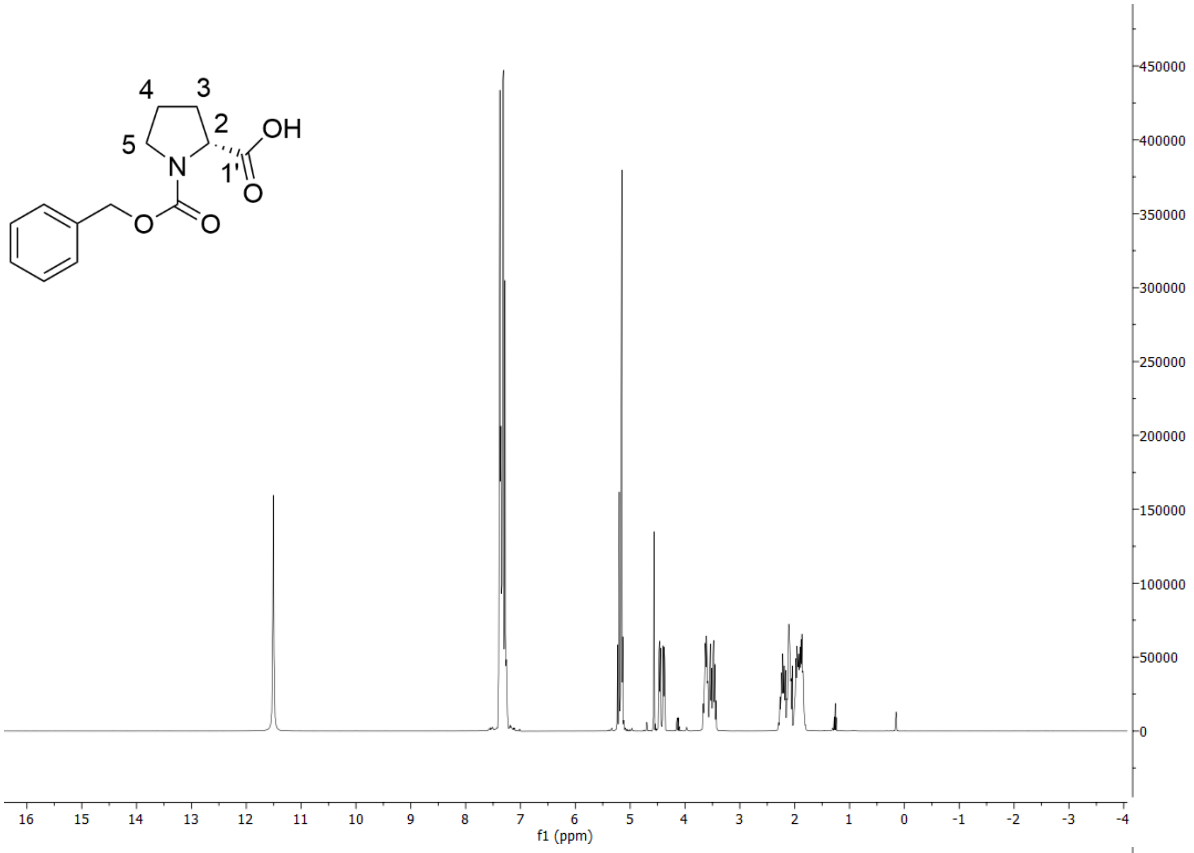

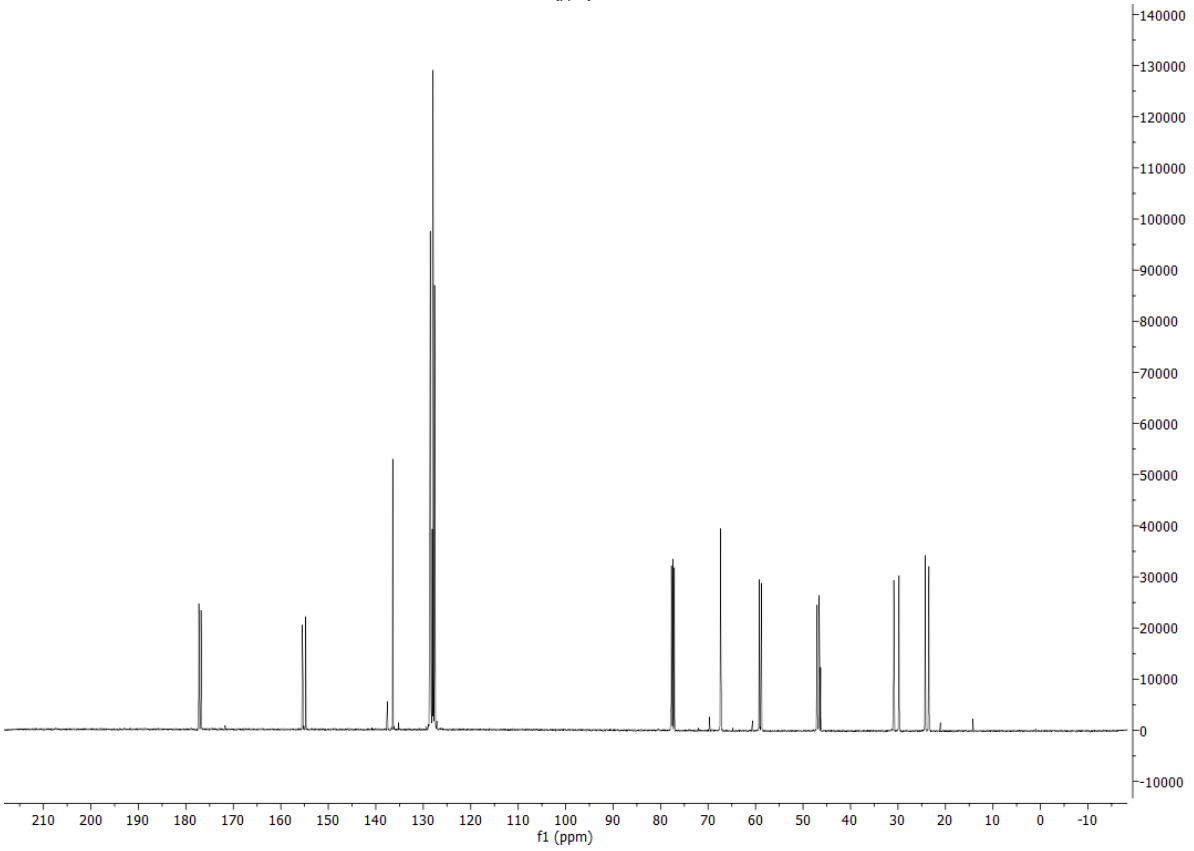

(2*R*)-1-(methoxycarbonyl)pyrrolidine-2-carboxylic acid 52b

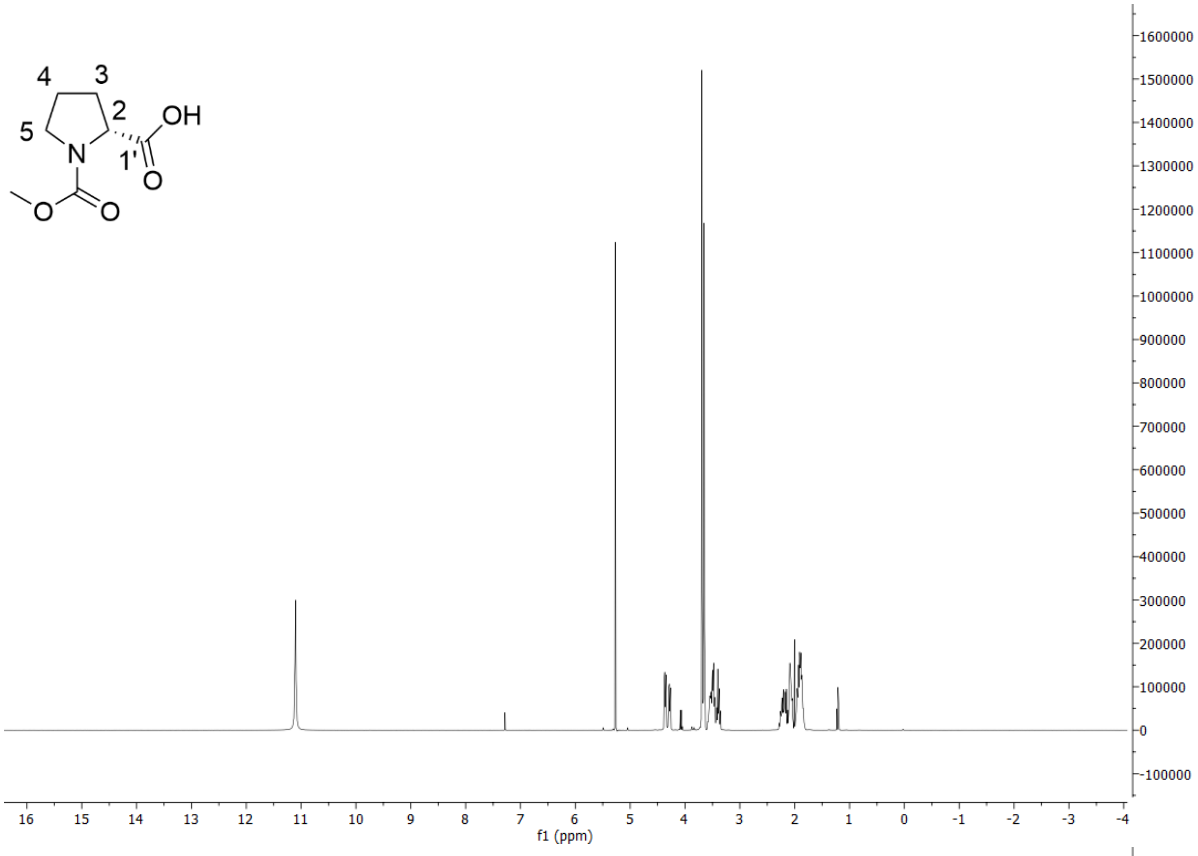

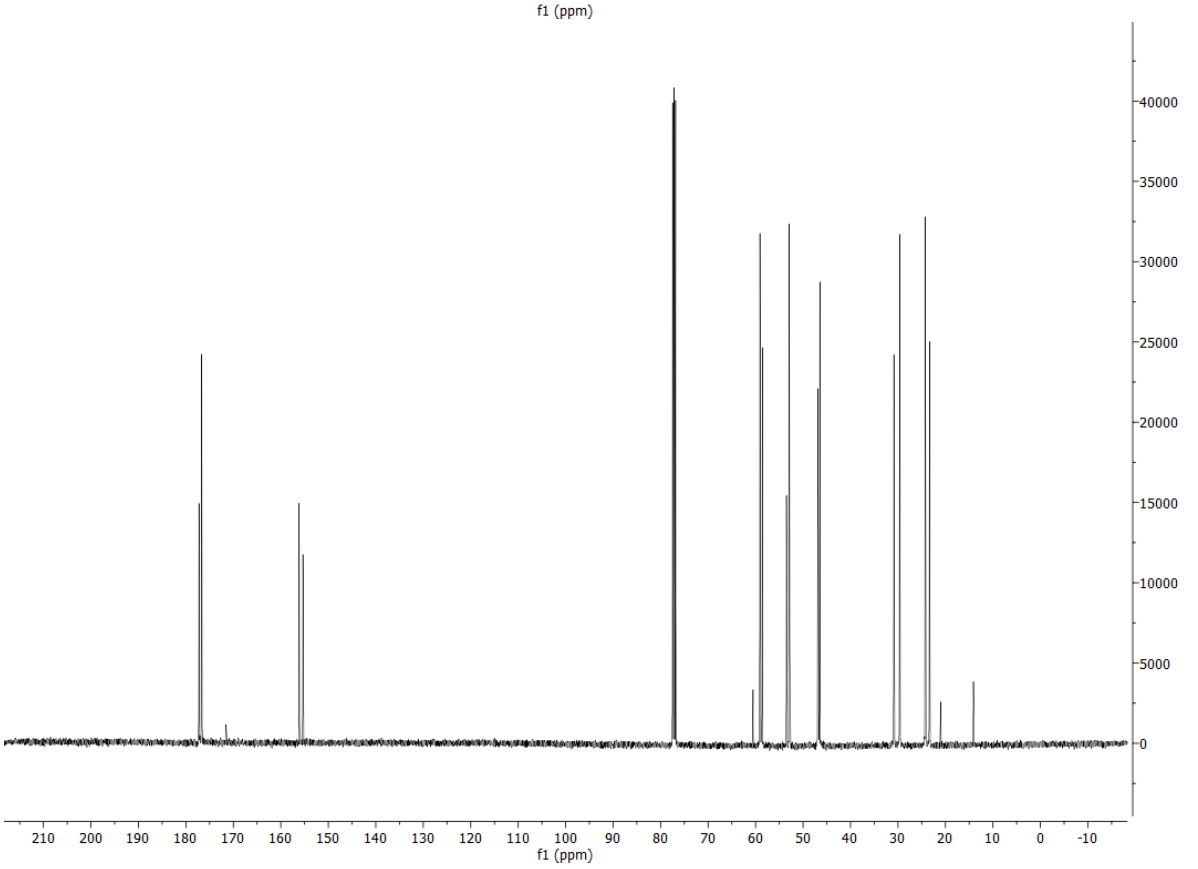

Benzyl (2*R*)-2-(2-diazoacetyl)pyrrolidine-1-carboxylate 53a

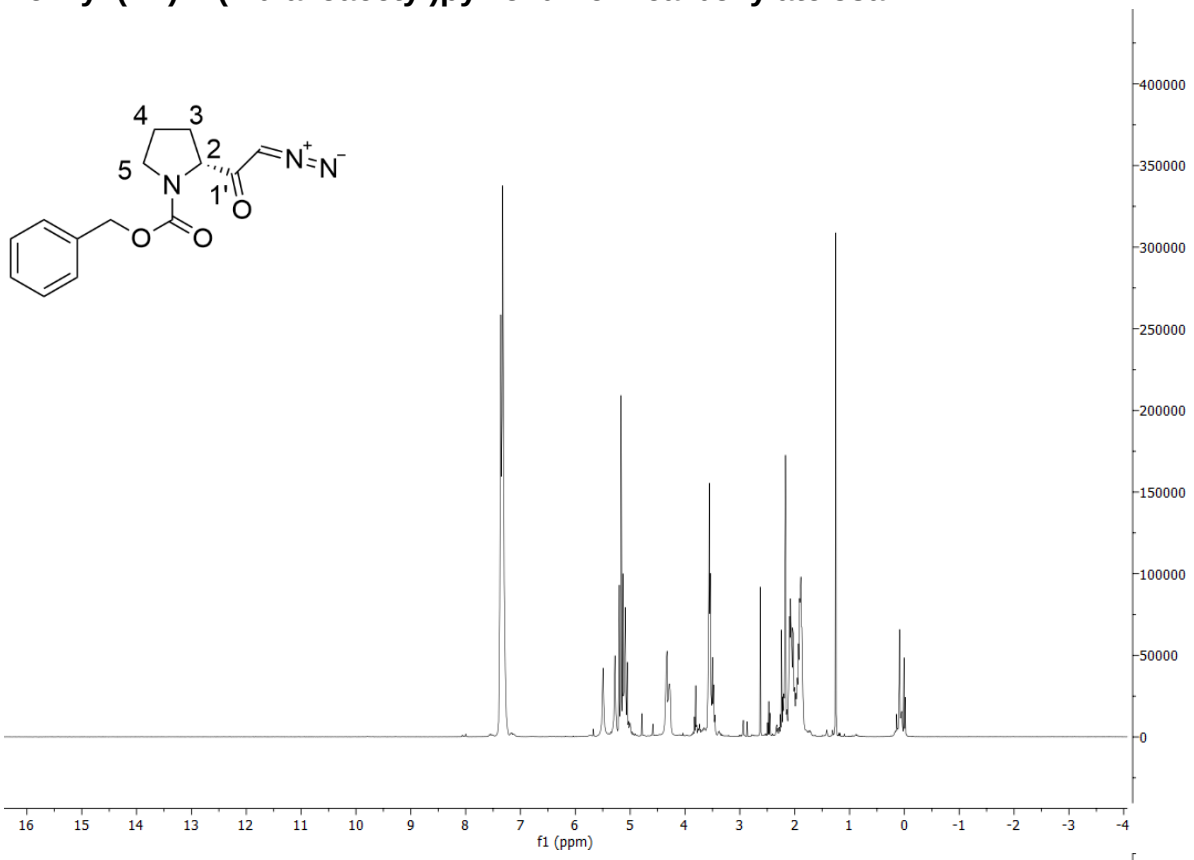

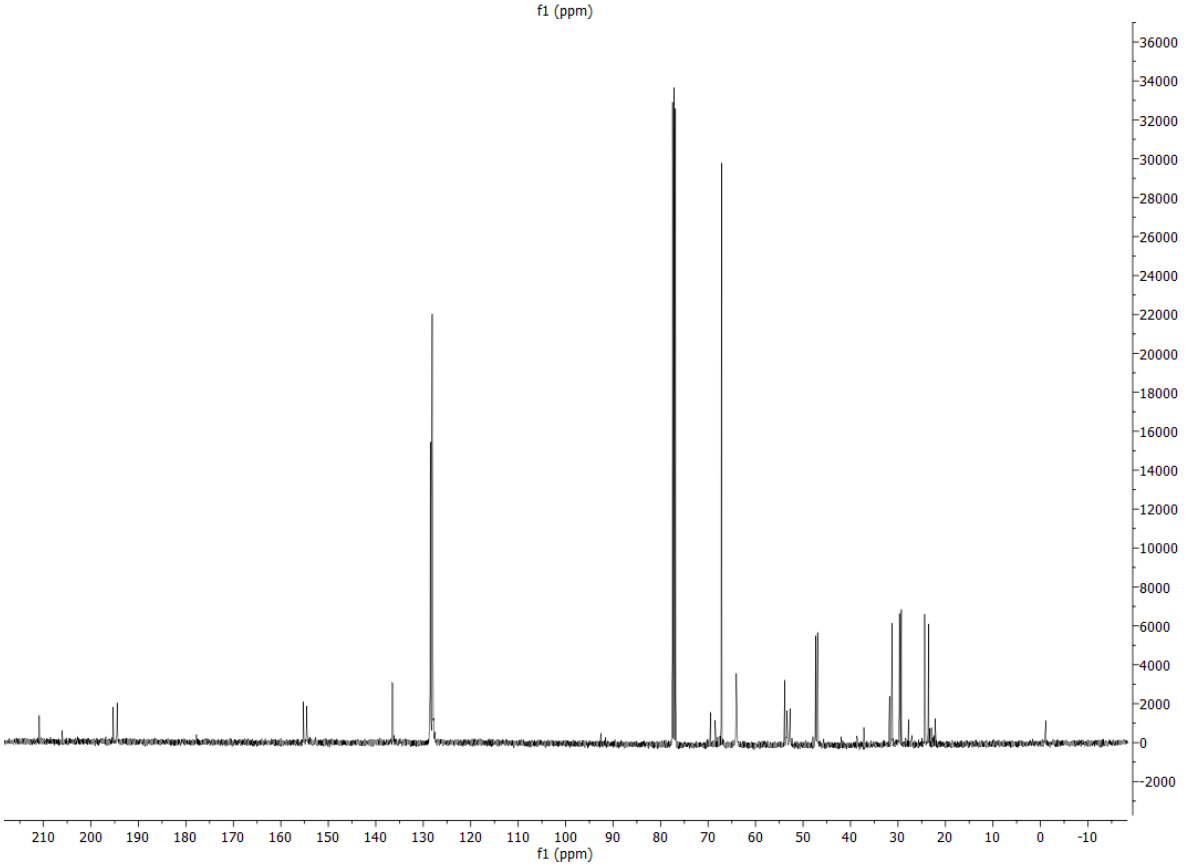

Methyl (2*R*)-2-(2'-diazoacetyl)pyrrolidine-1'-carboxylate 53b

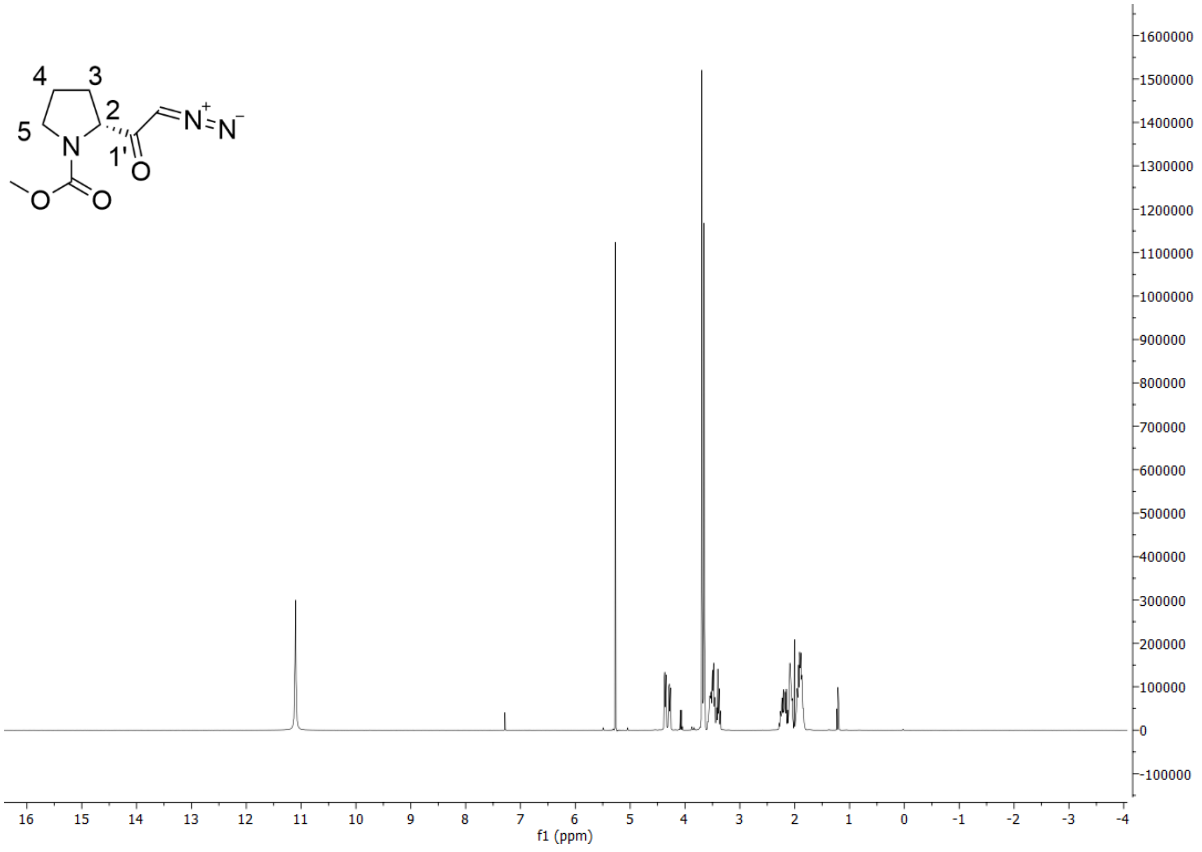

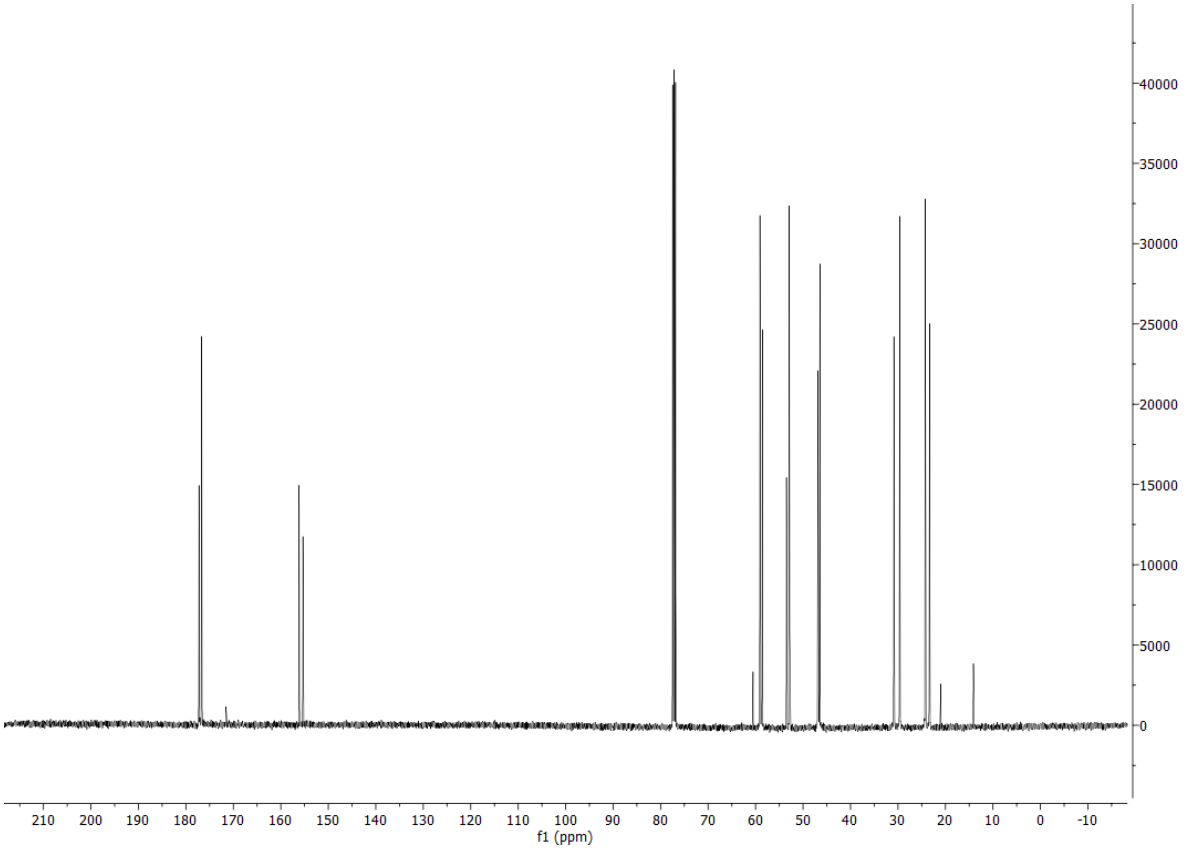

Benzyl-(2*R*)-2-(2'-methoxy-2-oxoethyl)pyrrolidine-1'-carboxylate 54a

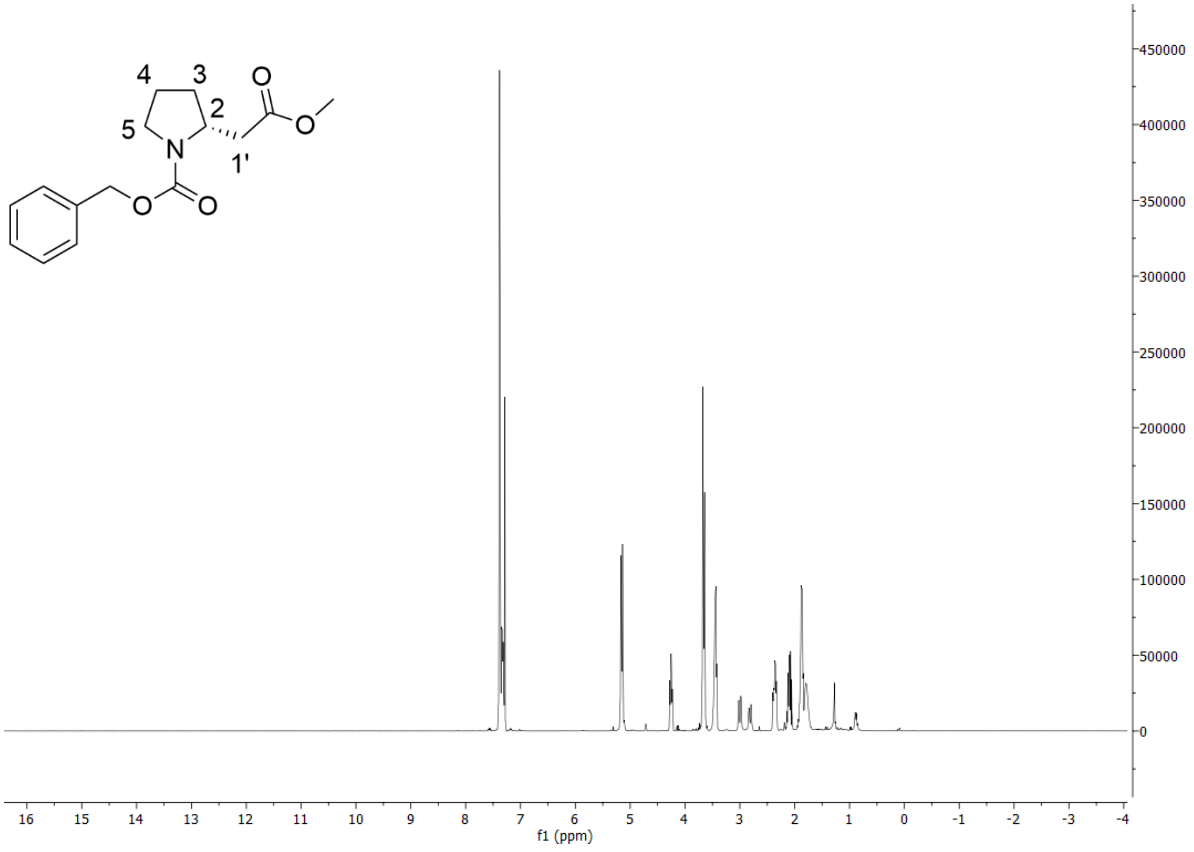

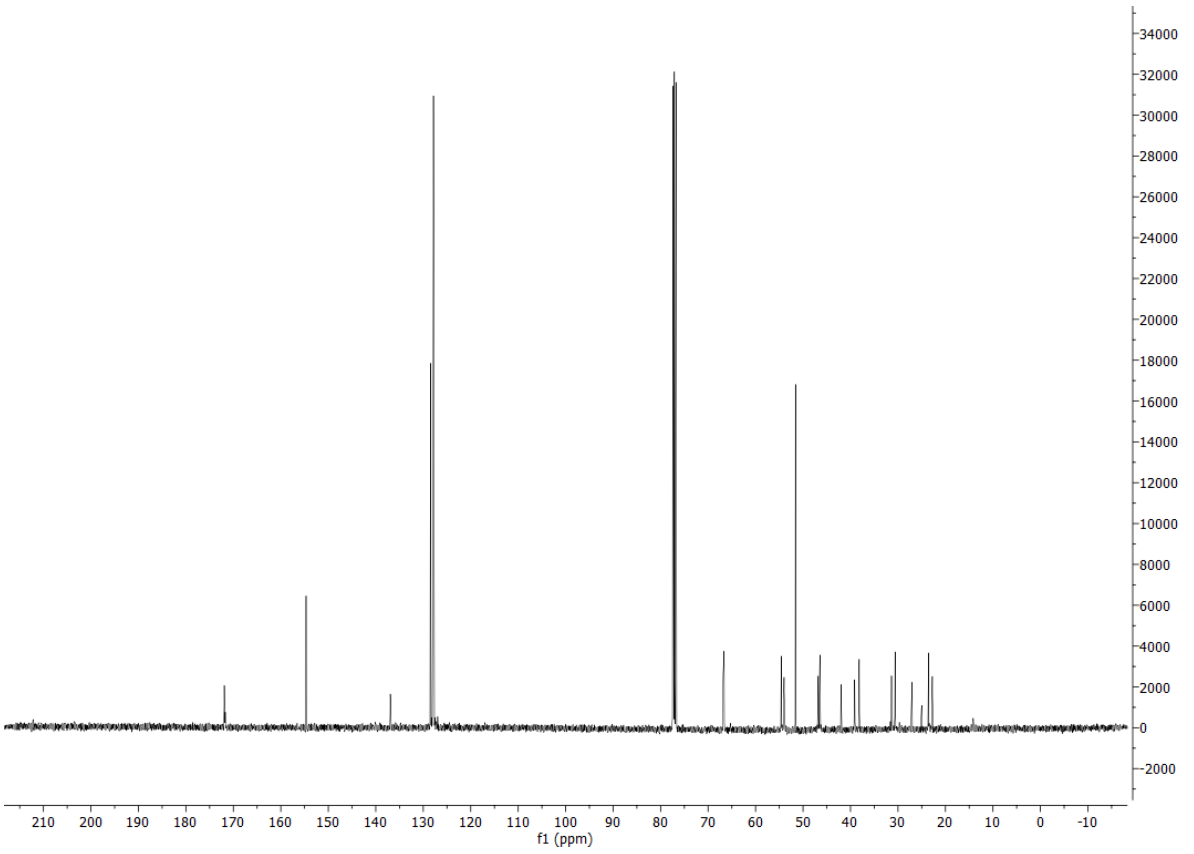

Methyl (2*R*)-2-(2'-methoxy-2-oxoethyl)pyrrolidine-1-carboxylate 54b

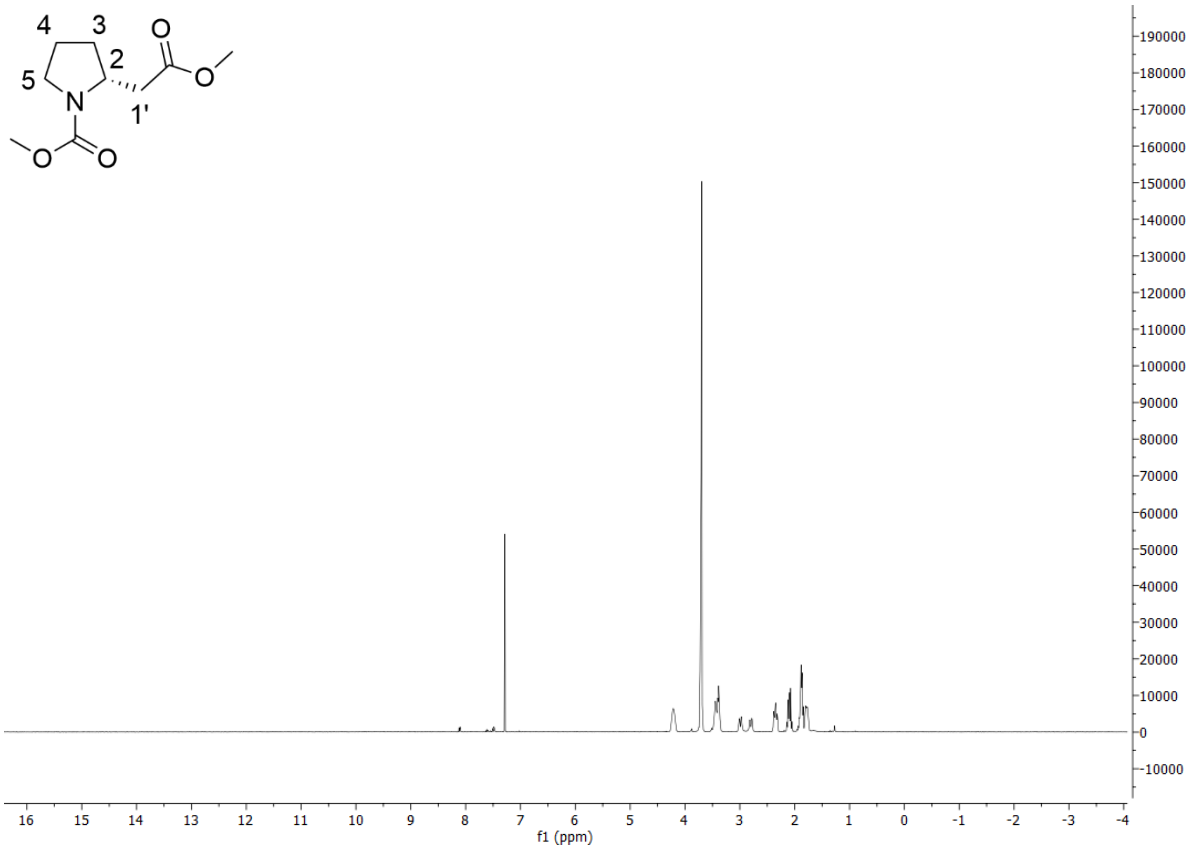

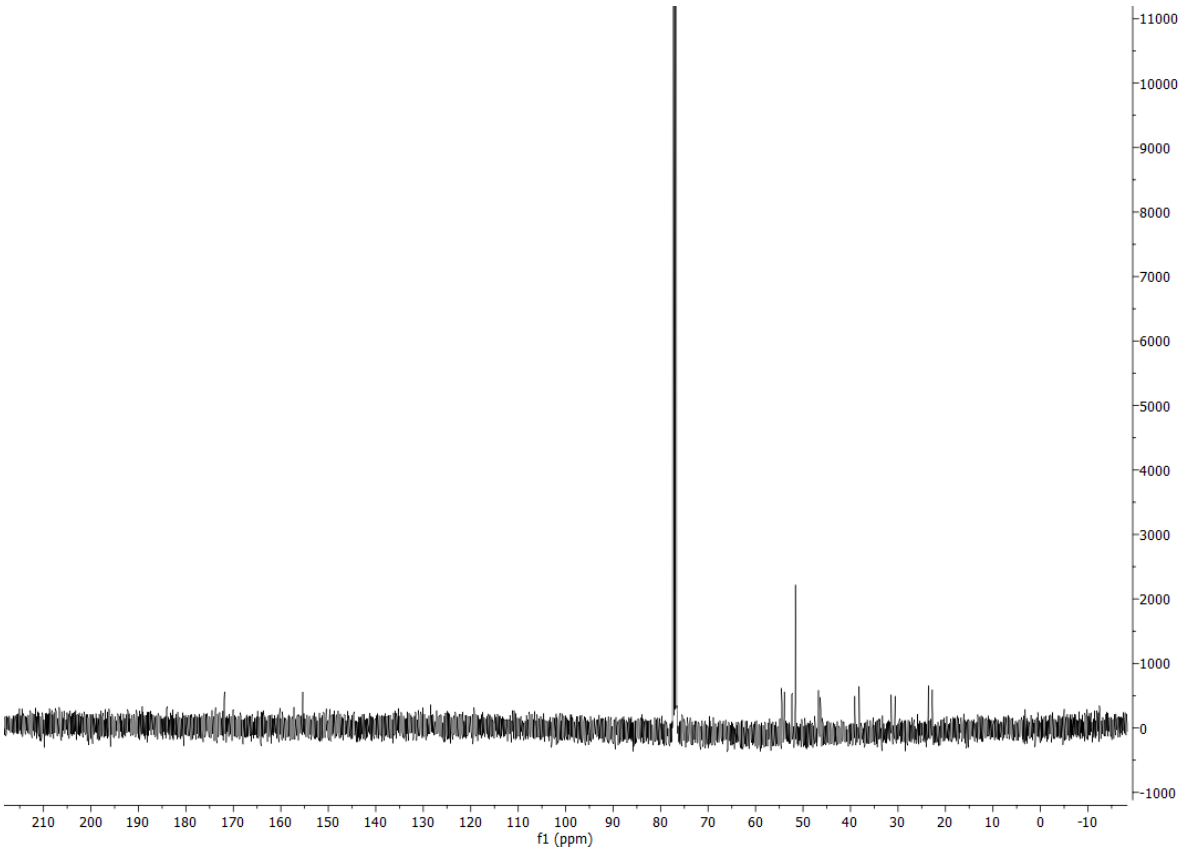

2-[(2*R*)-N-methylpyrrolidin-2’-yl]ethan-1’-ol 55

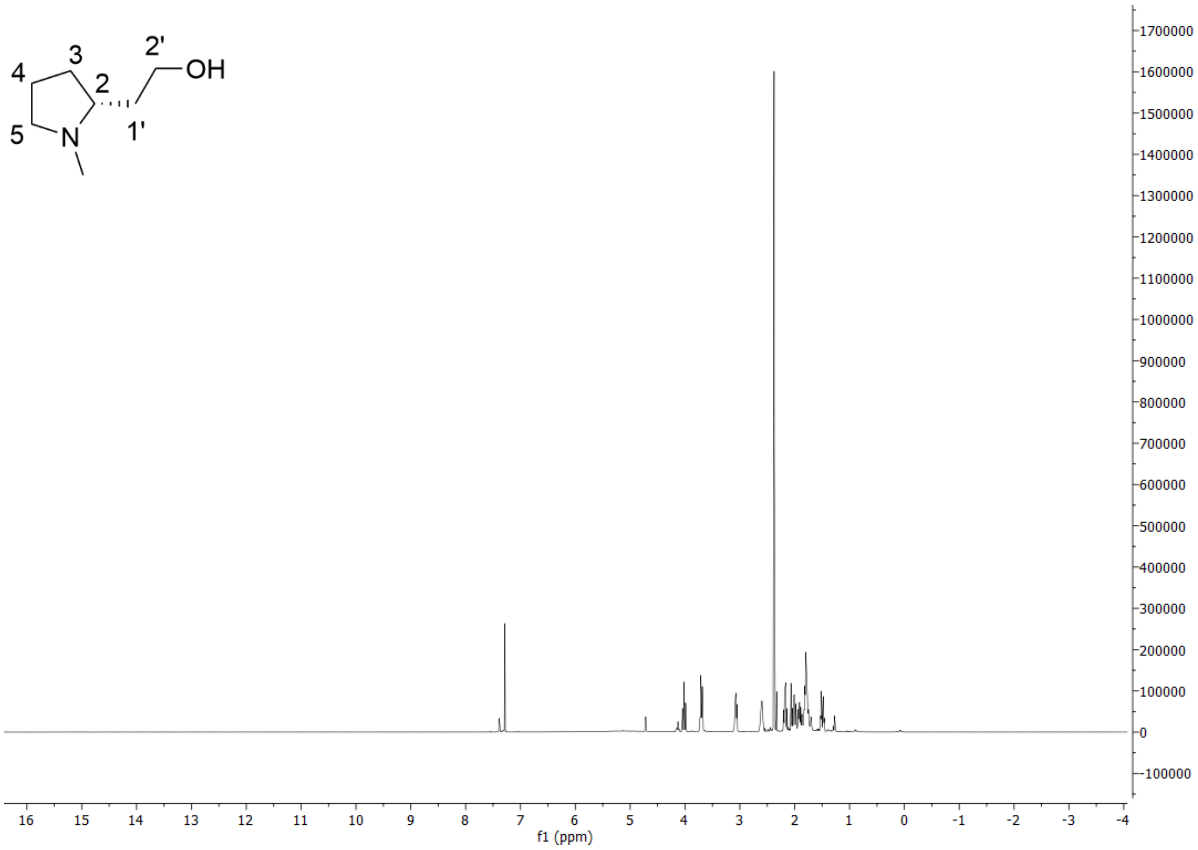

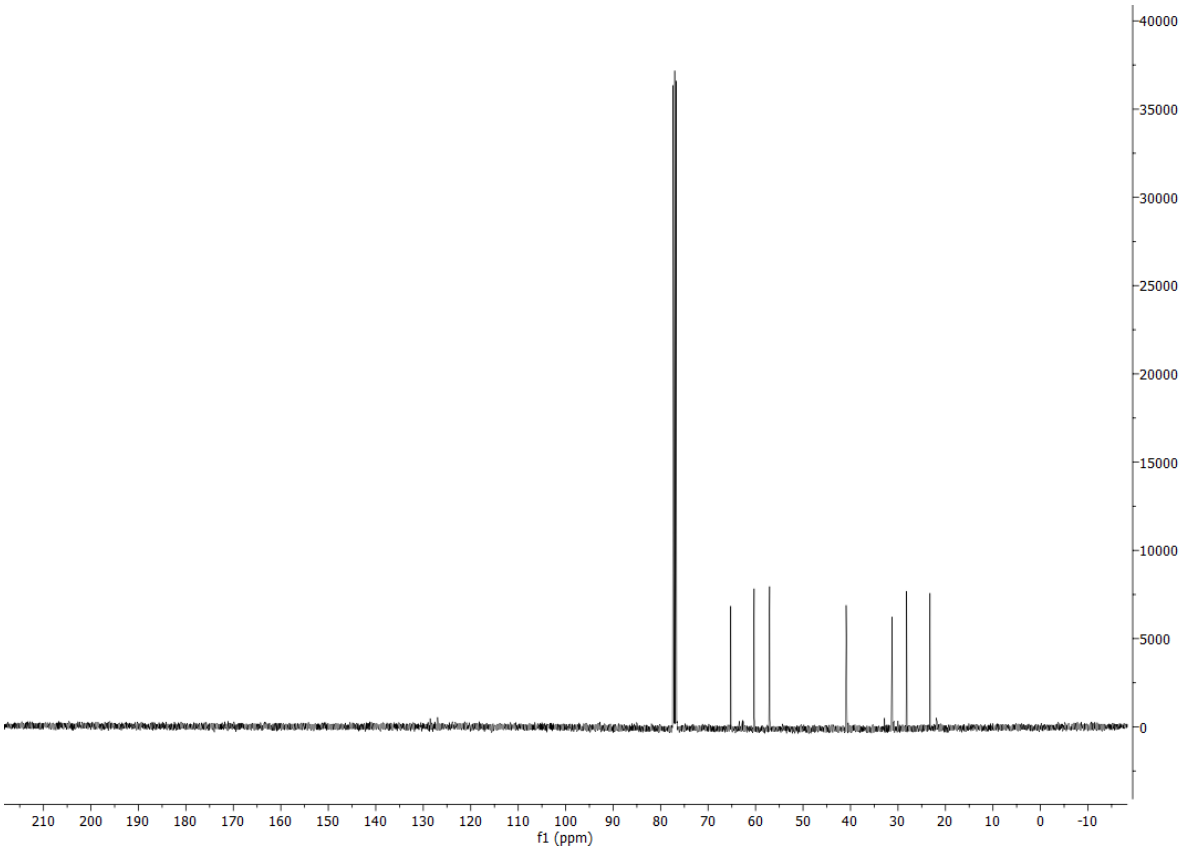

(2*R*)-2'-(2-chloroethyl)-*N*-methylpyrrolidine hydrochloride 56

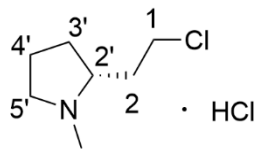

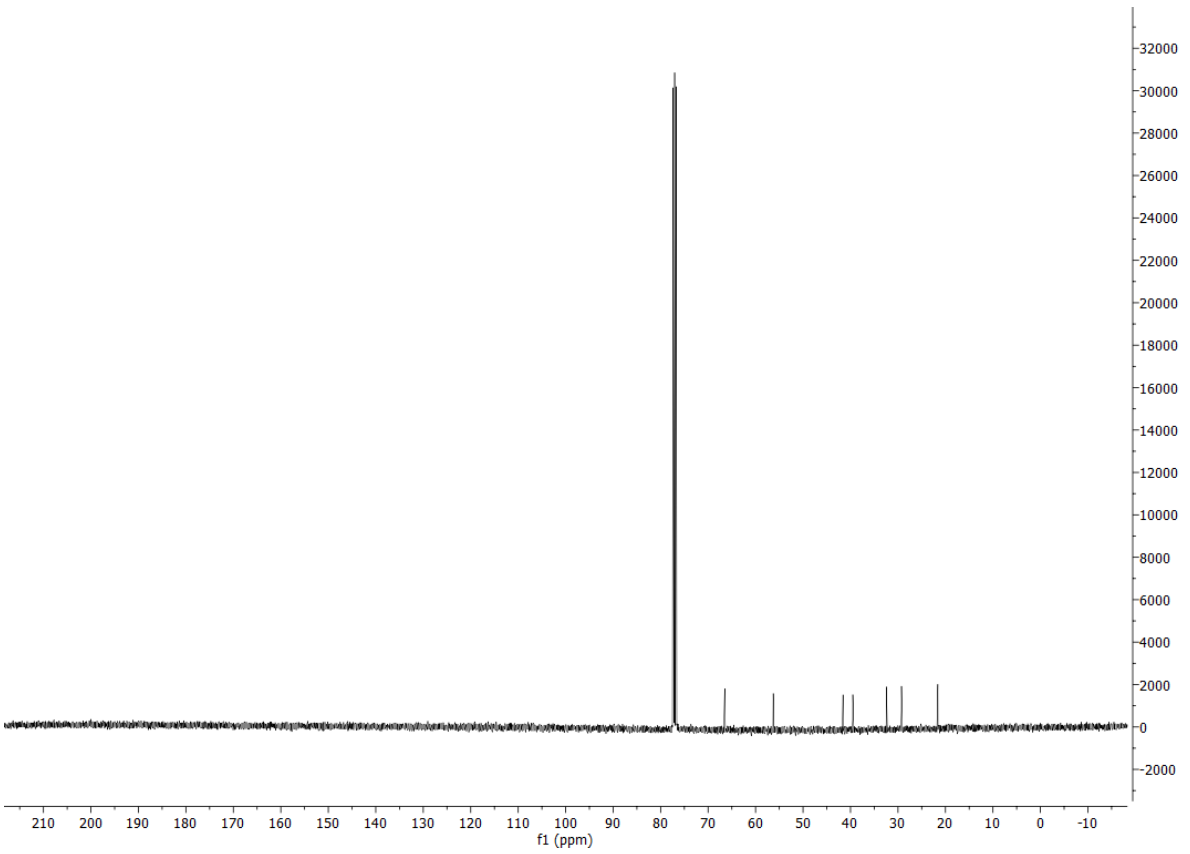

(2*R*)-2’’’-[2’’-(2-benzoylphenoxy)ethyl]-1’’’-methylpyrrolidine

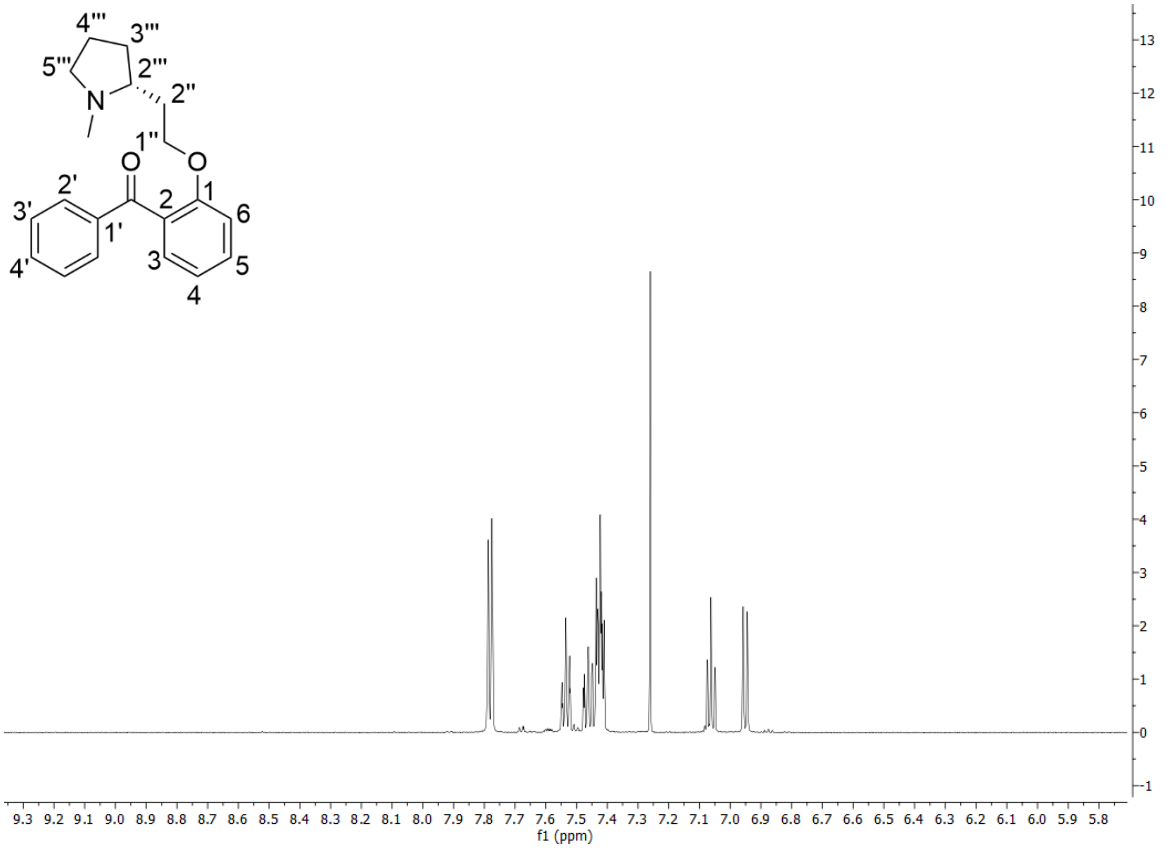

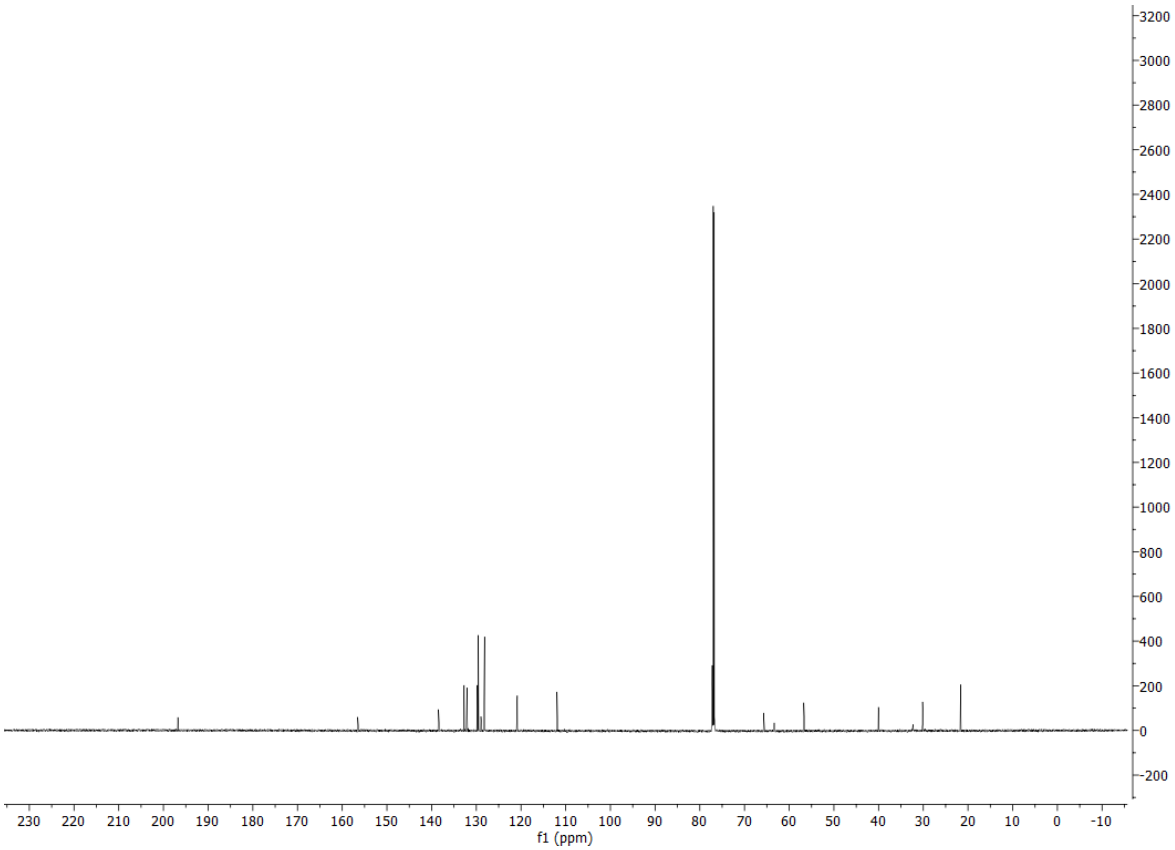

{2-[(2-bromophenyl)methoxy]ethyl}dimethylamine 32

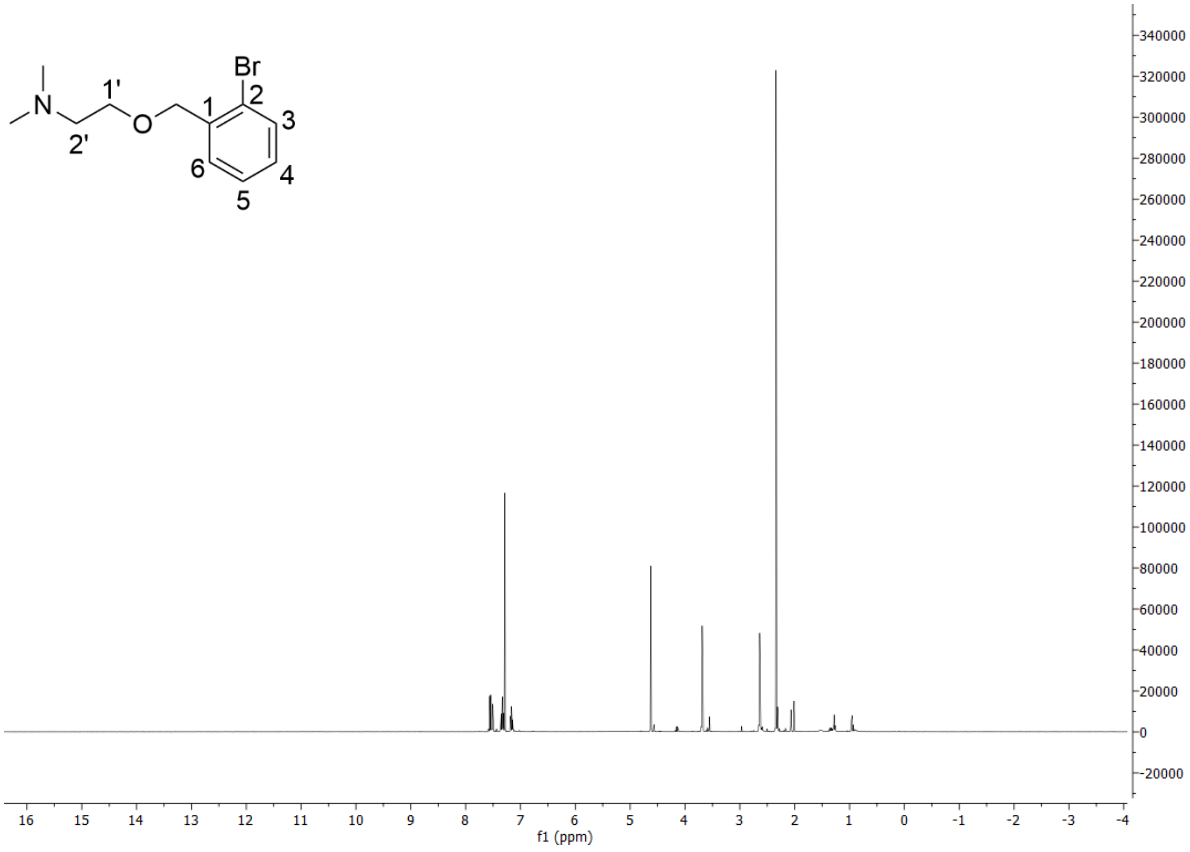

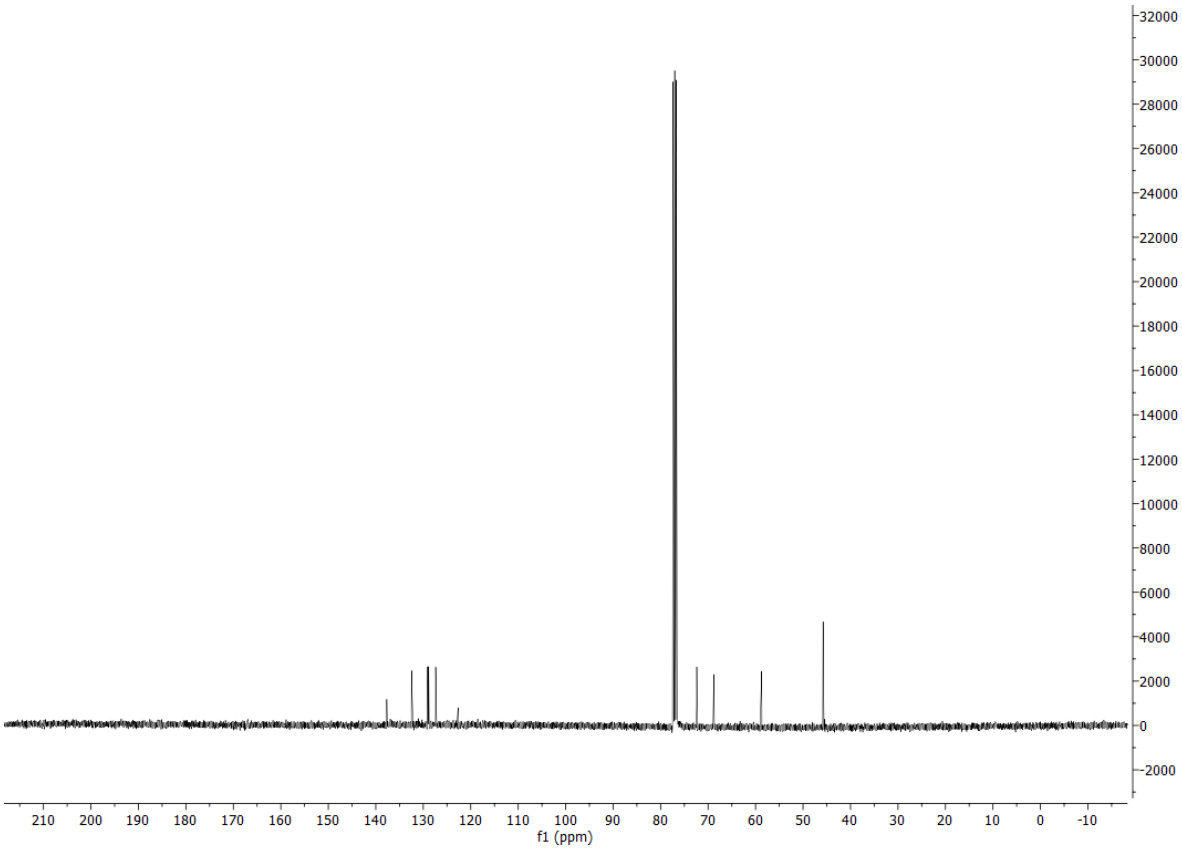

[(2-bromophenyl)methoxy](tert-butyl)dimethylsilane 35

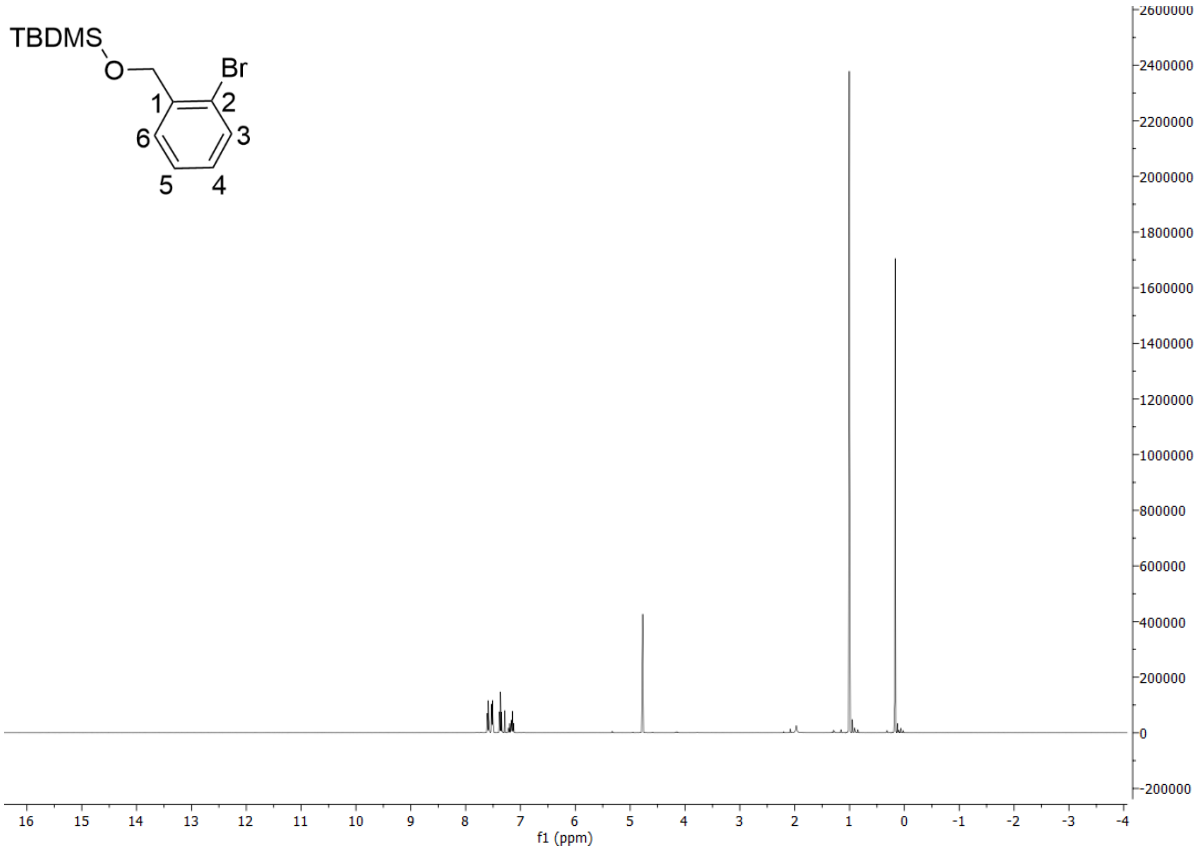

{2-[2''-(dimethylamino)ethoxy]phenyl}(phenyl)methanol

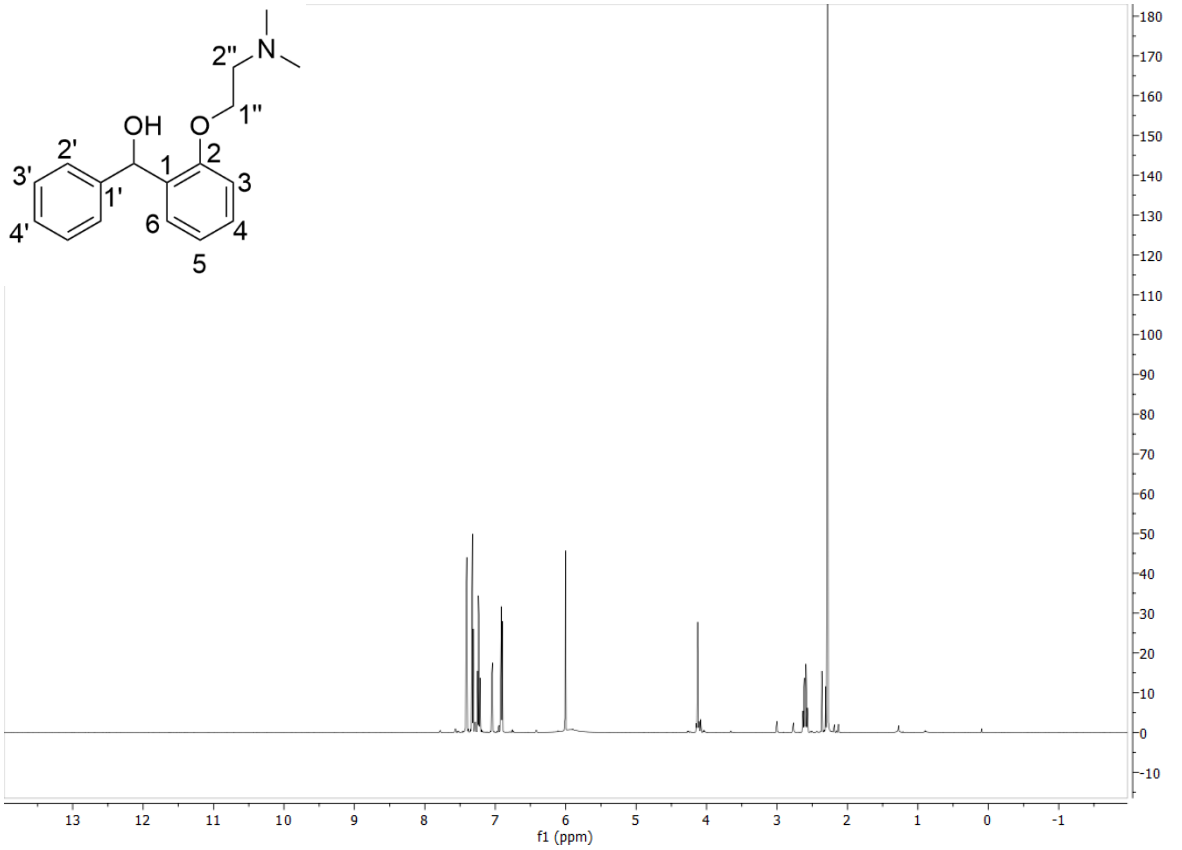

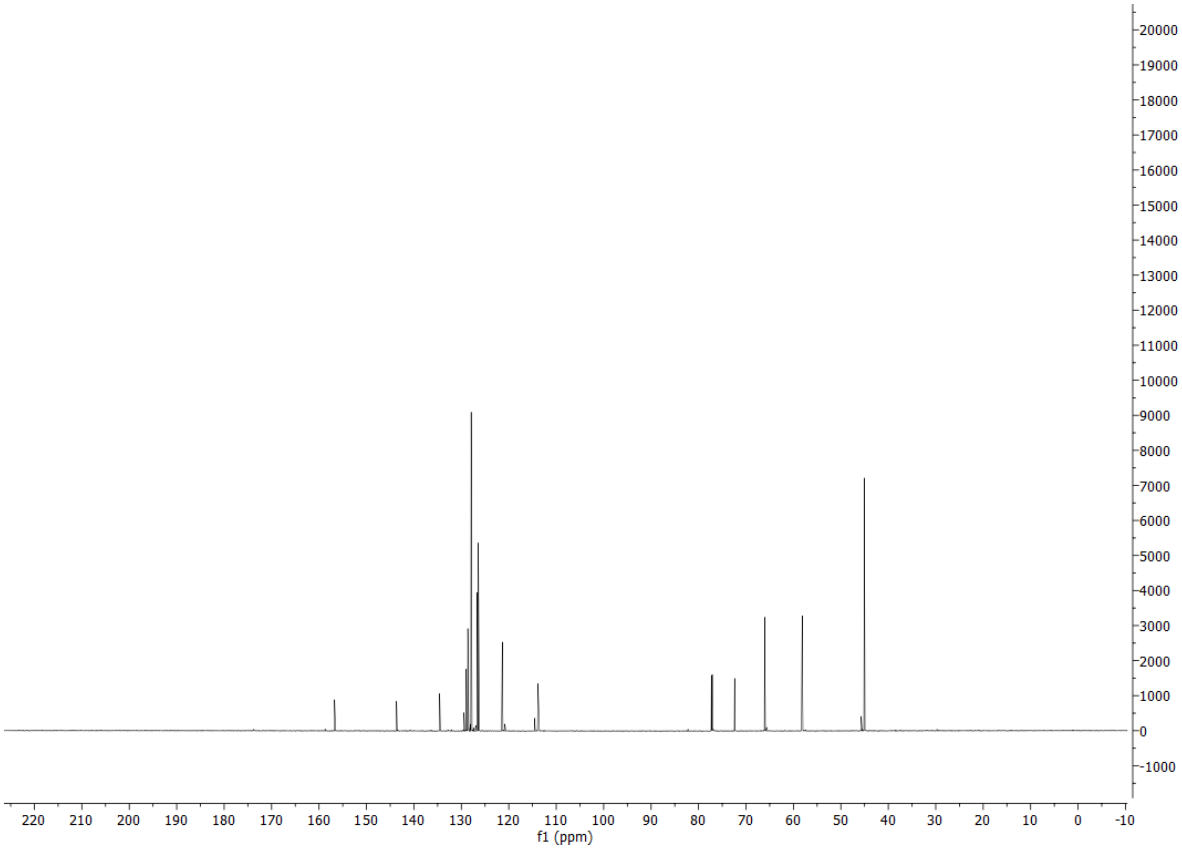

[2’’-(2-benzoylphenoxy)ethyl]dimethylamine 44

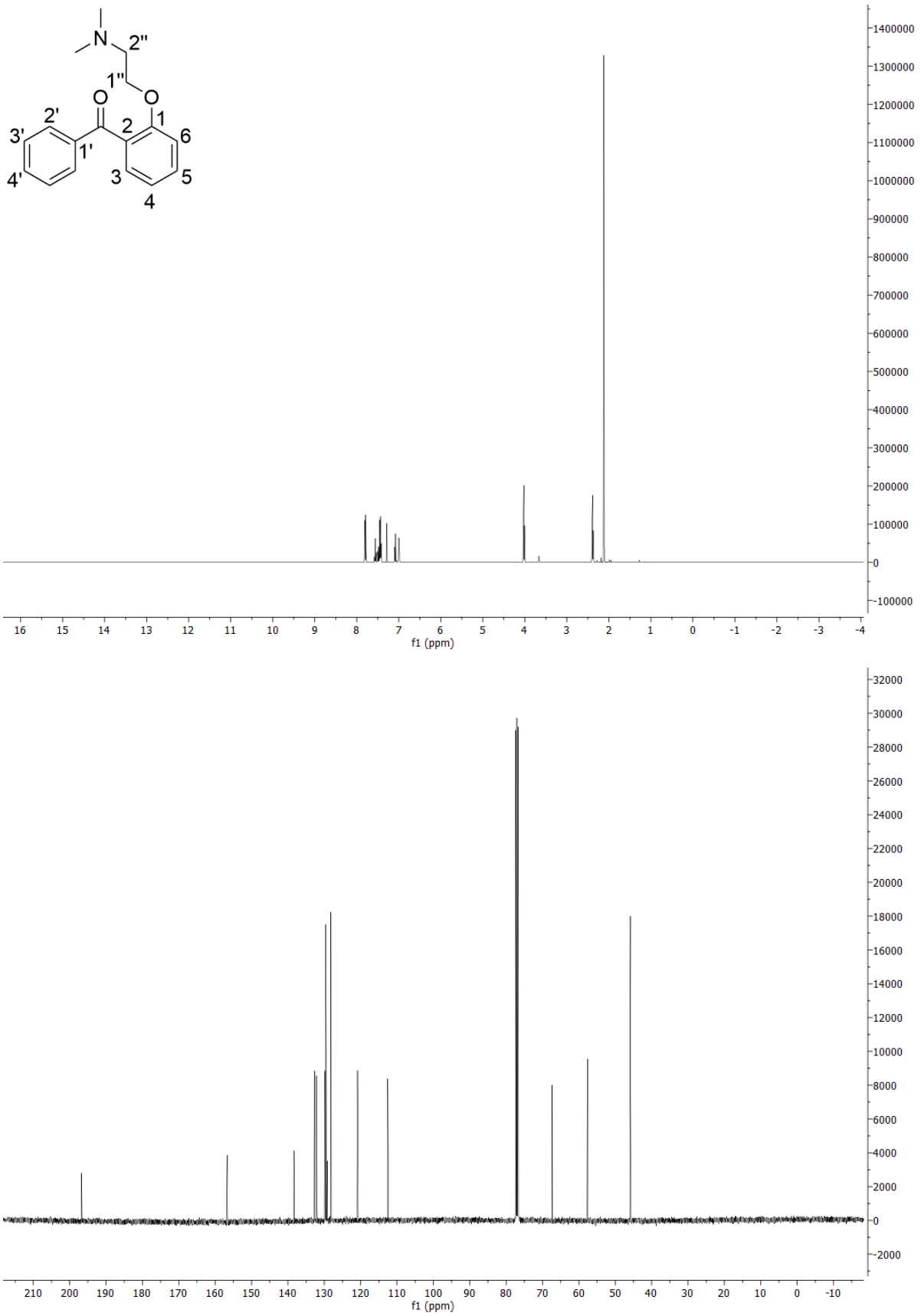

[3’’-(2-benzoylphenoxy)propyl]dimethylamine 46

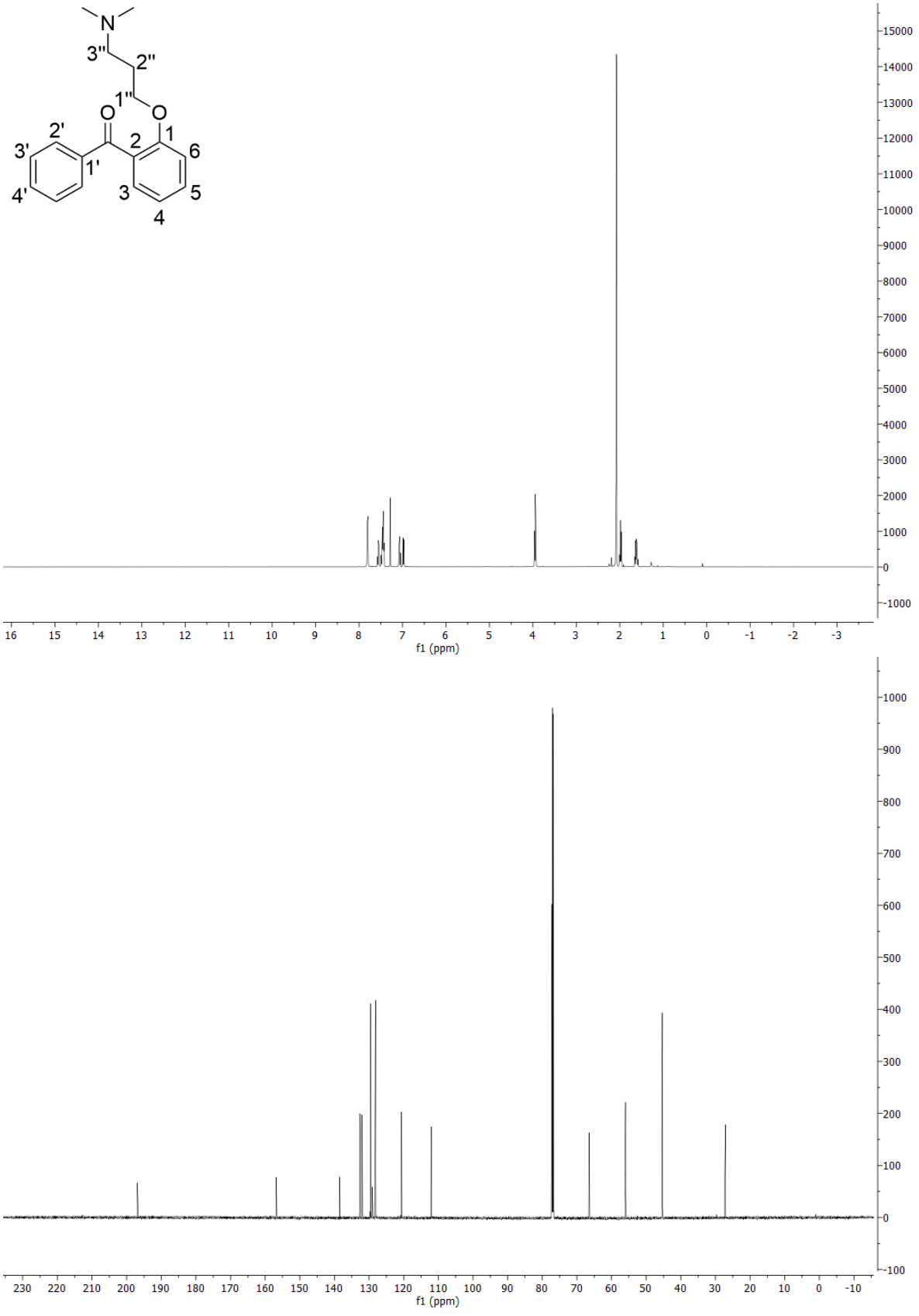

[2’’-(2-benzoyl-4-chlorophenoxy)ethyl]dimethylamine 48

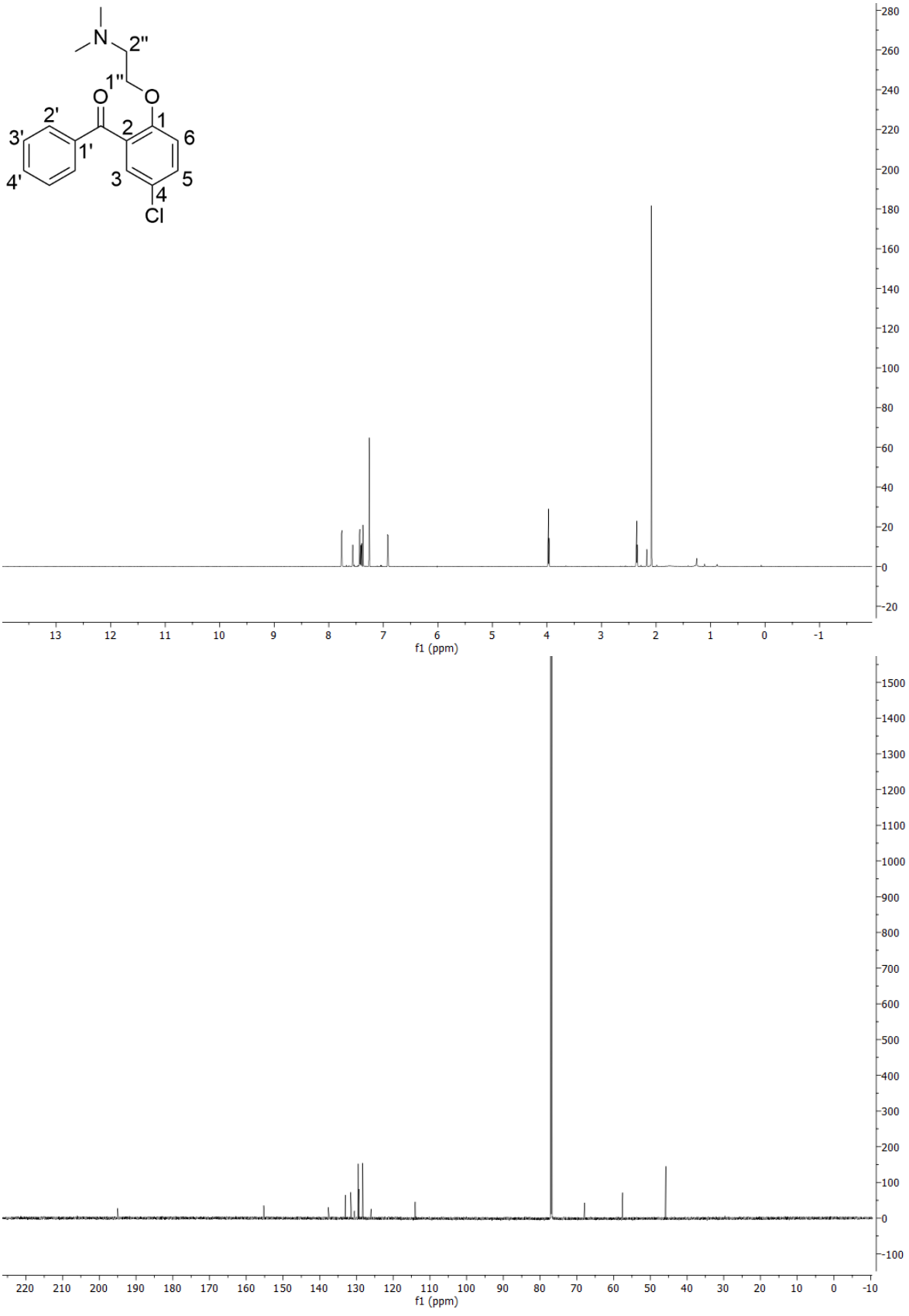

[3’’-(2-benzoyl-4-chlorophenoxy)propyl]dimethylamine 49

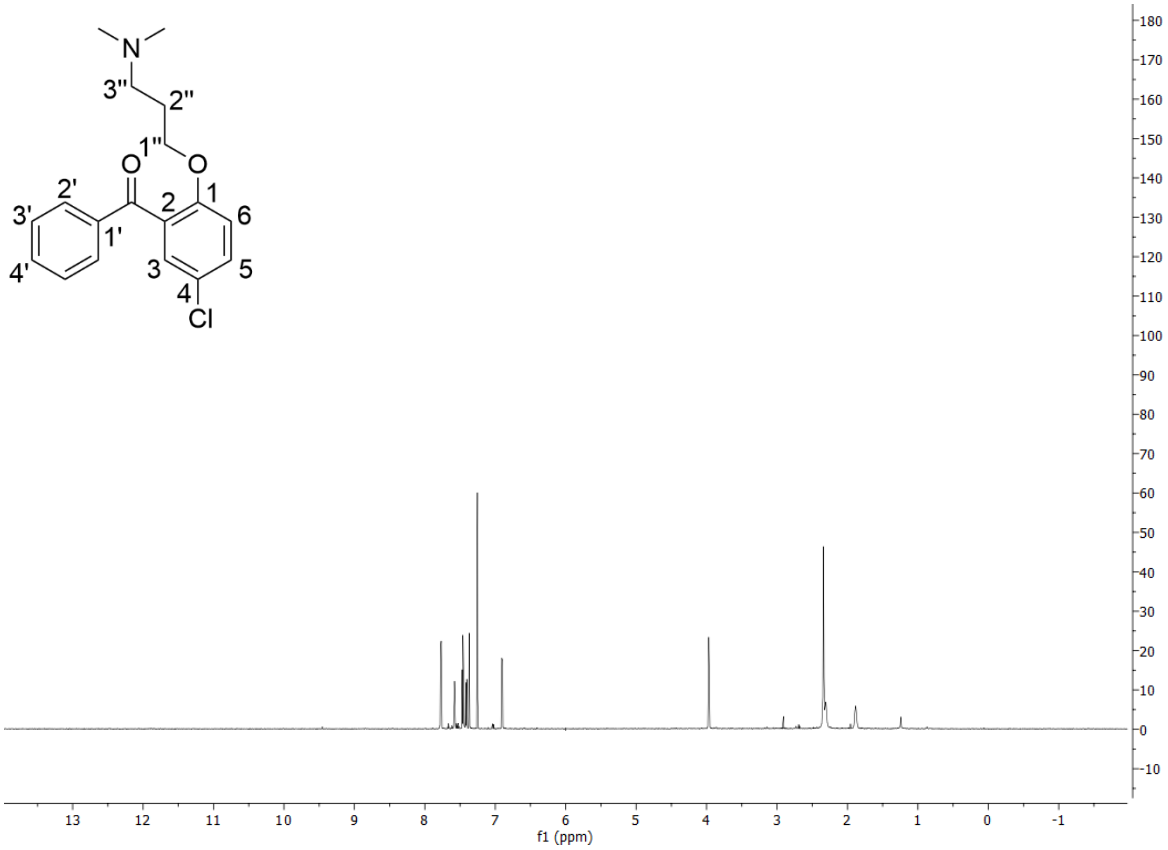

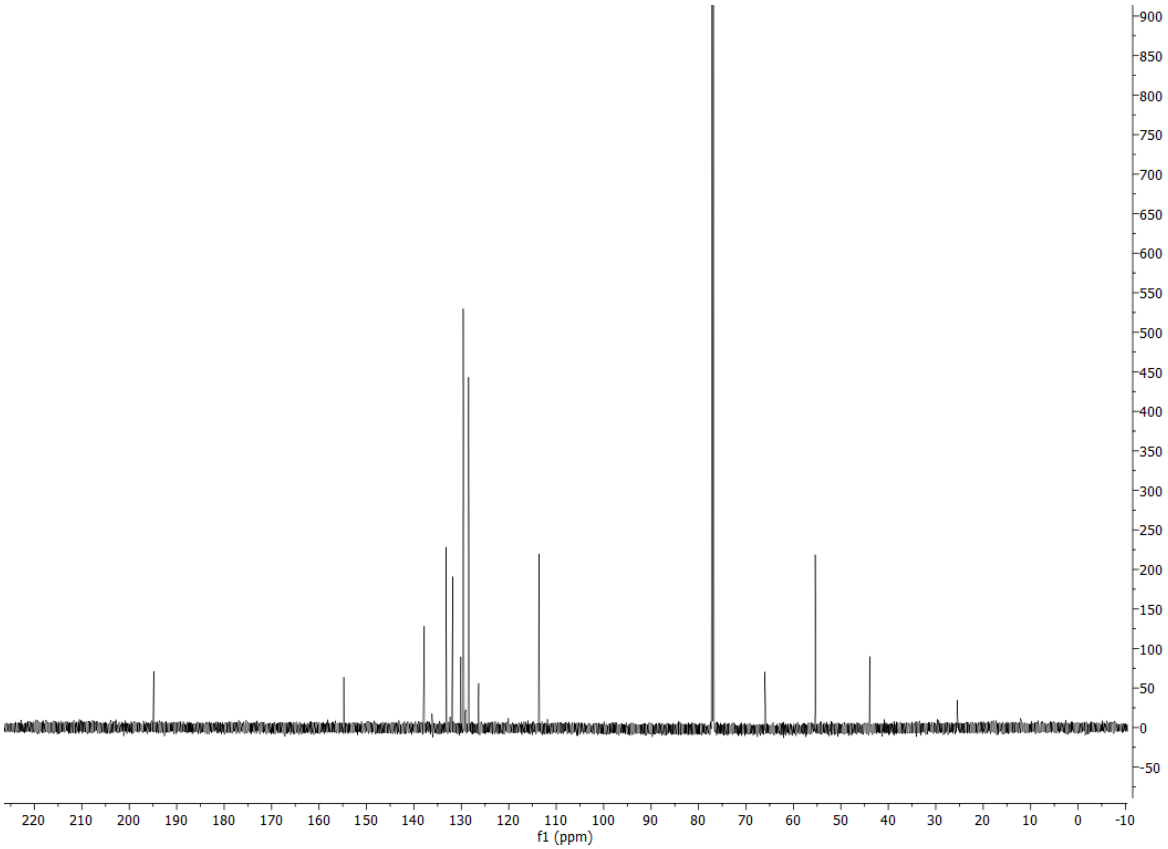

[2’’-(4-benzoylphenoxy)ethyl]dimethylamine 71

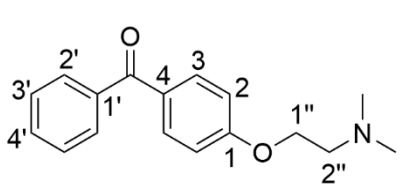

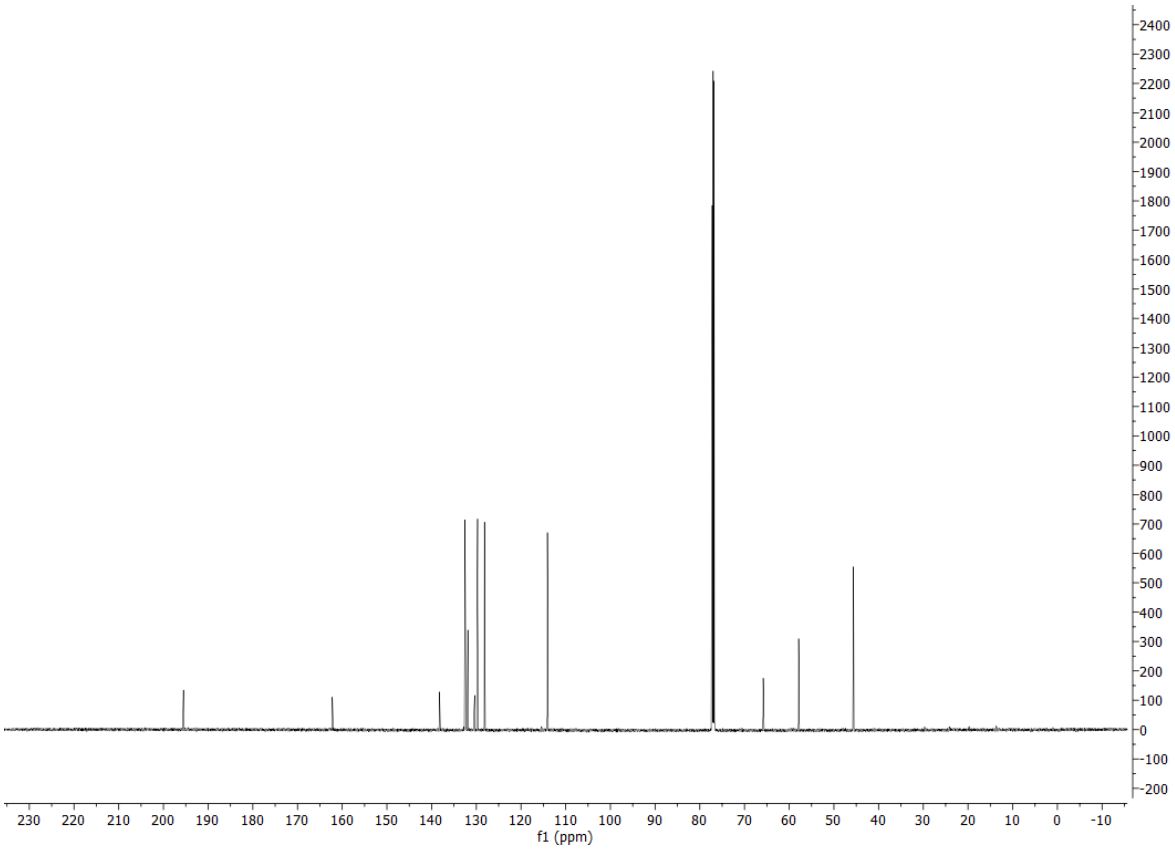

[3’’-(4-benzoylphenoxy)propyl]dimethylamine 72

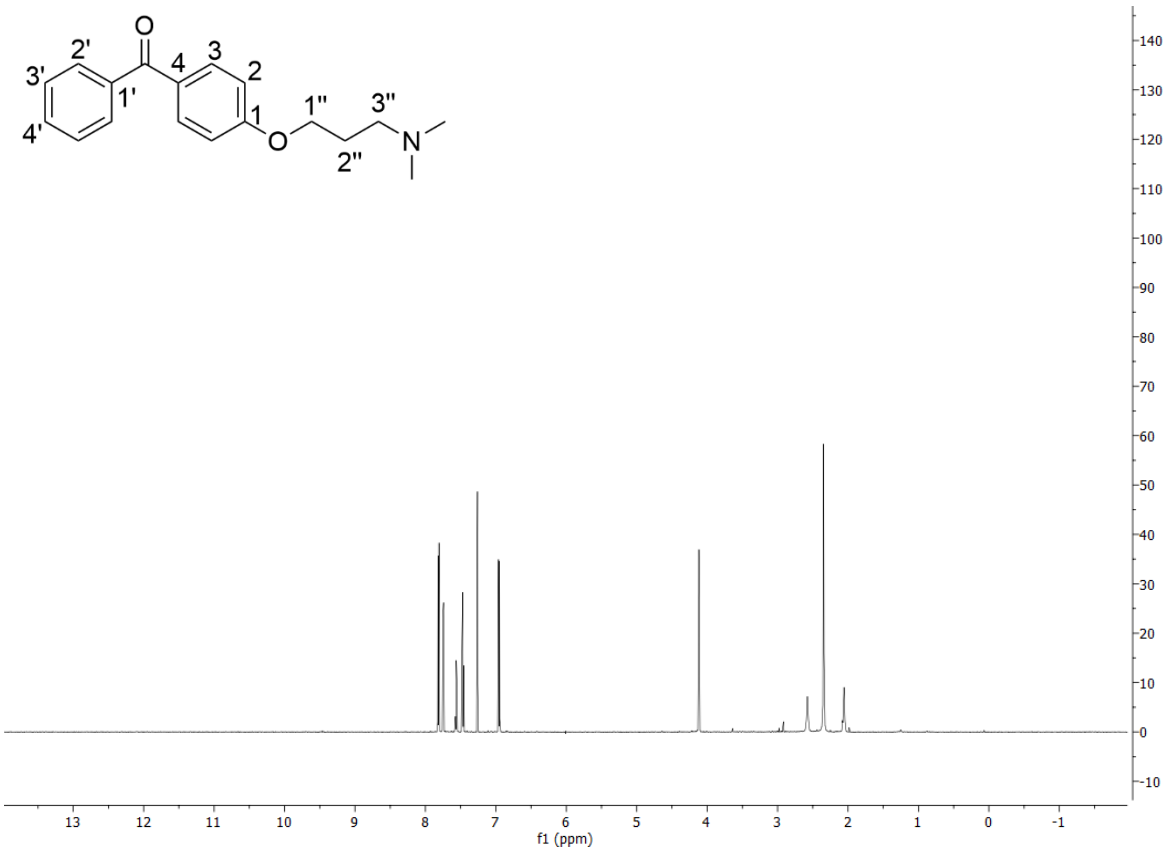

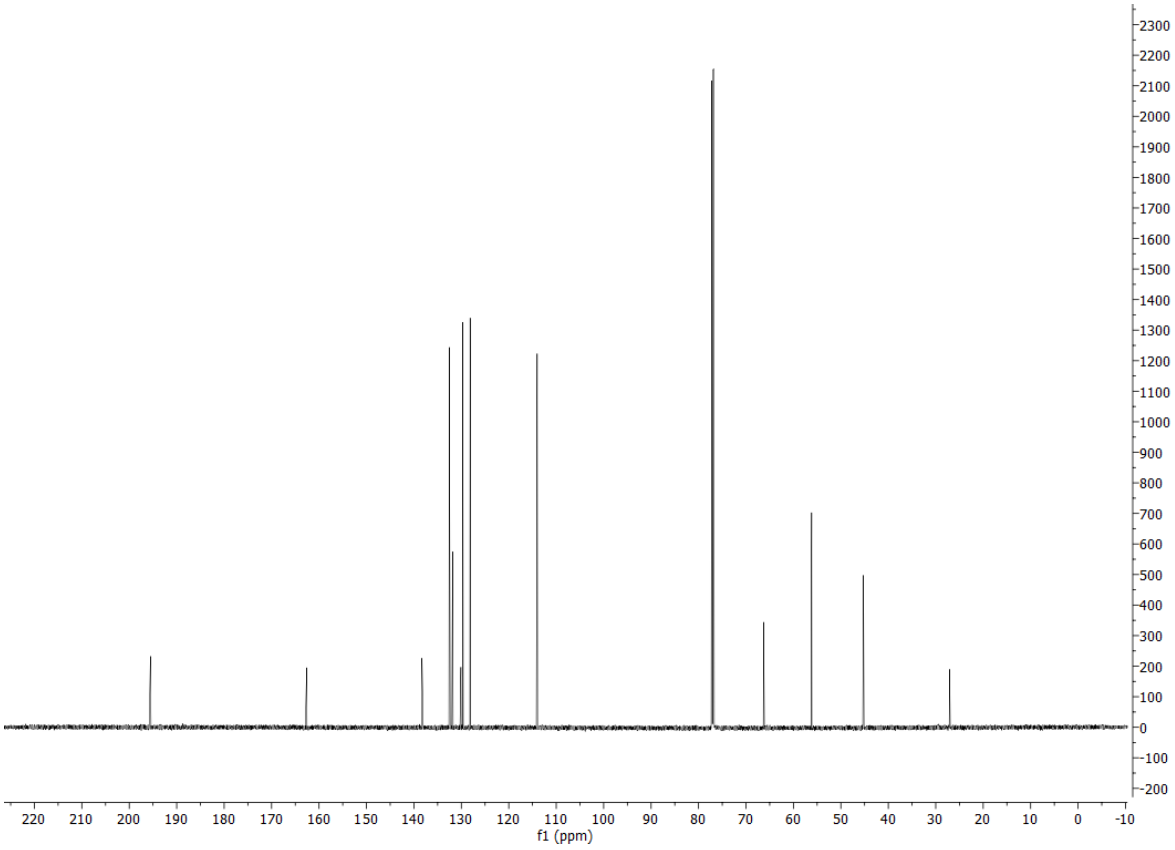

{2’’-[(4-benzoylphenyl)methoxy]ethyl}dimethylamine 118

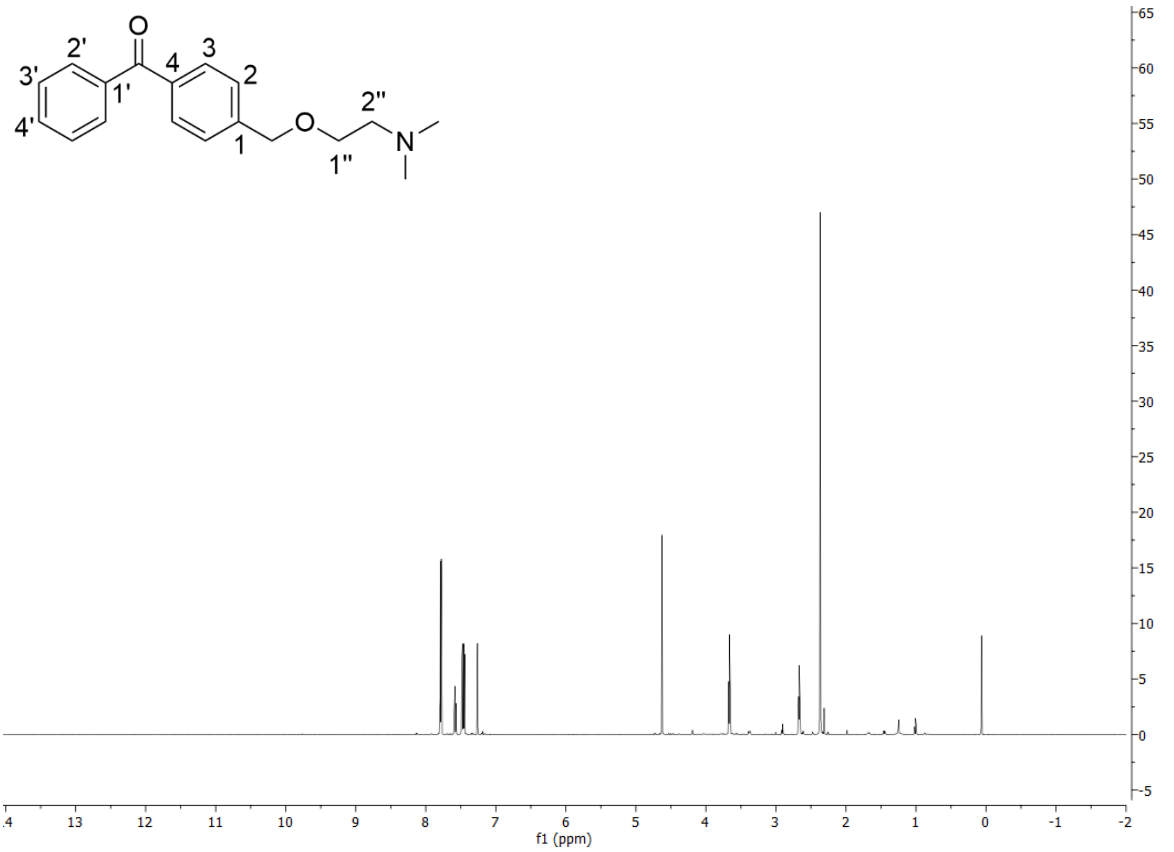

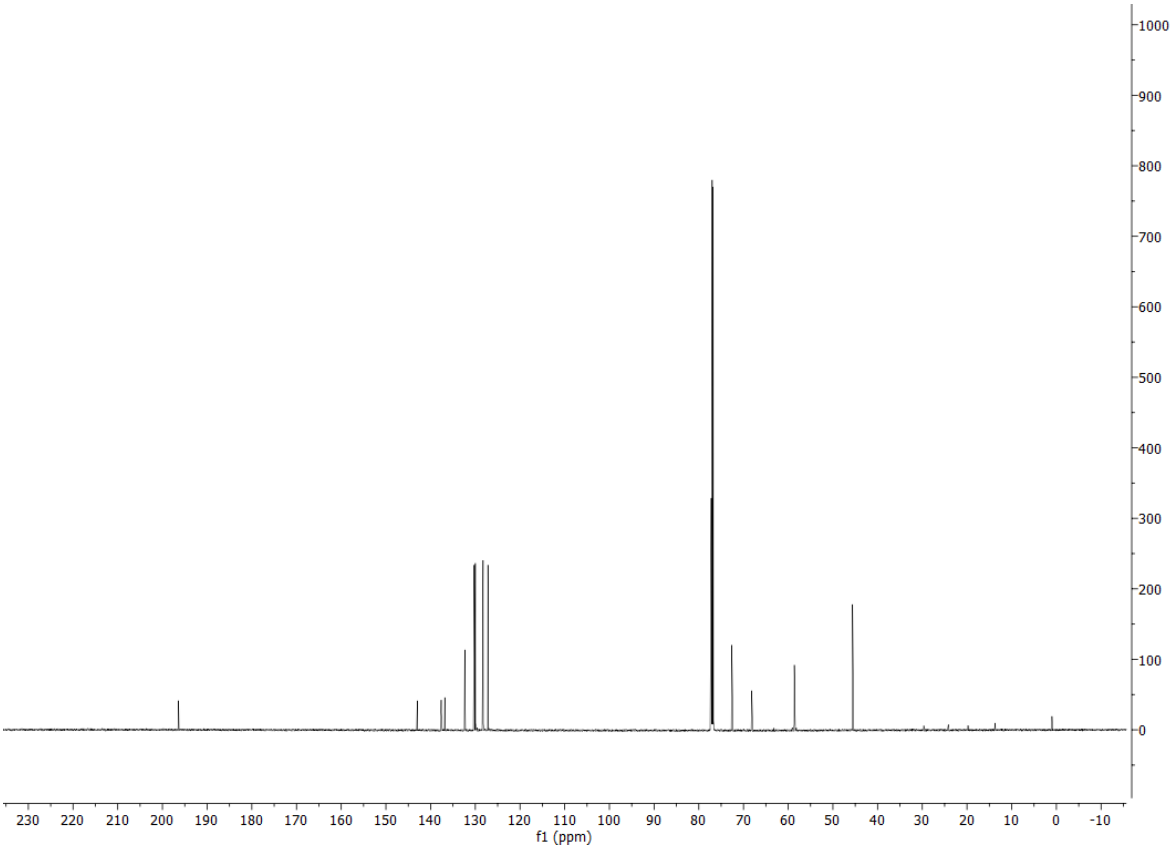

{3’’-[(4-benzoylphenyl)methoxy]propyl}dimethylamine 115

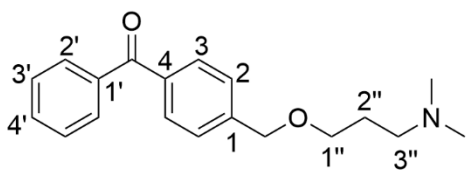

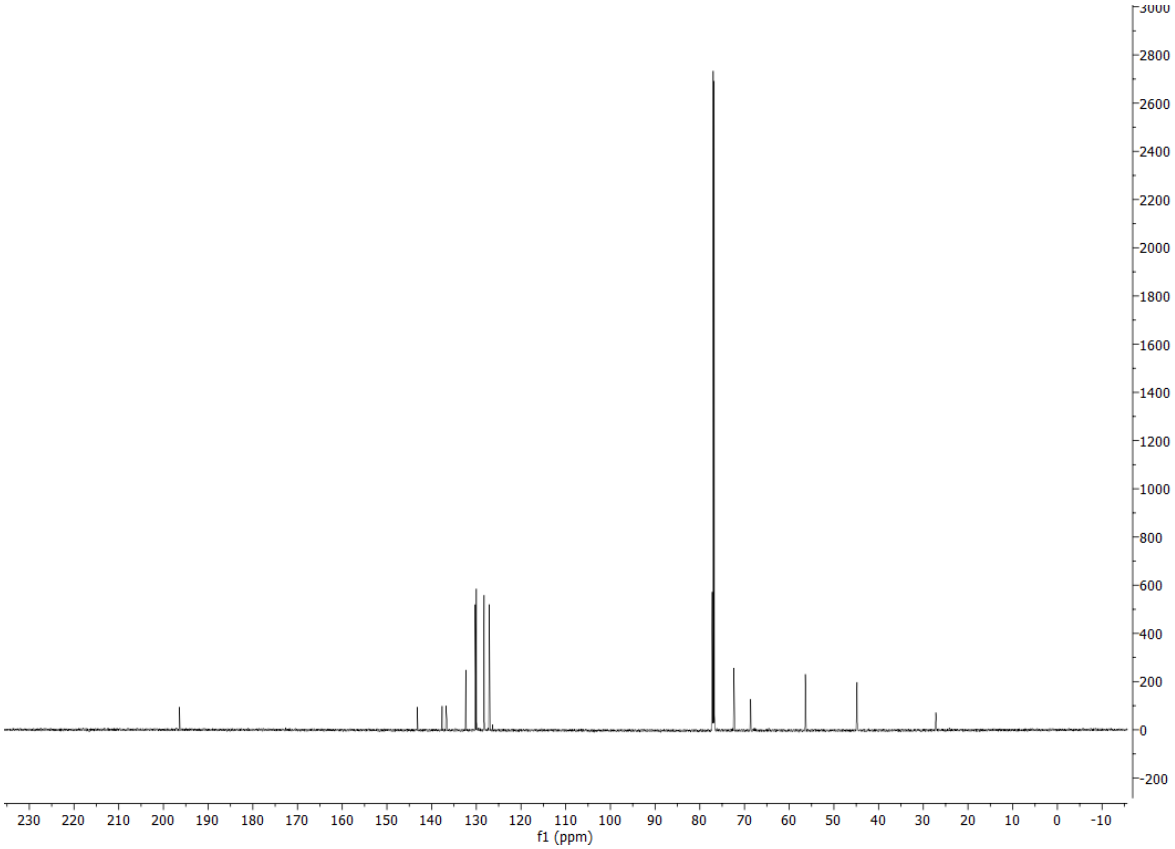

[(4-benzoylphenyl)methyl](3''-hydroxypropyl)dimethylazanium chloride 116

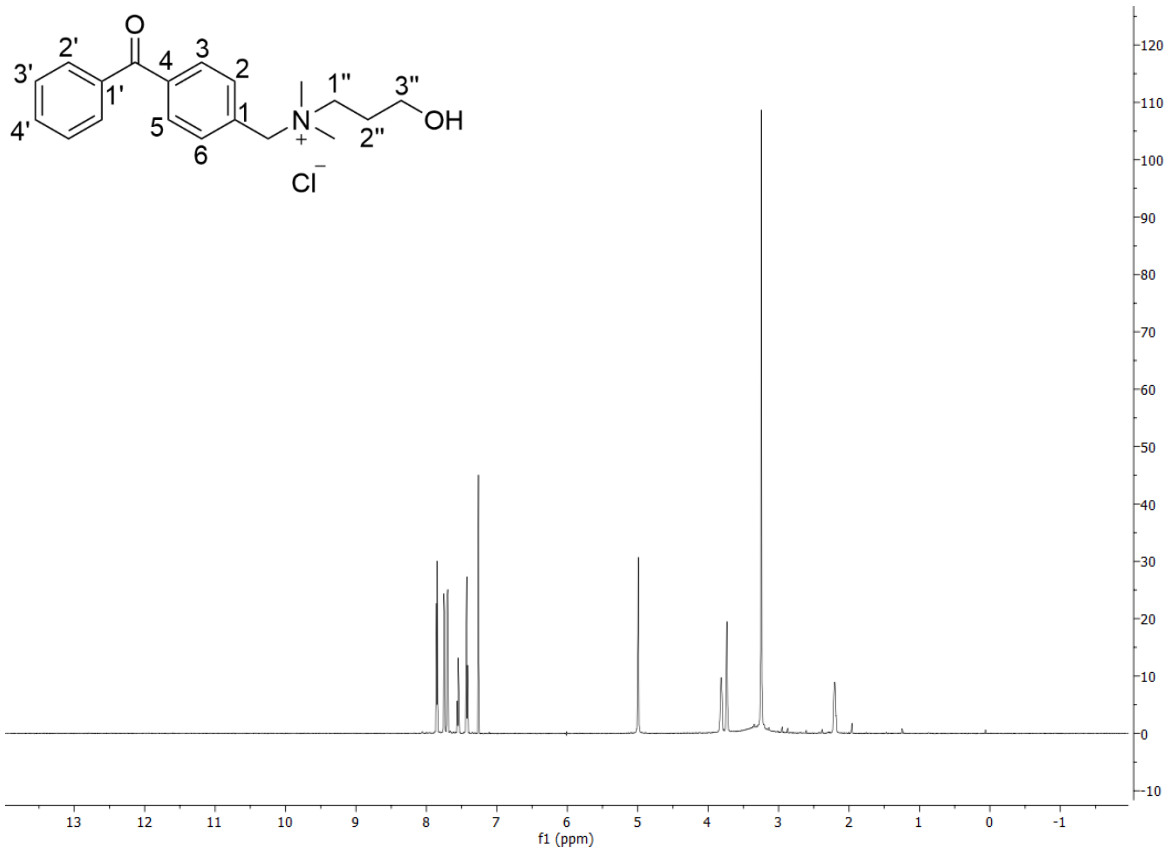

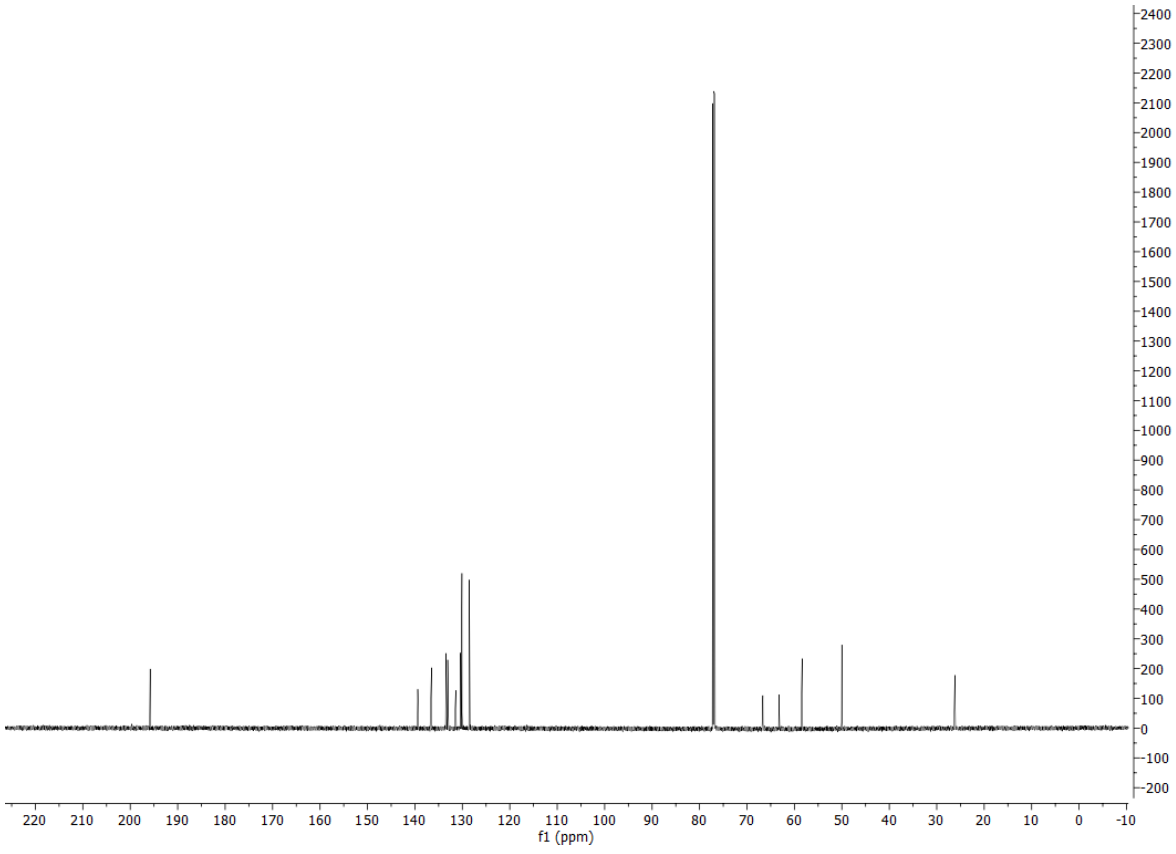

2-(2’’-bromoethoxy)phenyl](phenyl)methanone 61a

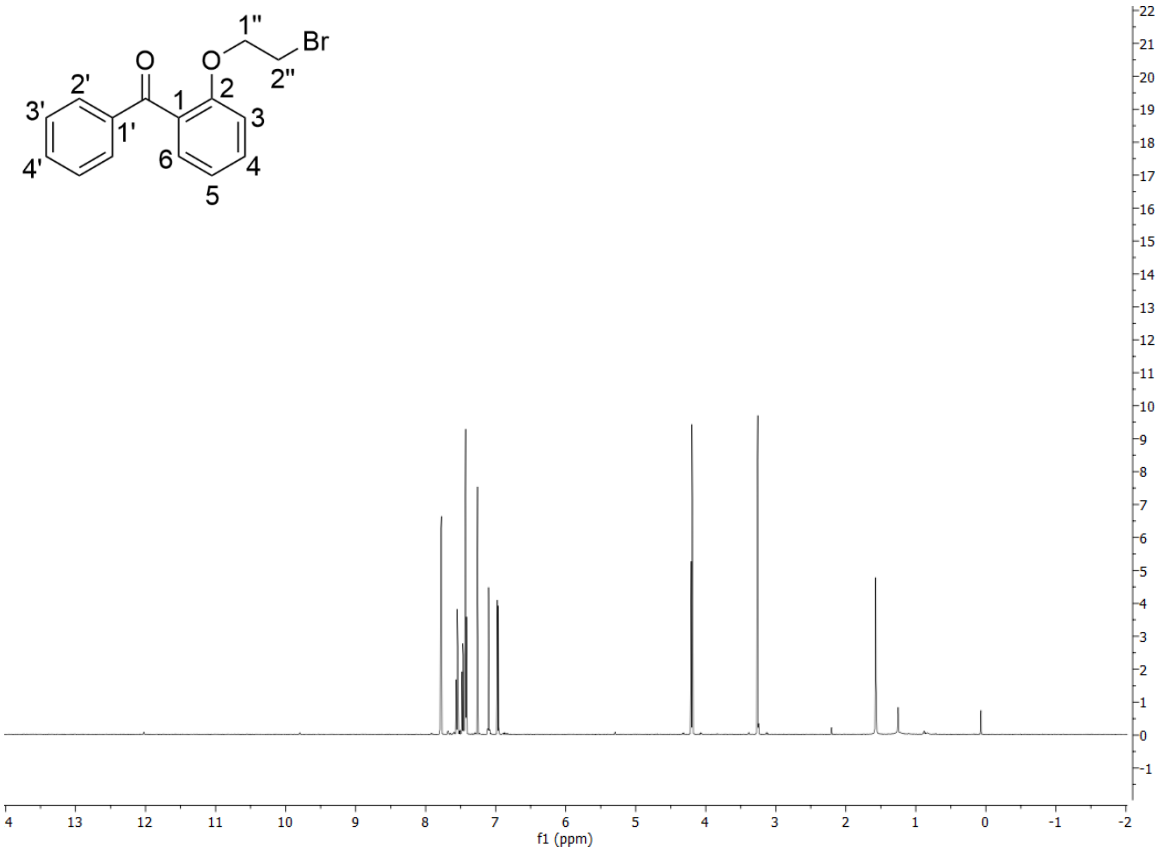

(2*R*)-*N*-[2’’-(2-benzoylphenoxy)ethyl]-2’’’-methylpyrrolidine 63

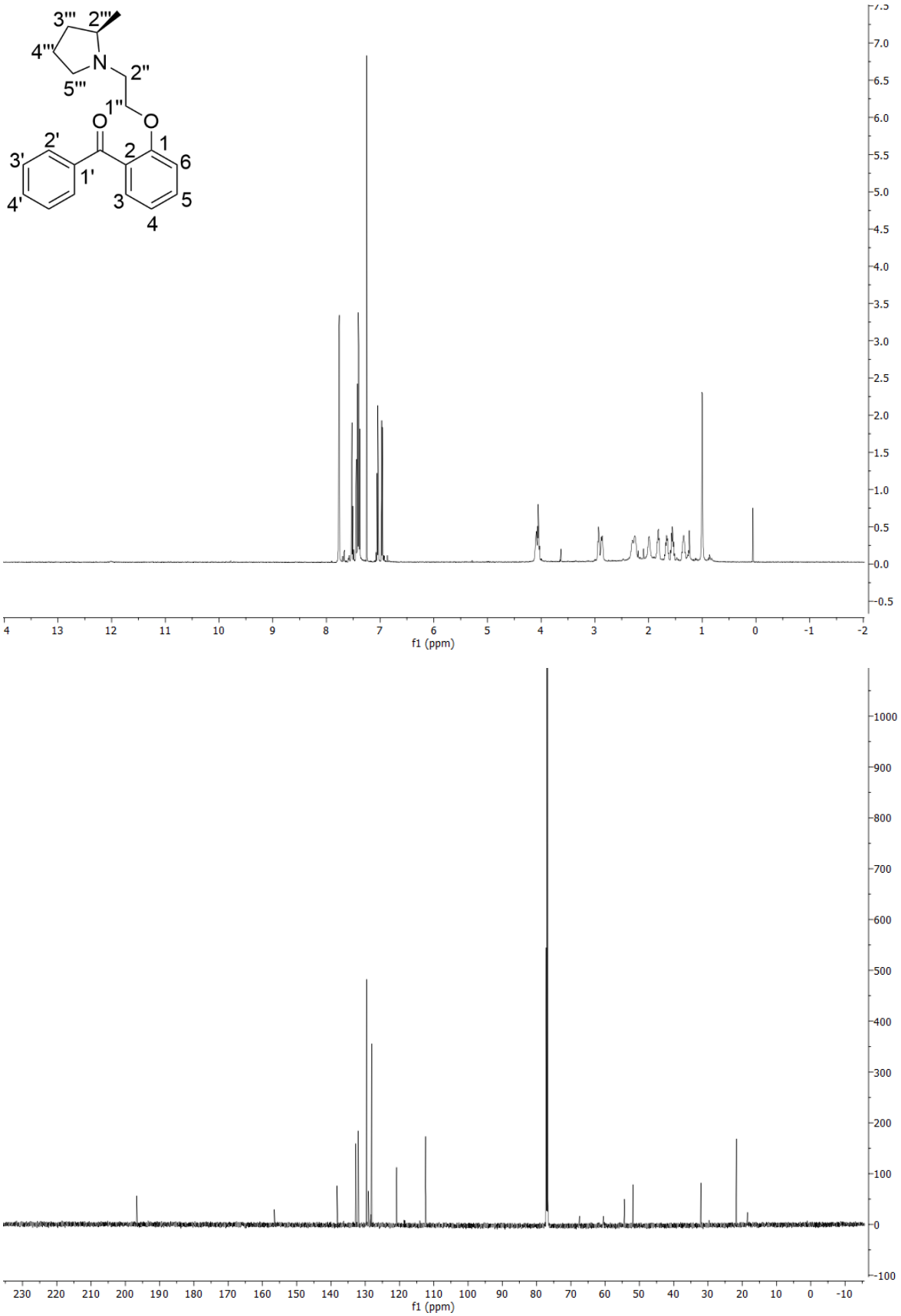

[2-(3’’-bromopropoxy)phenyl](phenyl)methanone 61b

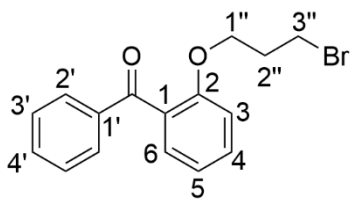

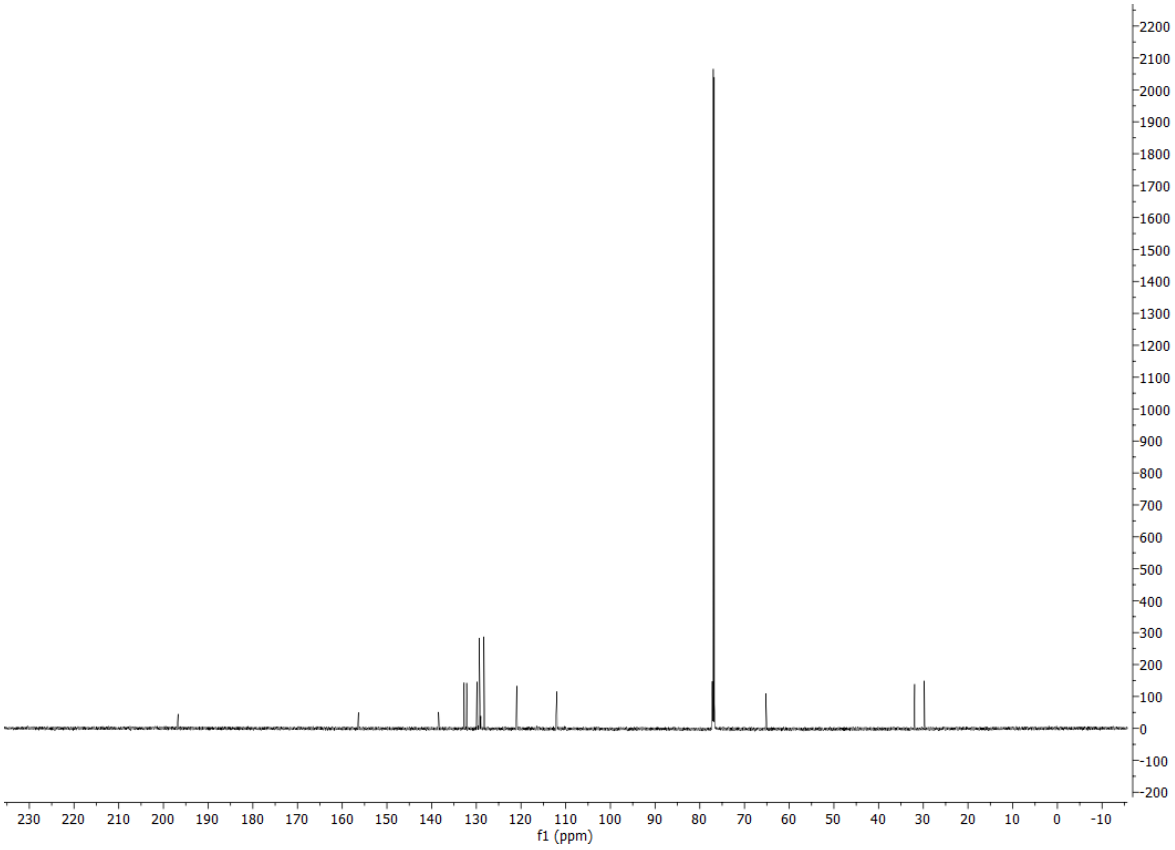

(2’’’*R*)-*N* -[3’’-(2-benzoylphenoxy)propyl]-2’’’-methylpyrrolidine 64

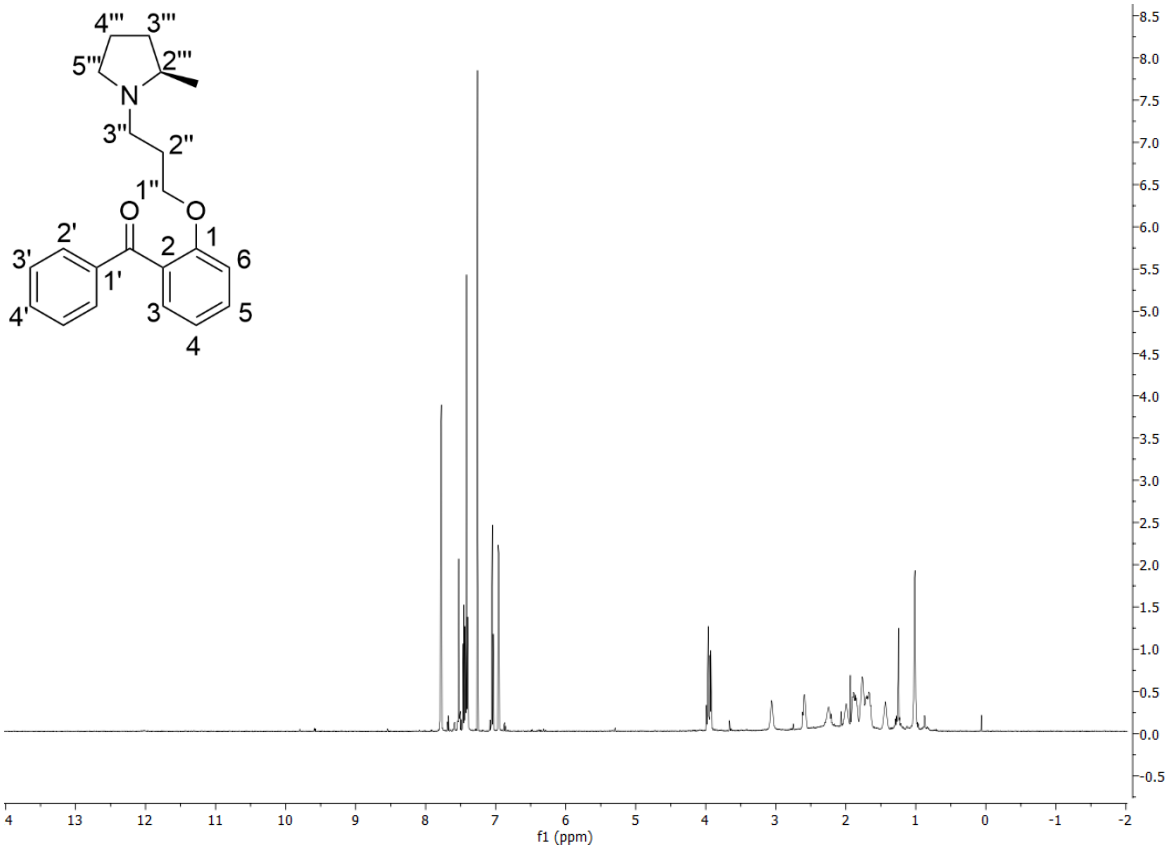

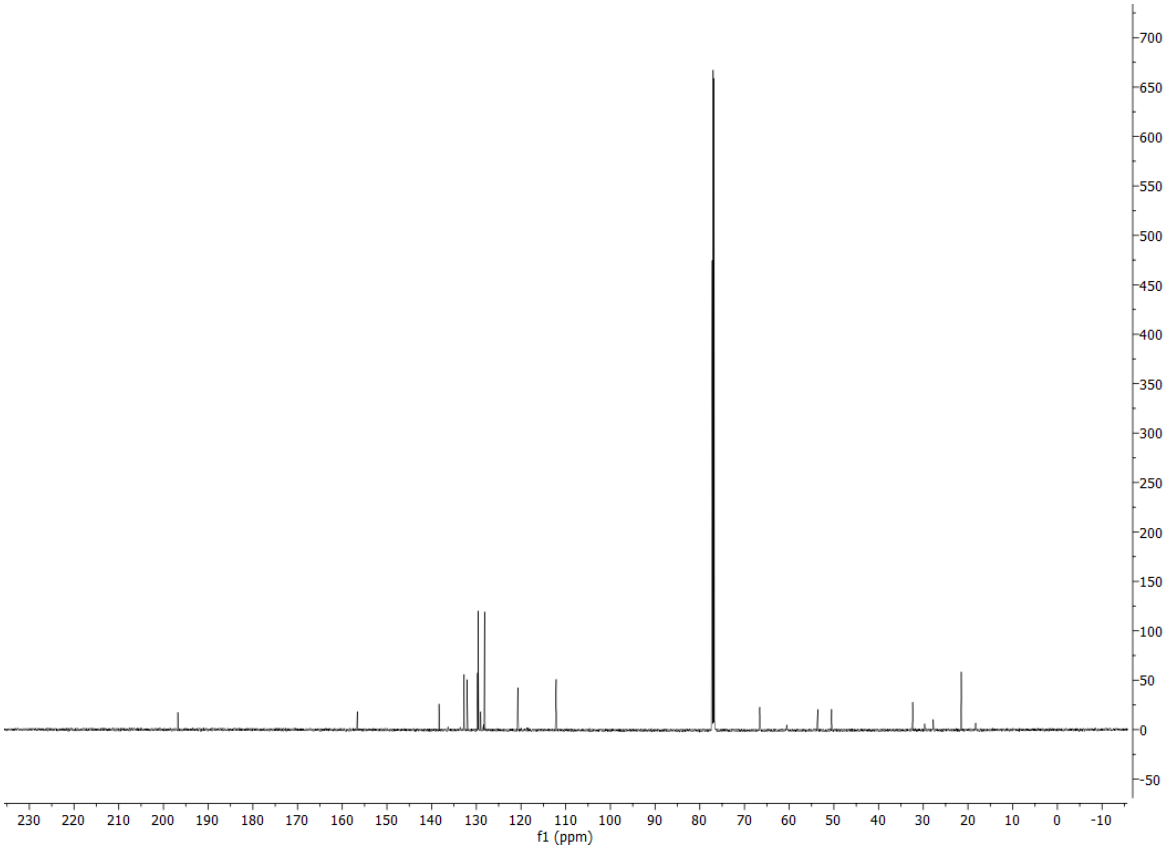

[2-(4’’-bromobutoxy)phenyl](phenyl)methanone 61c

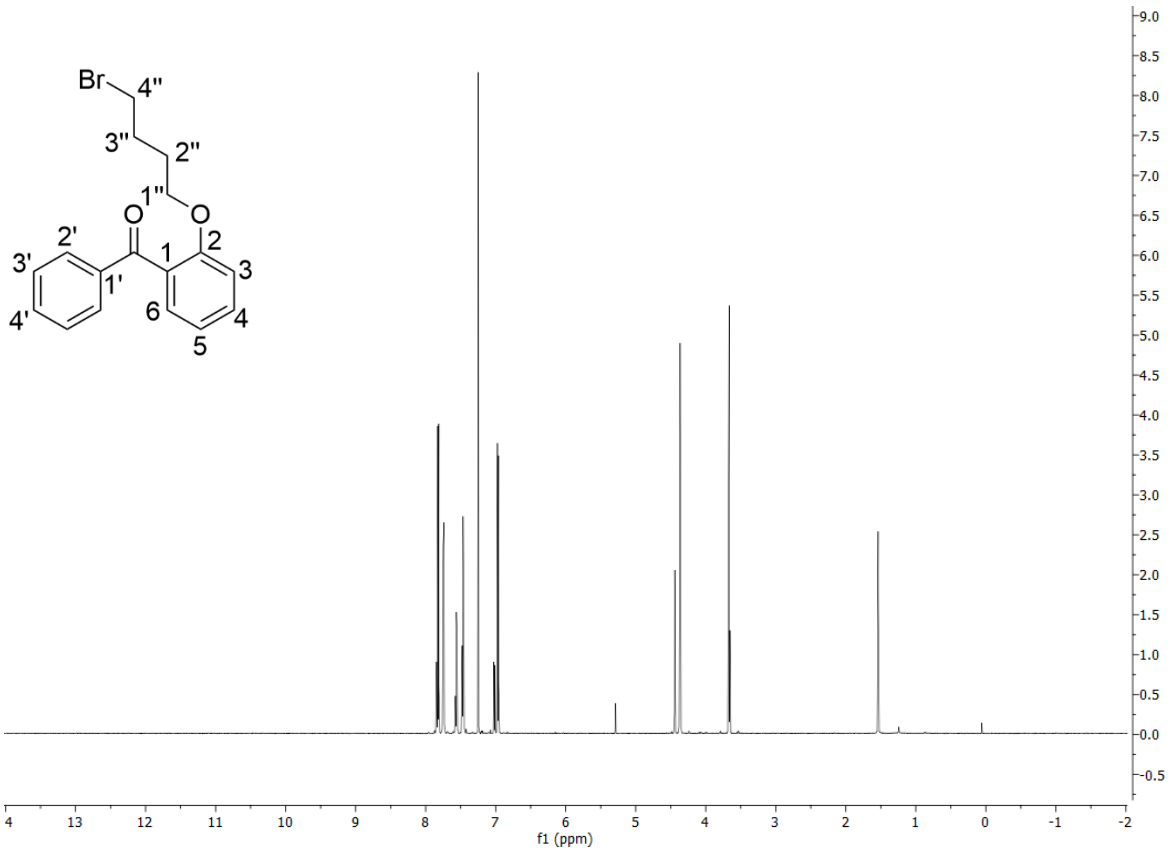

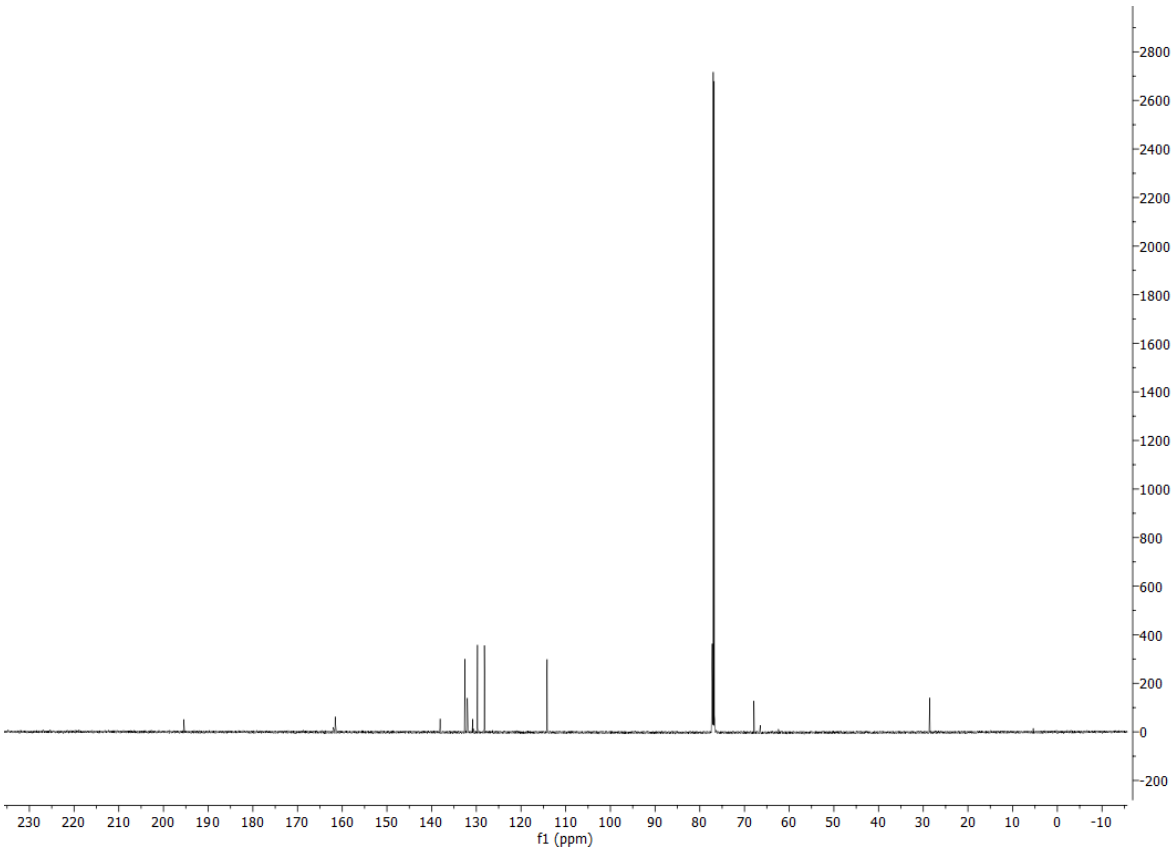

(2’’’*R*)- *N* -[4’’-(2-benzoylphenoxy)butyl]-2’’’-methylpyrrolidine 65

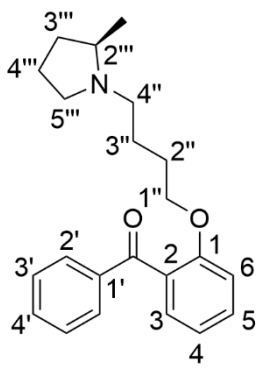

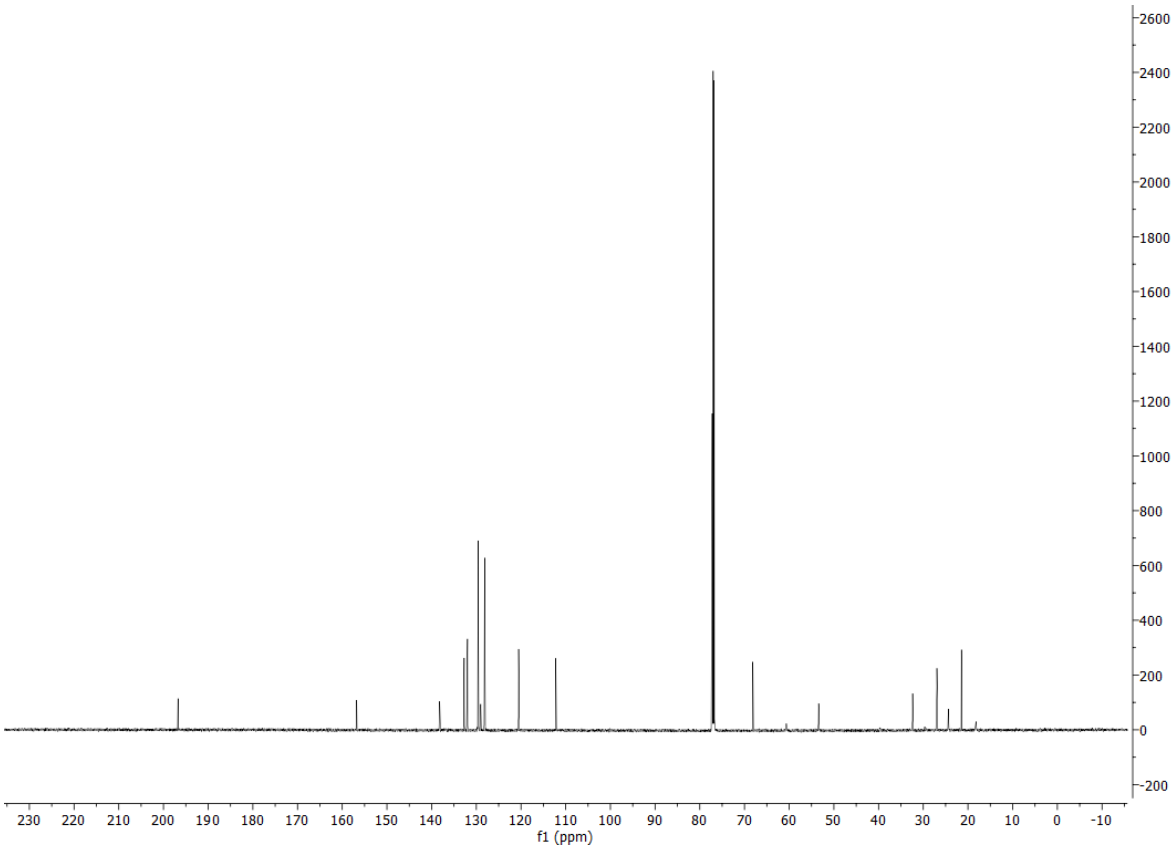

[2-(2’’-bromopropoxy)-5-chlorophenyl](phenyl)methanone 61d

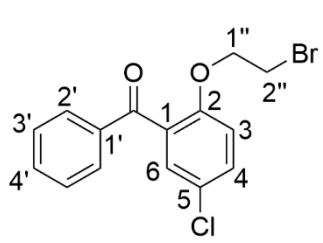

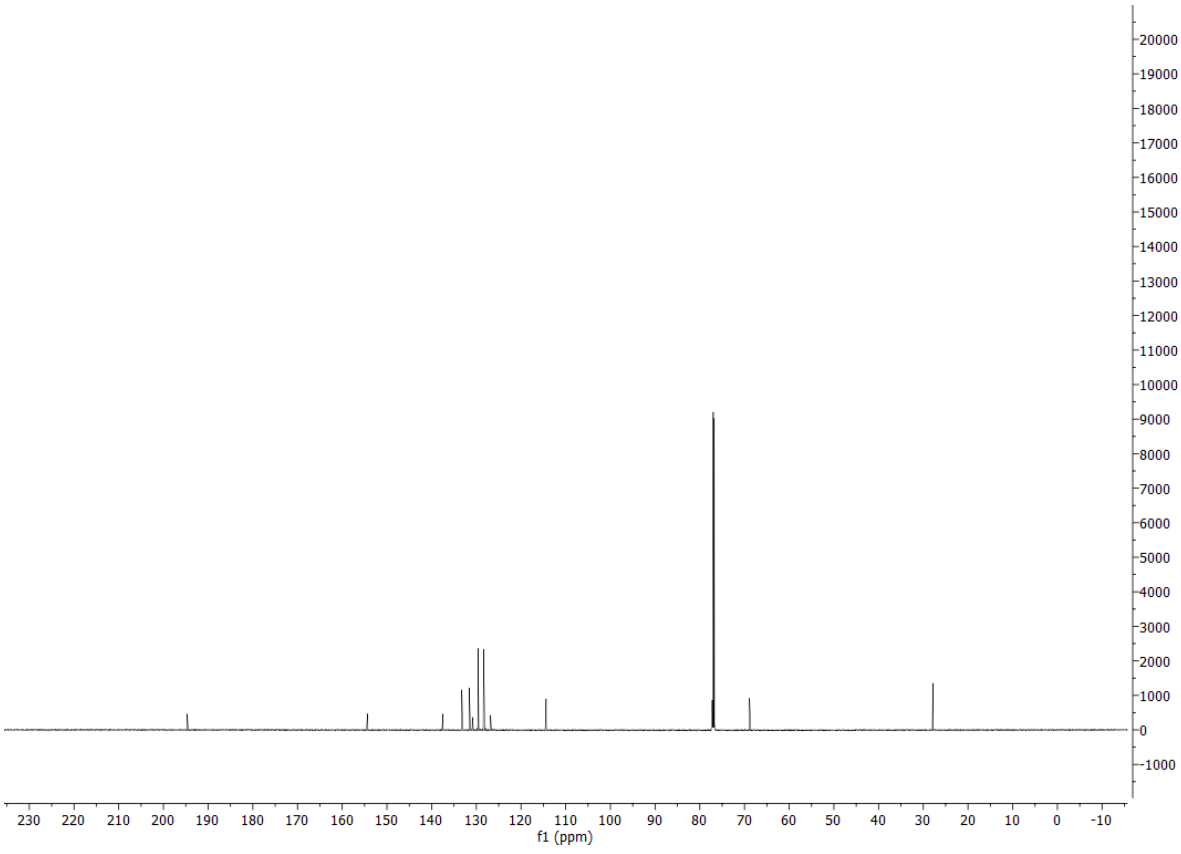

(2’’’*R*)-*N* -[2-(2’’-benzoyl-4-chlorophenoxy)ethyl]-2’’’-methylpyrrolidine 66

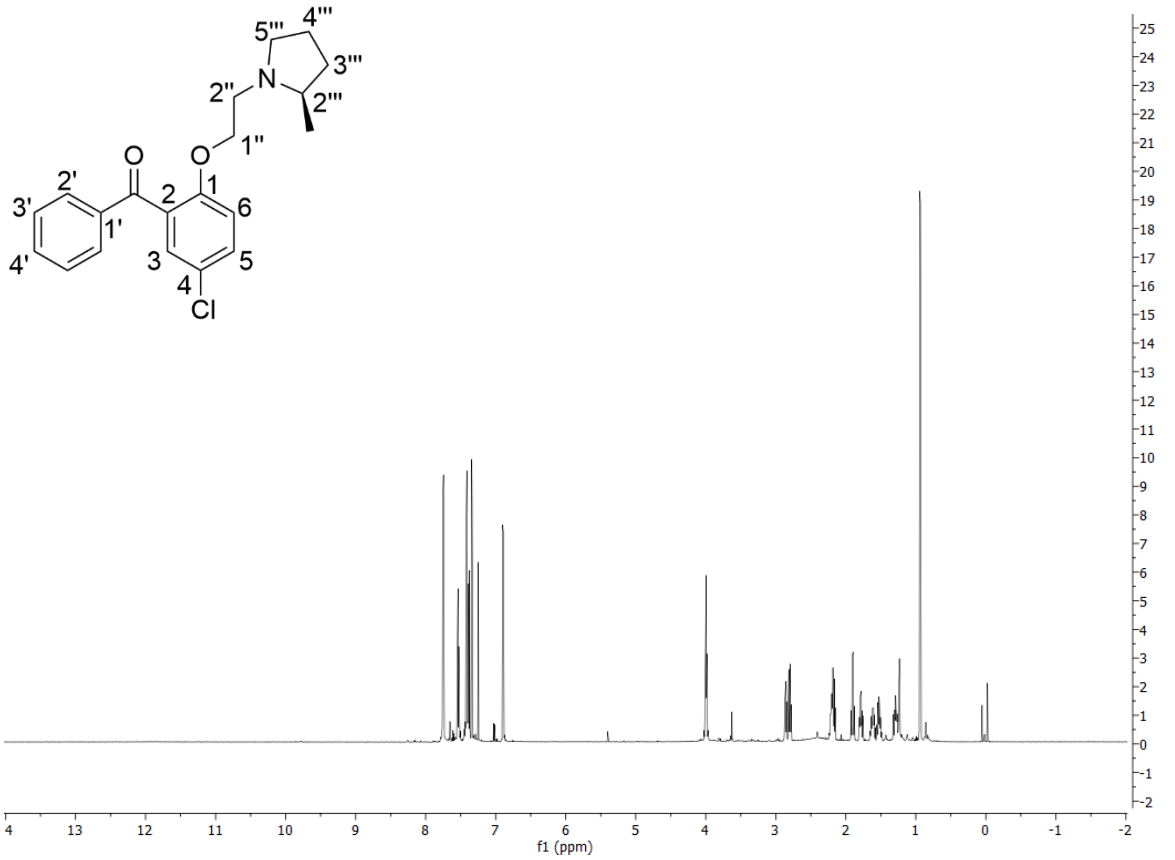

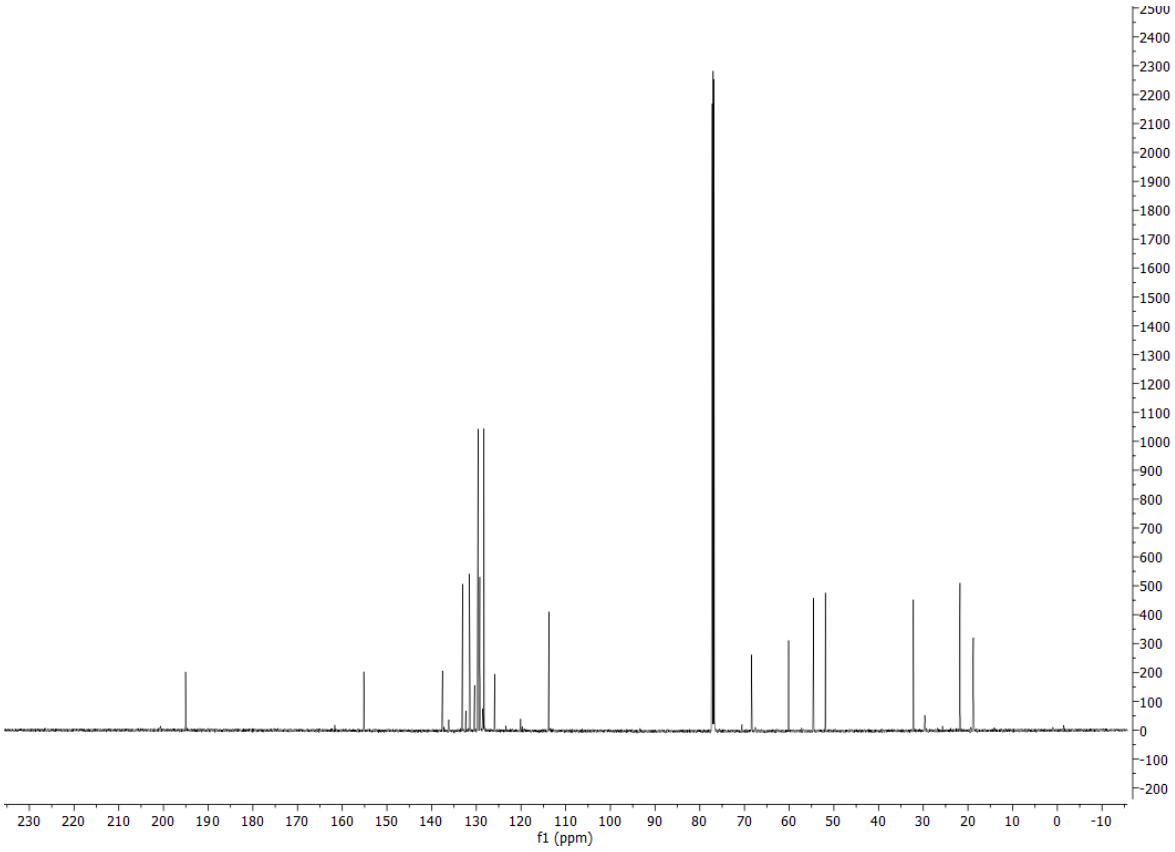

[2-(3’’-bromopropoxy)-5-chlorophenyl](phenyl)methanone 61e

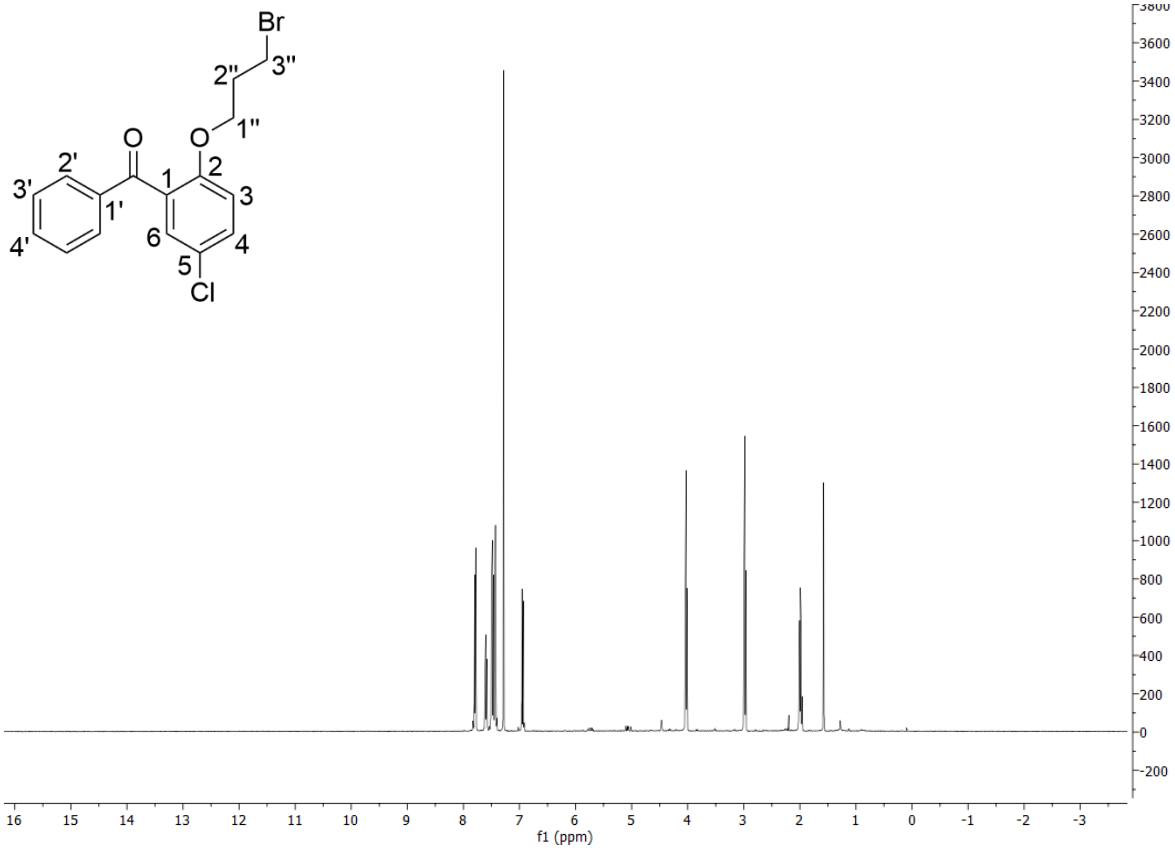

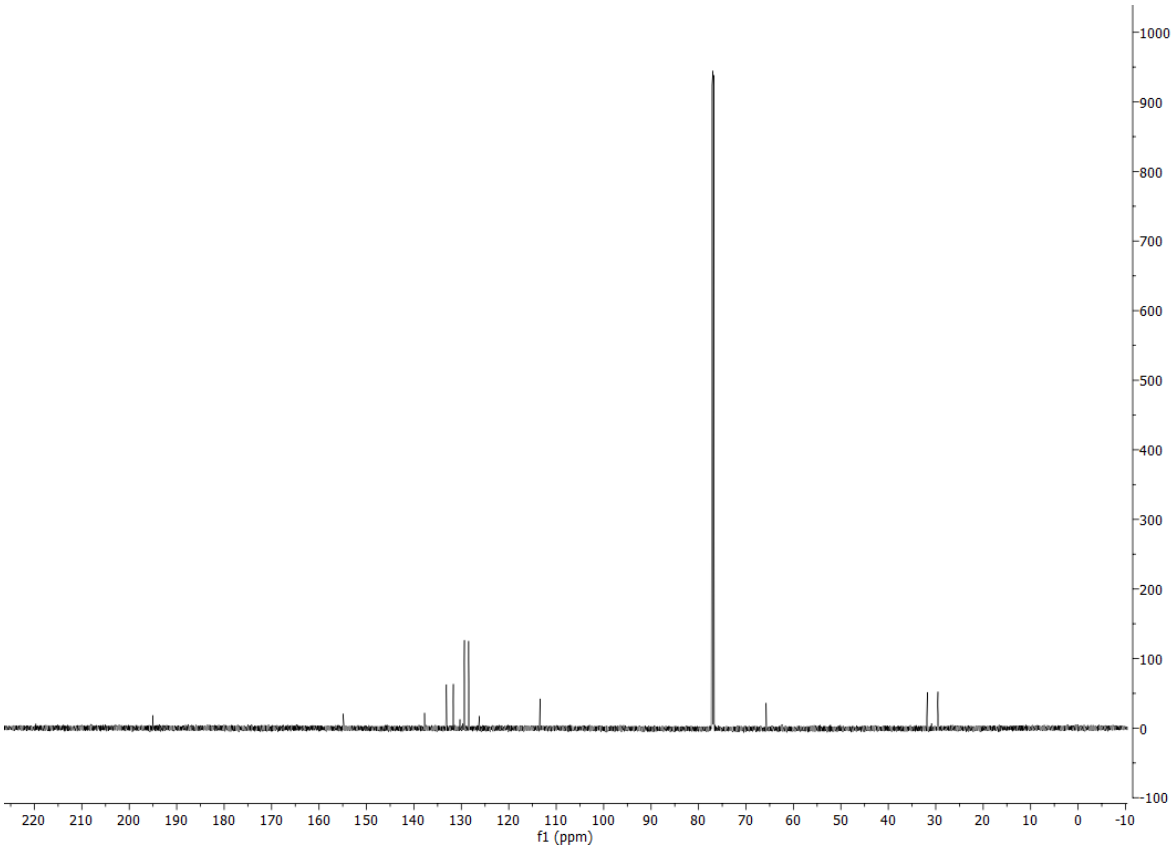

(2*R*)-*N*-[3''-(2-benzoyl-4-chlorophenoxy)propyl]-2'''-methylpyrrolidine 67

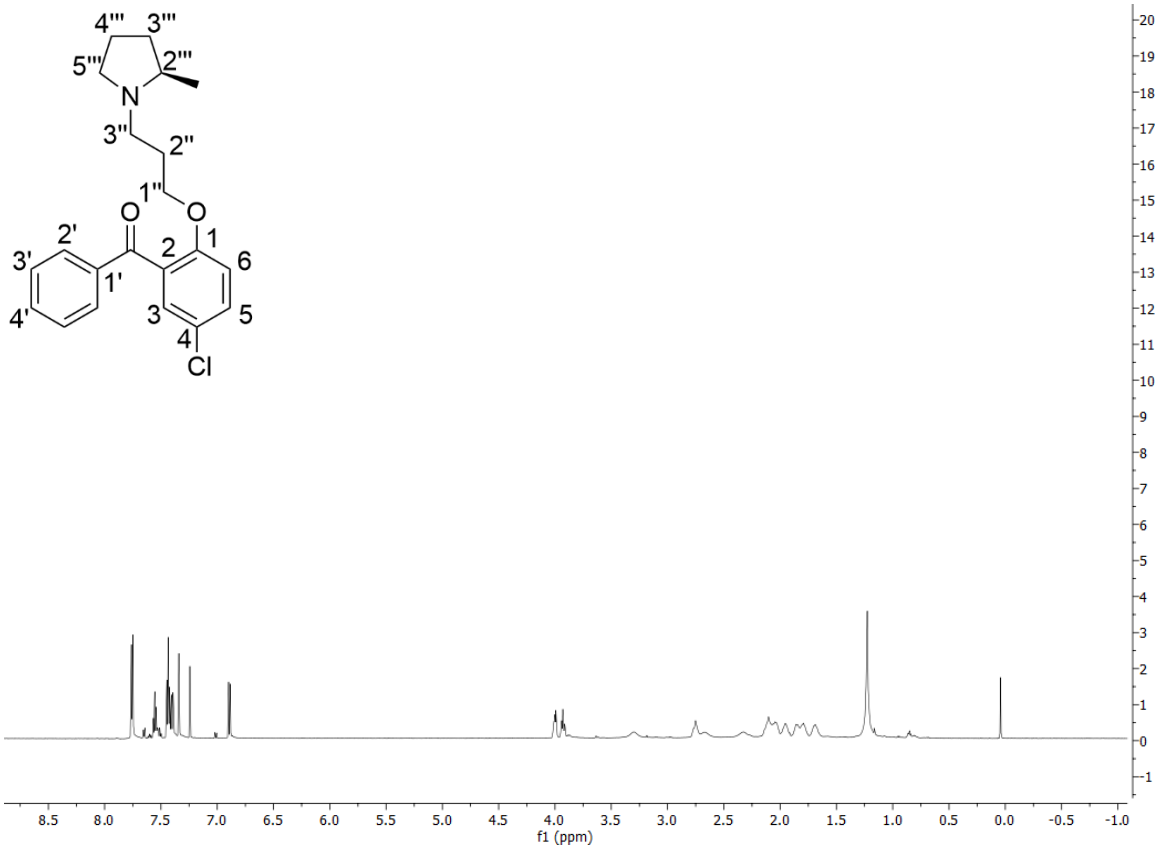

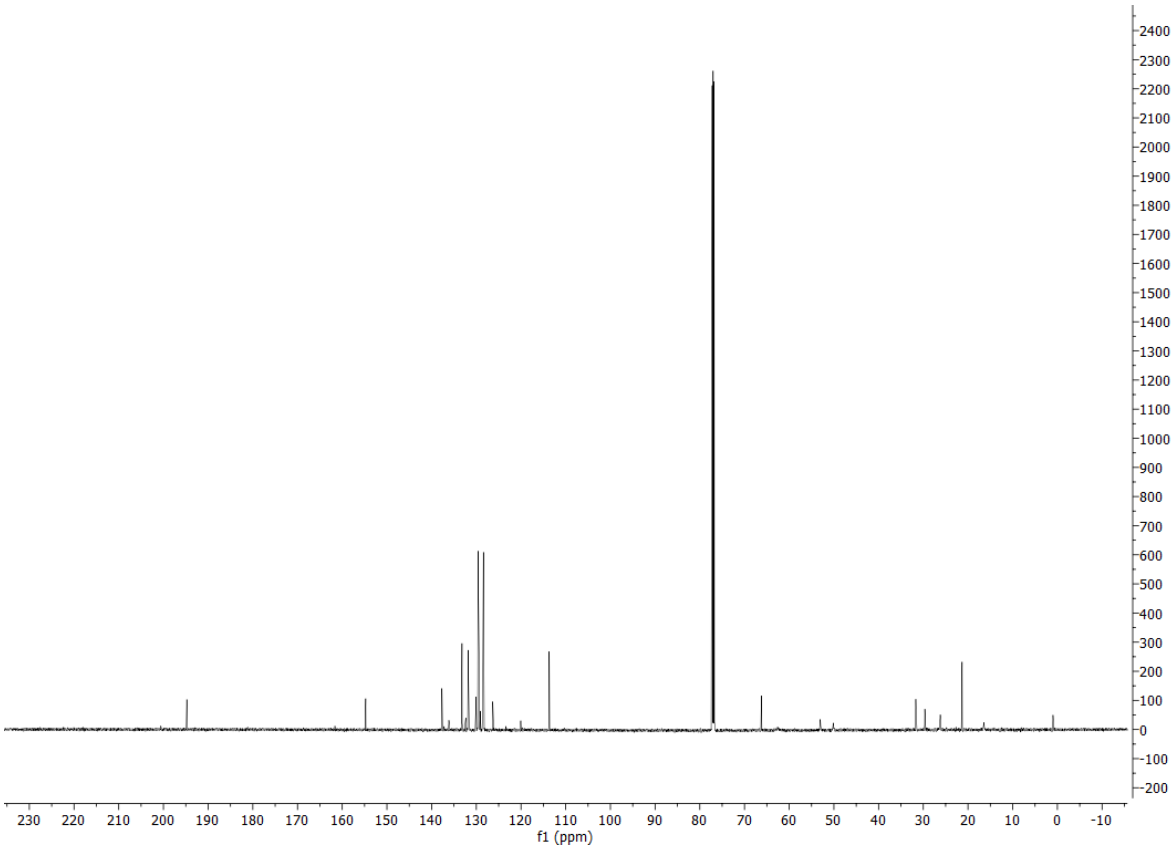

[2-(4’’-bromobutoxy)-5-chlorophenyl](phenyl)methanone 61f

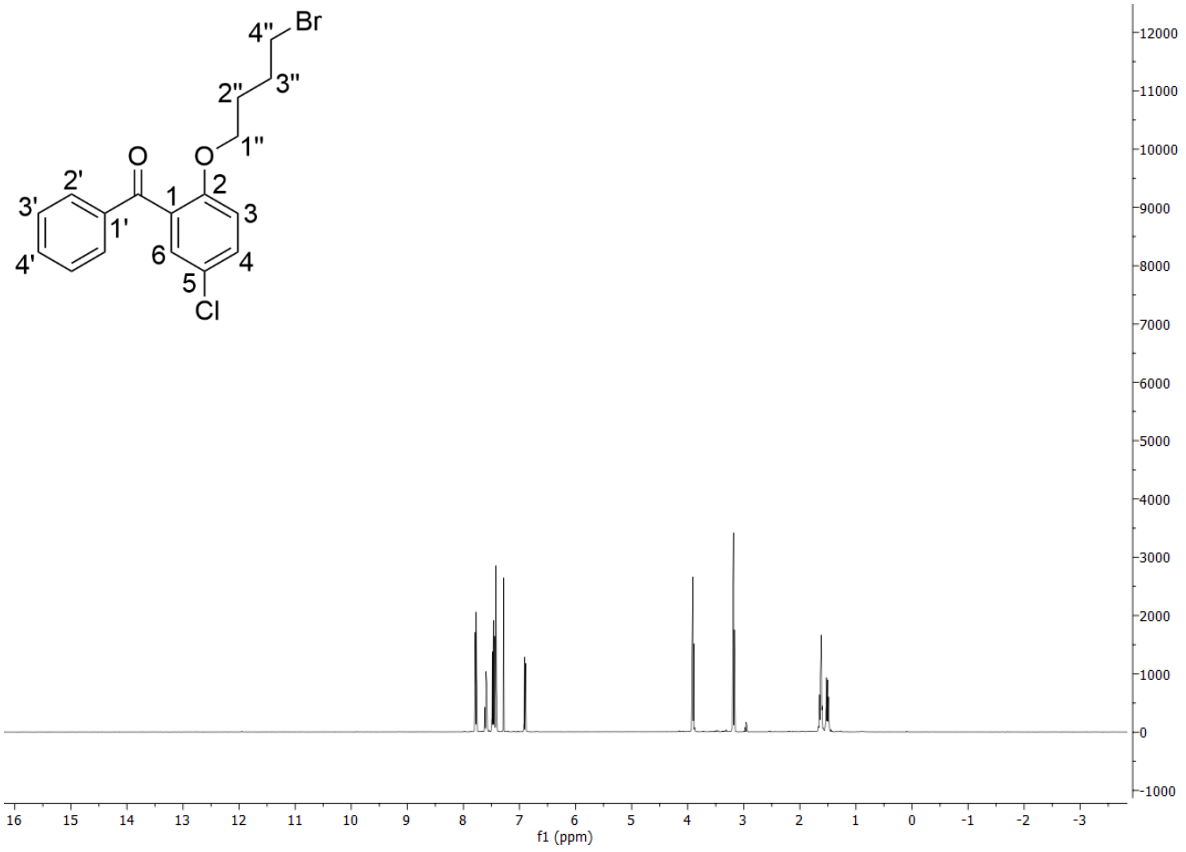

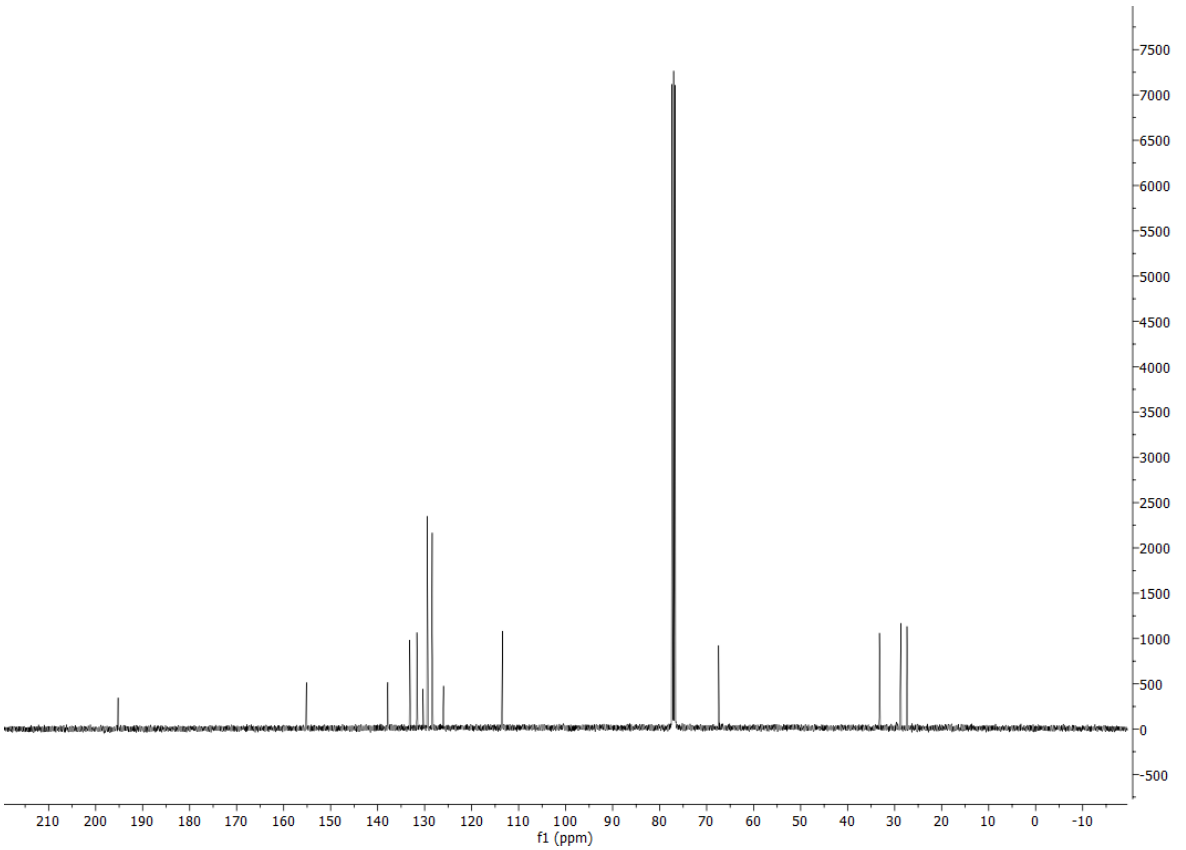

(2’’’*R*)-*N*-[4’’-(2-benzoyl-4-chlorophenoxy)butyl]-2’’’-methylpyrrolidine 68

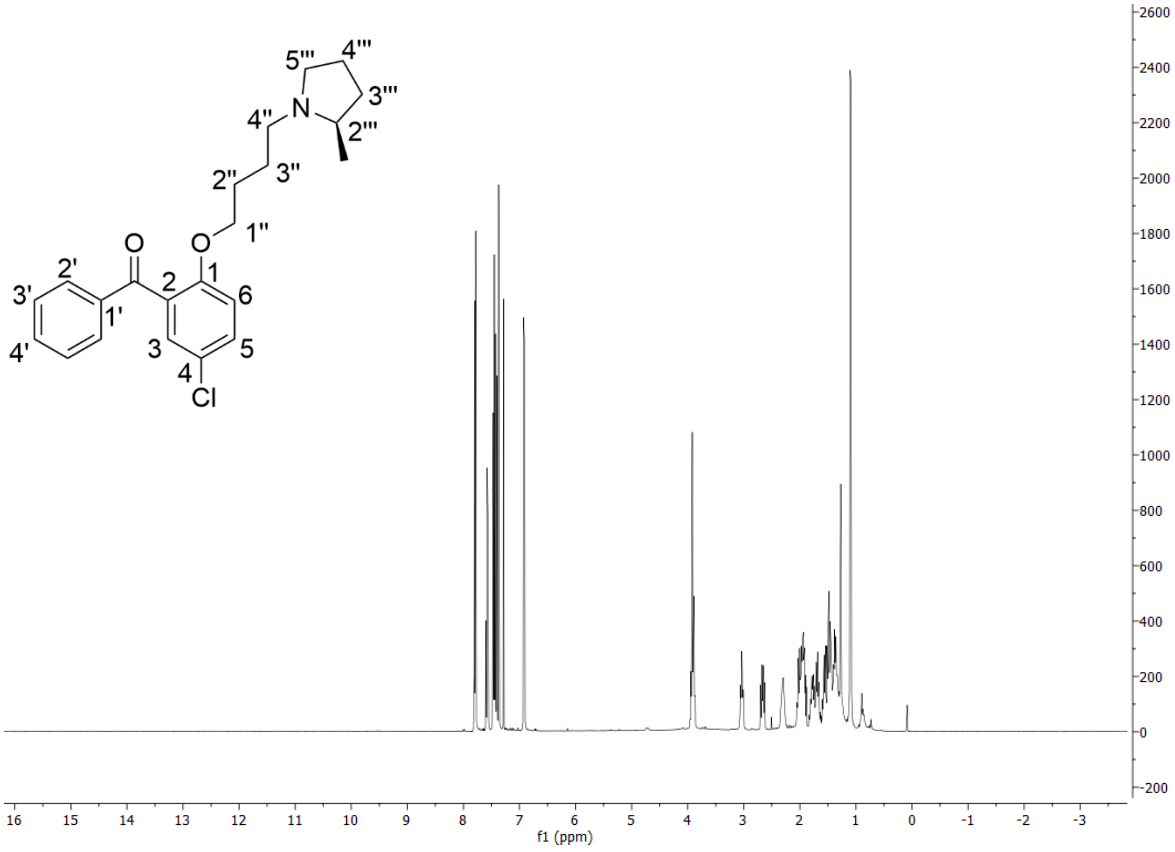

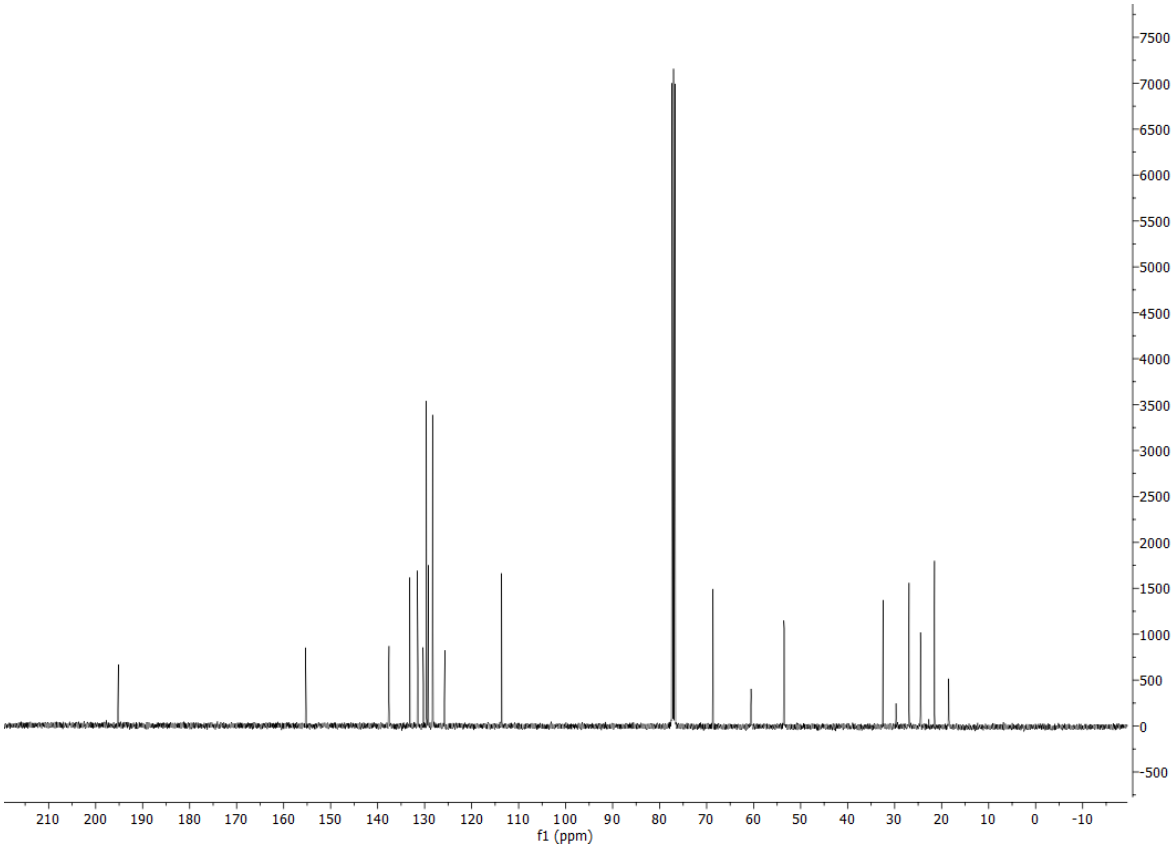

[3-(2’’-bromoethoxy)phenyl](phenyl)methanone 94a

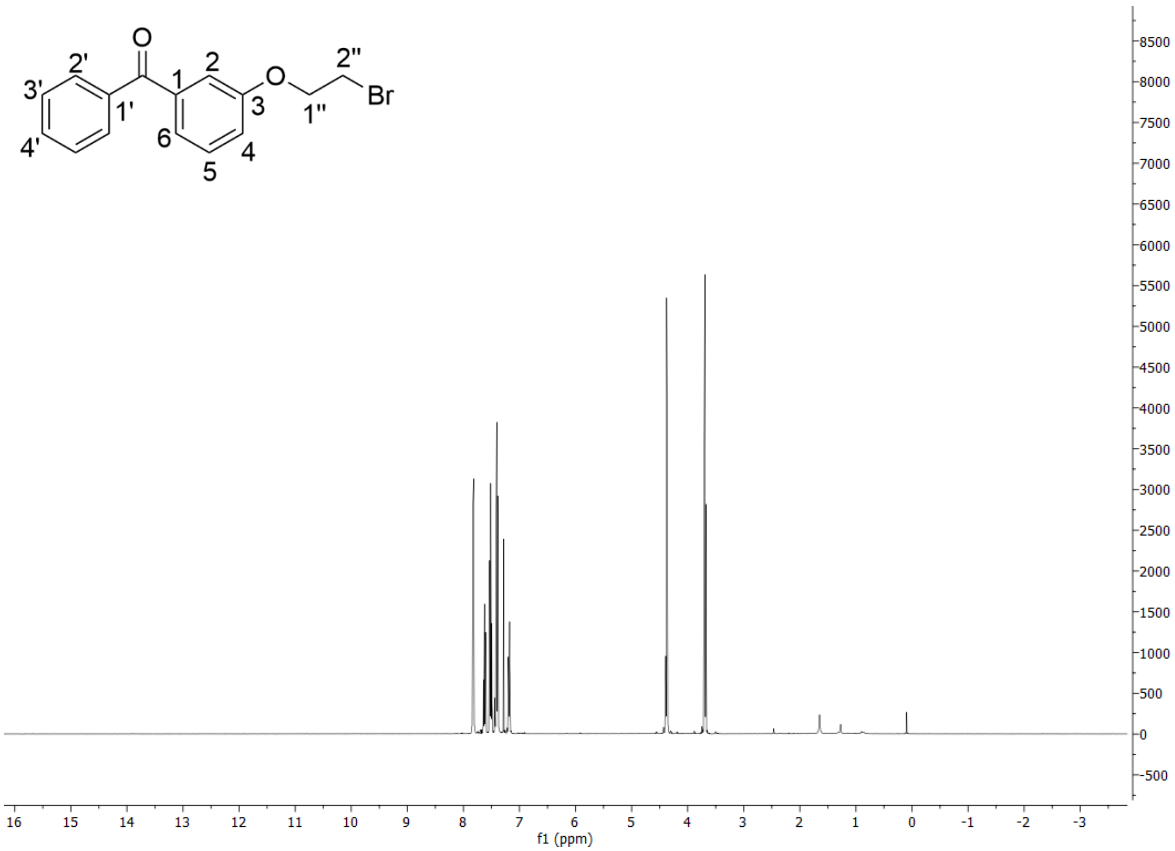

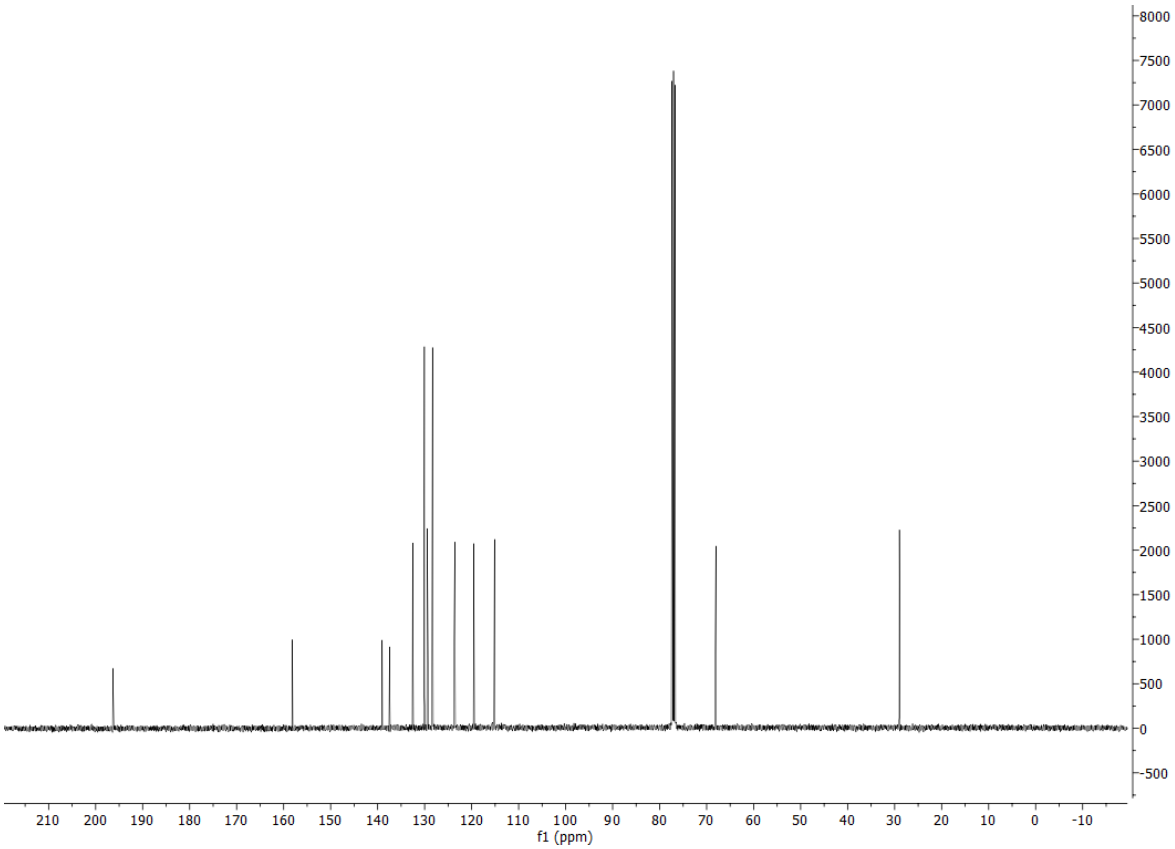

(2’’’*R*)- *N* -[2’’-(3-benzoylphenoxy)ethyl]-2’’’-methylpyrrolidine 95

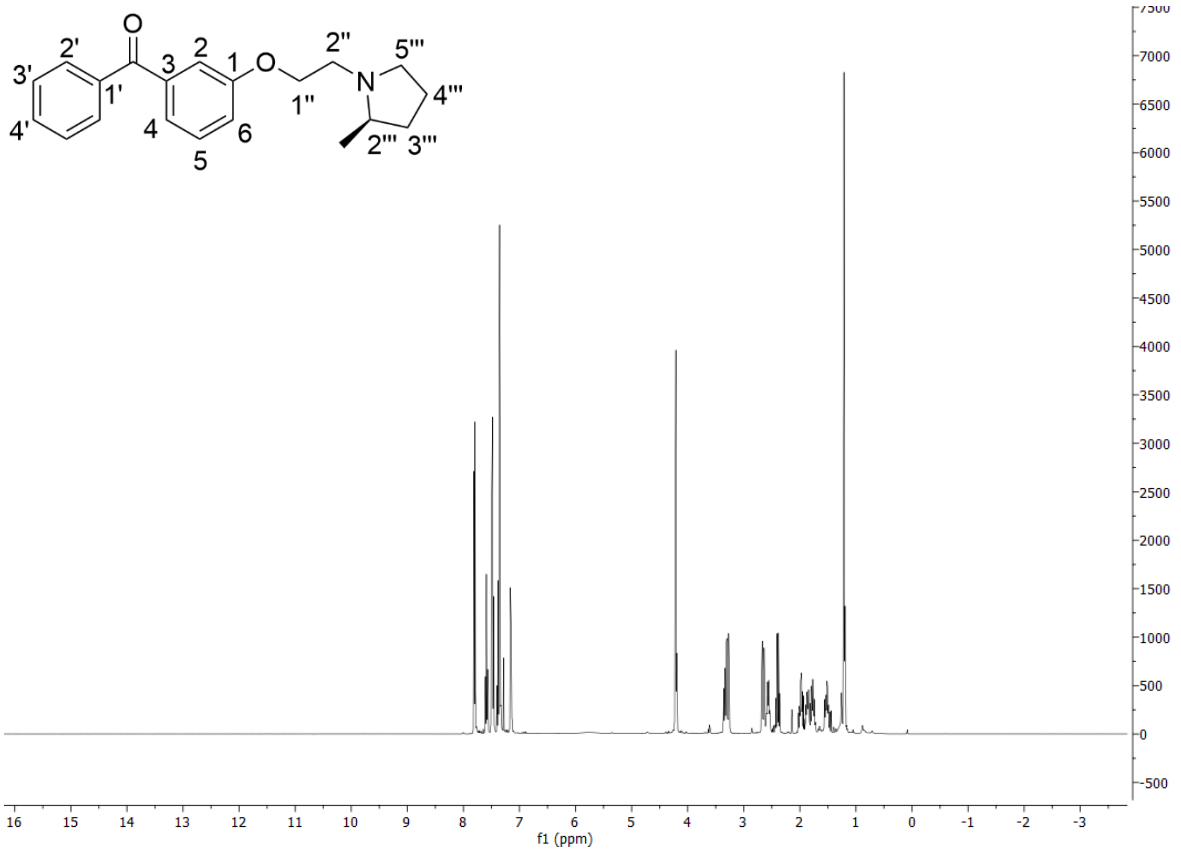

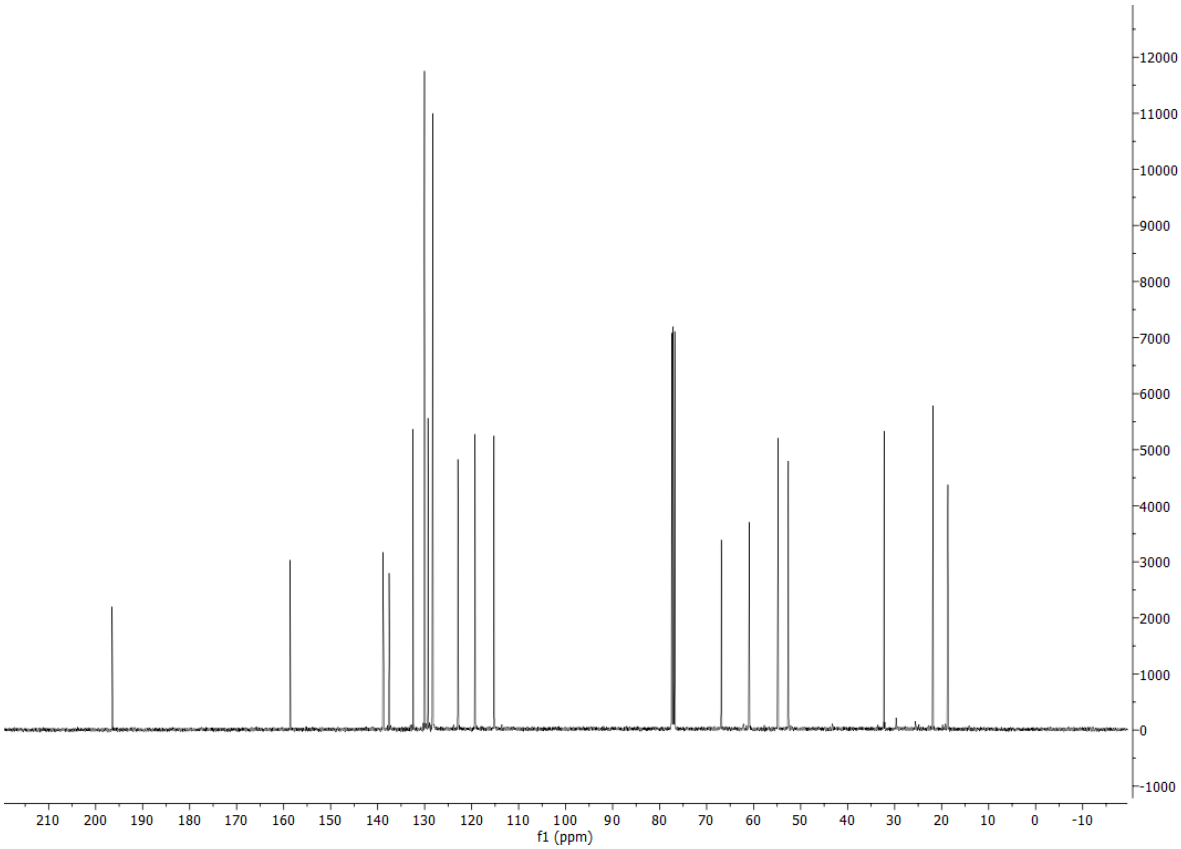

(2’’’*R*)-*N* -[3’’-(3-benzoylphenoxy)propyl]-2’’’-methylpyrrolidine 96

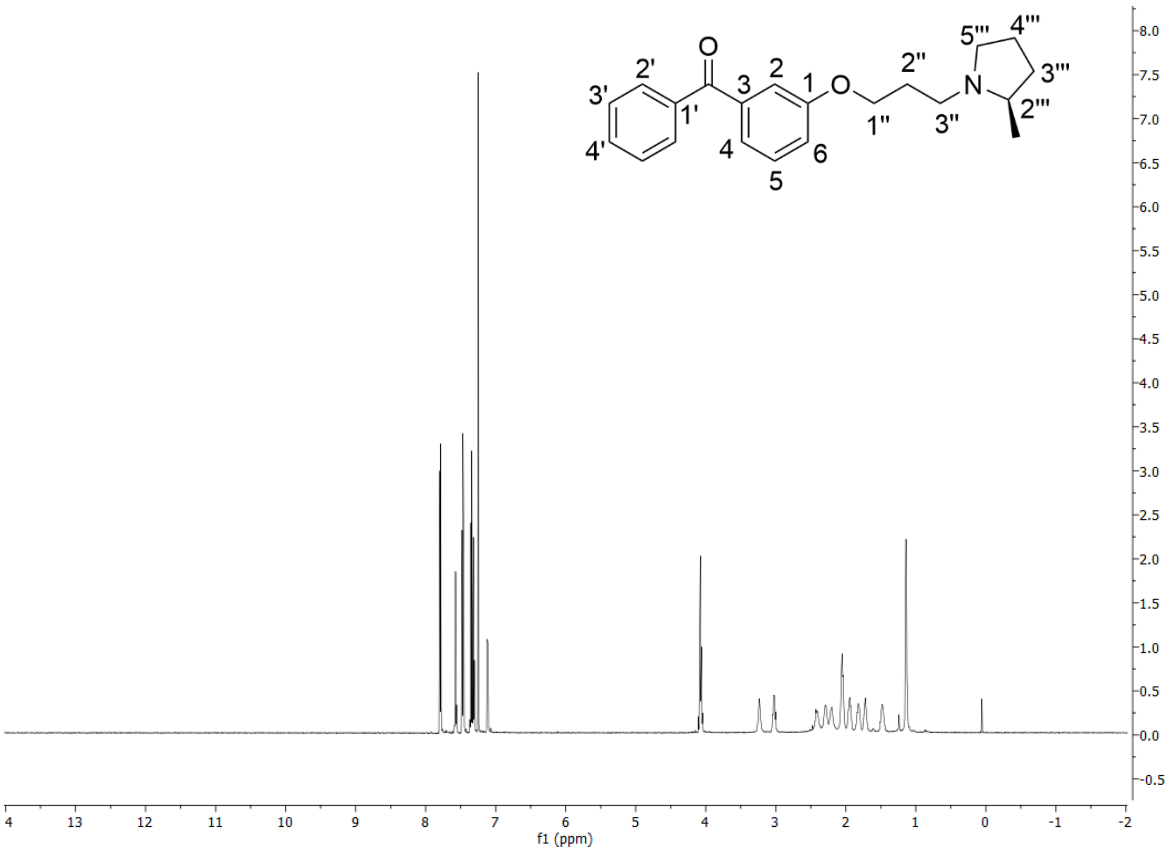

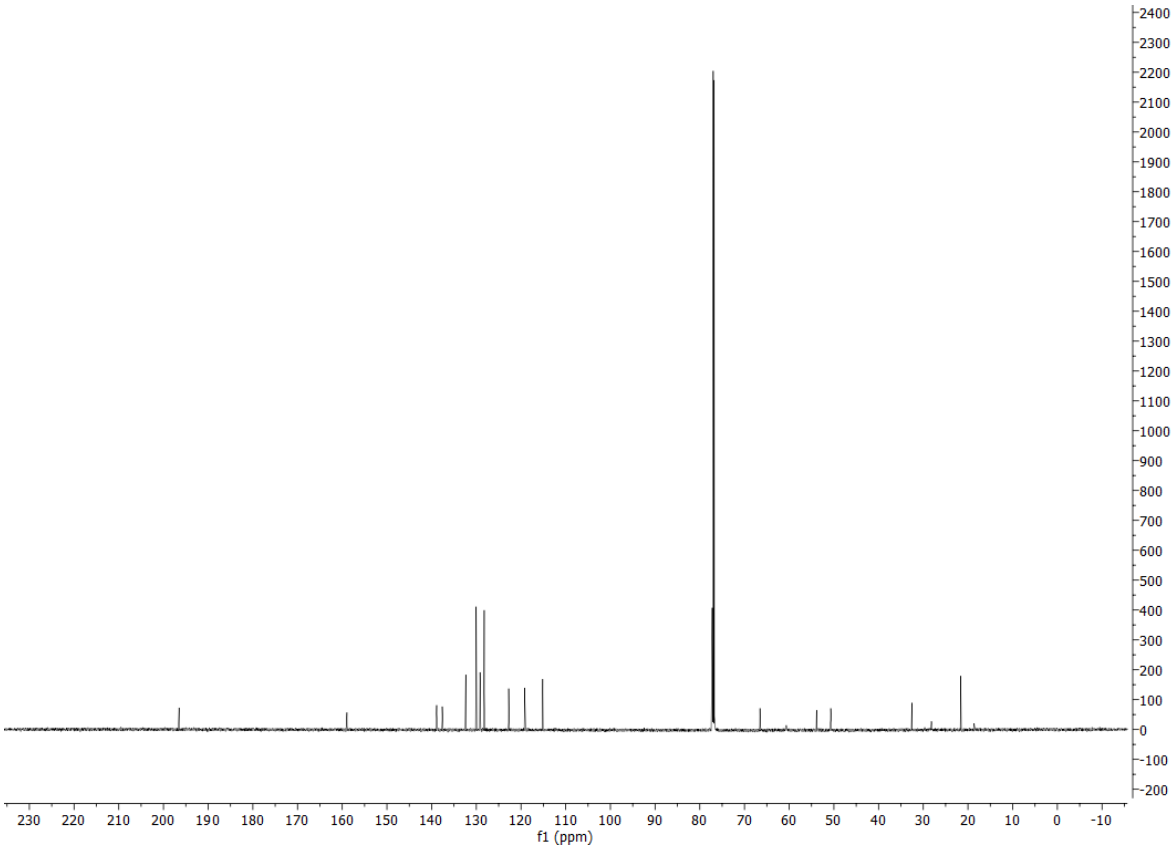

[3-(4’’-bromobutoxy)phenyl](phenyl)methanone 94c

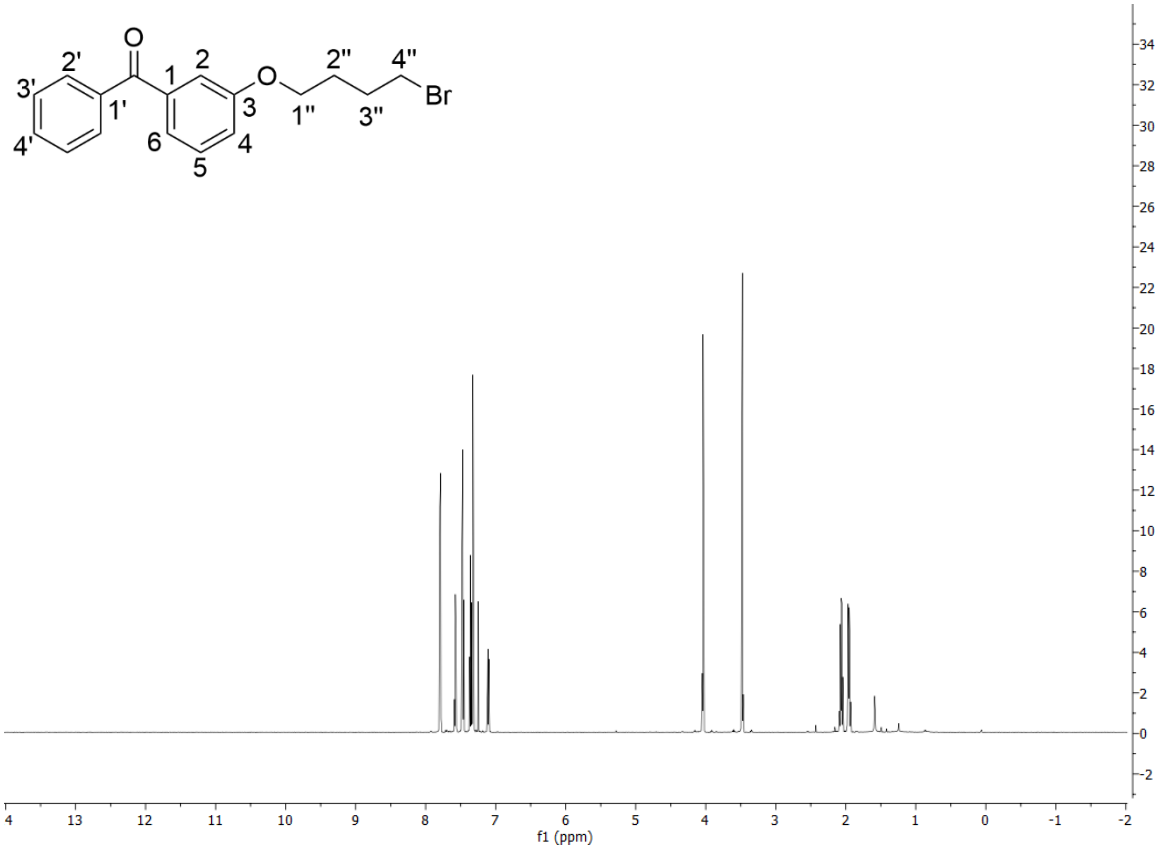

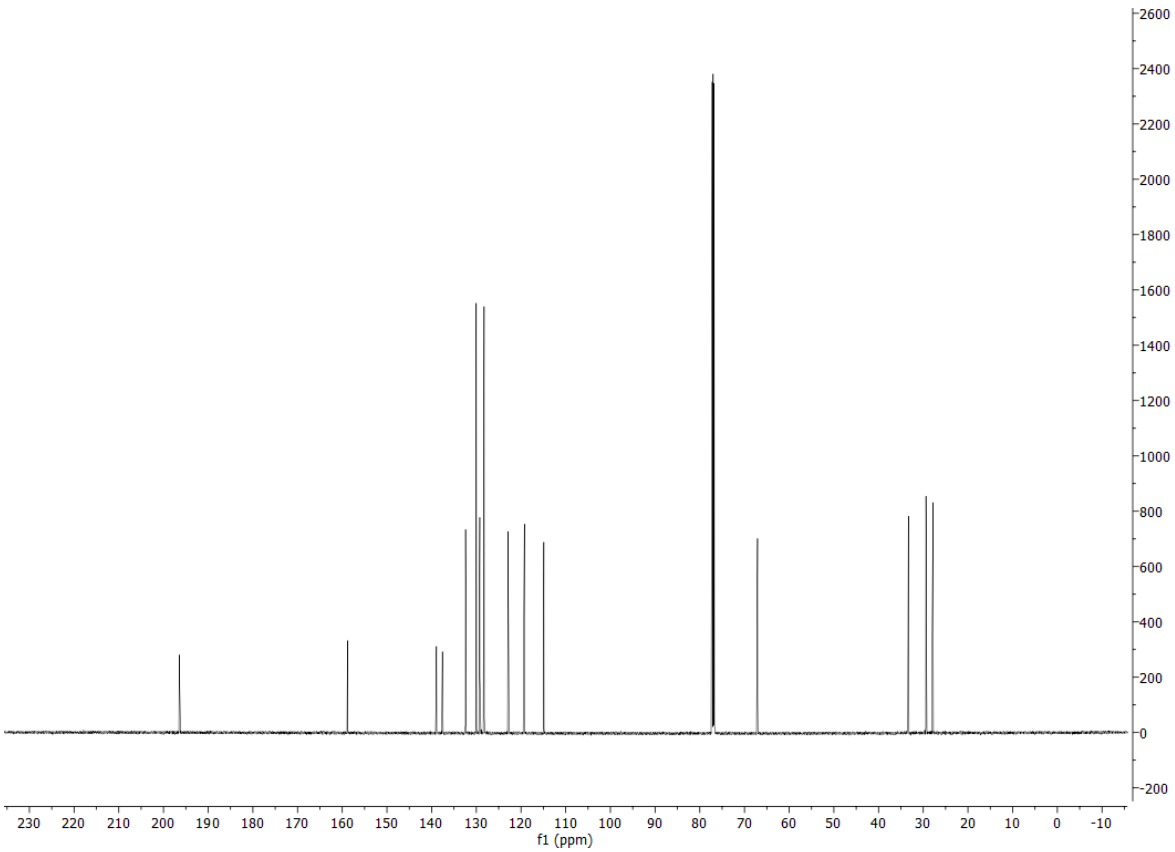

(2’’’*R*)-*N*-[4’’-(3-benzoylphenoxy)butyl]-2’’’-methylpyrrolidine 97

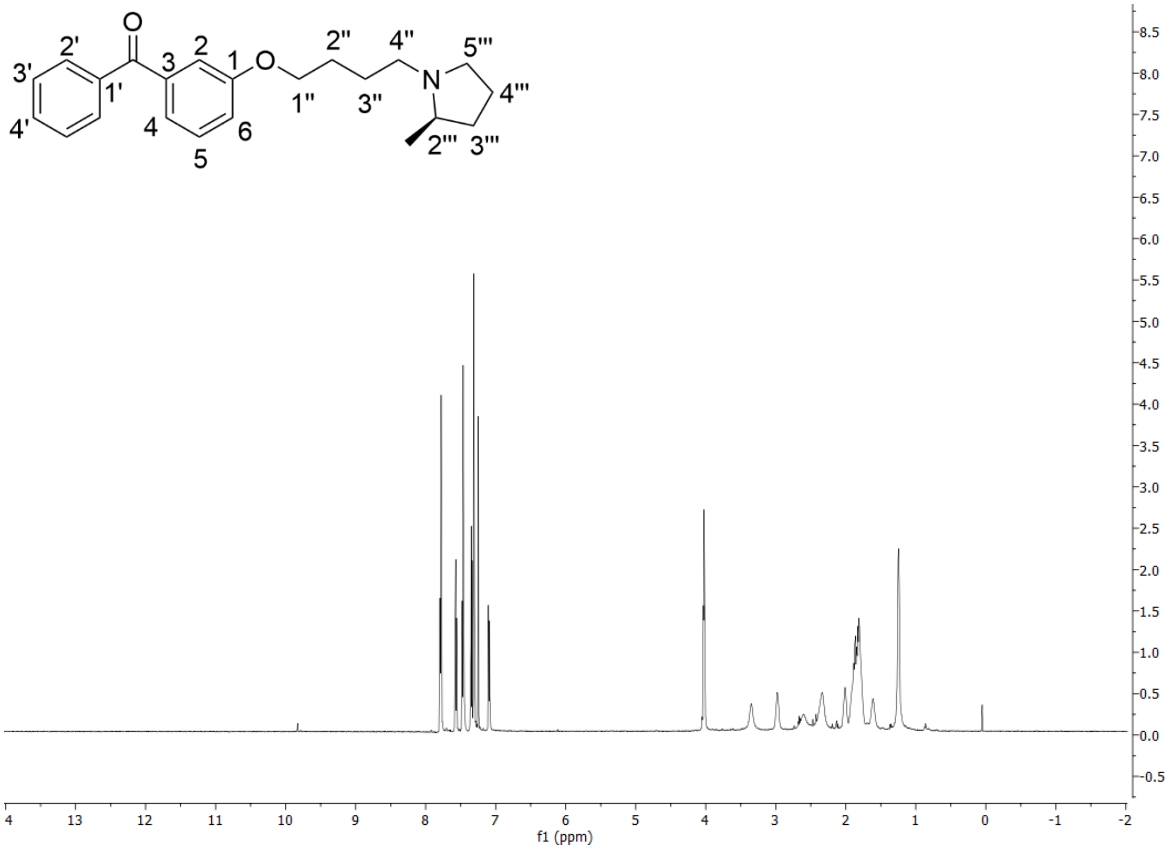

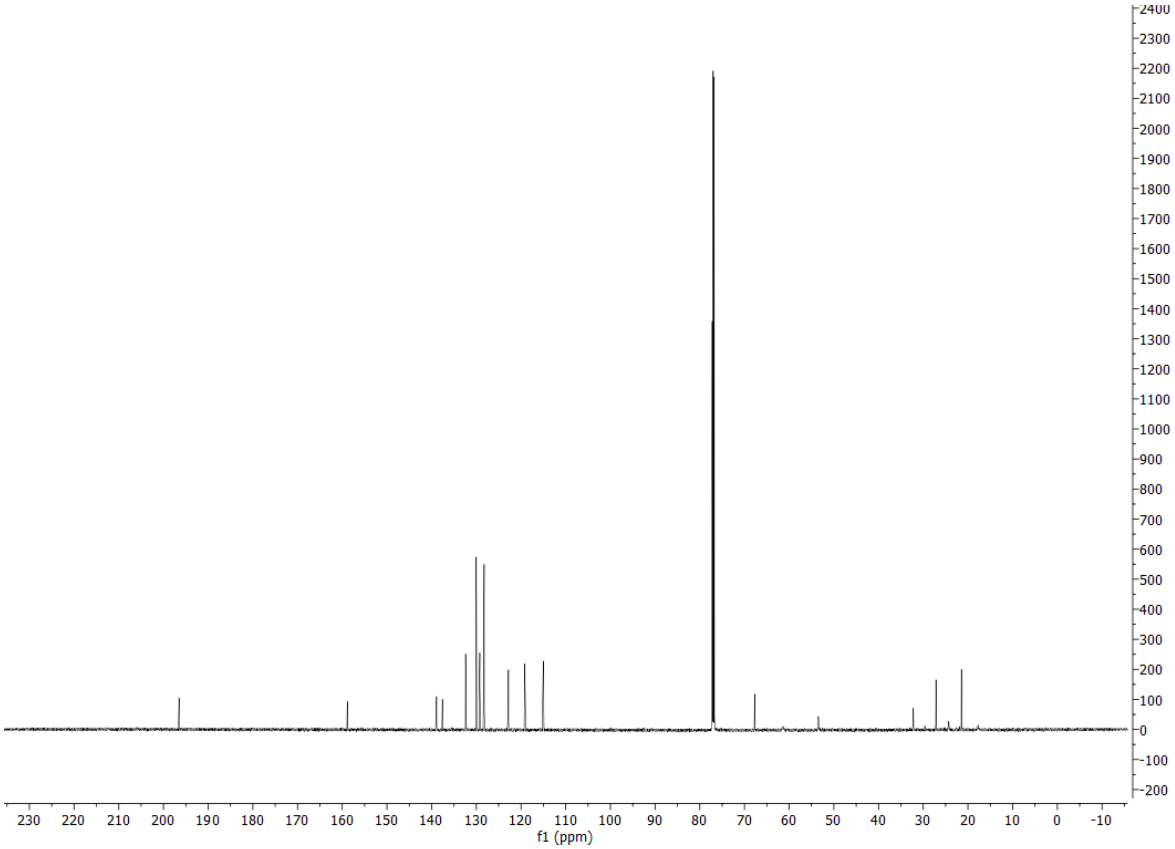

3-(4’-methylbenzoyl)phenol 106

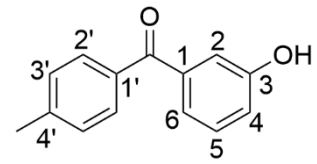

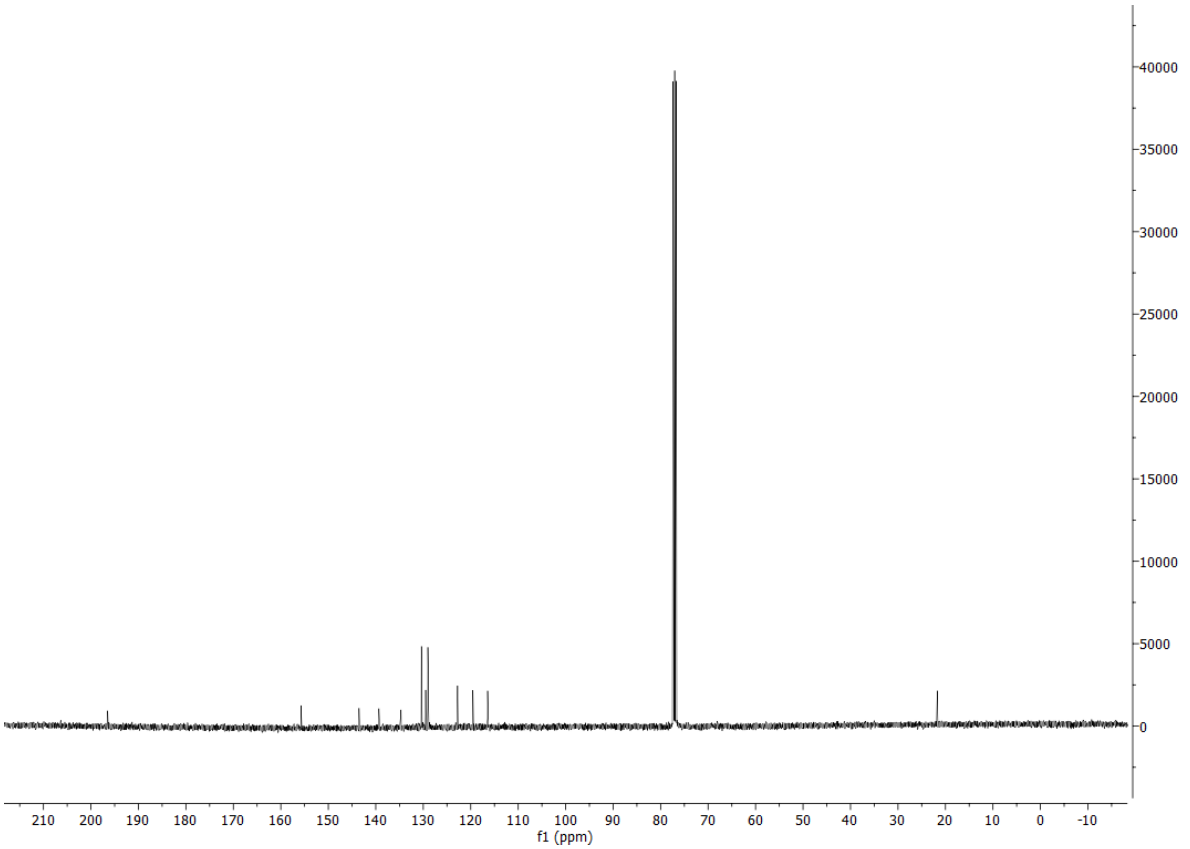

(2’’’*R*)-*N*-{3’’-[3-(4’-methylbenzoyl)phenoxy]propyl}2’’’-methylpyrrolidine 112

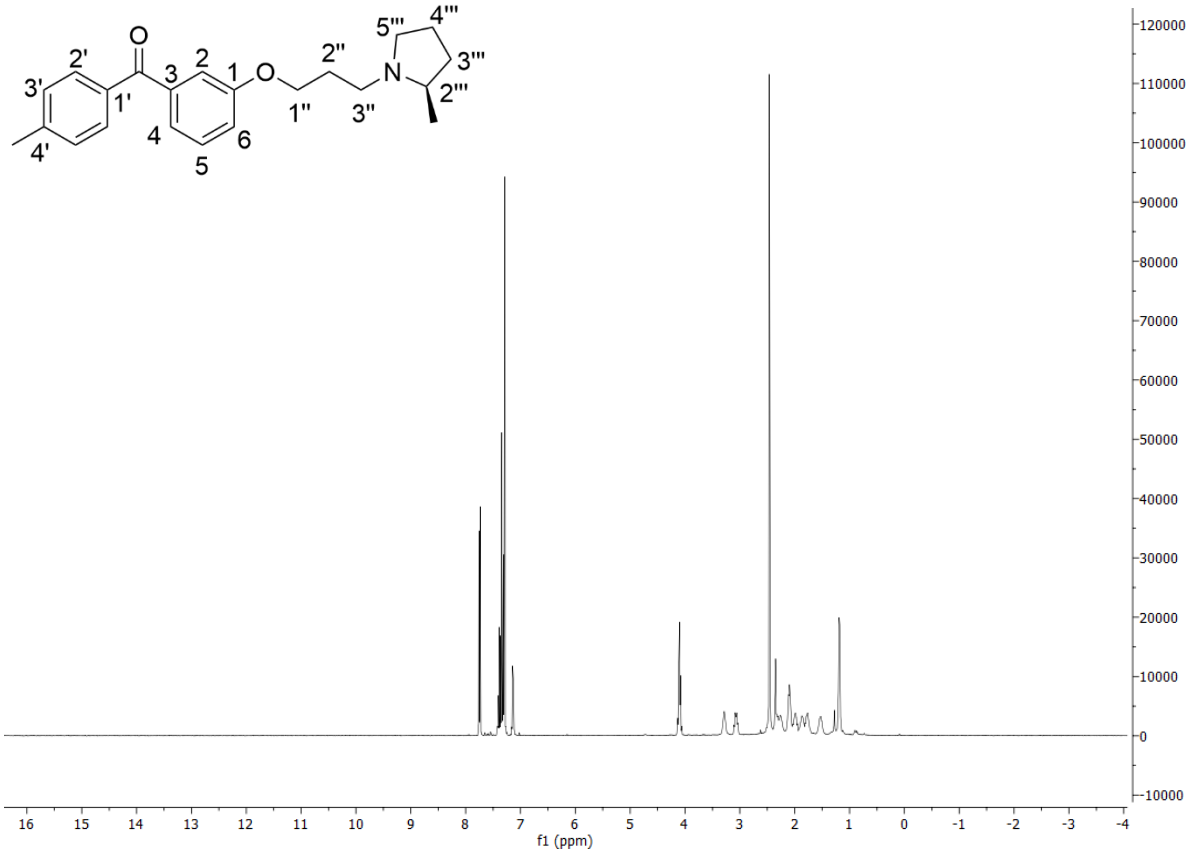

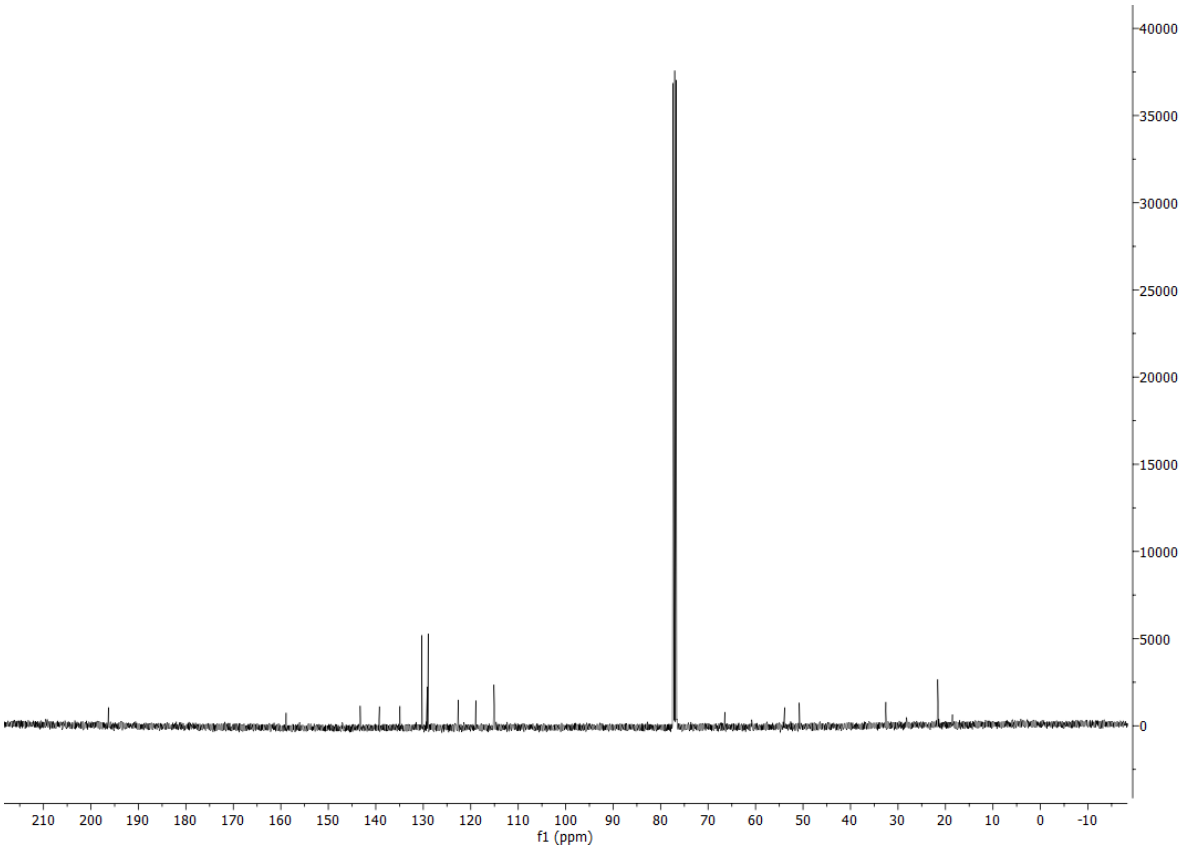

3-[4’-(isopropanyl)benzoyl]phenol 107

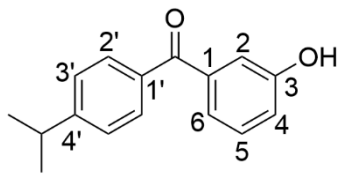

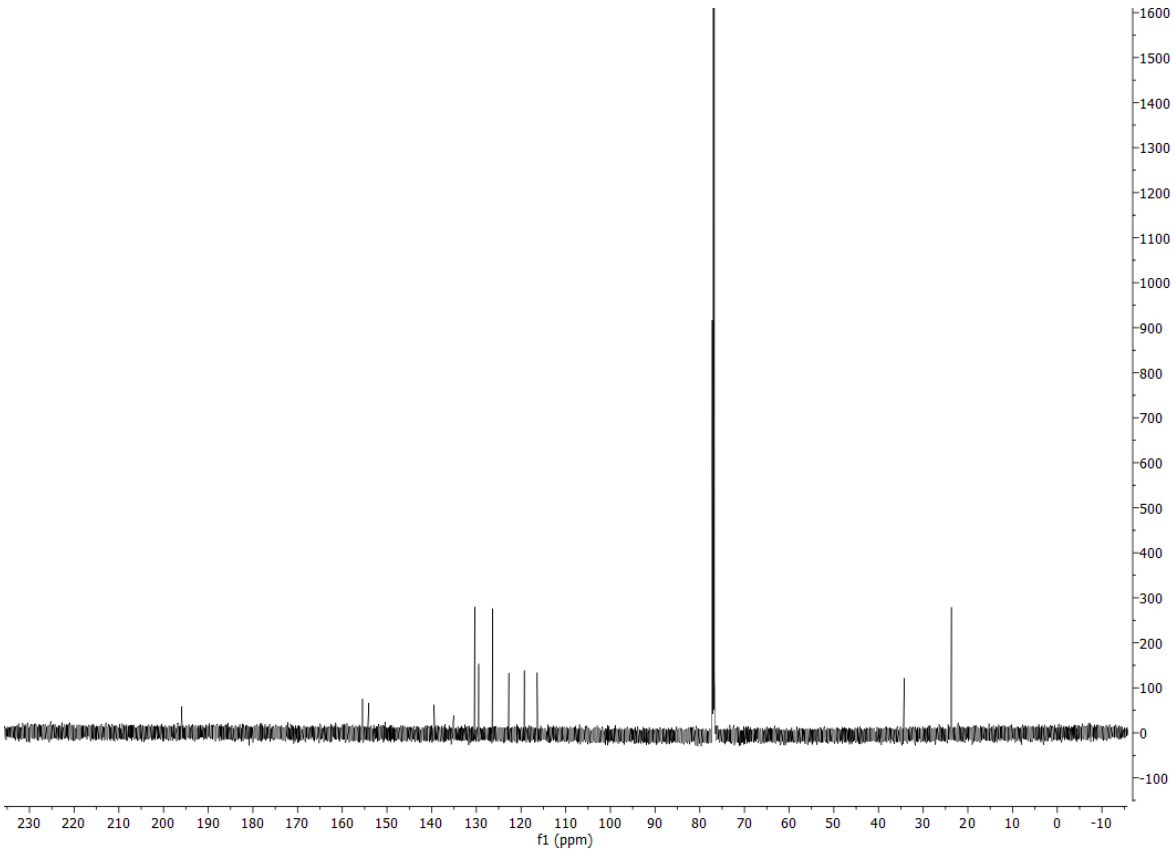

(2’’’*R*)-*N*-(3’’-{3-[4’-(propan-2’’’’-yl)benzoyl]phenoxy}propyl)-2’’’-methylpyrrolidine

113

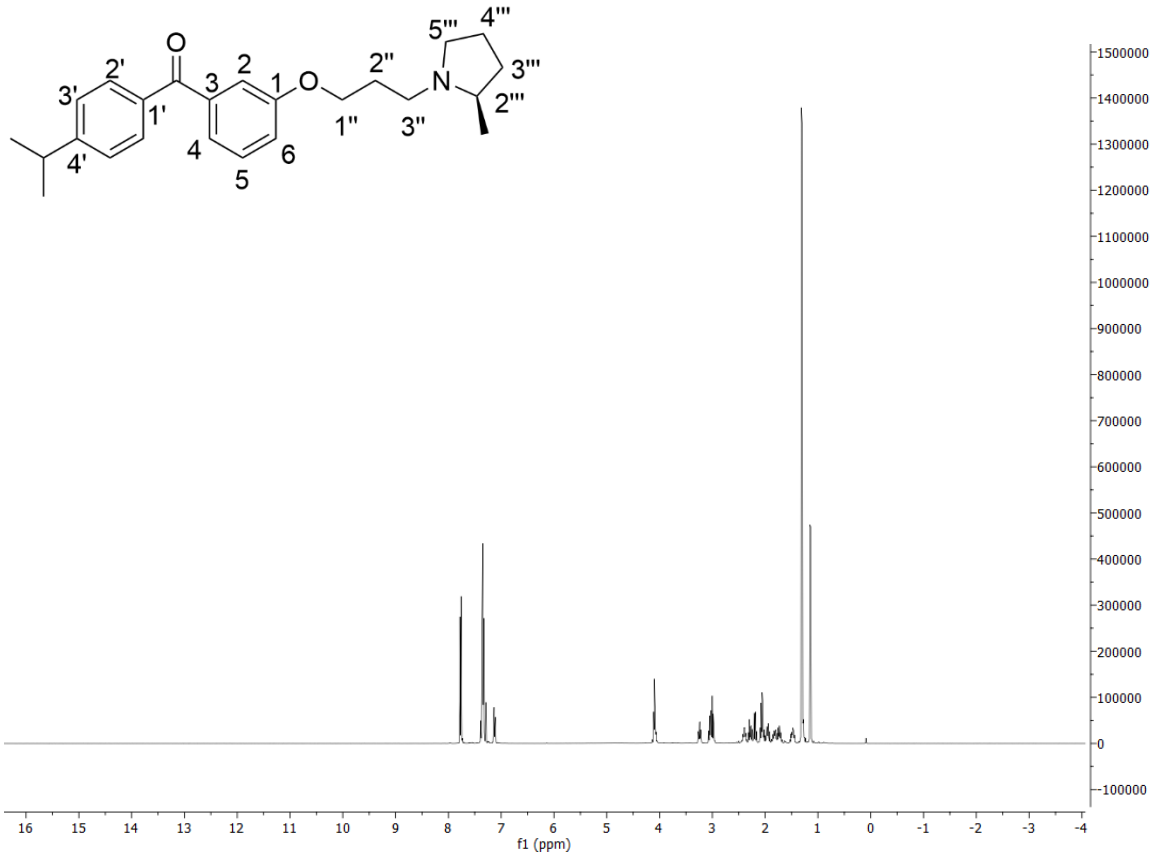

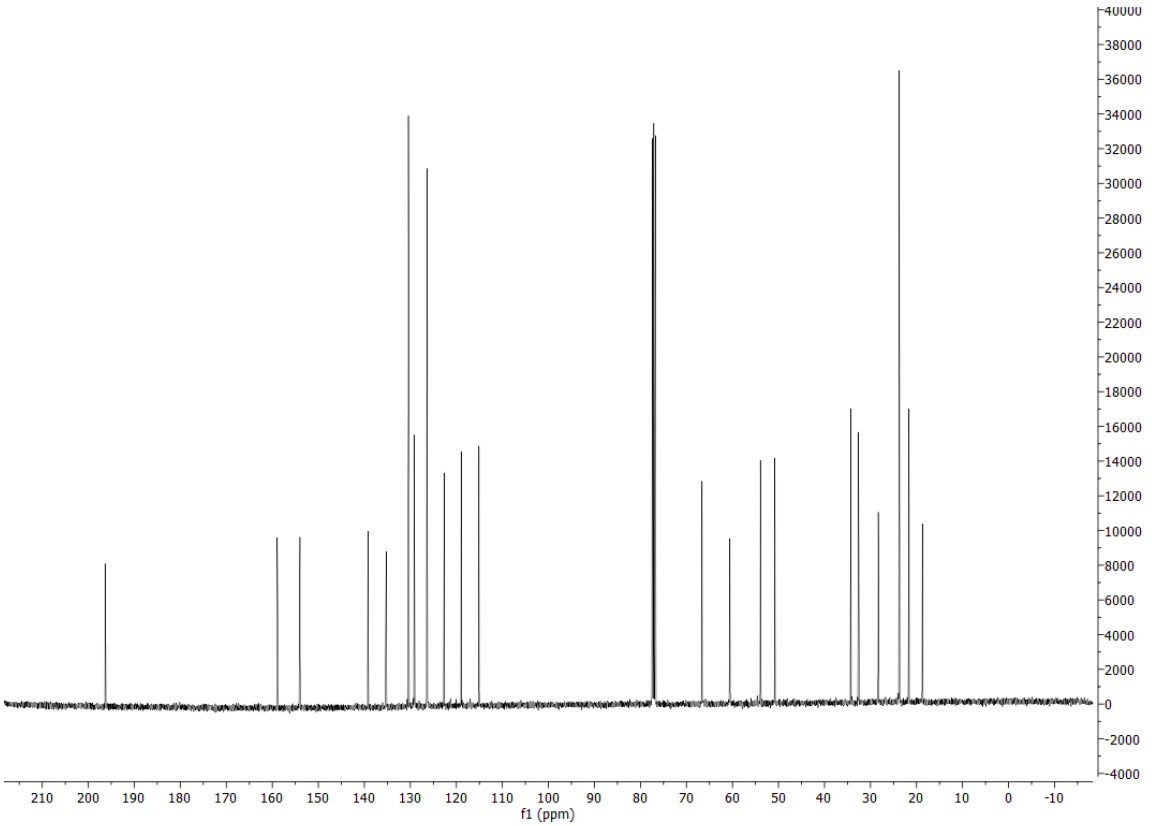

3-(4’-chlorobenzoyl)phenol 100

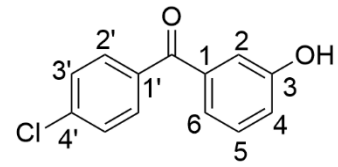

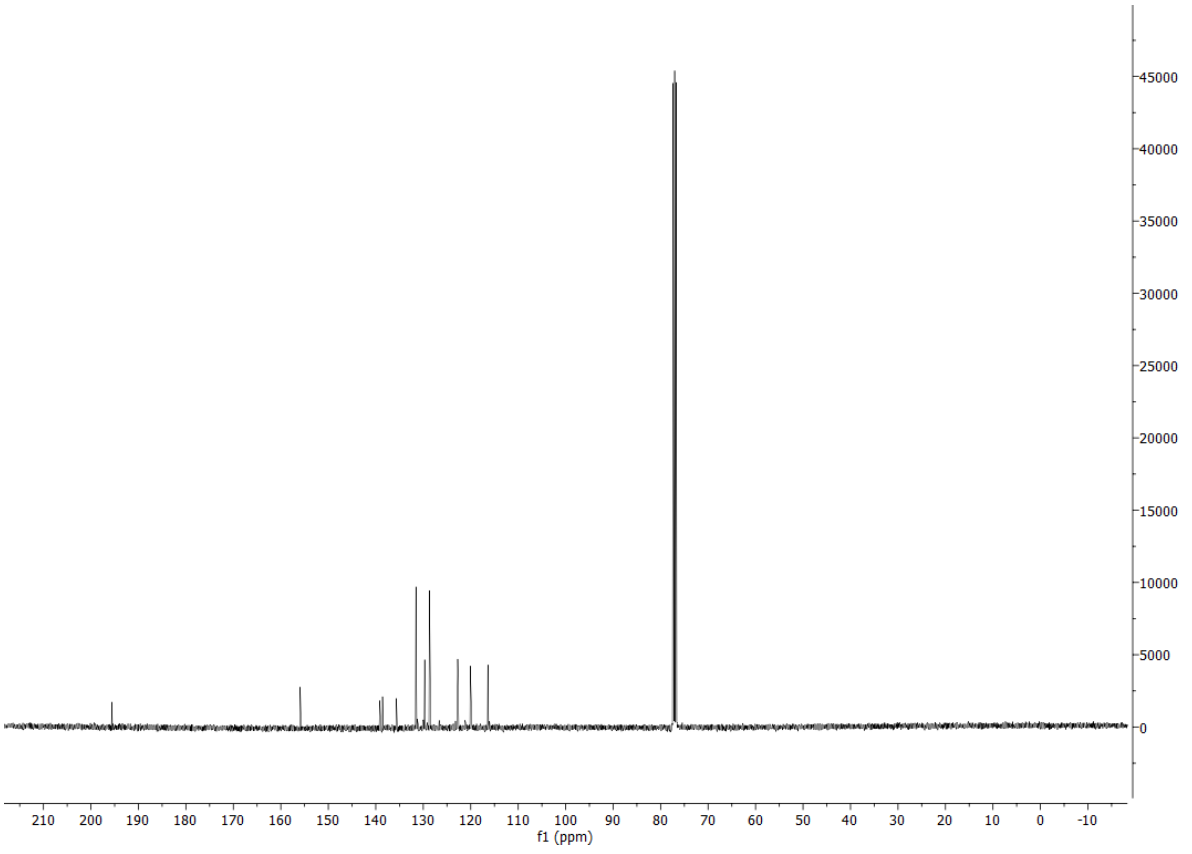

[3-(2’’-bromoethoxy)phenyl](4’-chlorophenyl)methanone 108a

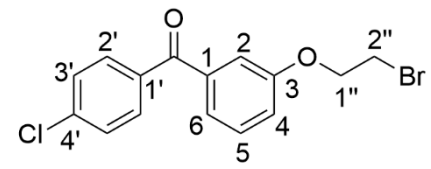

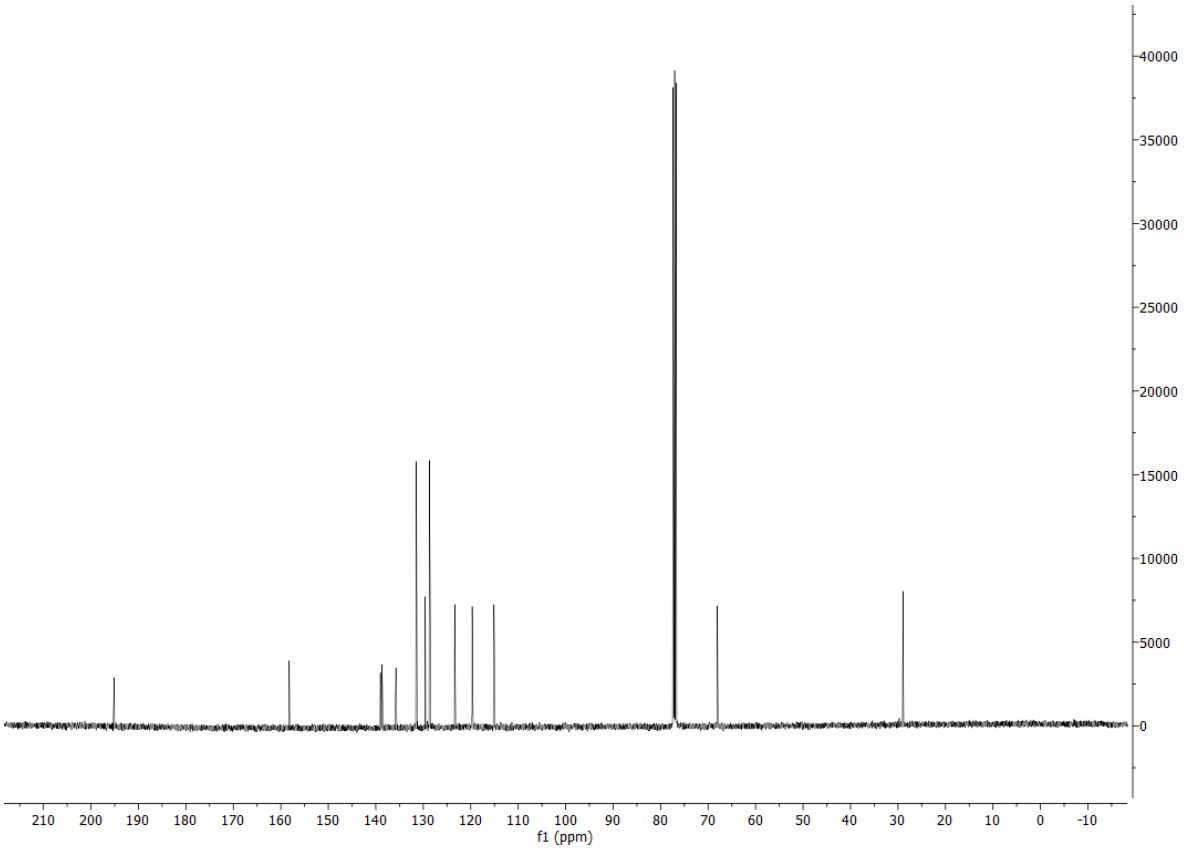

(2’’’*R*)-*N*-{2’’-[3-(4’-chlorobenzoyl)phenoxy]ethyl}-2’’’-methylpyrrolidine 109

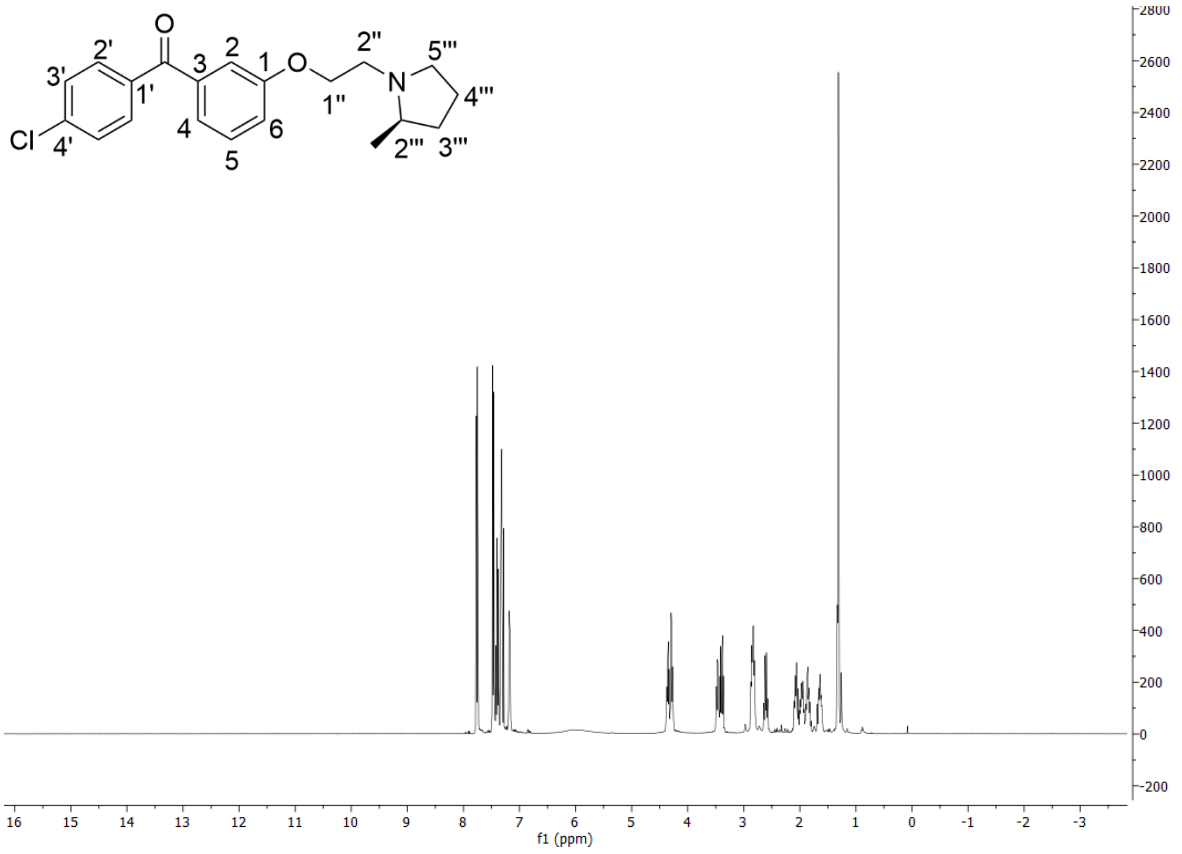

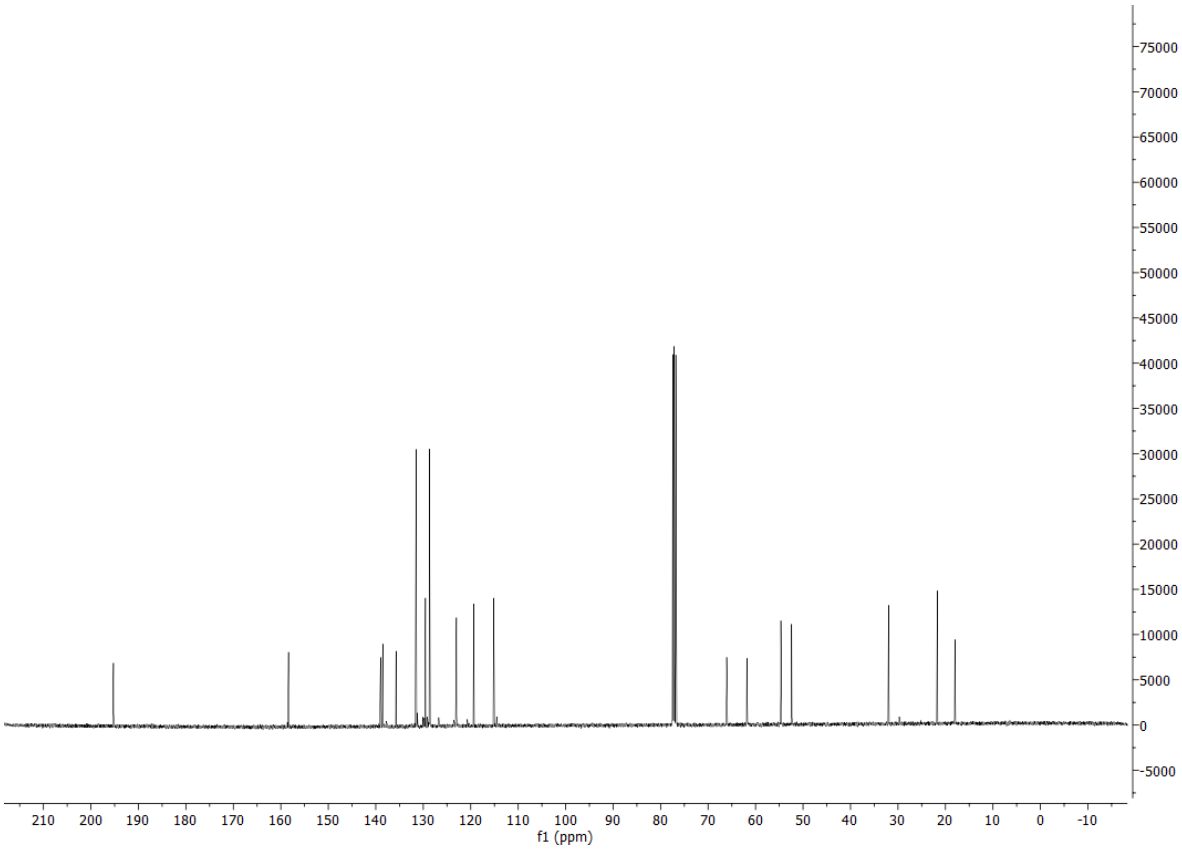

[3-(3’’-bromopropoxy)phenyl](4’-chlorophenyl)methanone 108b

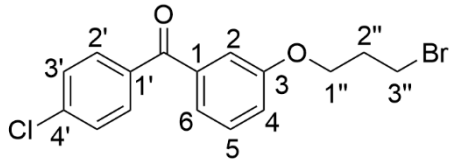

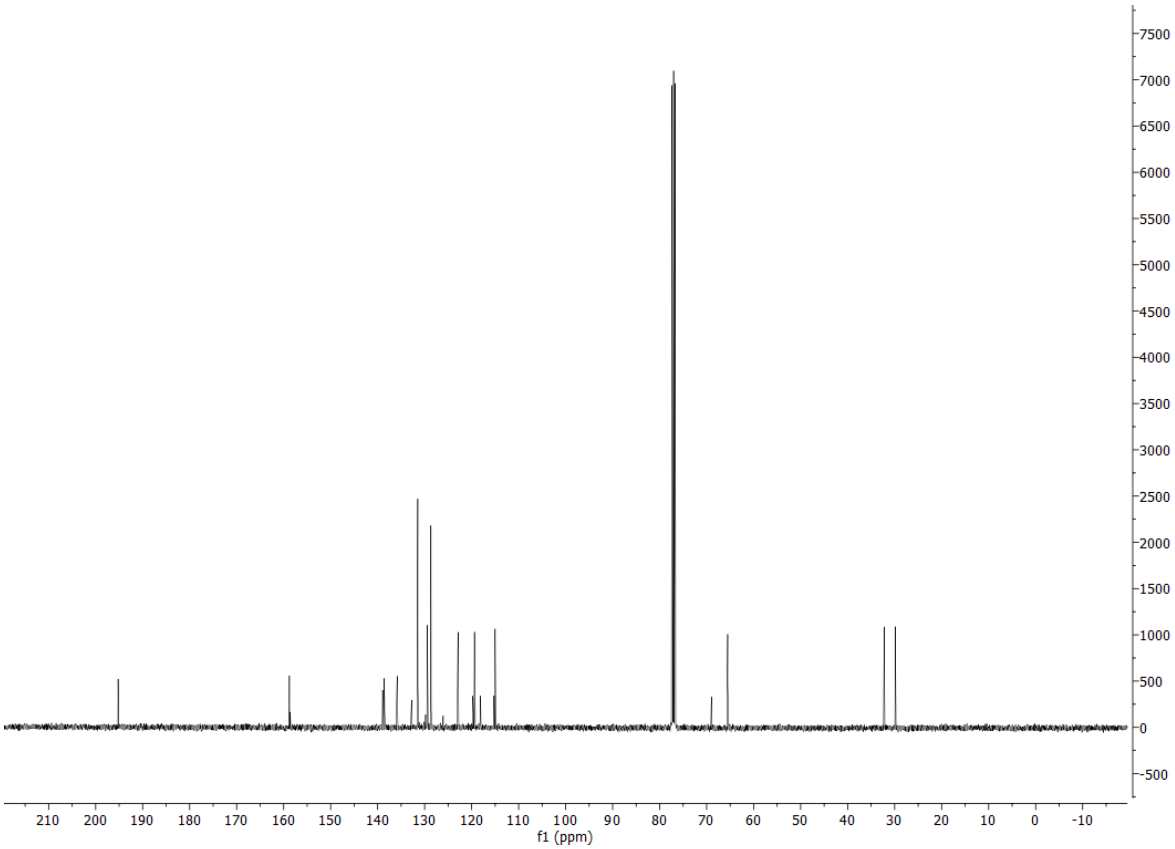

(2’’’R)-*N*-{3’’-[3-(4’-chlorobenzoyl)phenoxy]propyl}-2’’’-methylpyrrolidine 110

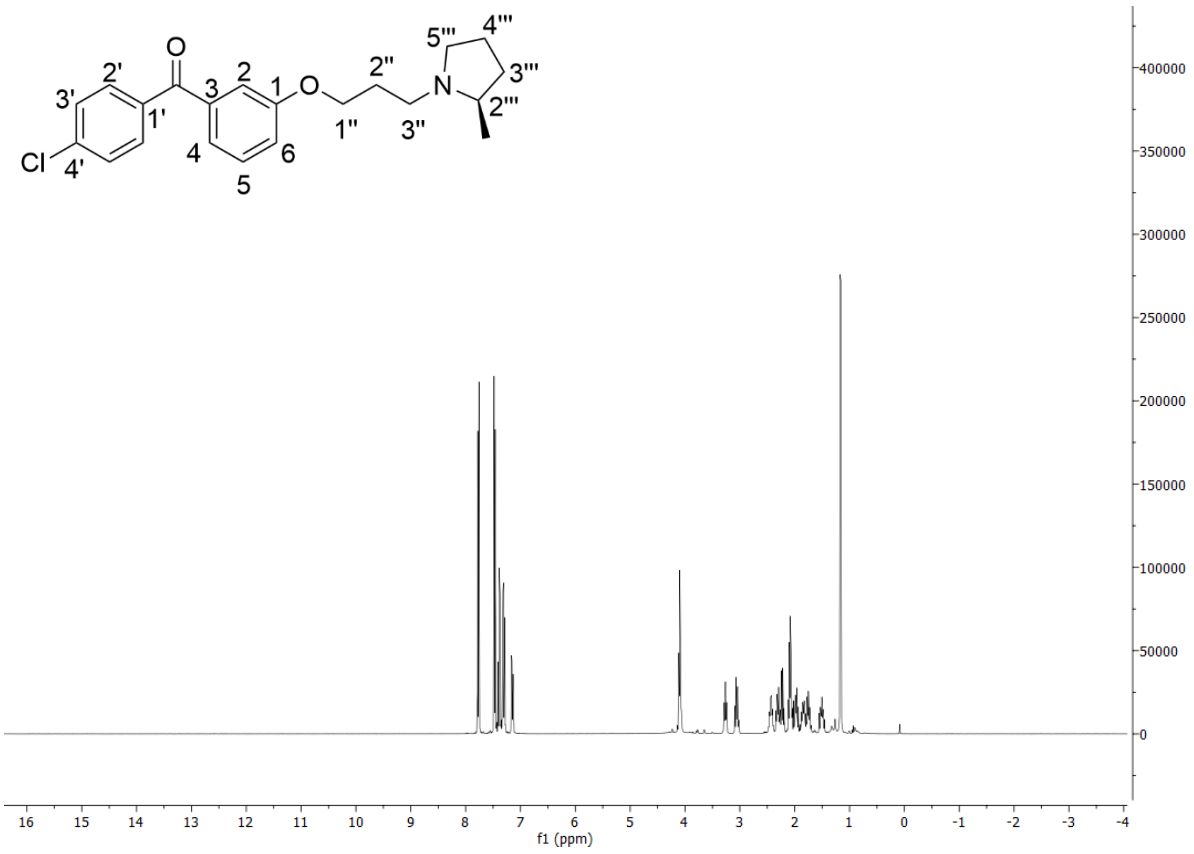

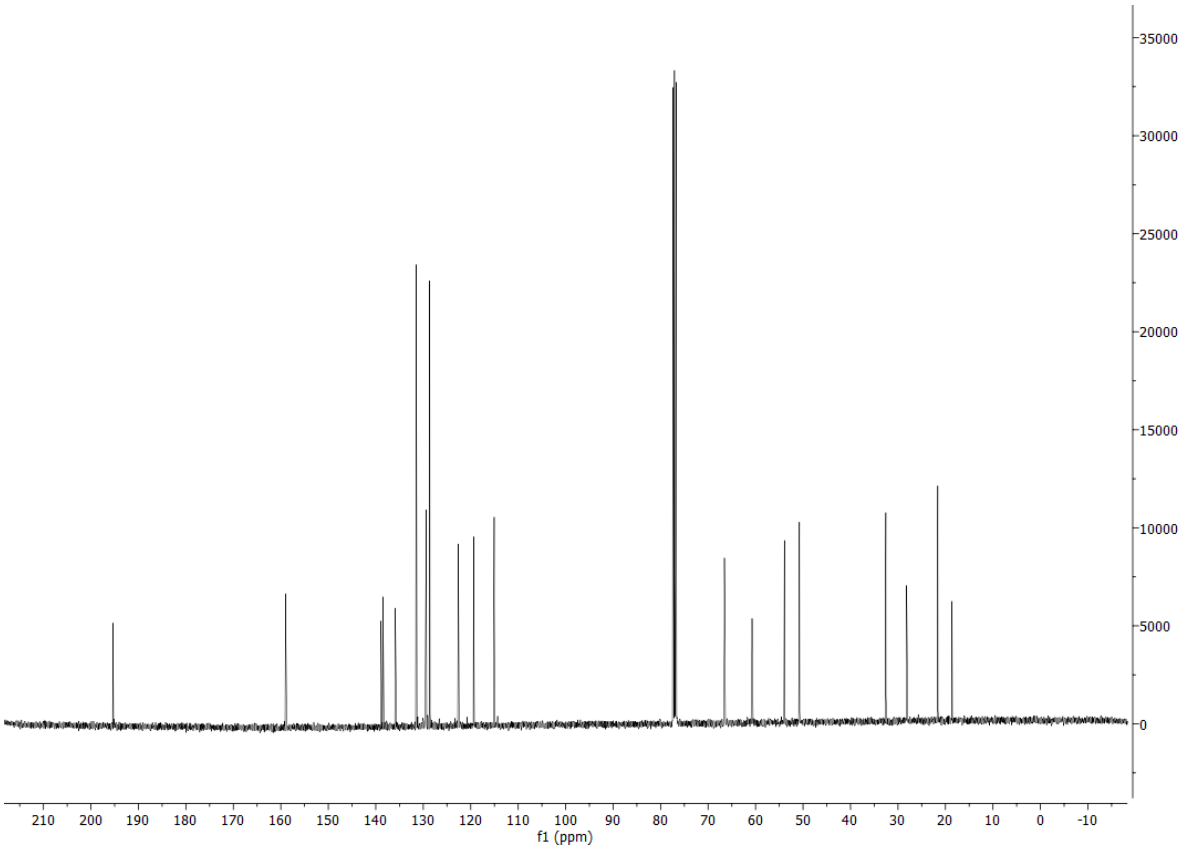

(2’’’*R*)-*N*-{4’’-[3-(4’-chlorobenzoyl)phenoxy]butyl}-2’’’-methylpyrrolidine 111

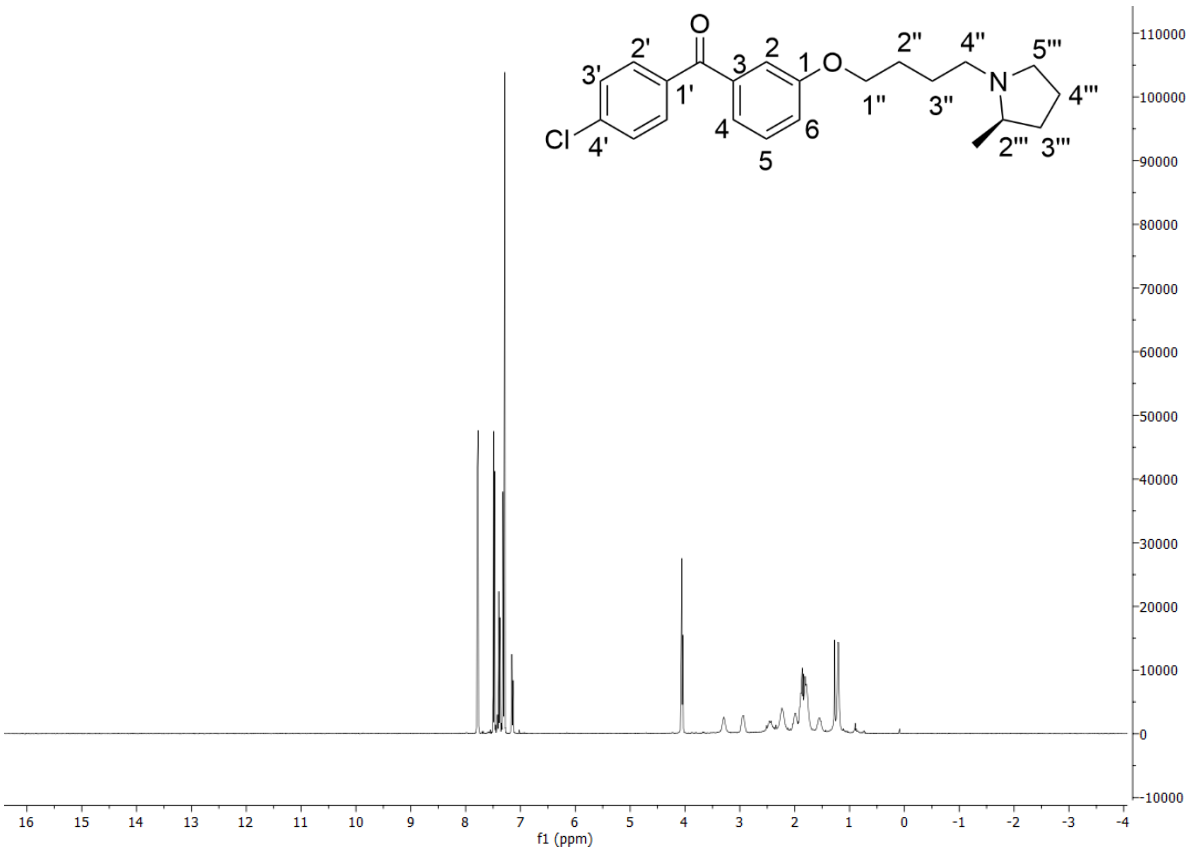

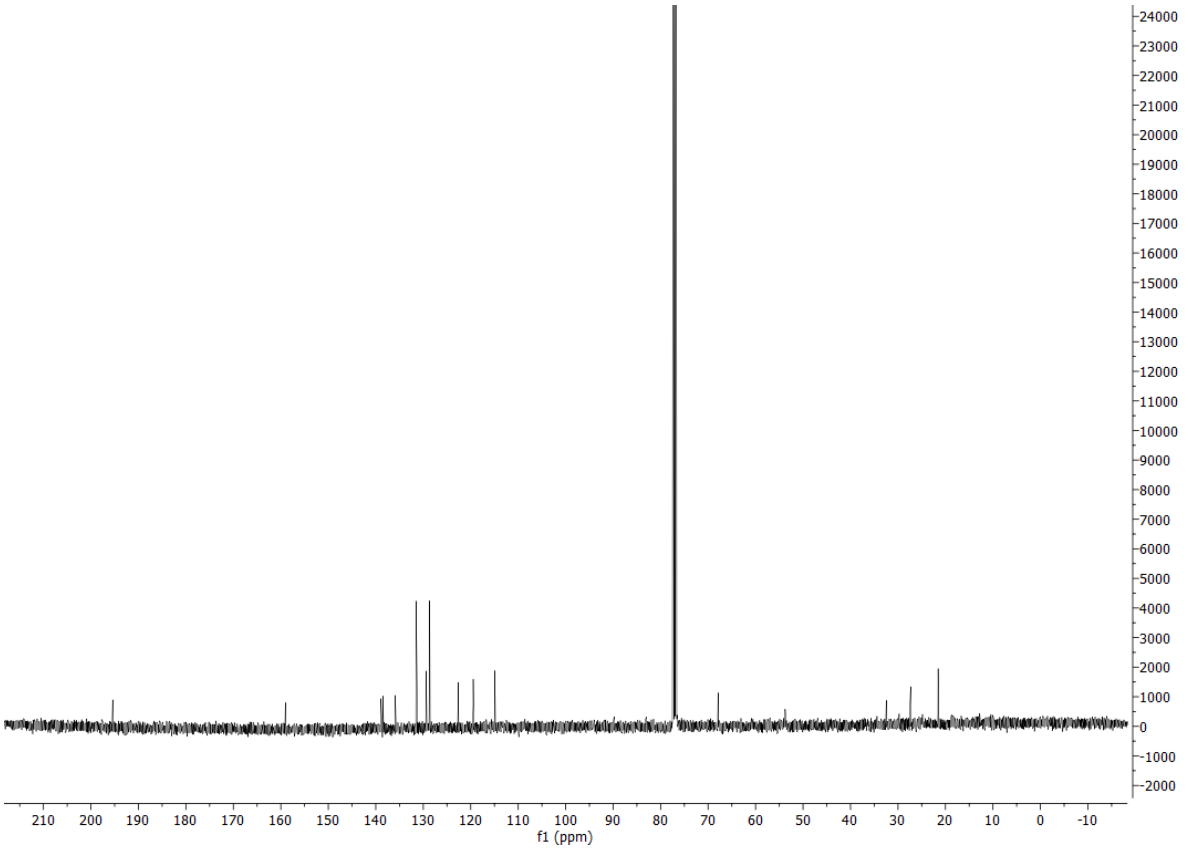

[4-(2’’-bromoethoxy)phenyl](phenyl)methanone 77a

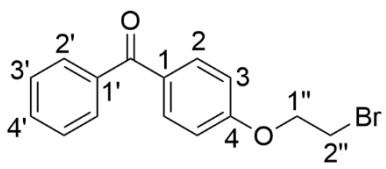

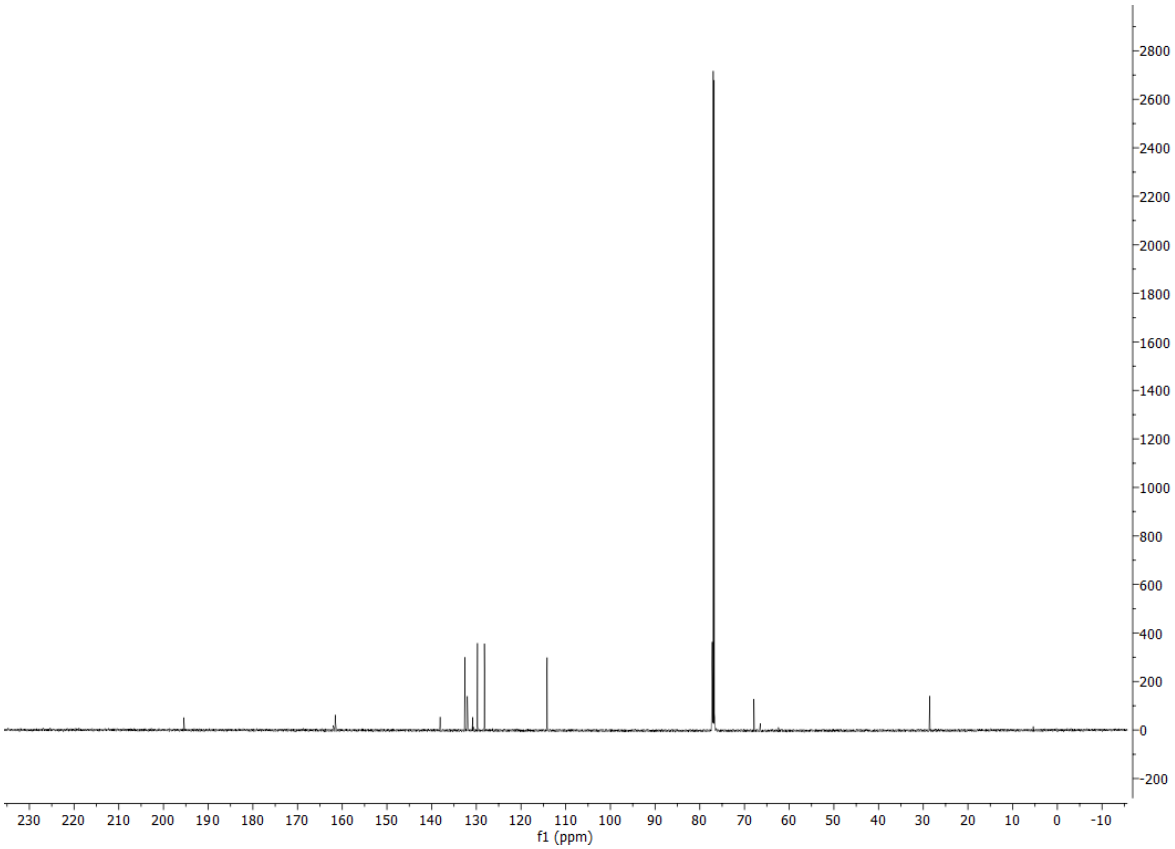

(2’’’*R*)-1’’’-[2’’-(4-benzoylphenoxy)ethyl]-2’’’-methylpyrrolidine 78

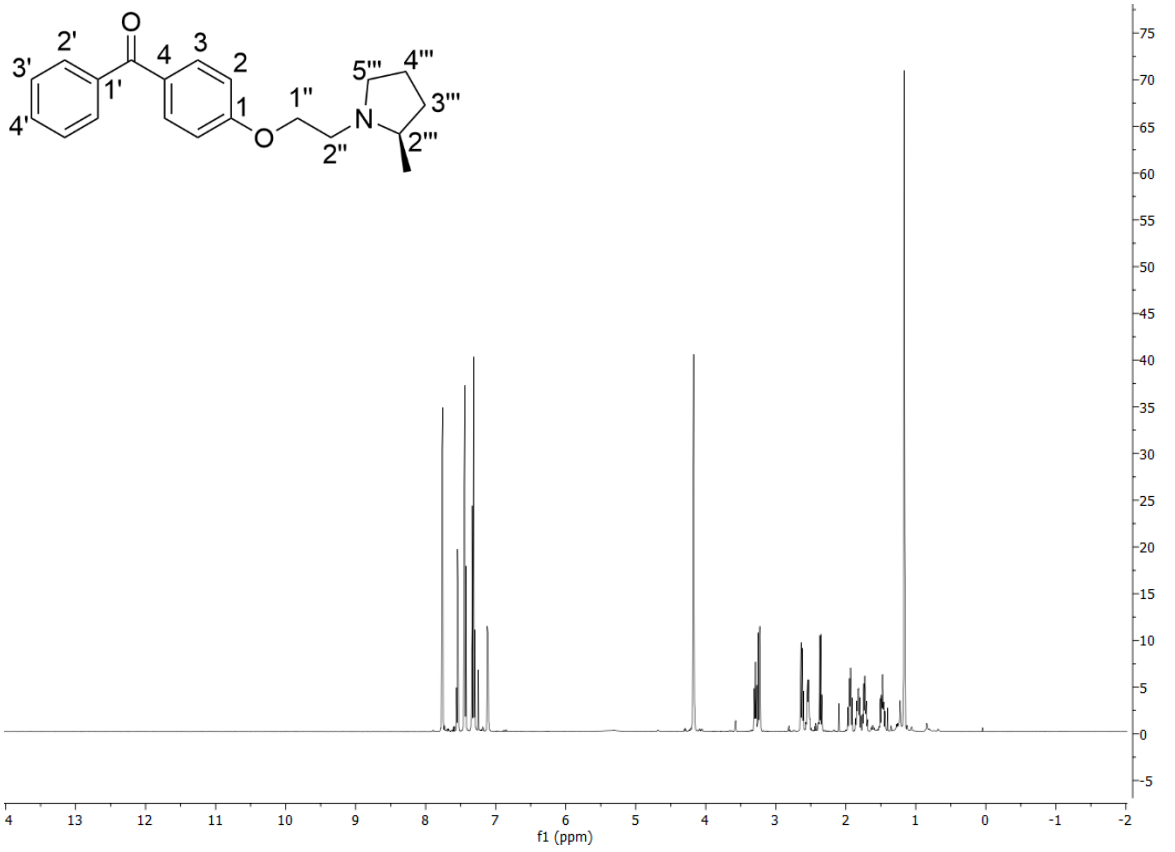

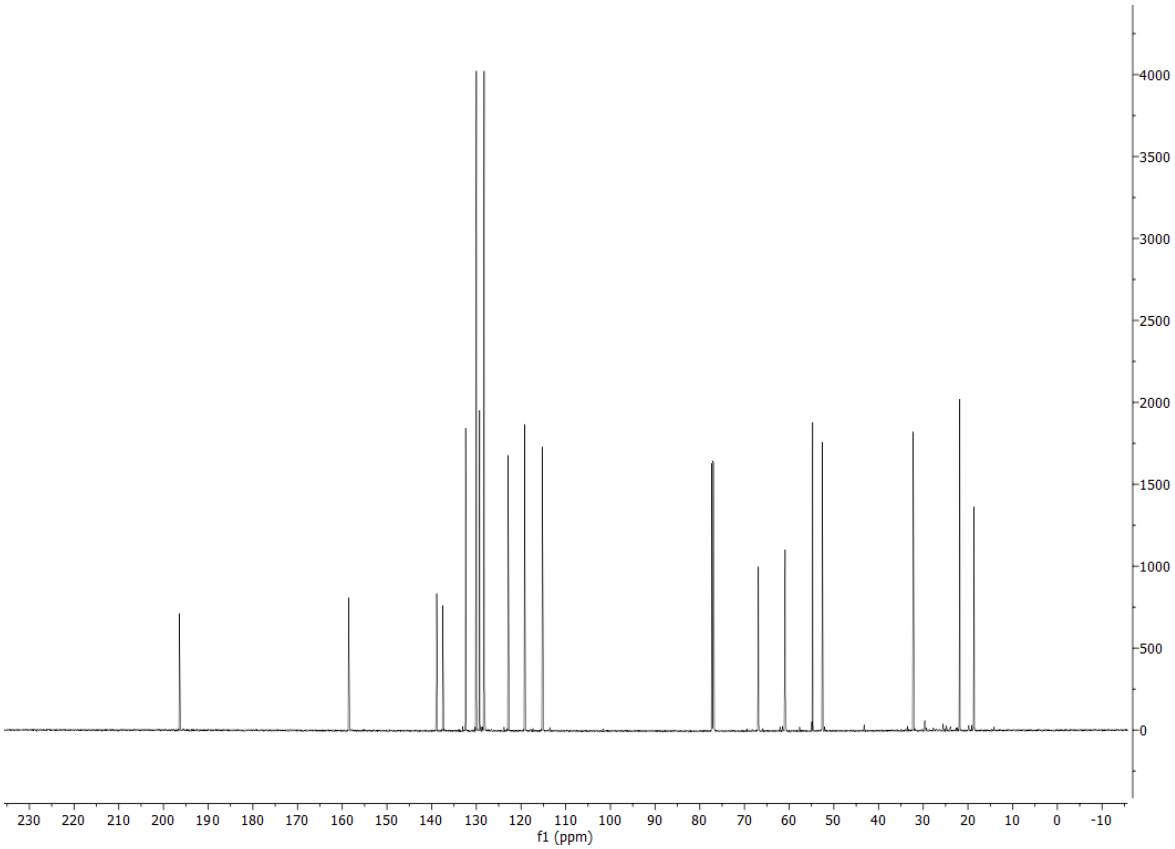

[4-(3’’-bromopropoxy)phenyl](phenyl)methanone 77b

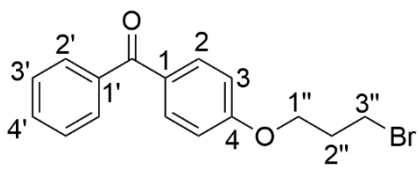

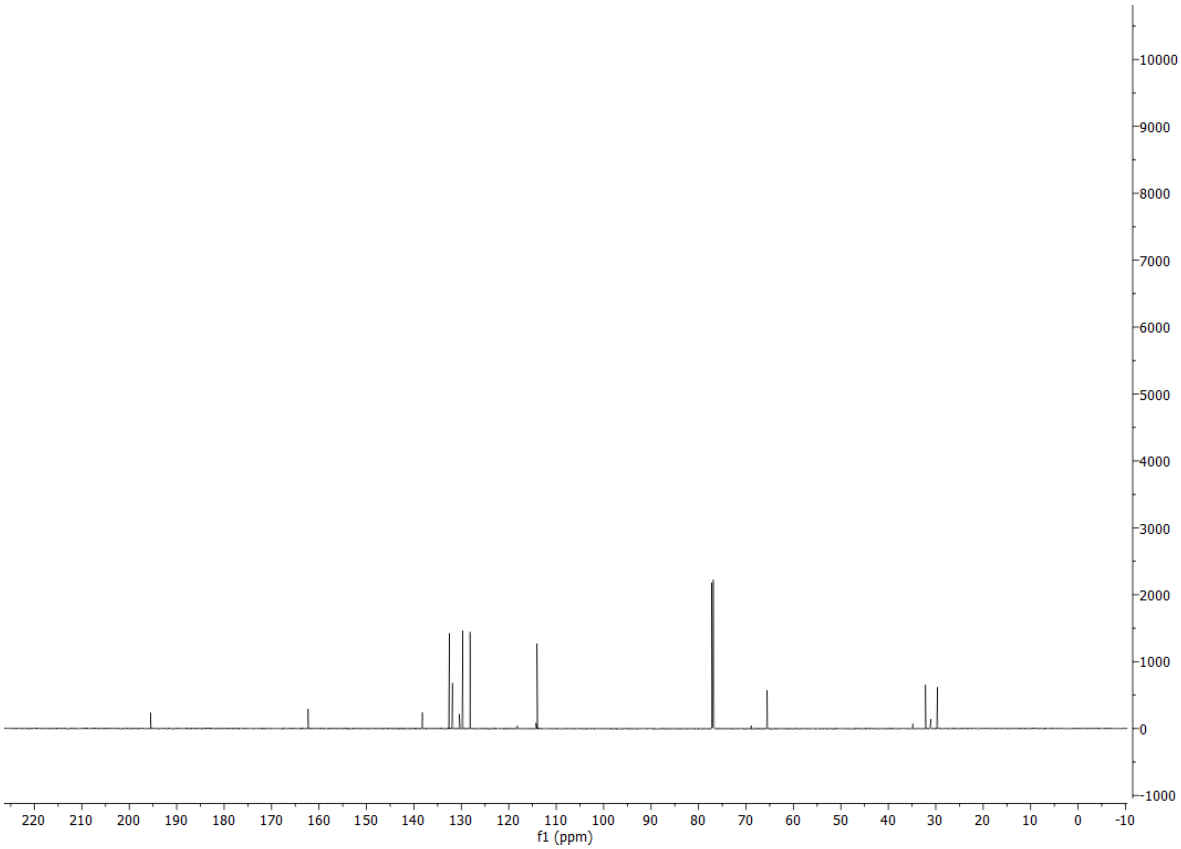

(2’’’*R*)-1’’’-[3’’-(4-benzoylphenoxy)propyl]-2’’’-methylpyrrolidine 79

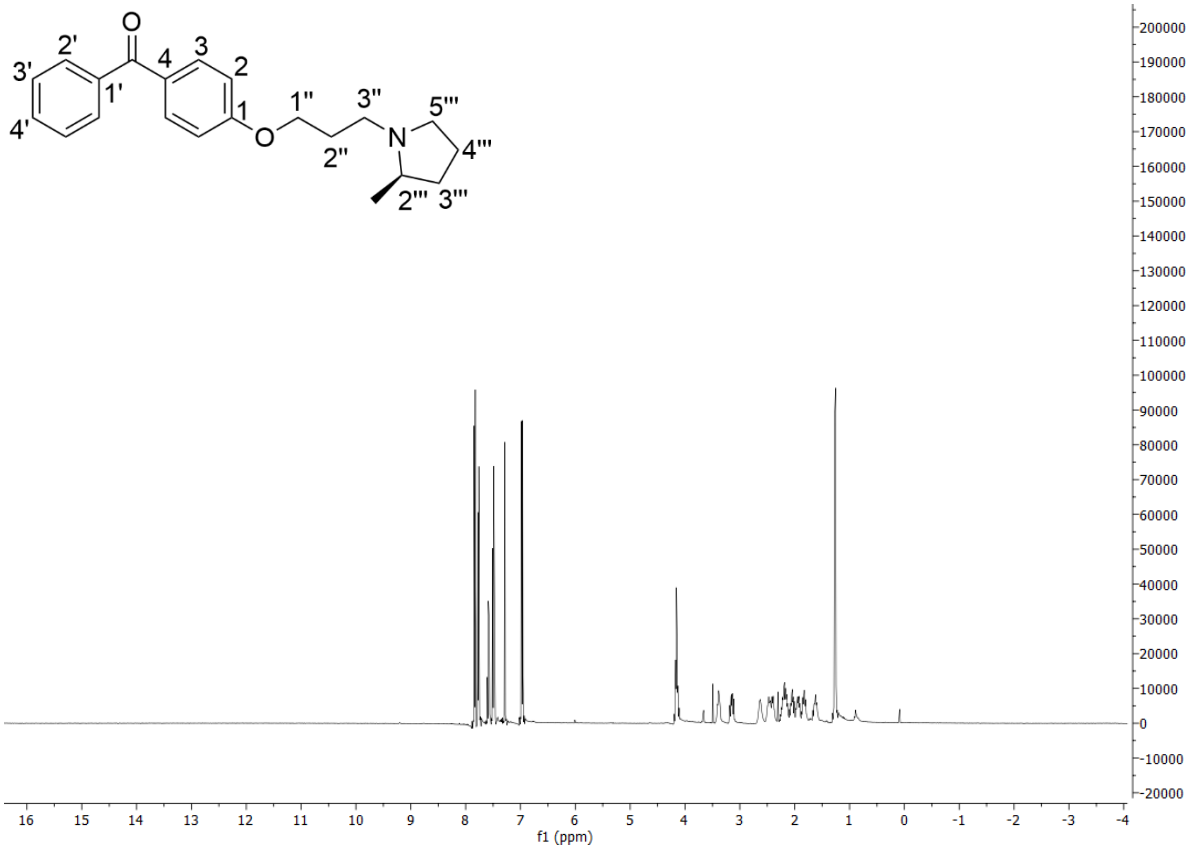

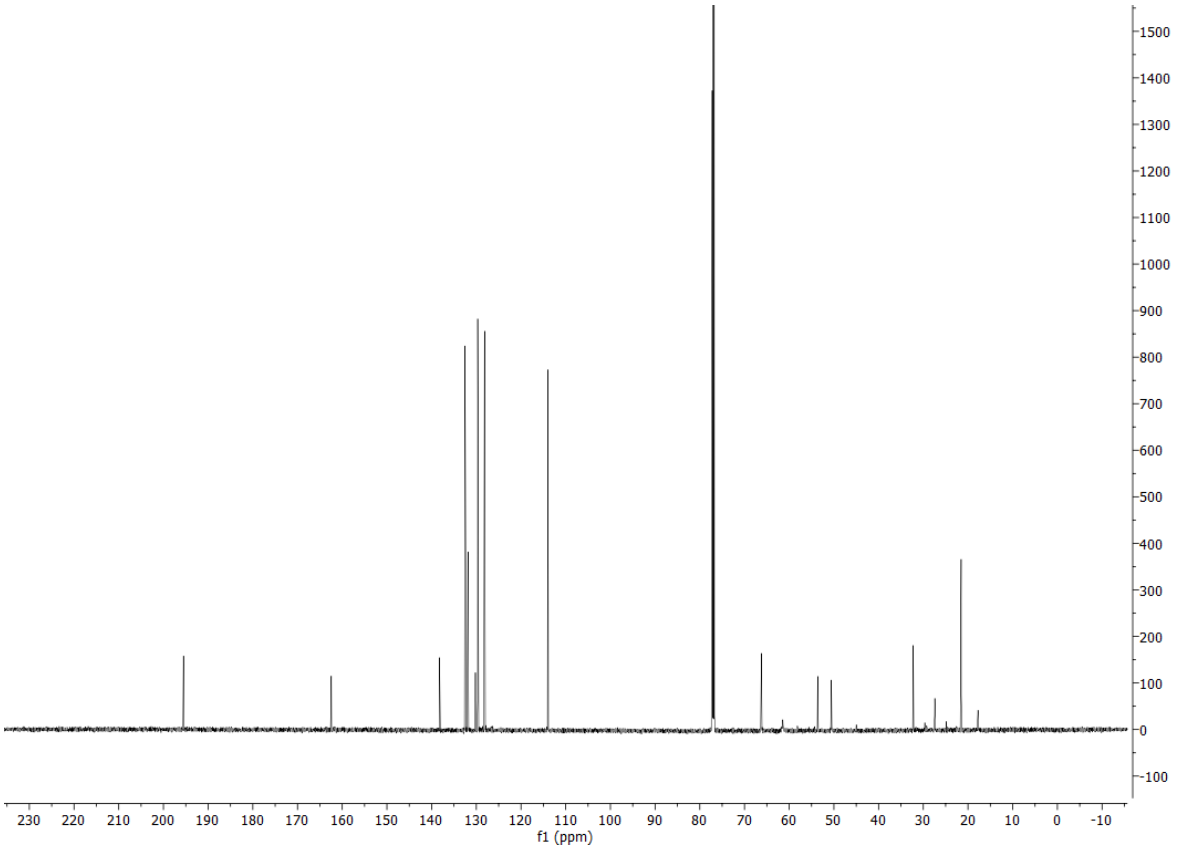

[4-(4’’-bromobutoxy)phenyl](phenyl)methanone 77c

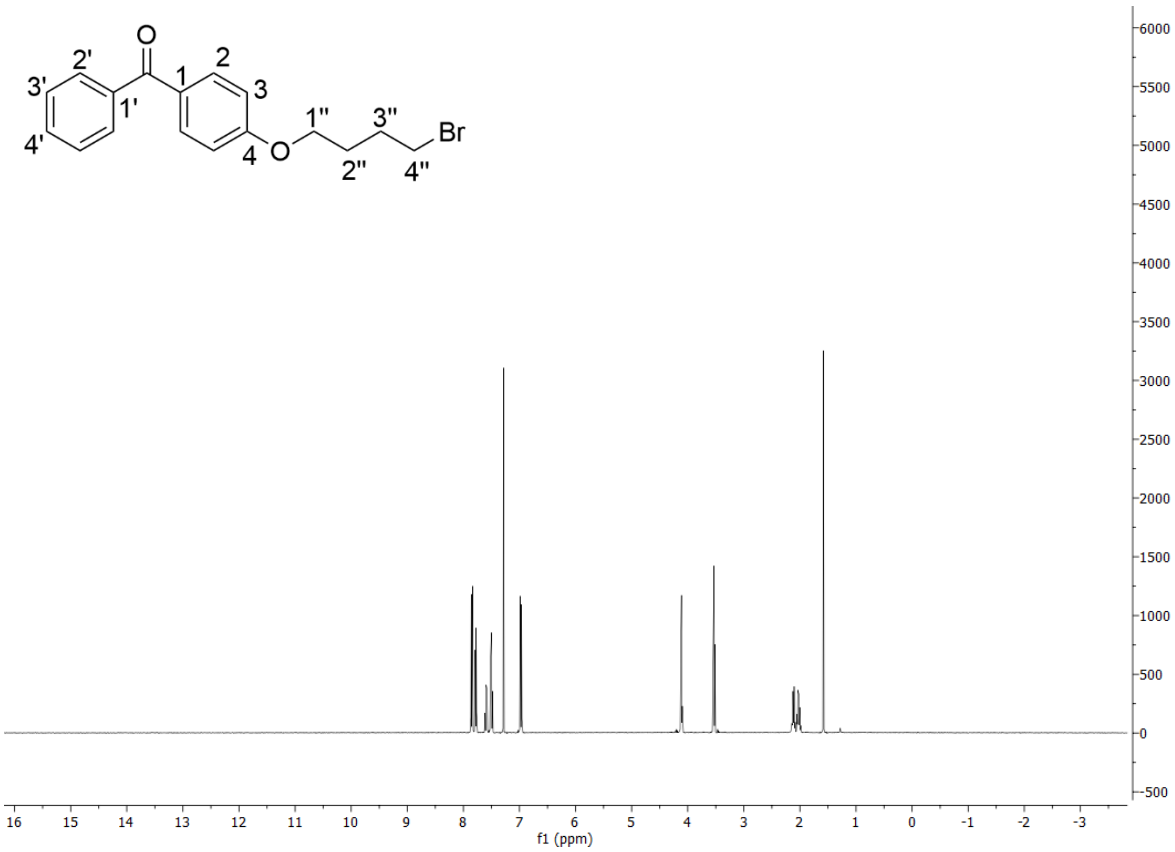

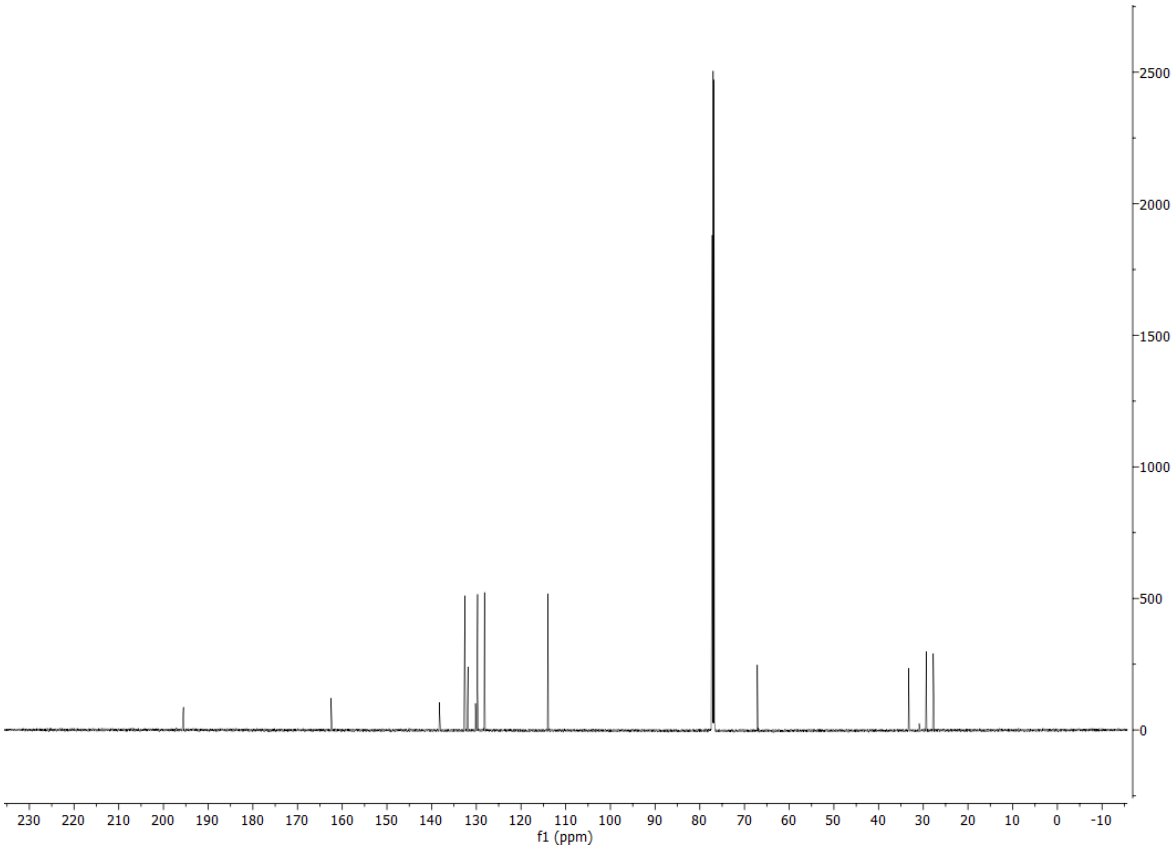

(2’’’*R*)-1’’’-[4’’-(4-benzoylphenoxy)butyl]-2’’’-methylpyrrolidine 80

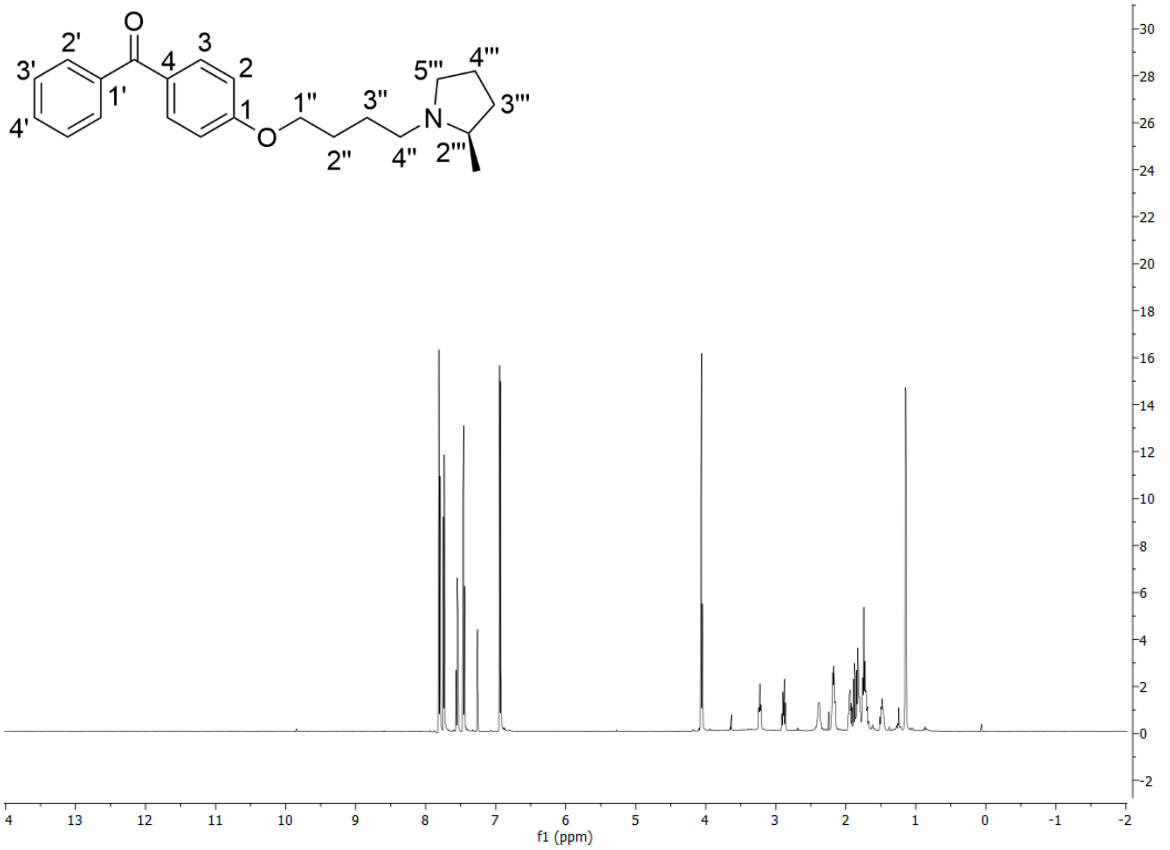

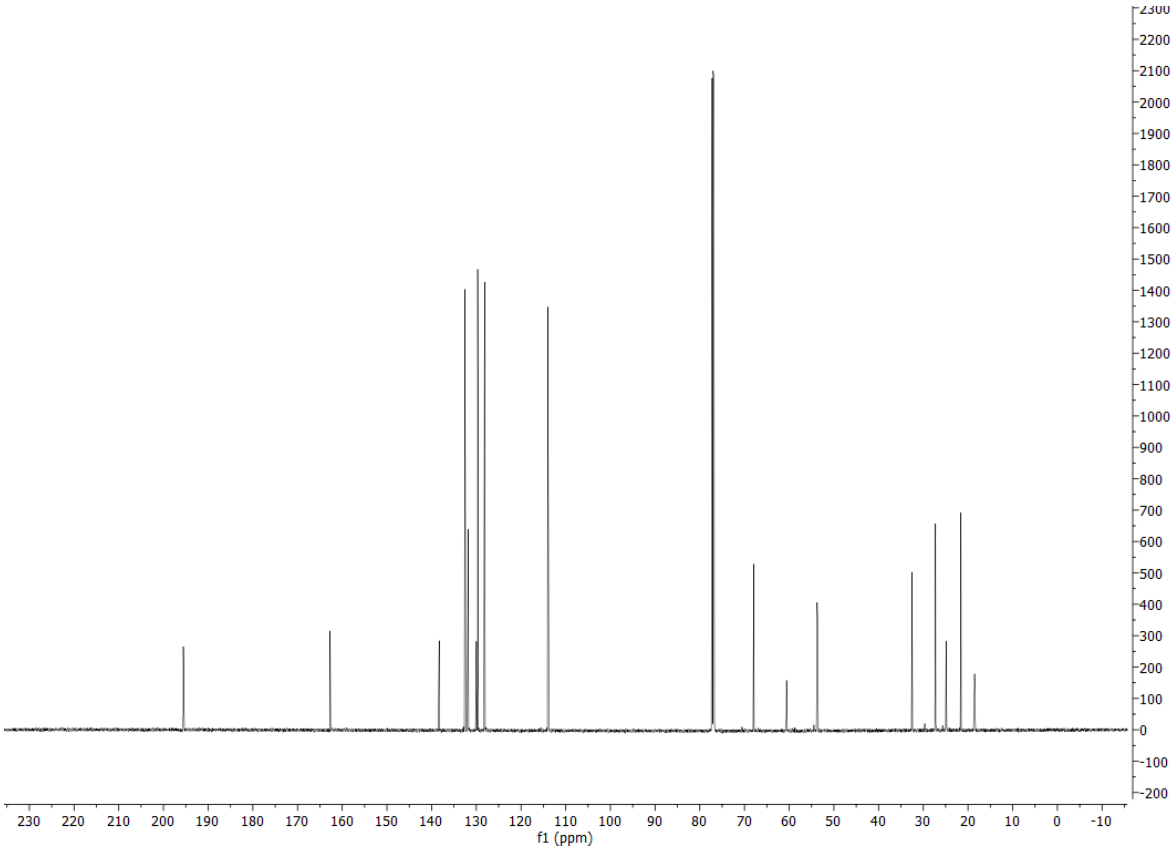

[4-(2’’-bromoethoxy)phenyl](4’-chlorophenyl)methanone 77d

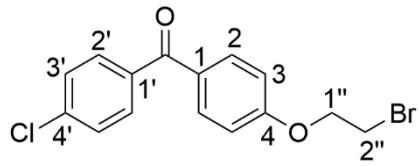

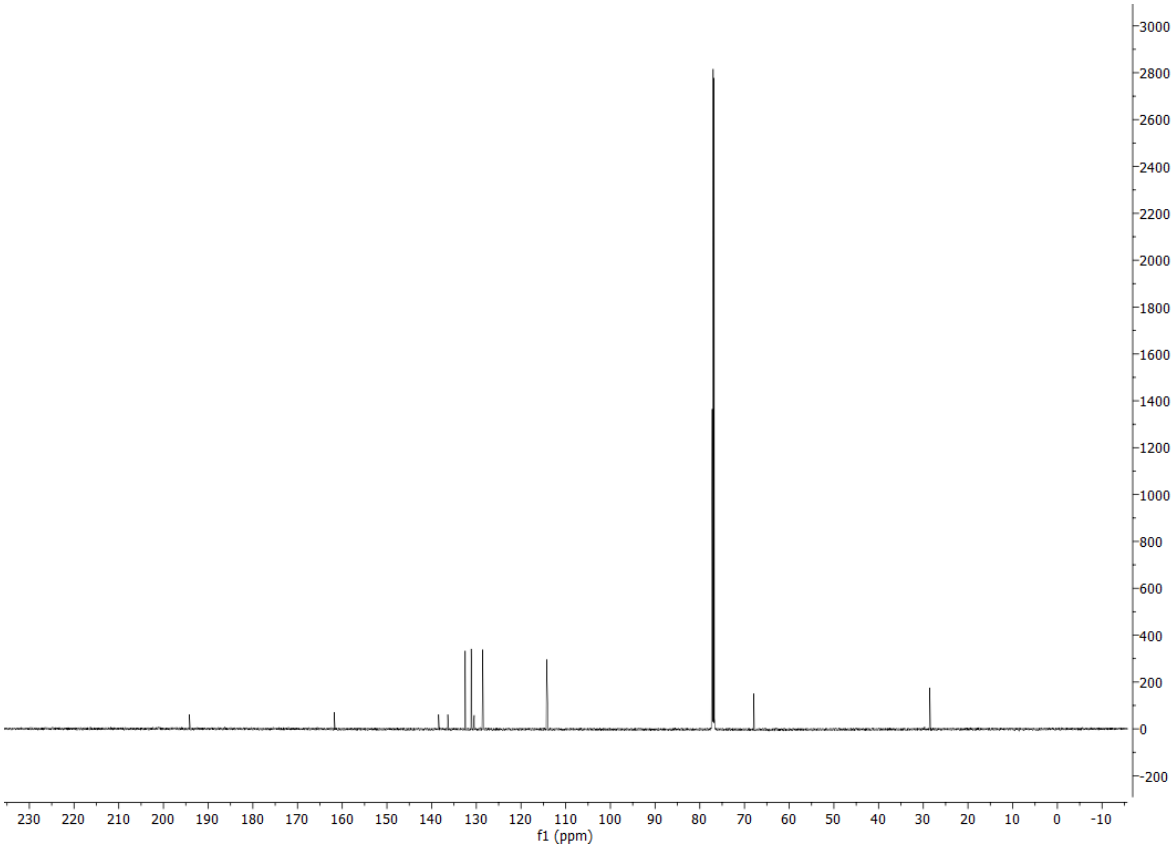

(2’’’*R*)-1’’’-{2’’-[4-(4’-chlorobenzoyl)phenoxy]ethyl}-2’’’-methylpyrrolidine 81

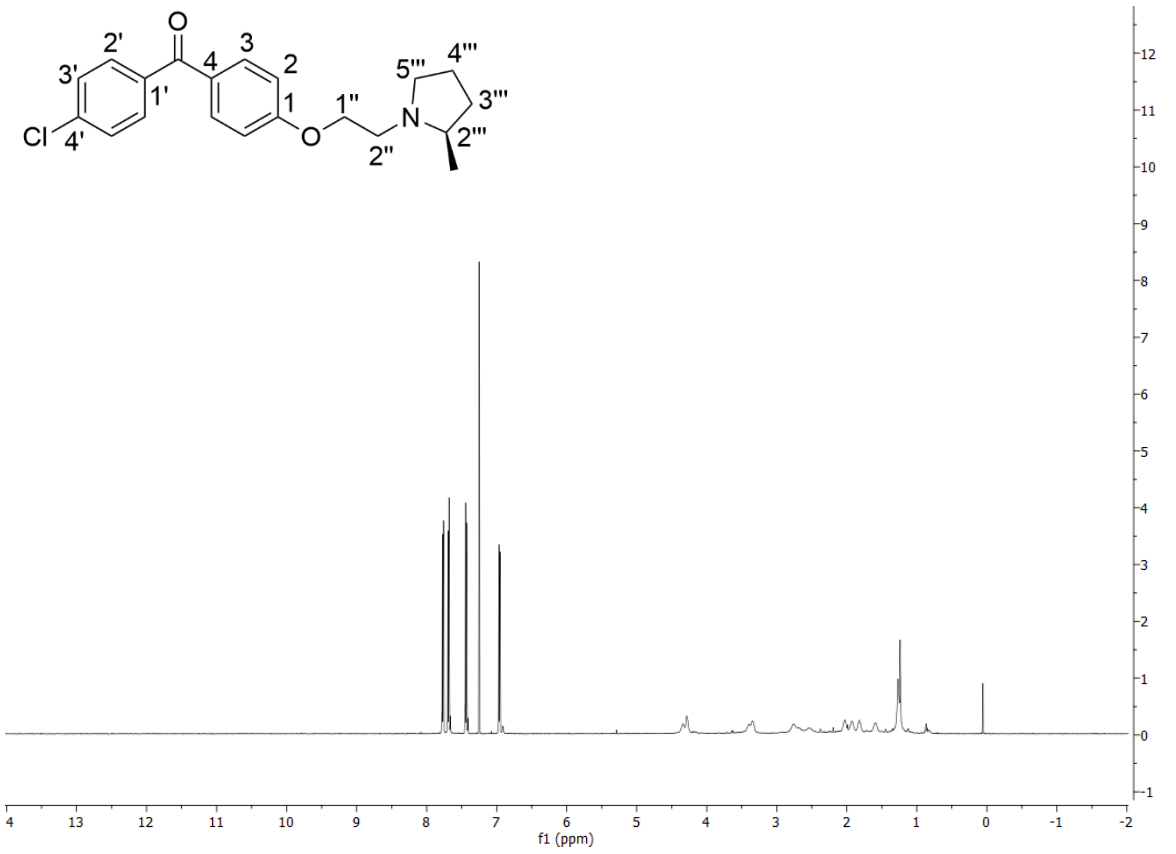

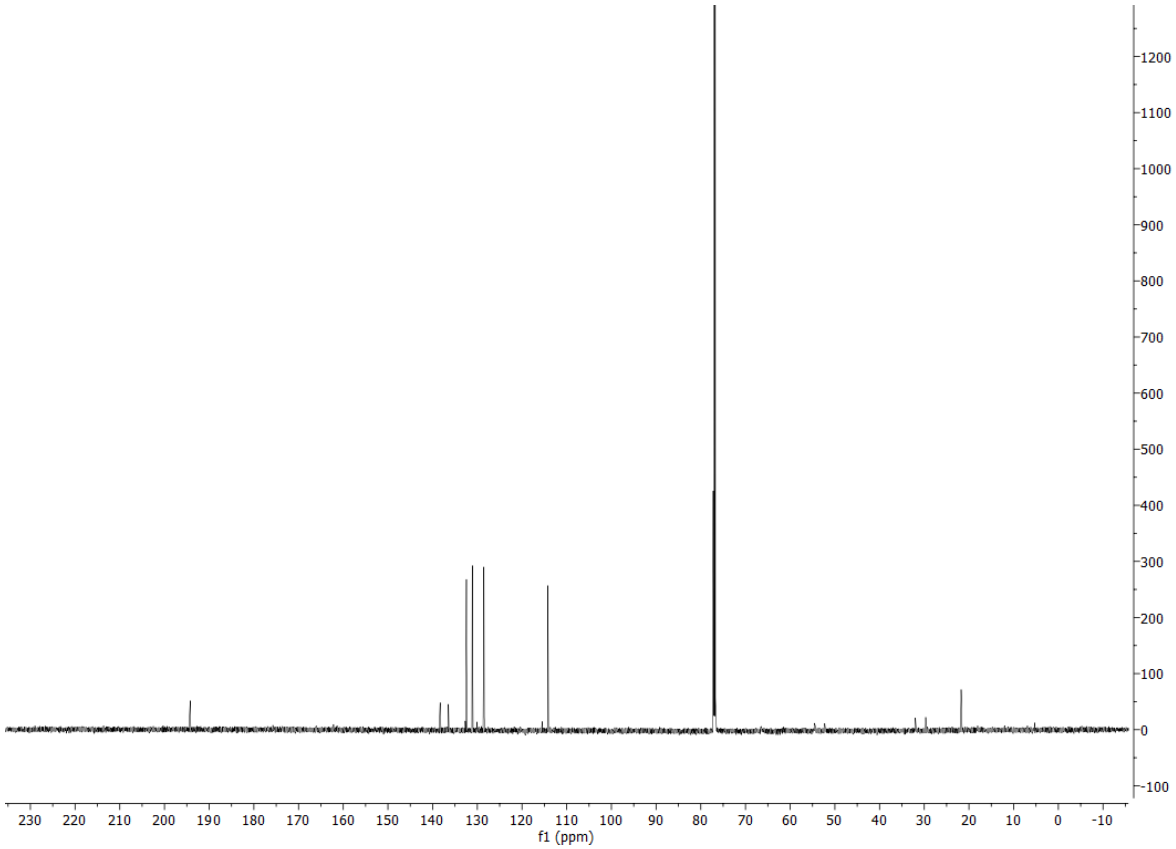

[4-(3’’-bromopropoxy)phenyl](4’-chlorophenyl)methanone 77e

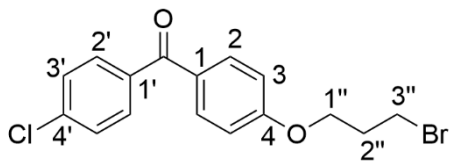

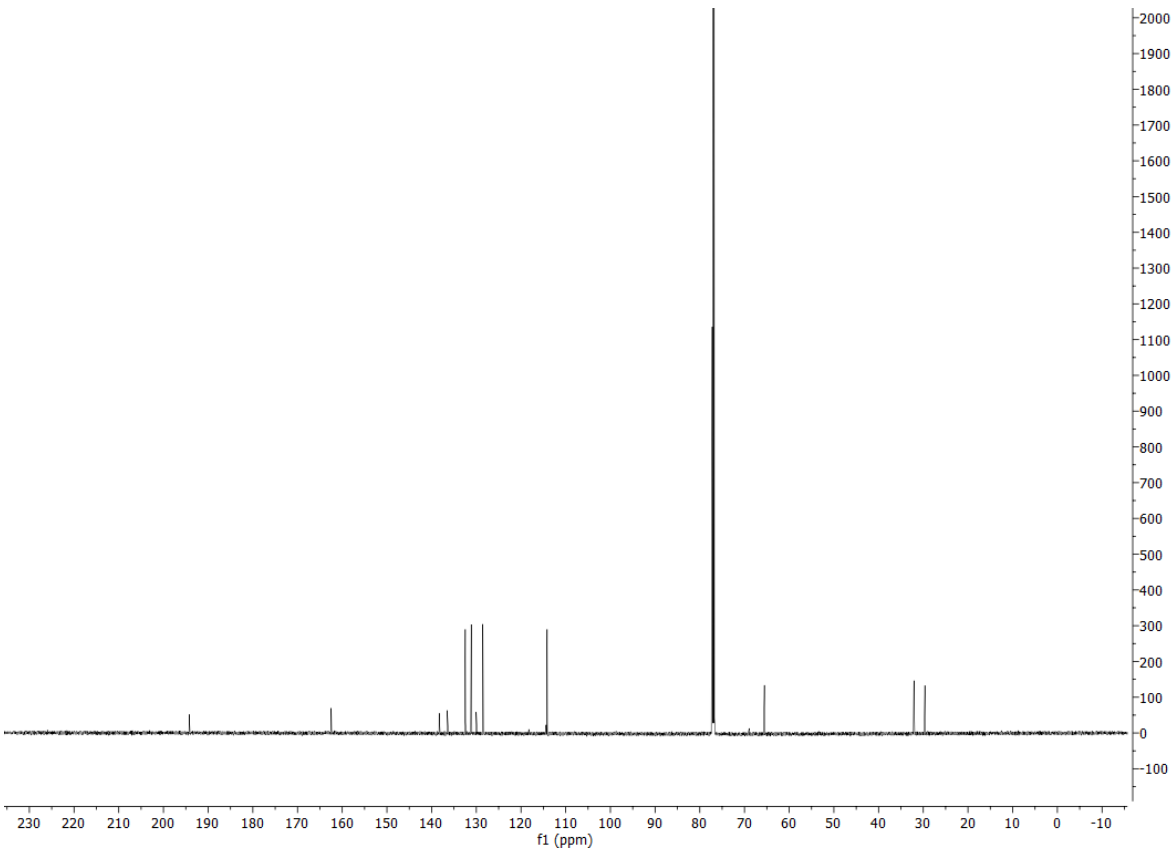

(2’’’*R*)-*N*-{3’’-[4-(4’-chlorobenzoyl)phenoxy]propyl}-2’’’-methylpyrrolidine 82

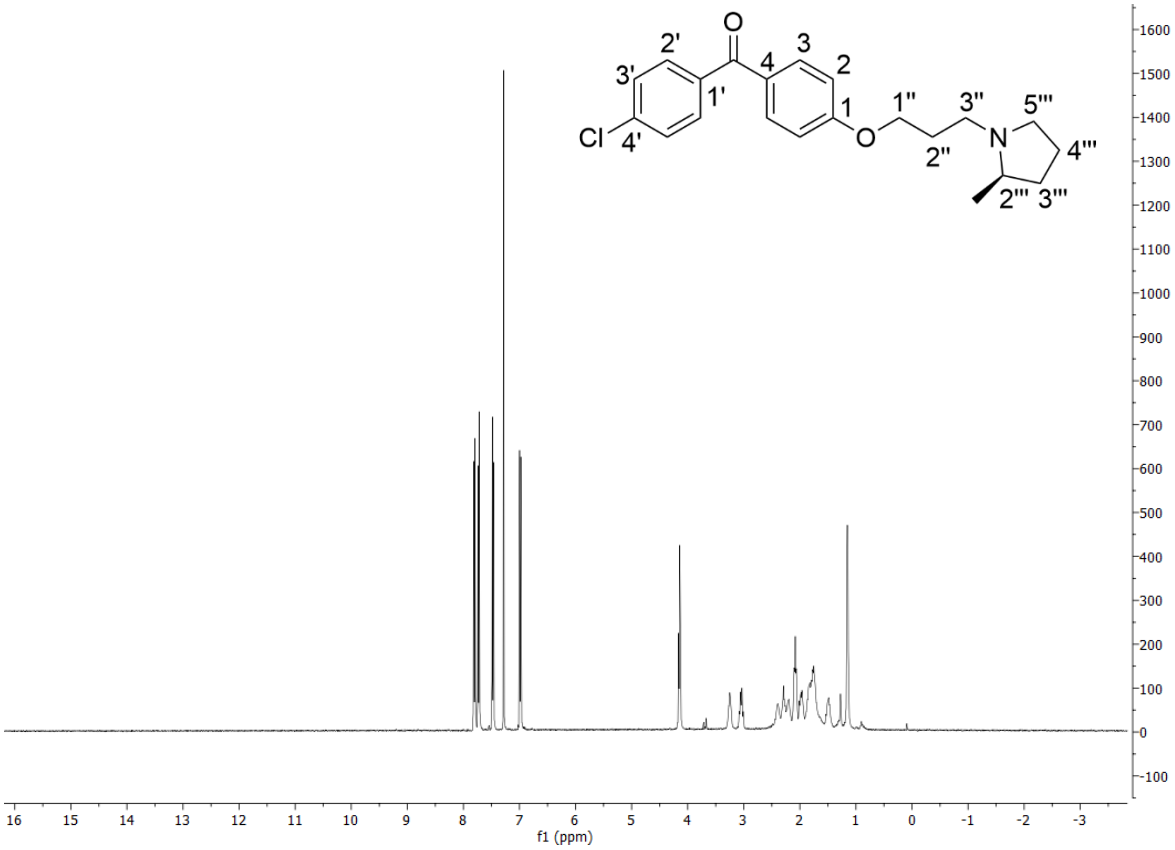

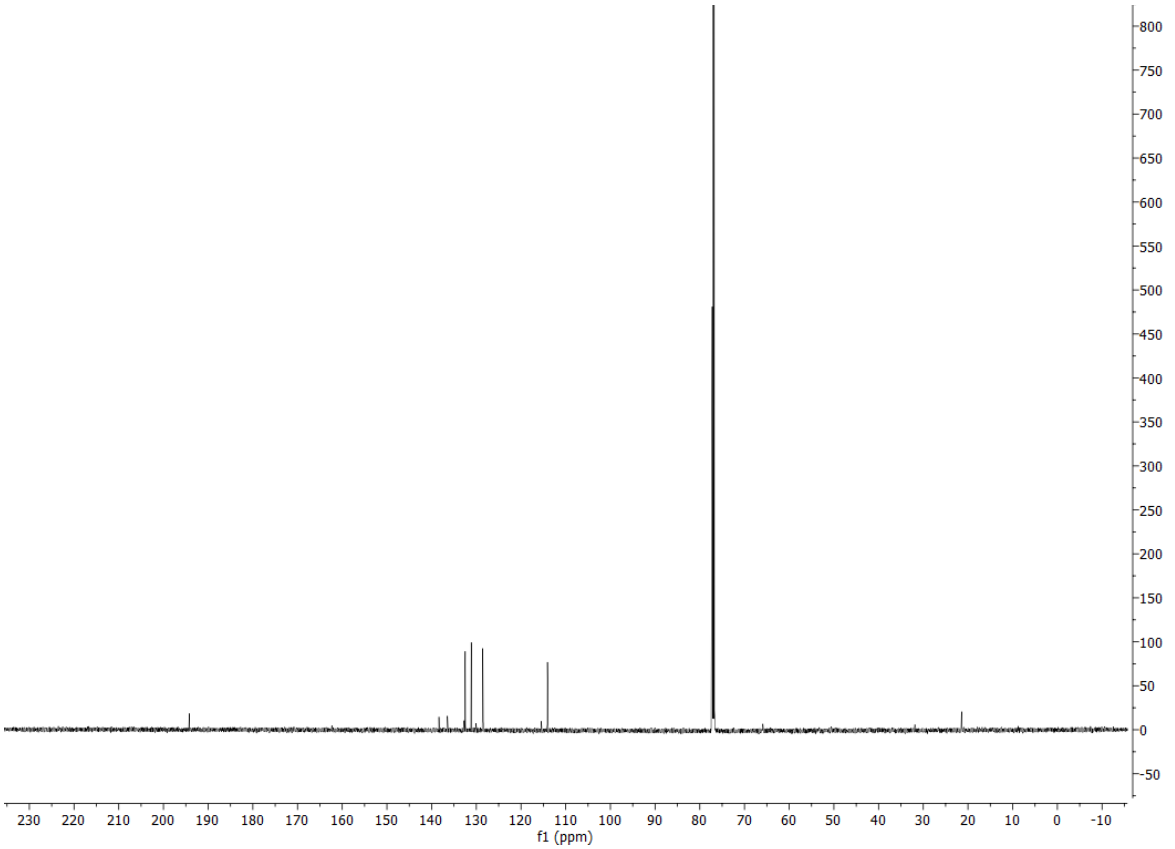

[4-(4’’-bromobutoxy)phenyl](4’-chlorophenyl)methanone 77f

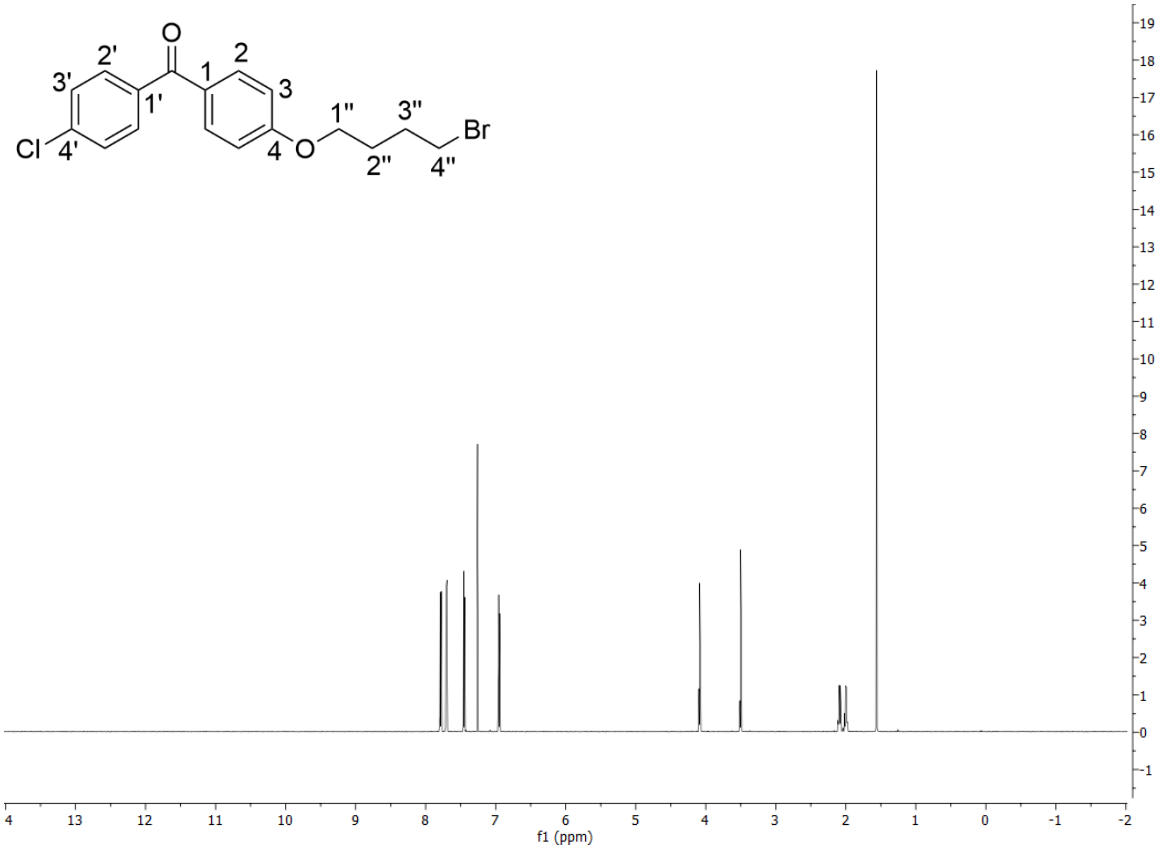

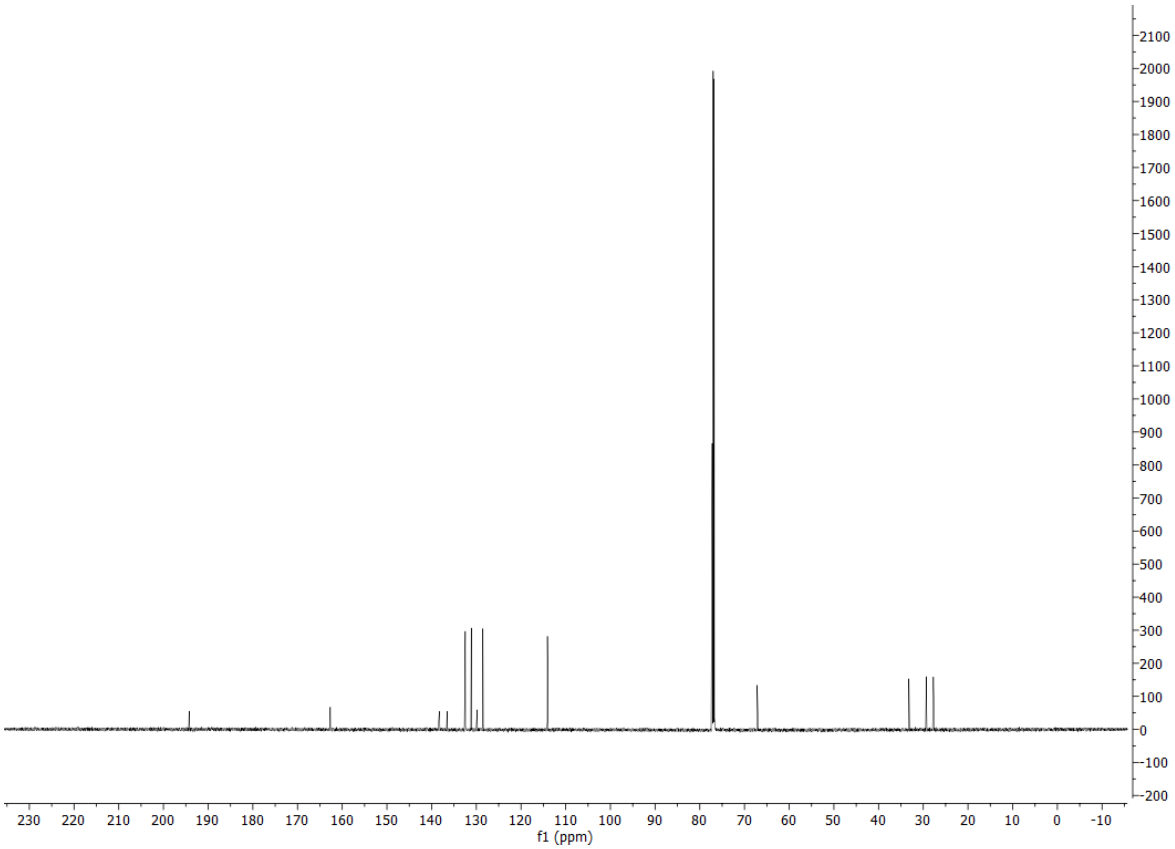

(2’’’*R*)-*N*-{4’’-[4-(4’-chlorobenzoyl)phenoxy]butyl}-2’’’-methylpyrrolidine 83

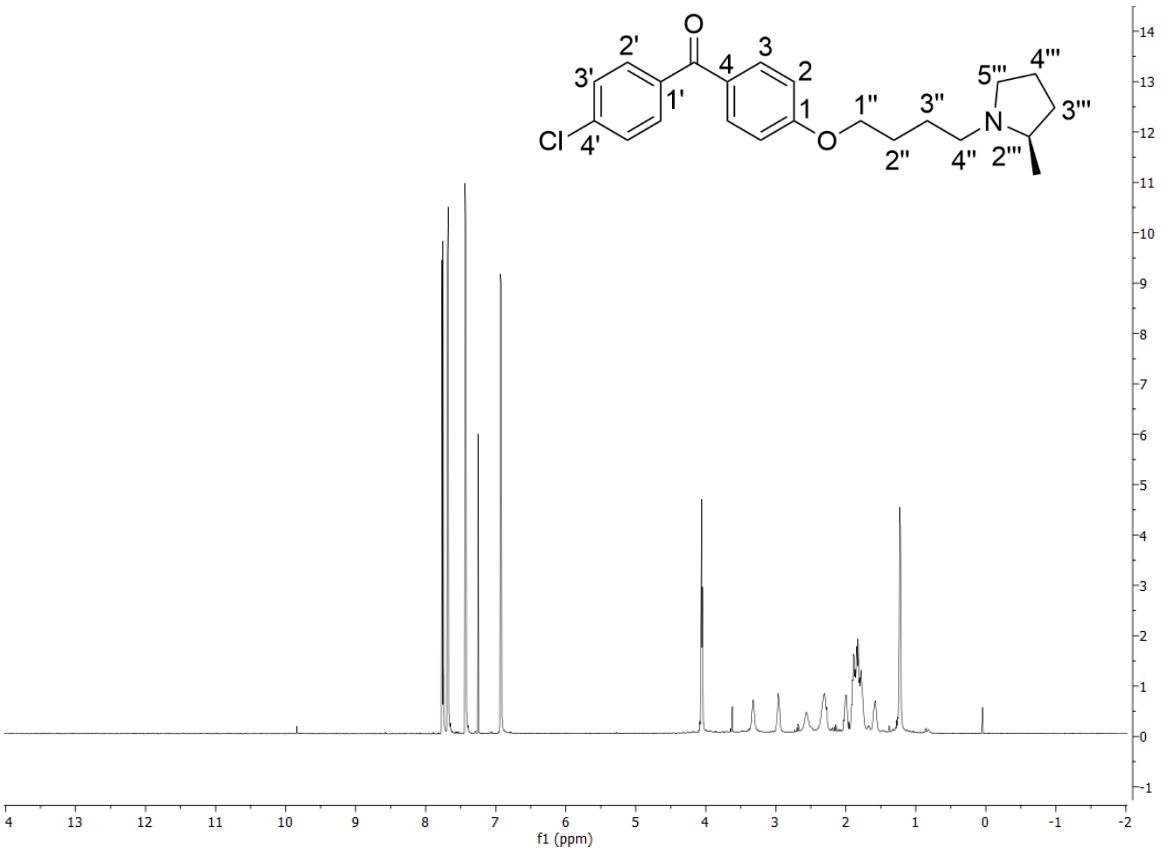

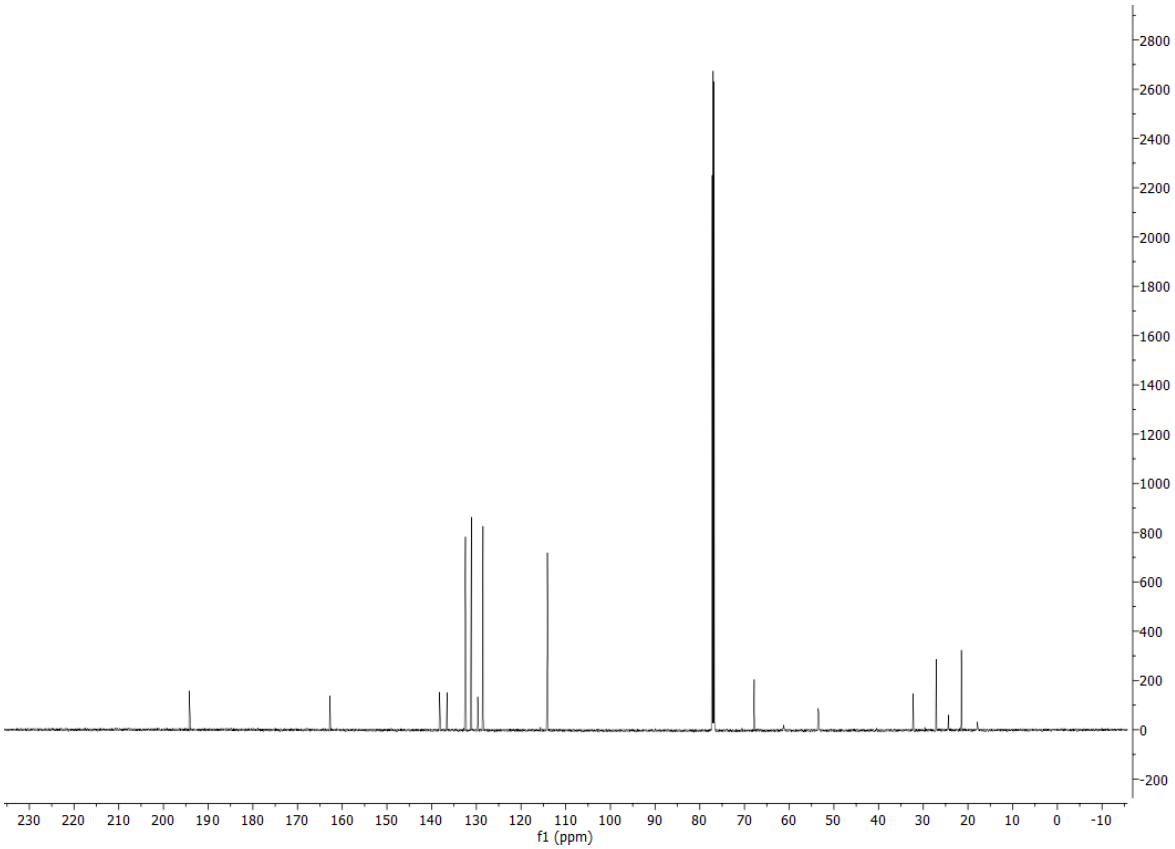

4-(3’-chlorobenzoyl)phenol 84

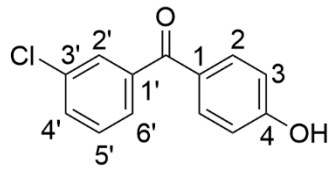

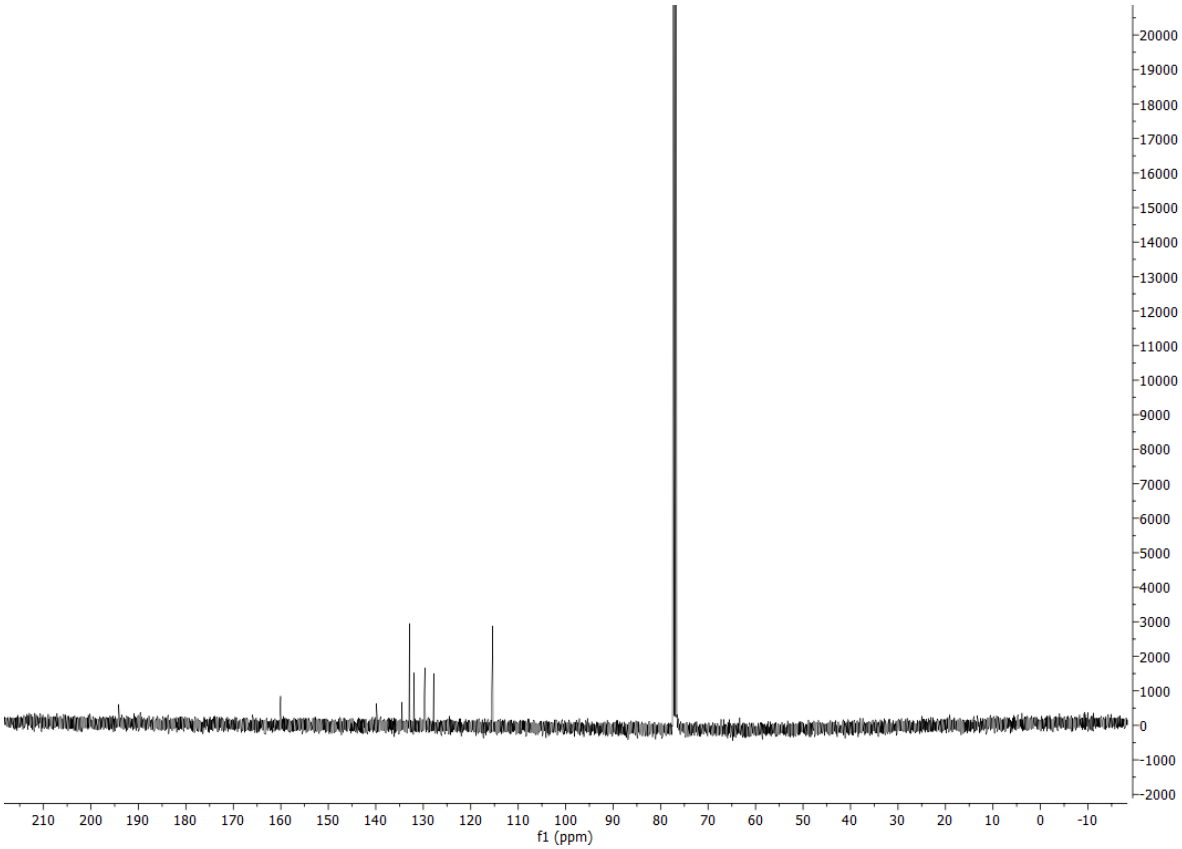

[4-(3’’-bromopropoxy)phenyl](3’-chlorophenyl)methanone 89

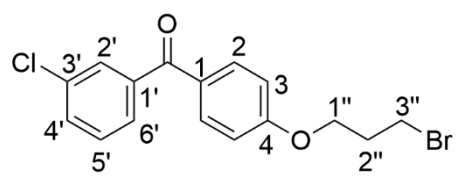

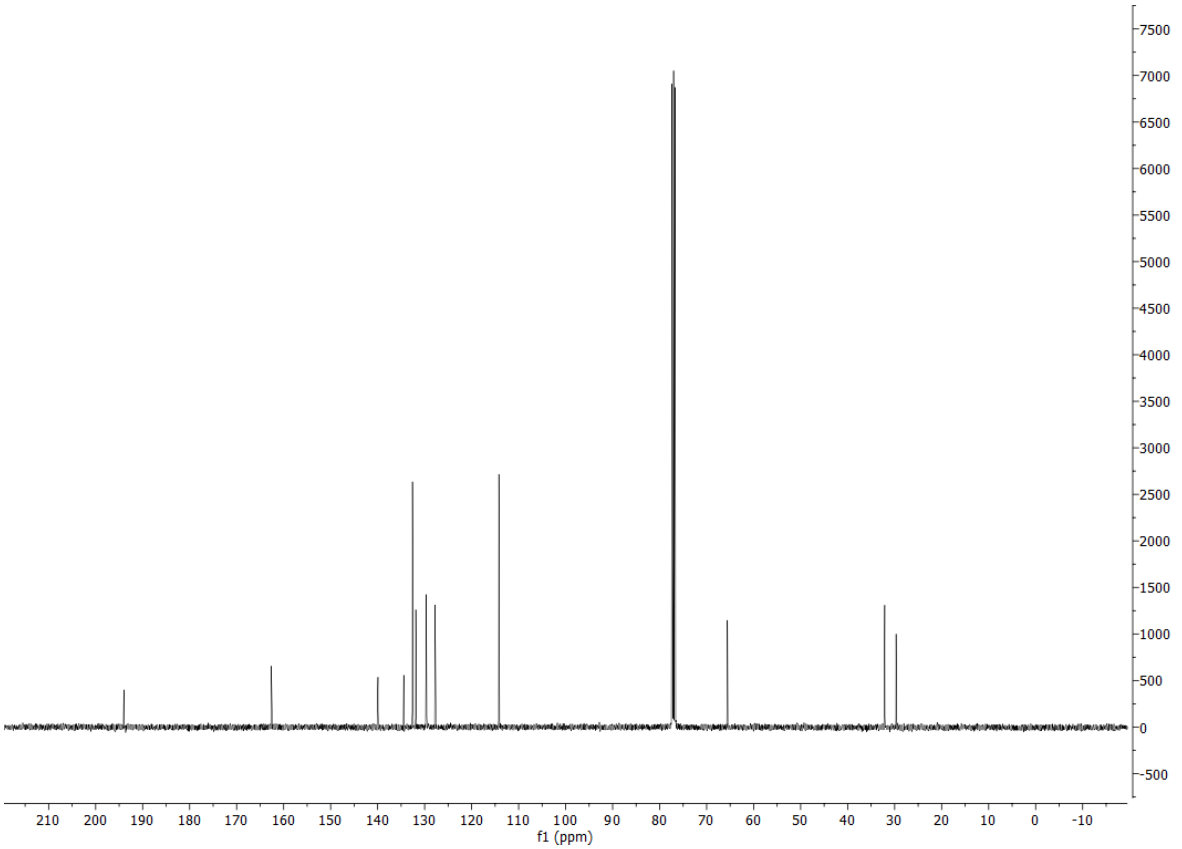

(2’’’*R*)-*N*-{3’’-[4-(3’-chlorobenzoyl)phenoxy]propyl}-2’’’-methylpyrrolidine 91

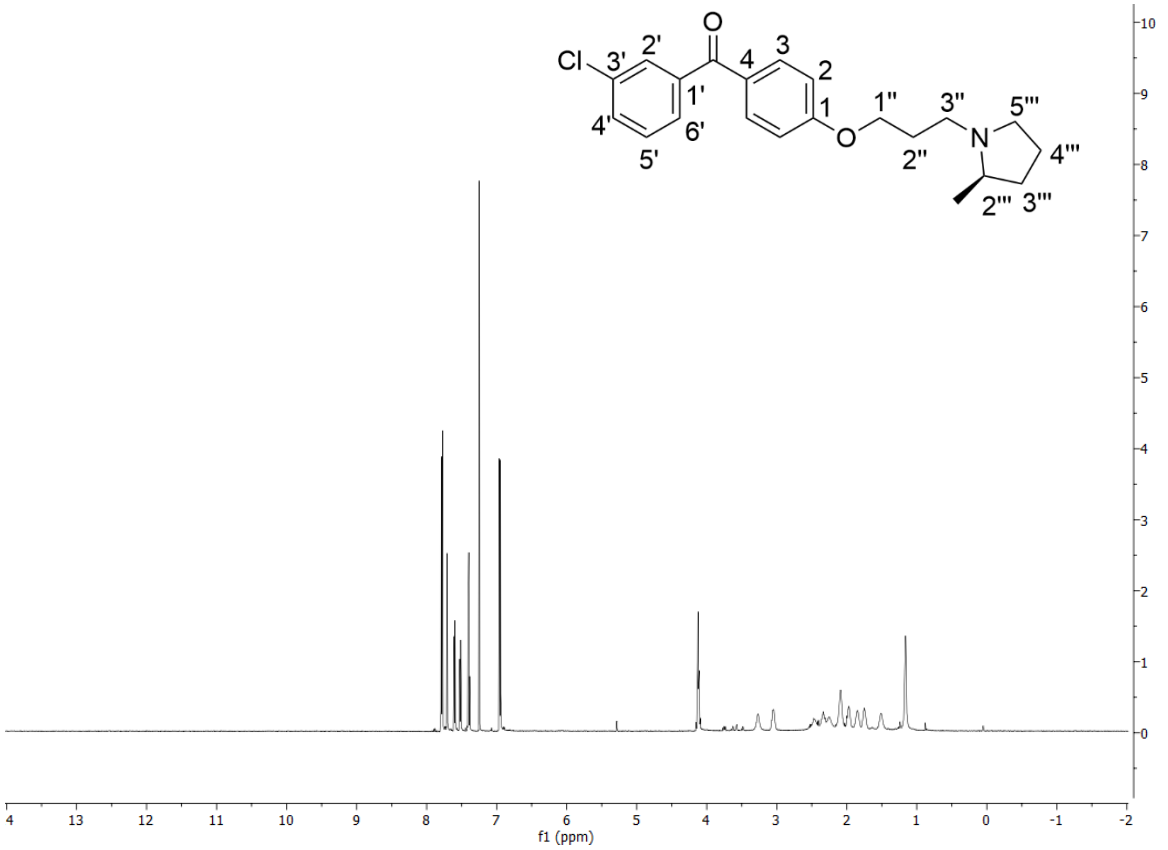

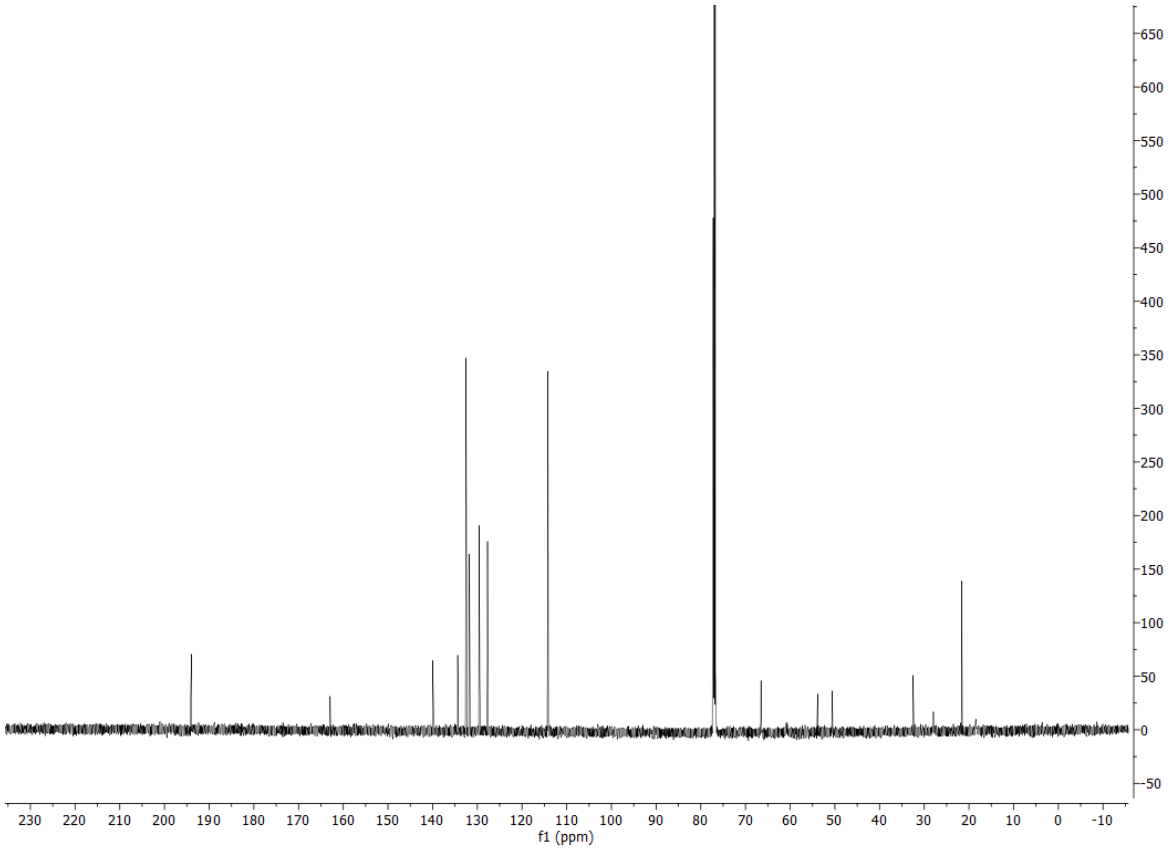

4-(2’-chlorobenzoyl)phenol 85

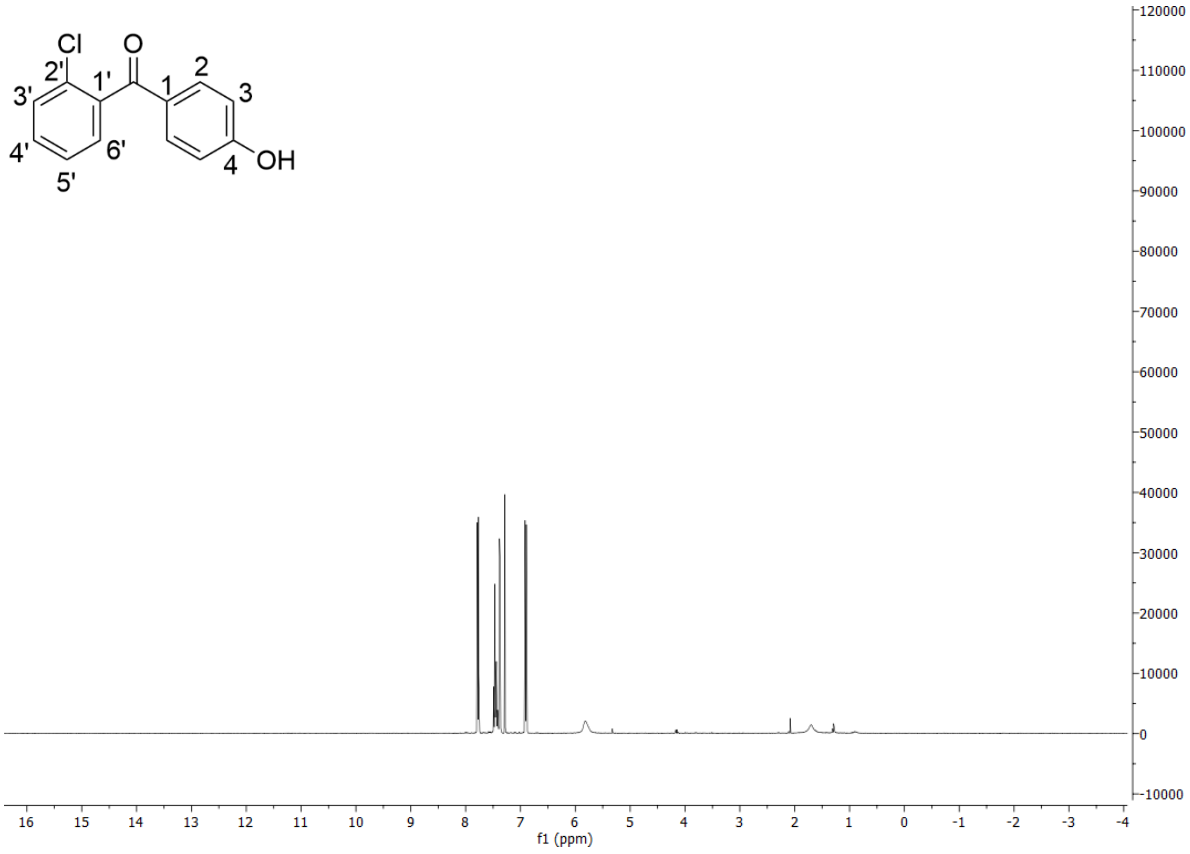

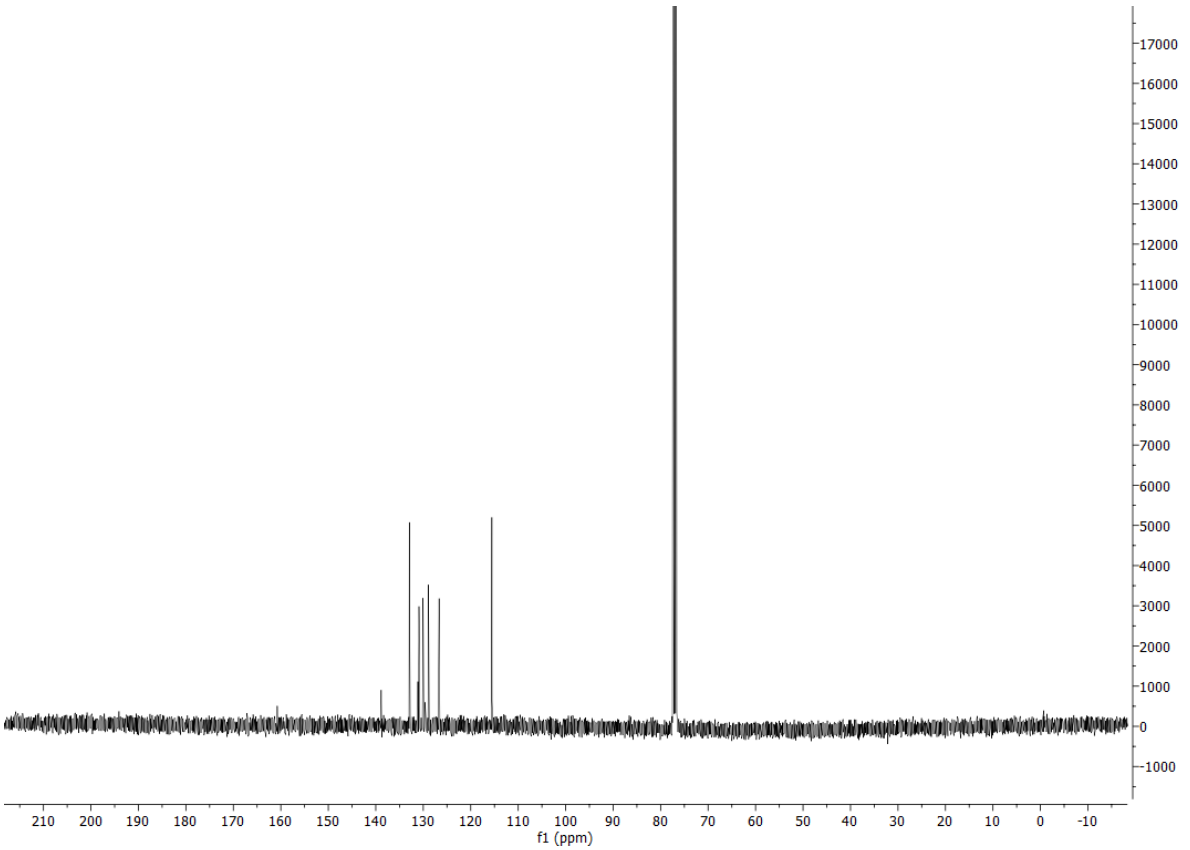

(2’’’*R*)-*N*-{3’’-[4-(2’-chlorobenzoyl)phenoxy]propyl}-2’’-methylpyrrolidine 92

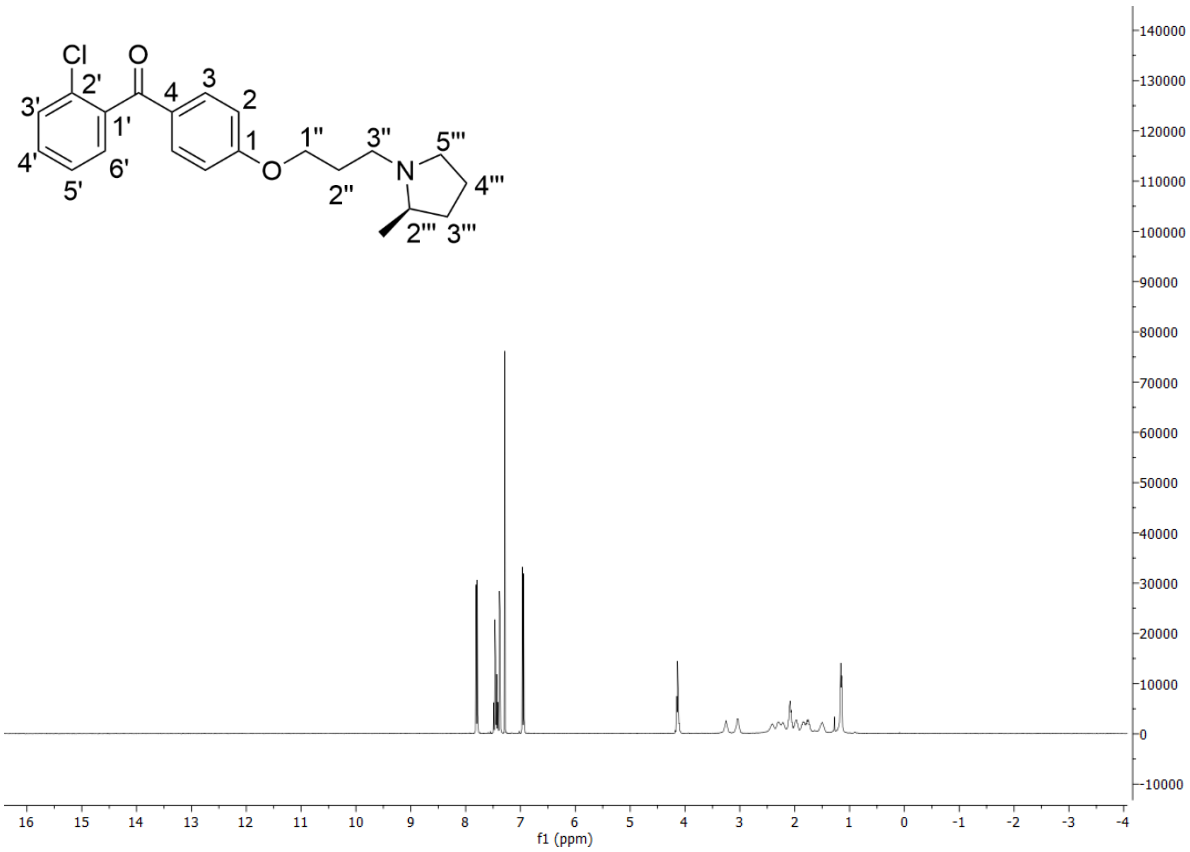

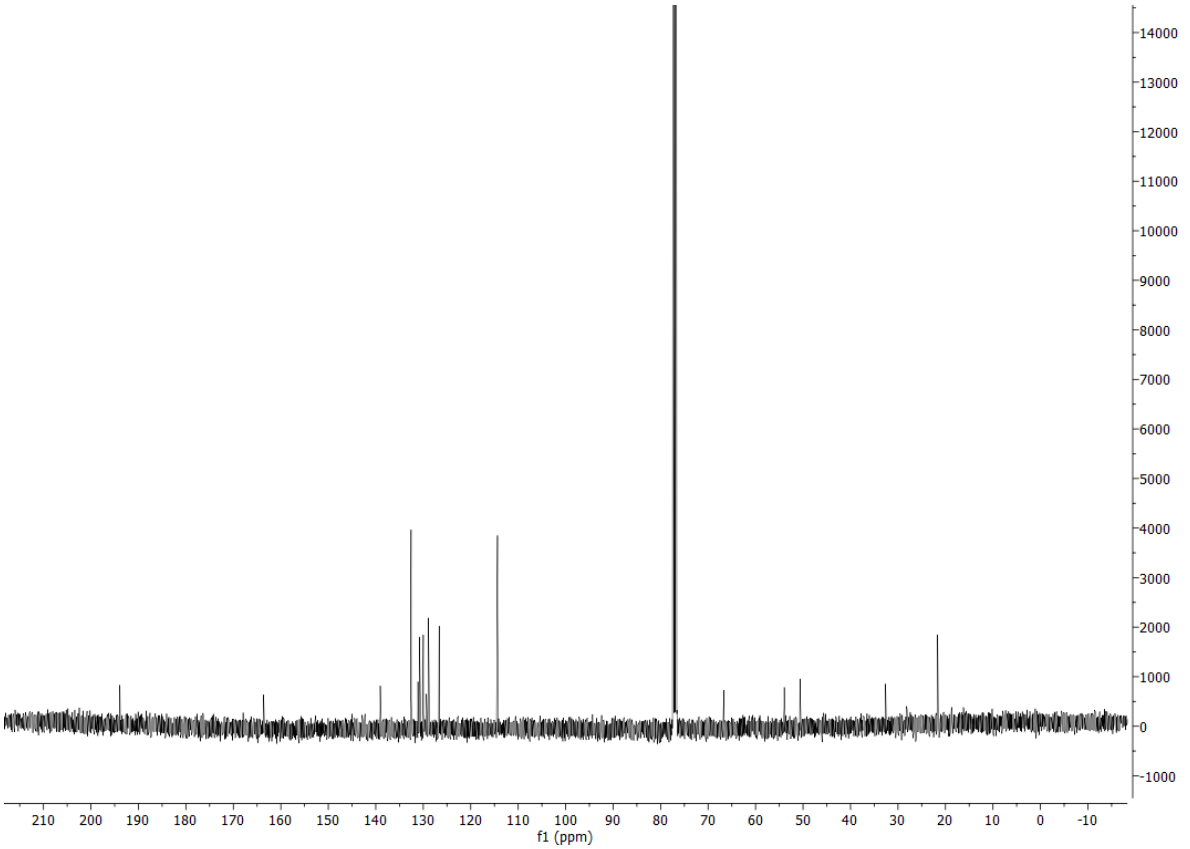

4-[1-(3’-bromopropoxy)phenyl]ethenone 123b

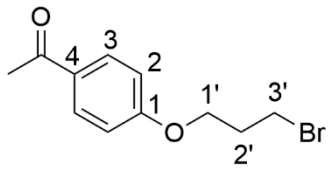

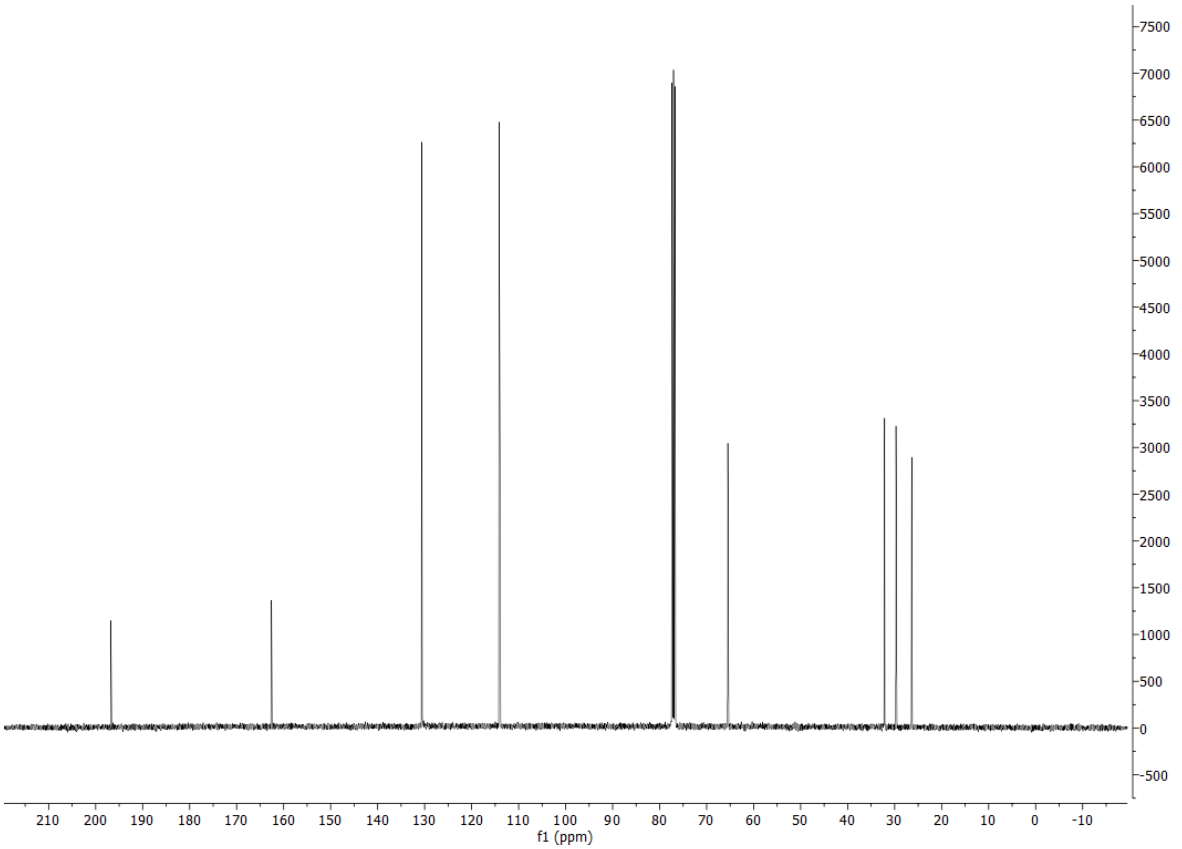

4-(1-{3’-[(2’’*R*)-2’’-methylpyrrolidine]propoxy}phenyl)ethenone 125

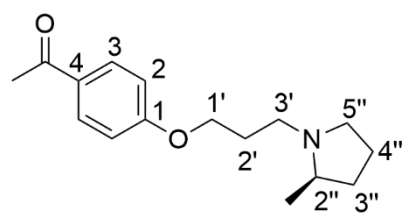

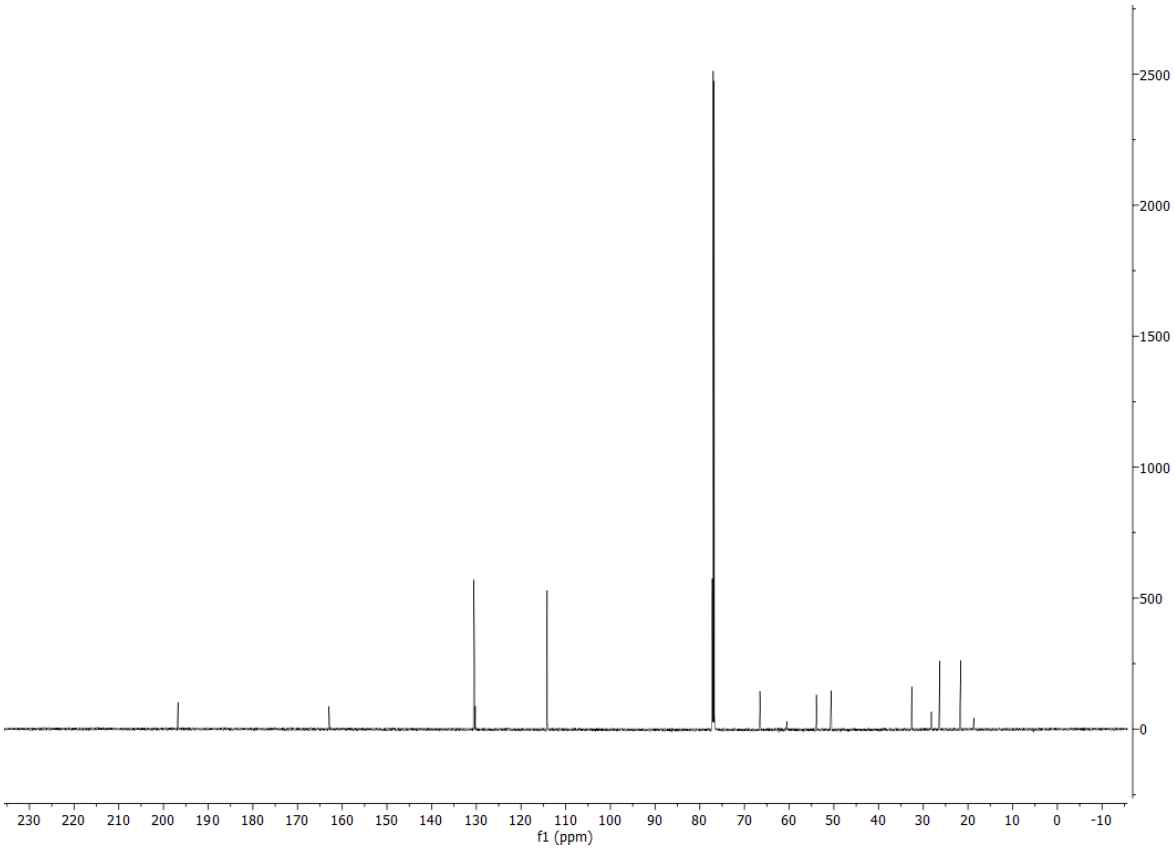

(2'*R*)-2'-methyl-*N*-(3-phenoxypropyl)pyrrolidine 124

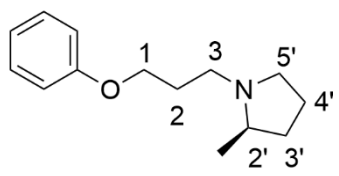

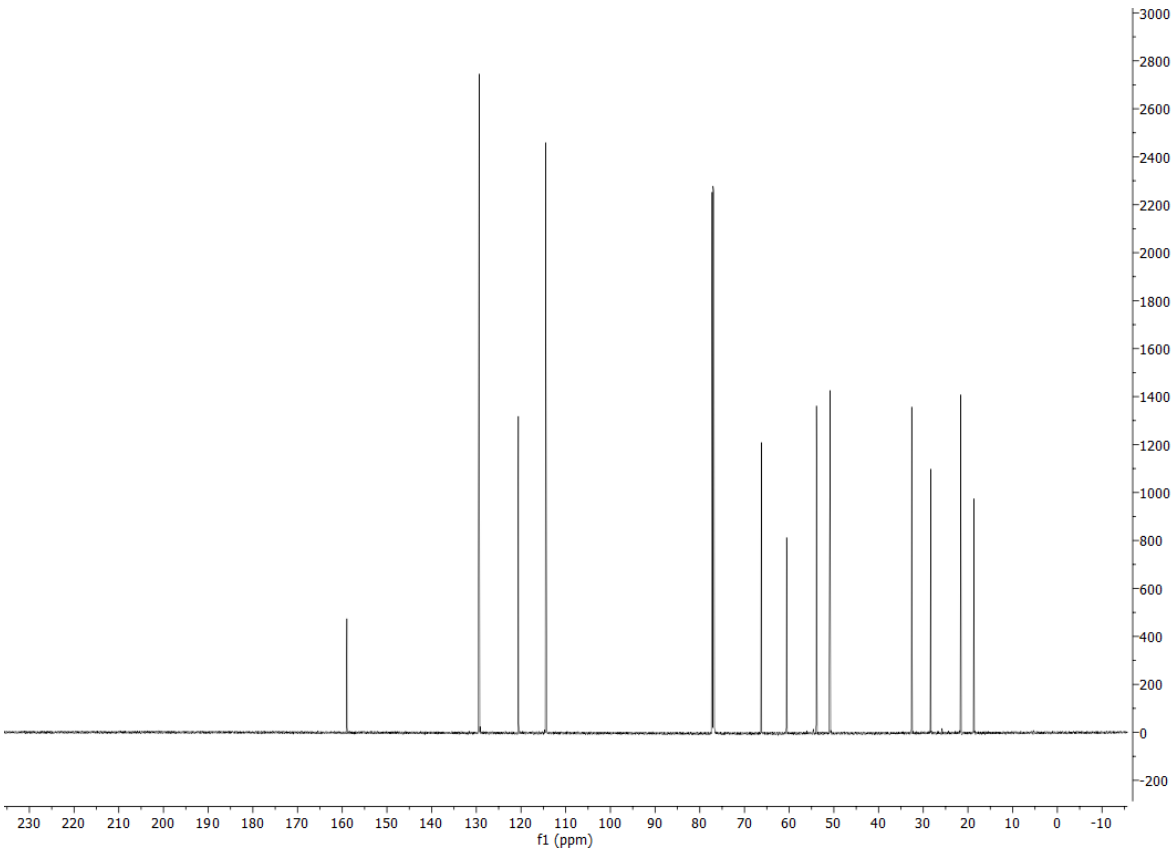

(4-chlorophenyl)(3’,5’-dimethoxyphenyl)methanone 141

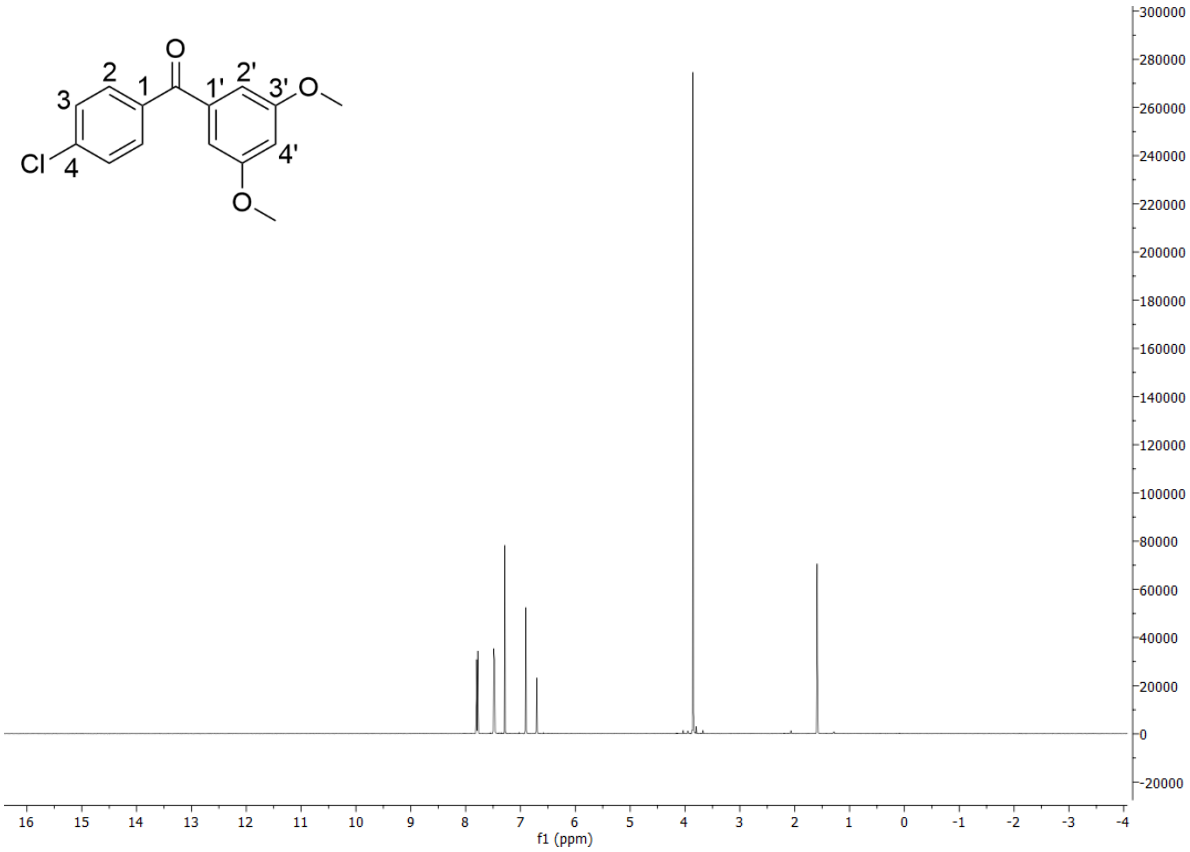

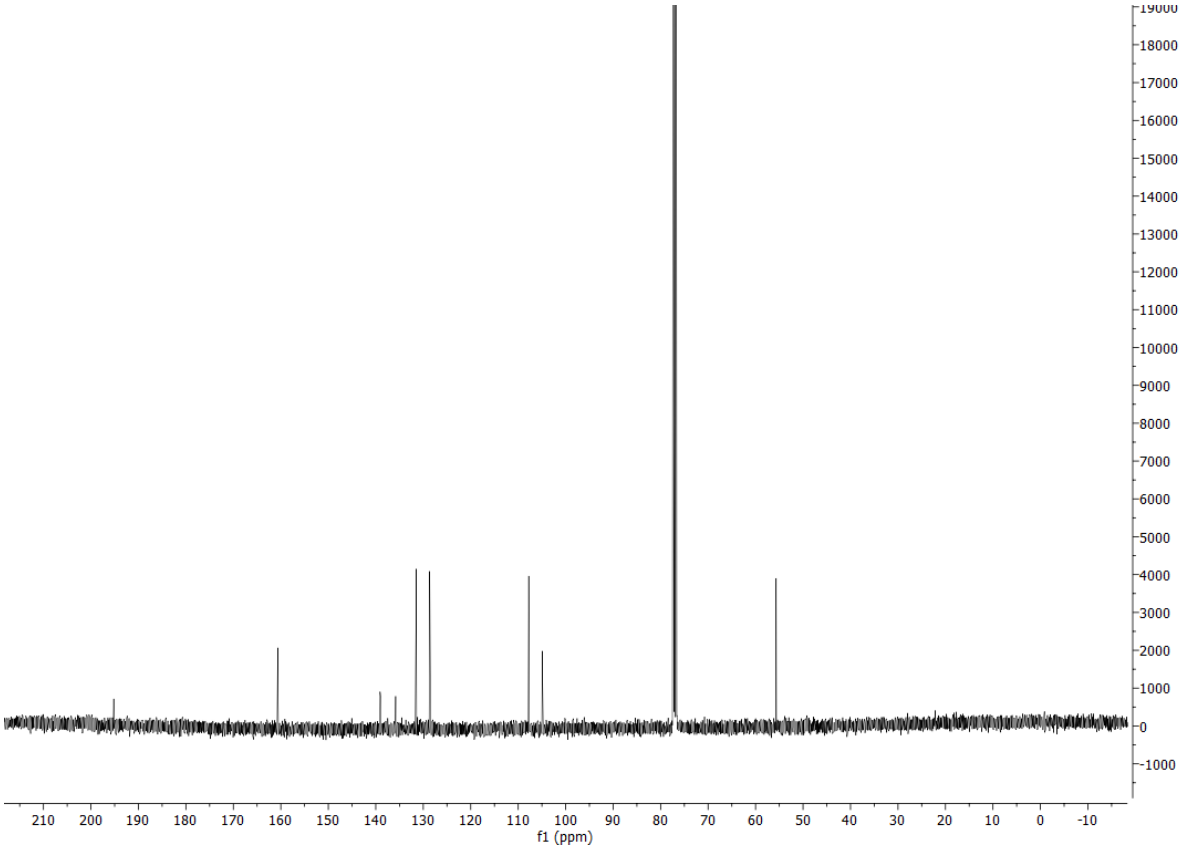

3’-(4-chlorobenzoyl)-5’-(hex-5’’-yn-1’’-yloxy)phenol 144

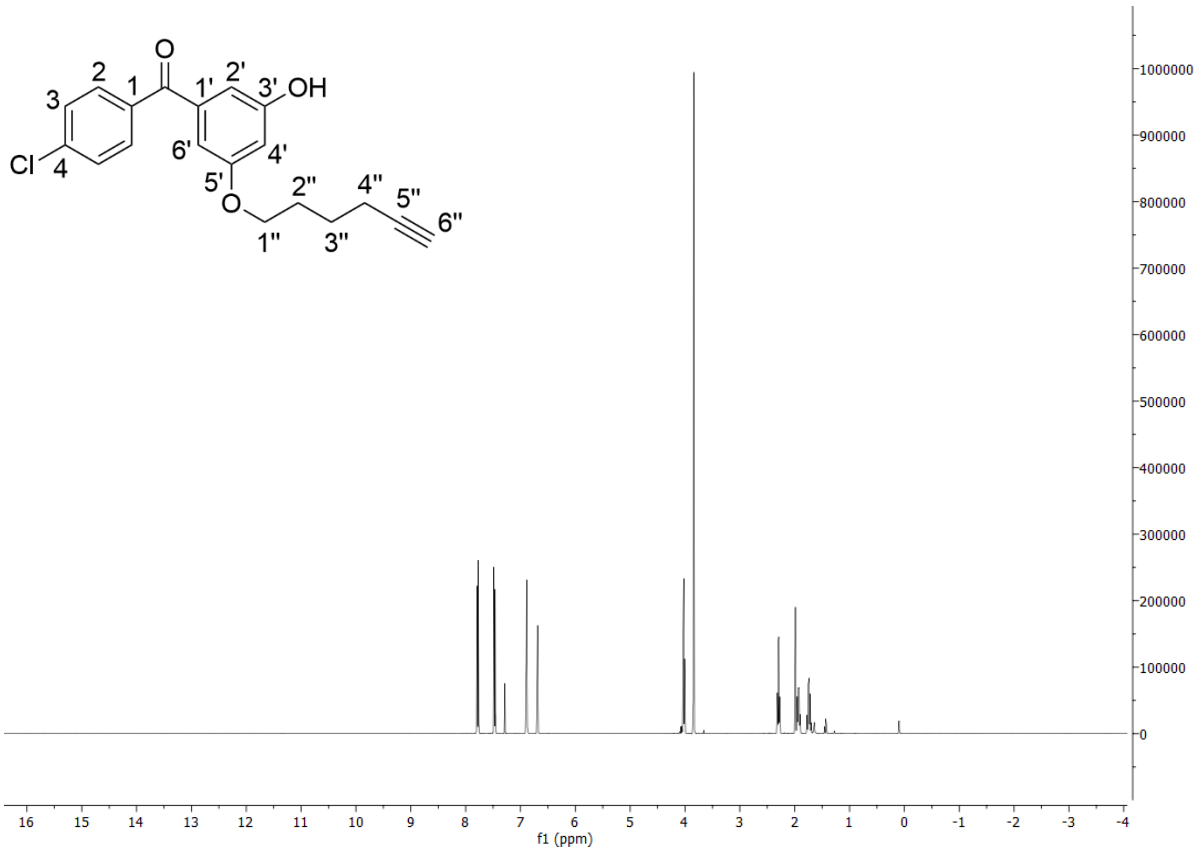

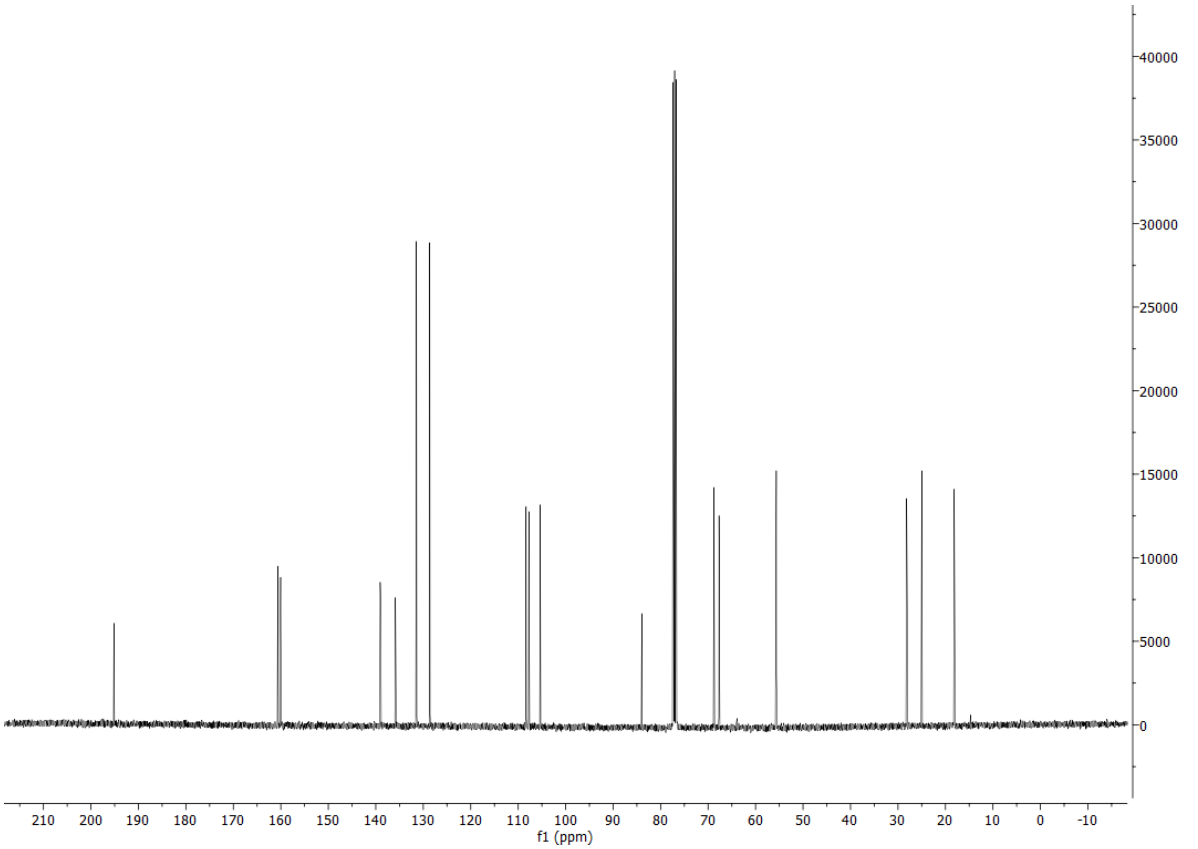

(2’’’*R*)-*N*-{3’’’-[3’-(4-chlorobenzoyl)-5’-(hex-5’’-yn-1’’-yloxy)phenoxy]propyl}-2’’’-methylpyrrolidine 138